

# MULTISCALE FLOWS GENERATED IN MULTISCALE WAYS: FUNDAMENTALS AND APPLICATIONS

J.C. Vassilicos

Department of Aeronautics

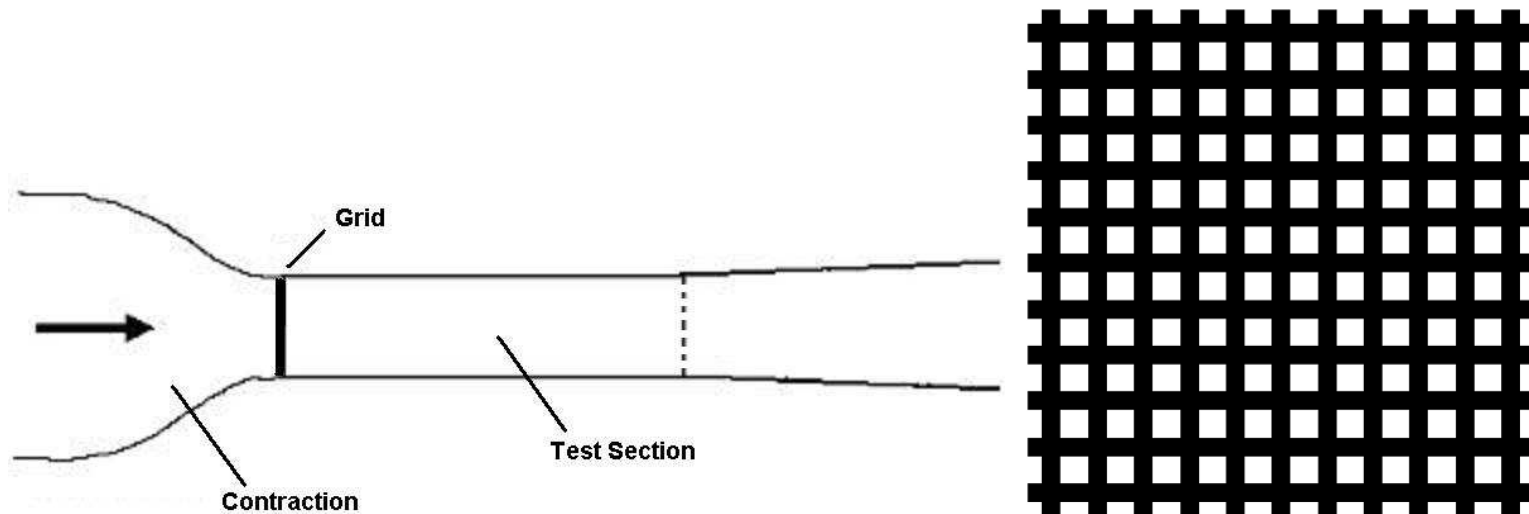
Imperial College London, U.K.

Work done with Chris Coffey, Daryl Hurst, N. Kerl, Sylvain Laizet, Nicolas Mazellier, Jovan Nedic, Richard Seoud, Nikos Soulopoulos, Thomas Sponfeldner and Pedro Valente.

see <http://www3.imperial.ac.uk/tmfc>

# Grid-generated turbulence

1. Attempt at reasonably homogeneous isotropic turbulence to check theories of turbulence: 1934 to this day.
2. Attempt at more stirring/mixing than with canonical free-shear flows such as individual wakes, jets, mixing layers.

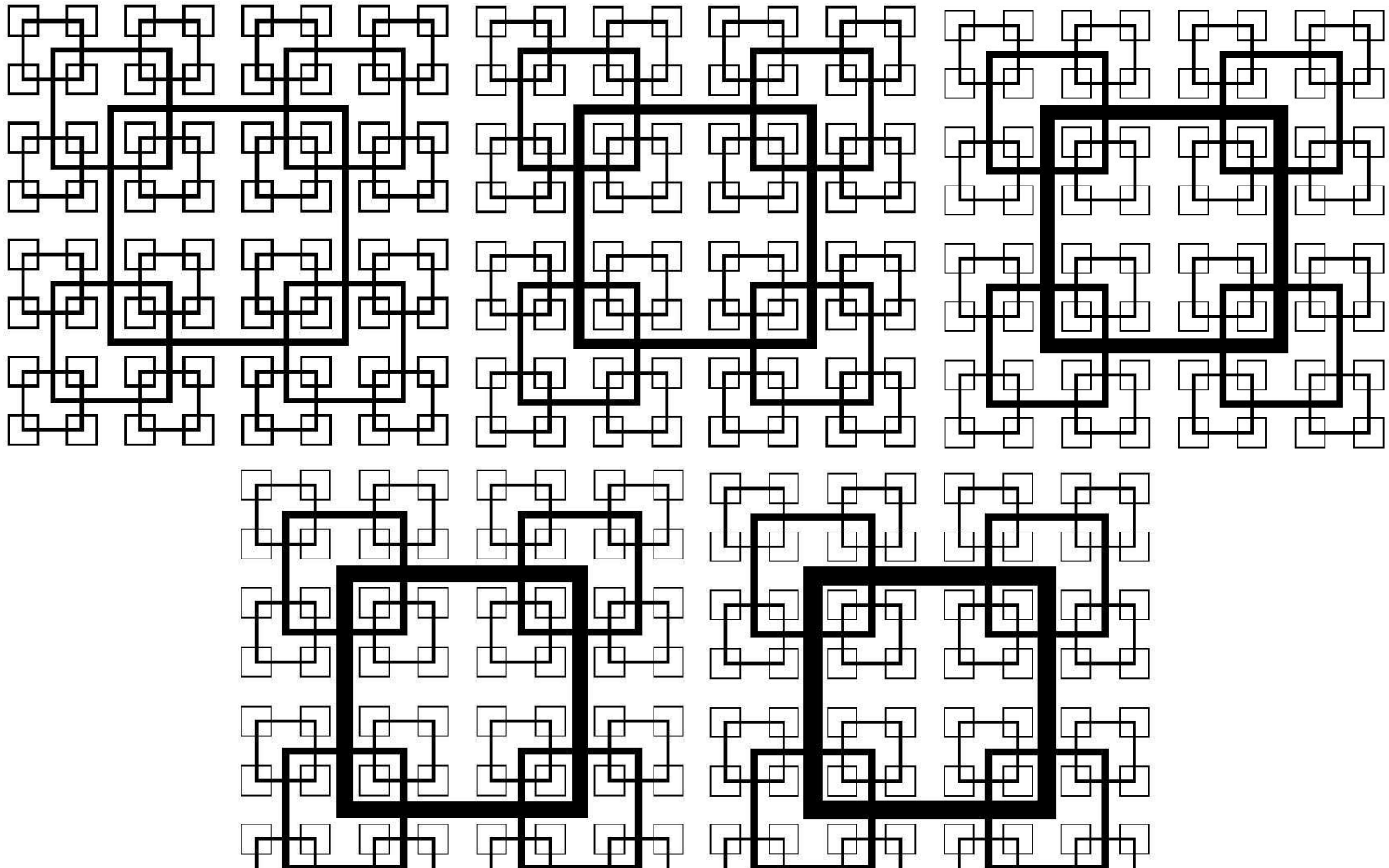


Starting point: very basic issue of how to scale grid-generated turbulence; with the bar width or the mesh-size?

# $D_f = 2, \sigma = 25\%$ fractal square grids

and equal  $M_{eff} \approx 2.6cm$ ,  $L_{max} \approx 24cm$ ,  $L_{min} \approx 3cm$ ,  $N = 4$ ,  
 $T = 0.46m$ .

**BUT**  $t_r = 2.5, 5.0, 8.5, 13.0, 17.0$



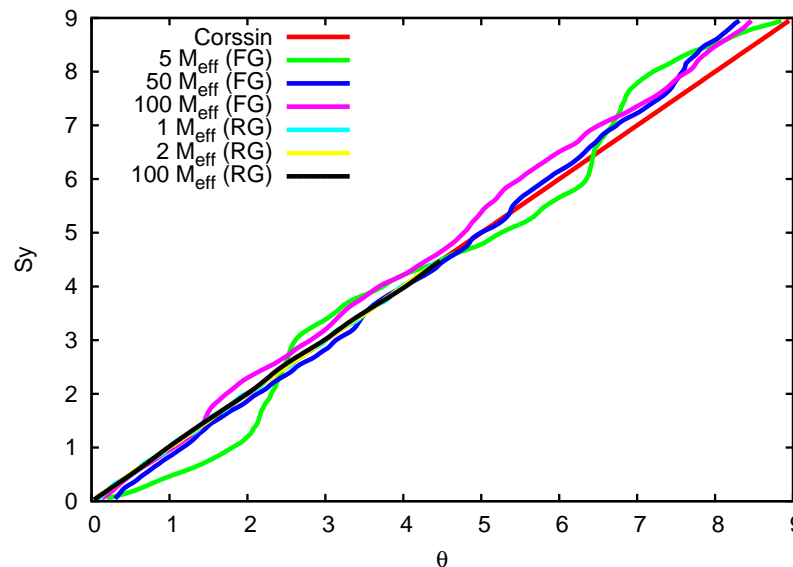
# Direct Numerical Simulations

We use Incompact3D which originates from Eric Lamballais (Poitiers) and his coworkers: solves incompressible

$$\text{Navier-Stokes and } \frac{\partial \theta}{\partial t} + \mathbf{u} \cdot \nabla \theta = \kappa \nabla^2 \theta$$

Immersed Boundary Method for modelling the grid in the flow.

Inflow/outflow boundary conditions in the streamwise direction, periodic boundary conditions in the lateral directions.



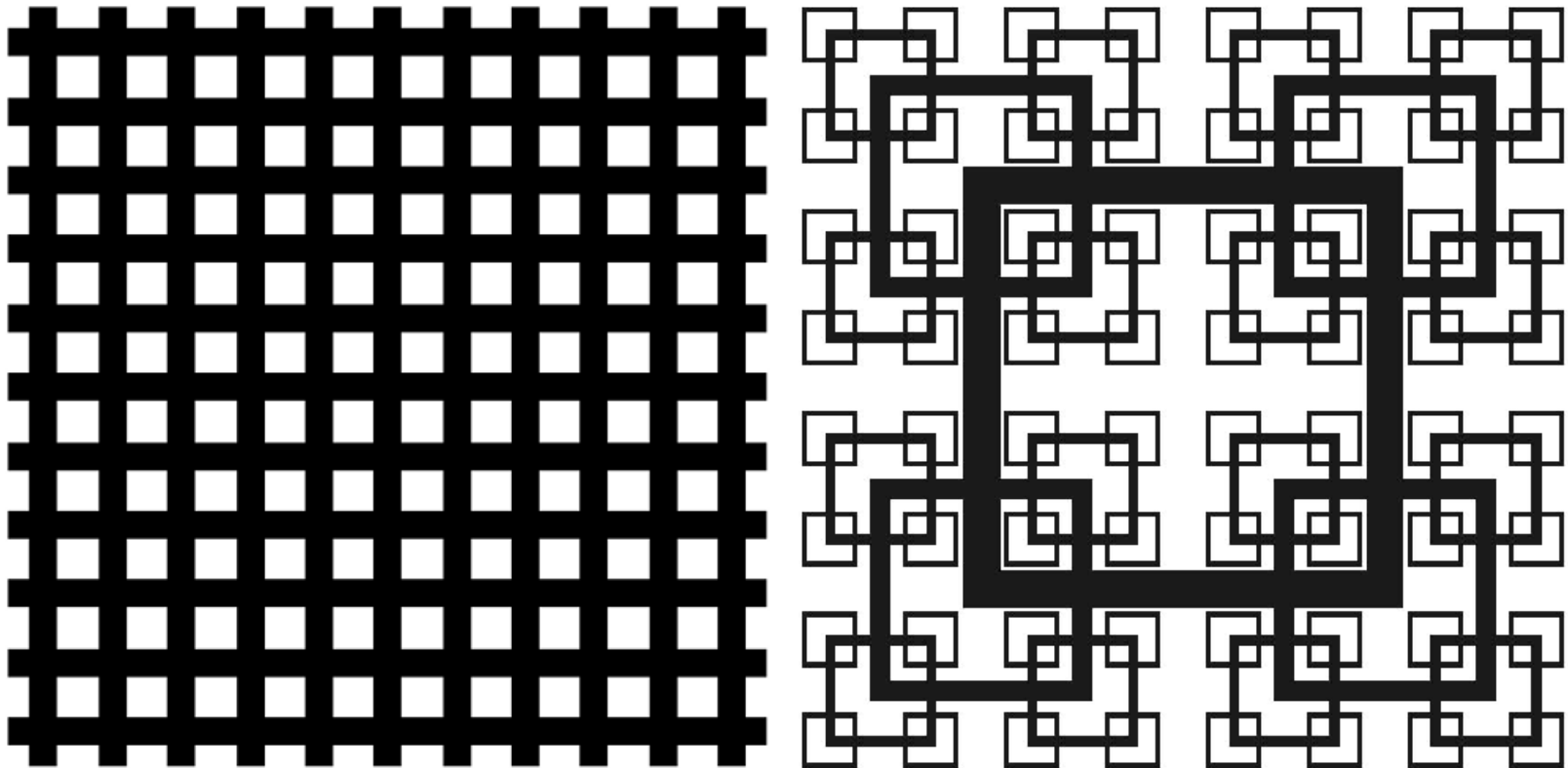


# Grids with same $\sigma = 50\%$

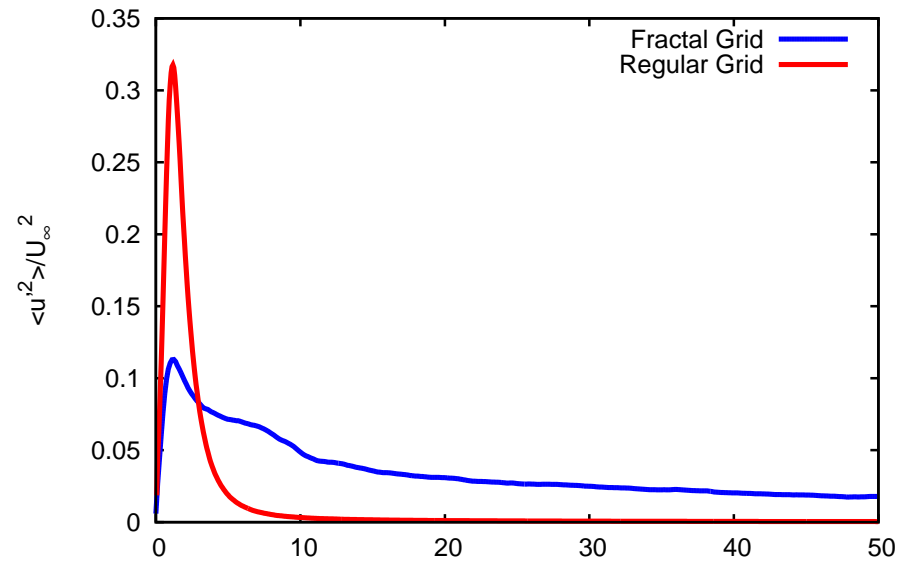
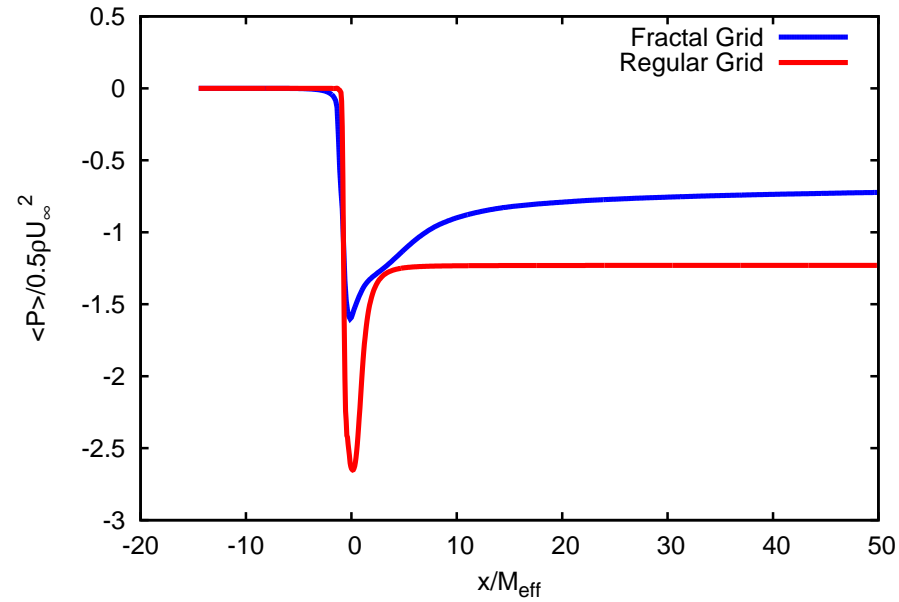
and same  $M_{eff} \equiv \frac{4T^2}{P} \sqrt{1 - \sigma}$ .

Fractal grid:  $D_f = 2$ ,  $N = 4$ ,  $t_r = 8.5$

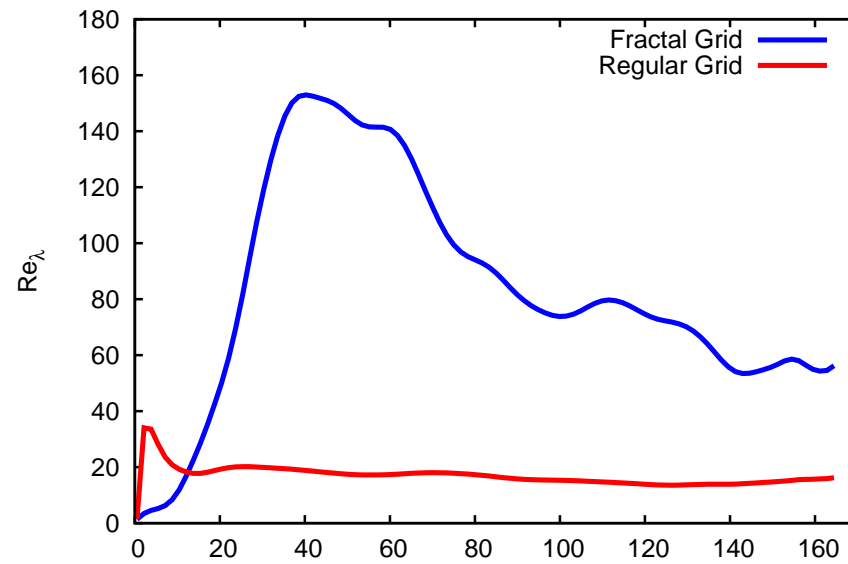
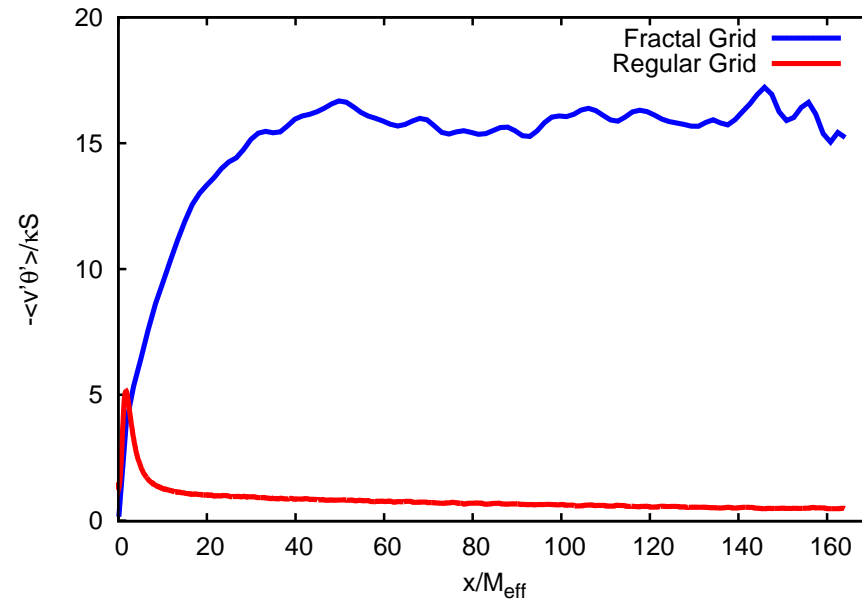
Regular grid:  $b = 2t_{min}$



# Turbulence and pressure drop



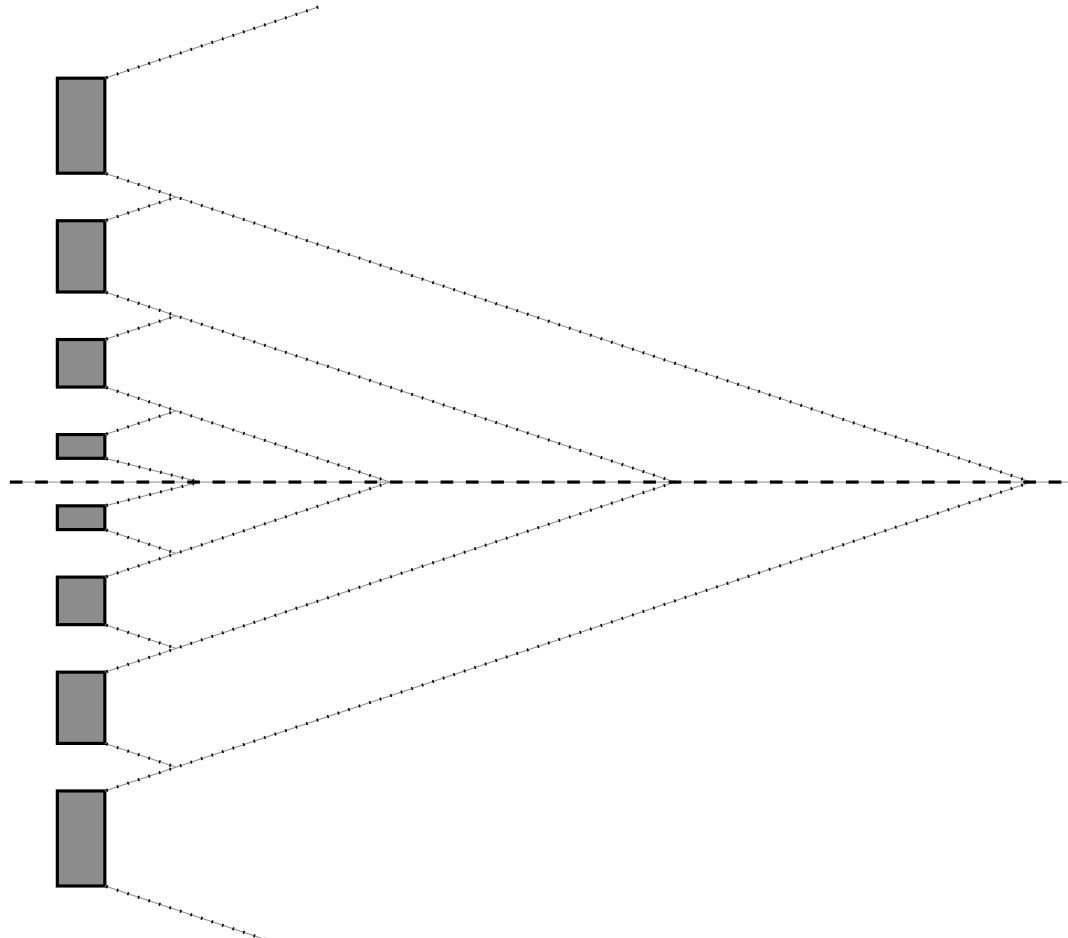
# Turbulence and scalar transfer



# Wake-interaction length-scales

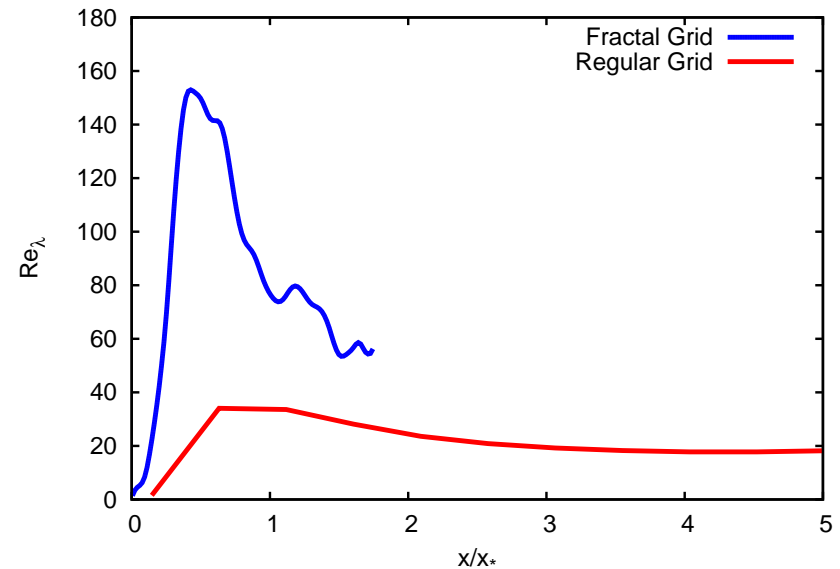
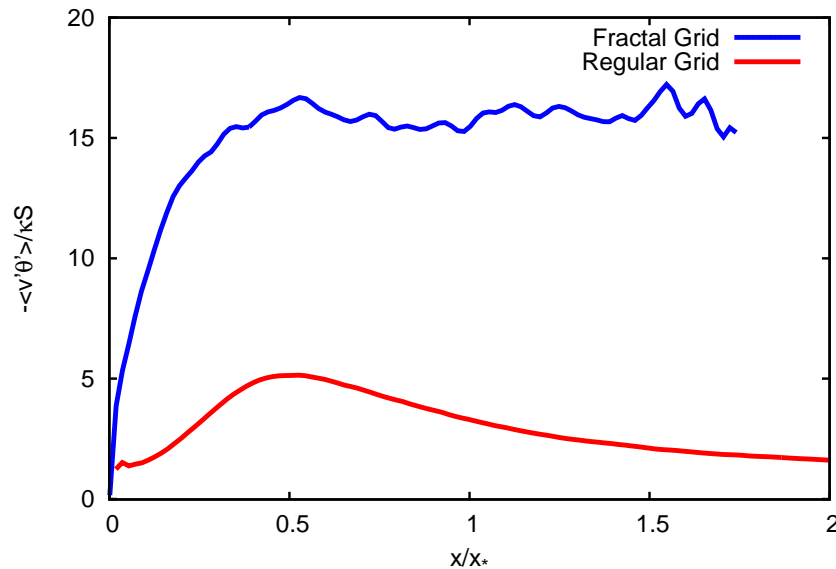
Regular grid:  $\frac{1}{2}M^2/b$

Fractal grid:  $\frac{1}{2}L_3^2/t_3 \approx 6.25M_{eff} < \frac{1}{2}L_2^2/t_2 \approx 12.255M_{eff} < \frac{1}{2}L_1^2/t_1 \approx 24M_{eff} < \frac{1}{2}L_0^2/t_0 \approx 47M_{eff}$



# Space-scale unfolding (SSU)

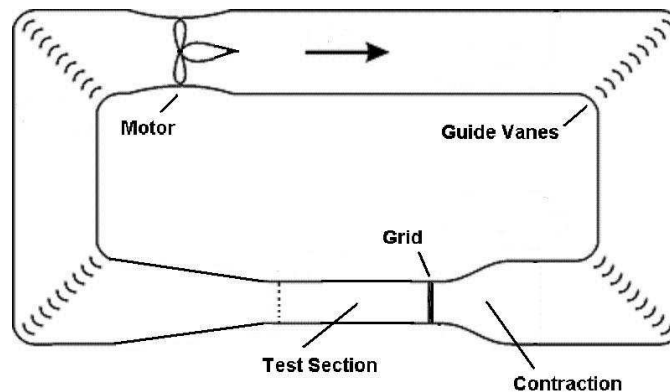
The fractal grid's SSU mechanism can cause a 50% drop in pressure drop and enhancements of scalar transfer and turbulent diffusion of at least one order of magnitude.



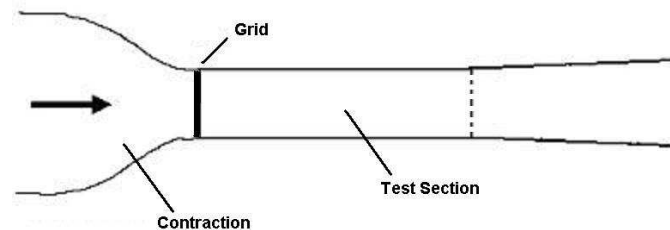
$$x_* = L_0^2/t_0 \text{ or } M^2/b$$

# Wind tunnels

$0.91^2 m^2$  width; test section  $4.8m$ ; max speed  $45m/s$ ;  
background turbulence  $\approx 0.25\%$ .



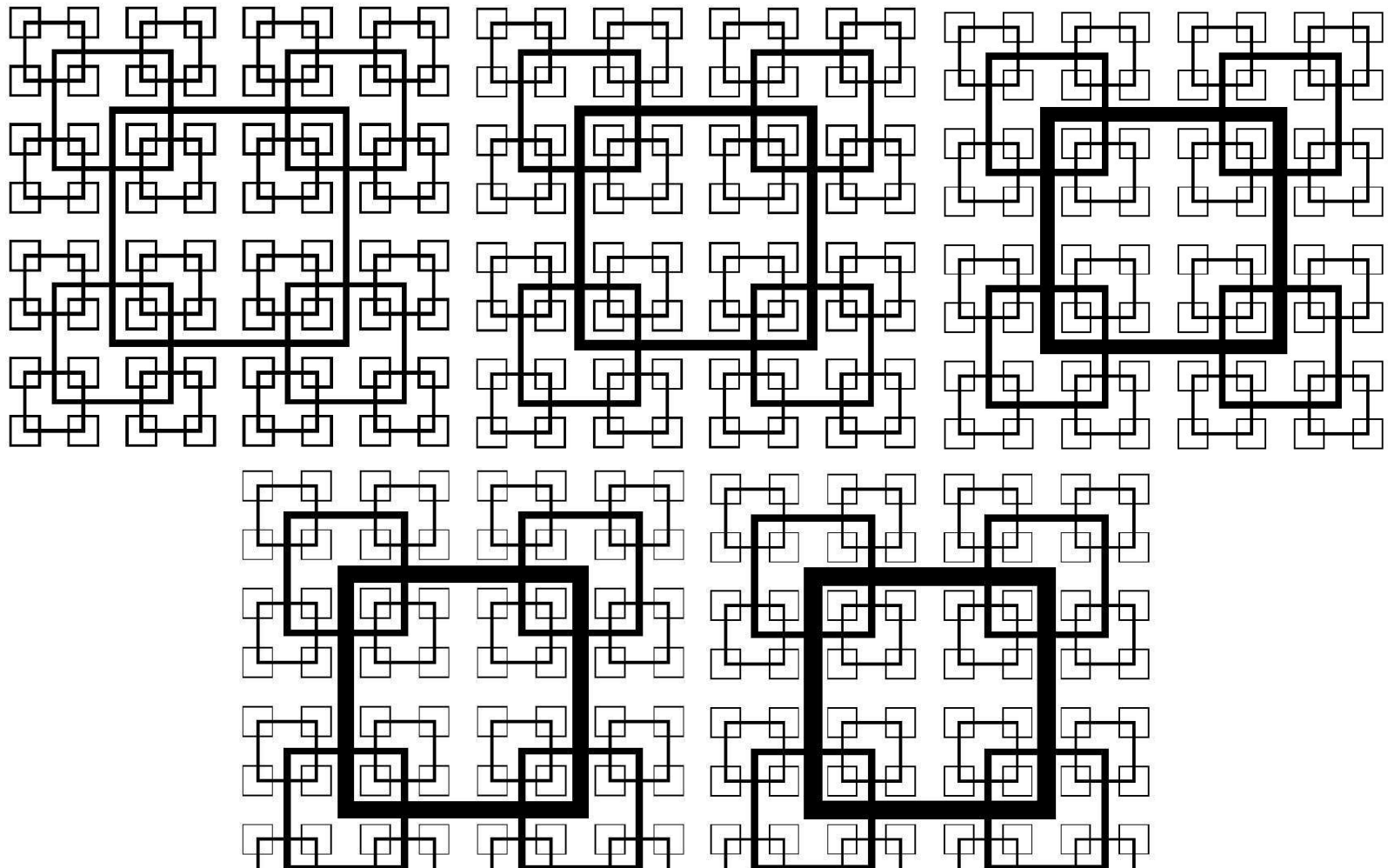
$0.46^2 m^2$  width; test section  $\approx 4.0m$ ; max speed  $33m/s$ ;  
background turbulence  $\approx 0.4\%$ .



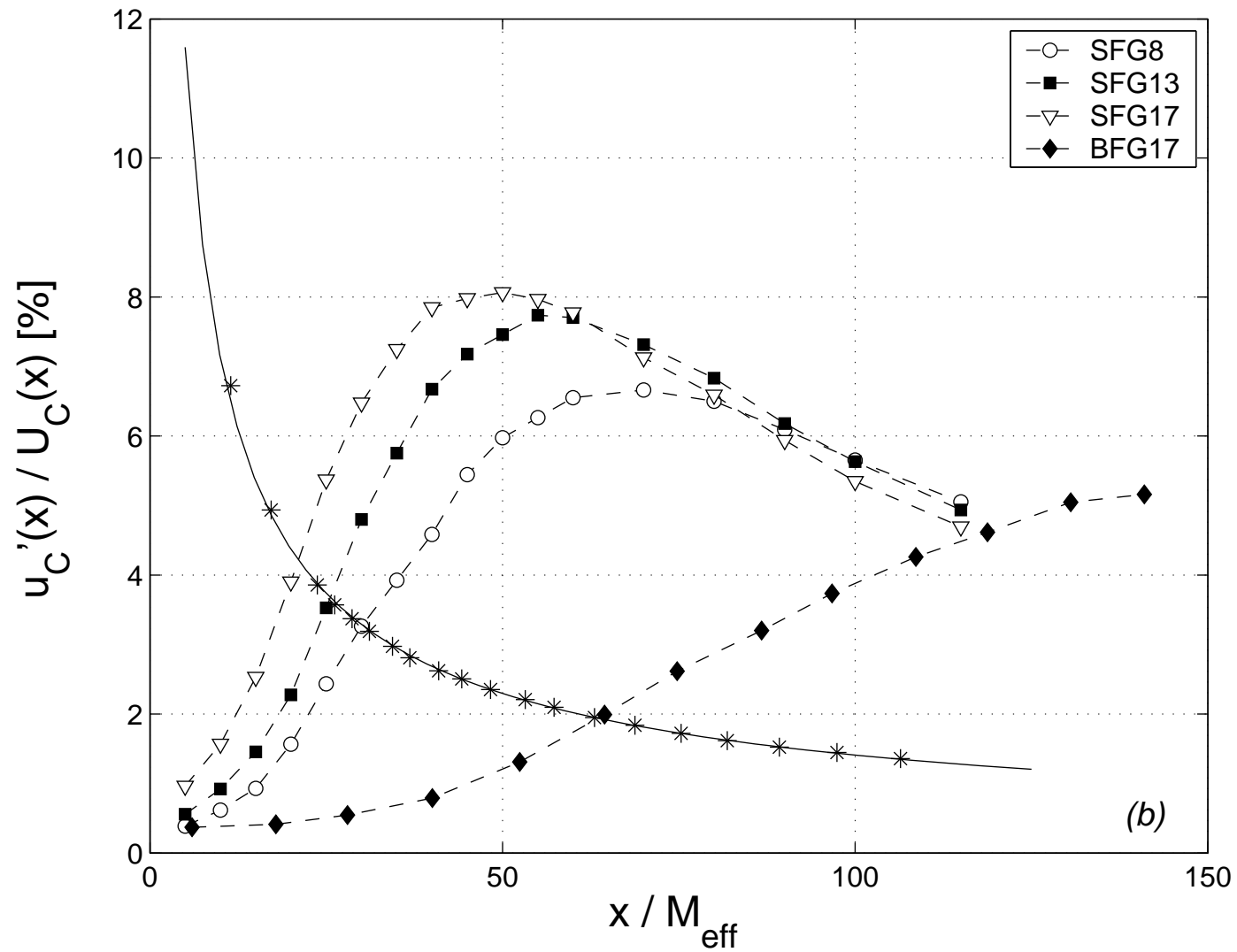
# $D_f = 2, \sigma = 25\%$ fractal square grids

and equal  $M_{eff} \approx 2.6cm$ ,  $L_{max} \approx 24cm$ ,  $L_{min} \approx 3cm$ ,  $N = 4$ ,  
 $T = 0.46m$ .

**BUT**  $t_r = 2.5, 5.0, 8.5, 13.0, 17.0$

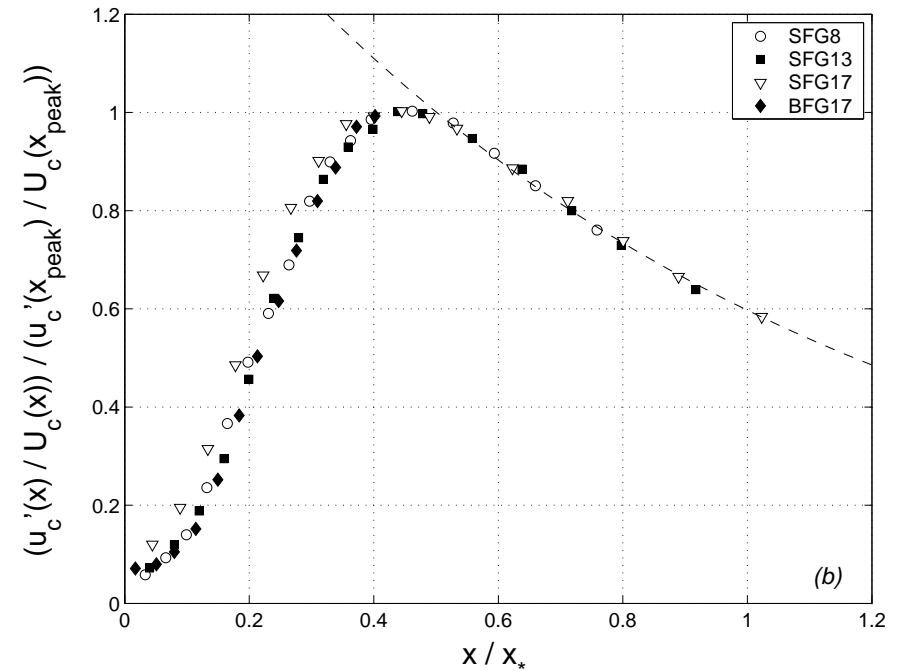
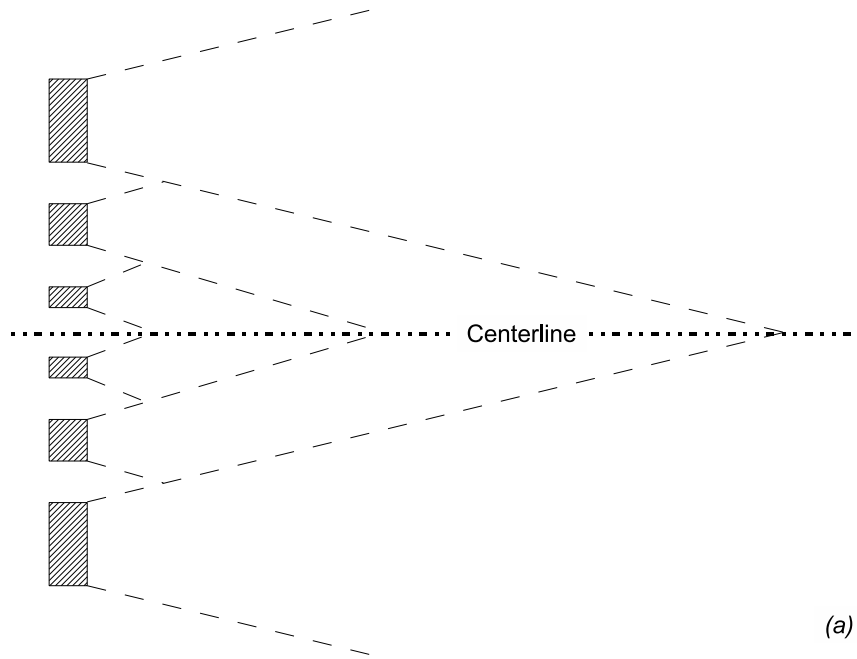


# Streamwise turbulence intensity





# Wake-interaction length-scale

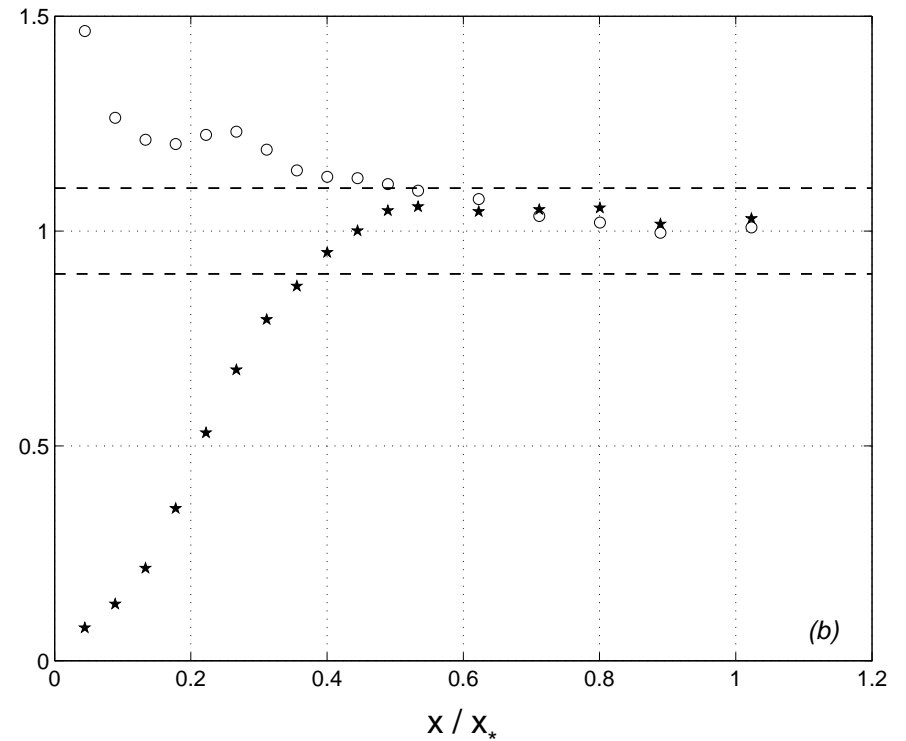
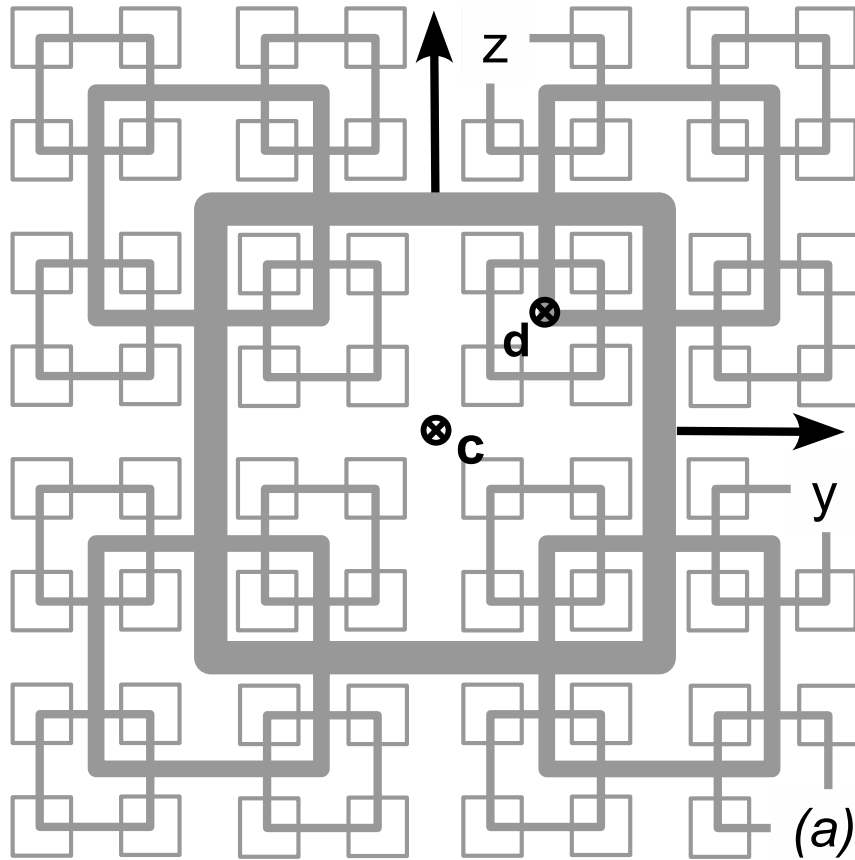


$(u'/U)/(u'/U)_{peak}$  versus  $x/x_*$  where  $L_0 = \sqrt{t_0 x_*}$

$$x_{peak} \approx 0.5x_*$$

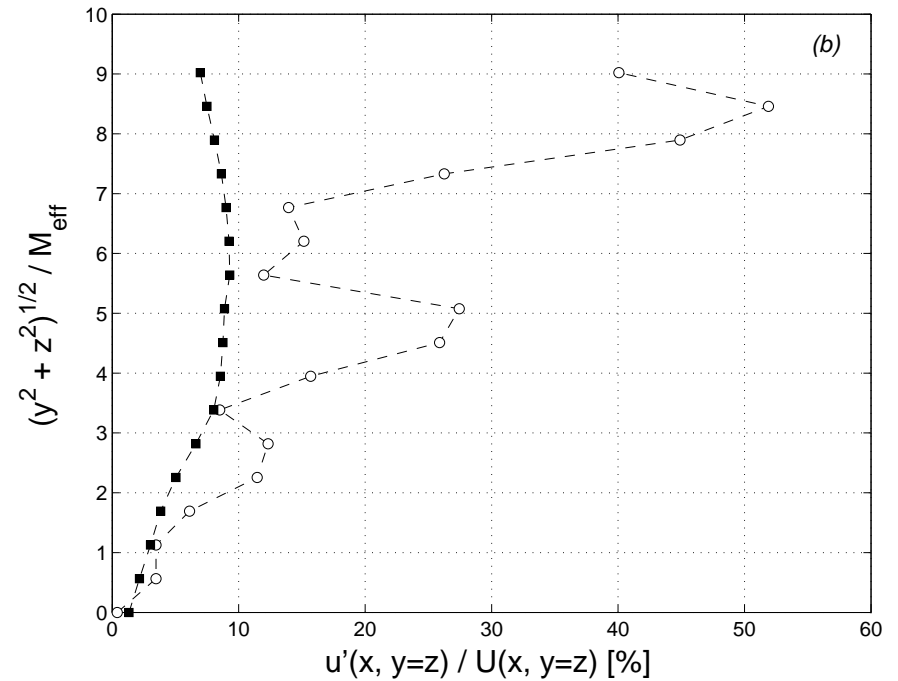
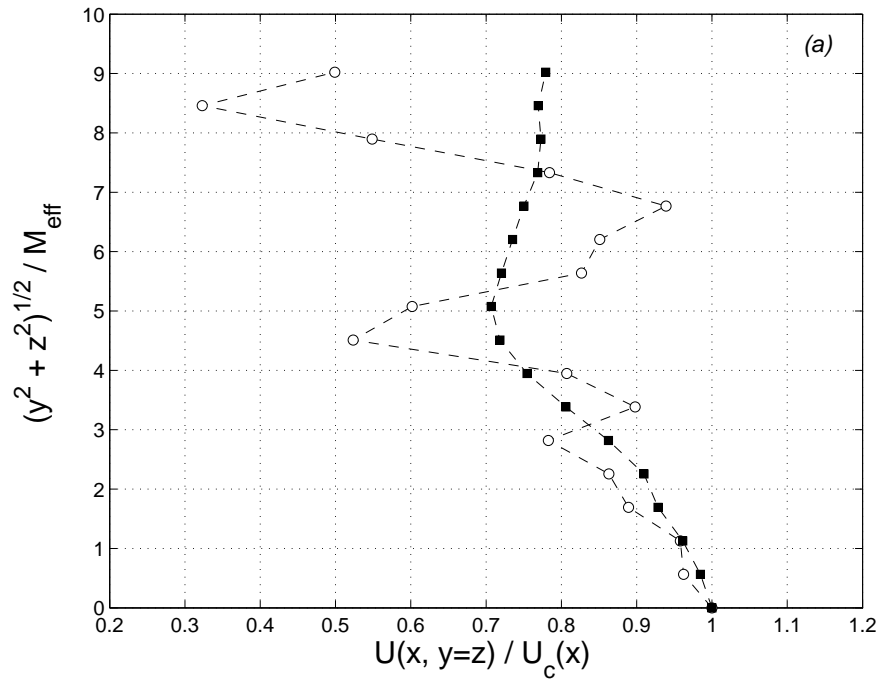
$u'/U \sim \exp(-Bx/x_*)$  where  $x_{peak} < x < x_*$ , with  $B \approx 2.06$  is good approximation

# Homogeneity where $x > x_{peak}$



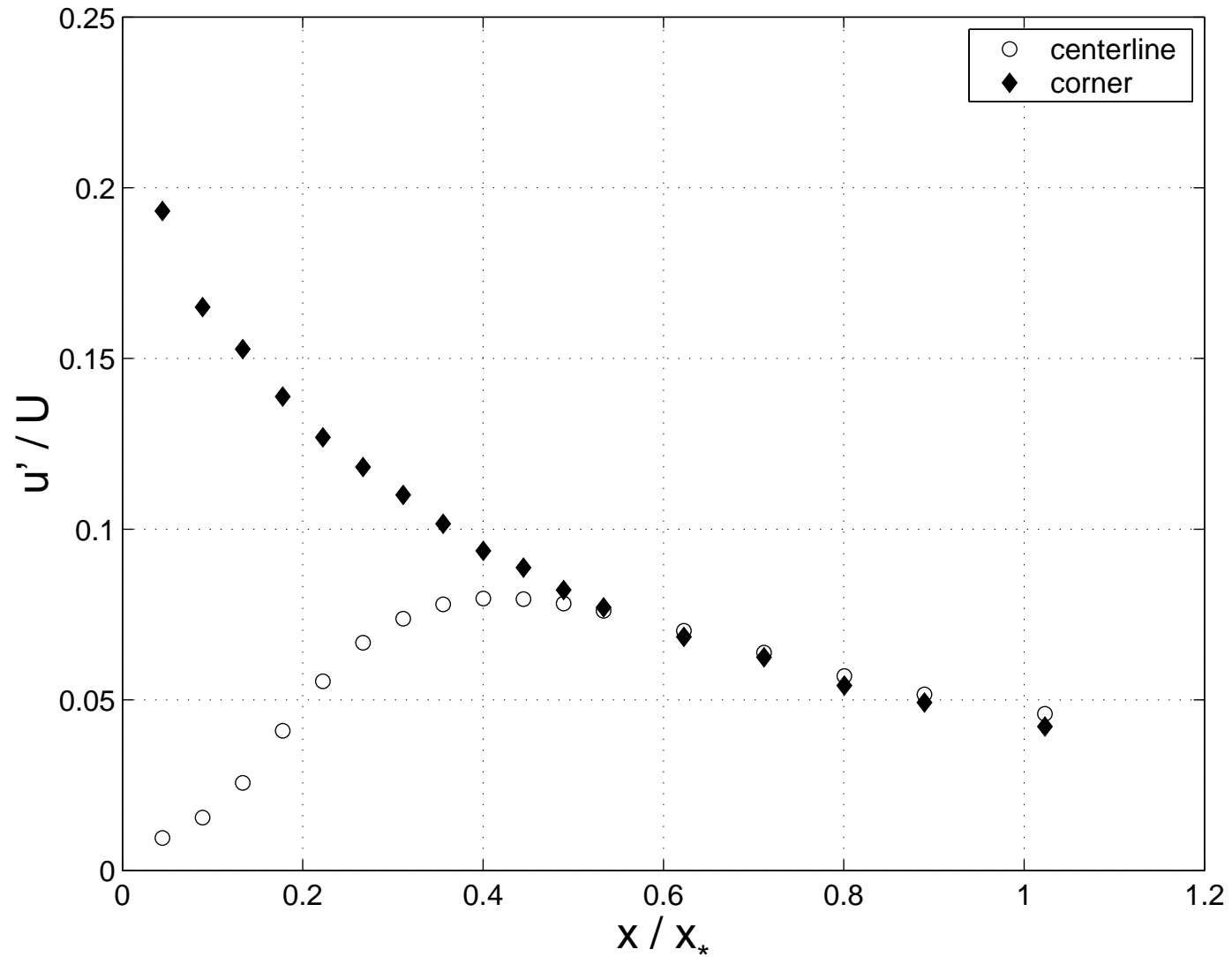
$U_c/U_d$  and  $u'_c/u'_d$  versus  $x/x_*$

# From inhomogeneity to homogeneity

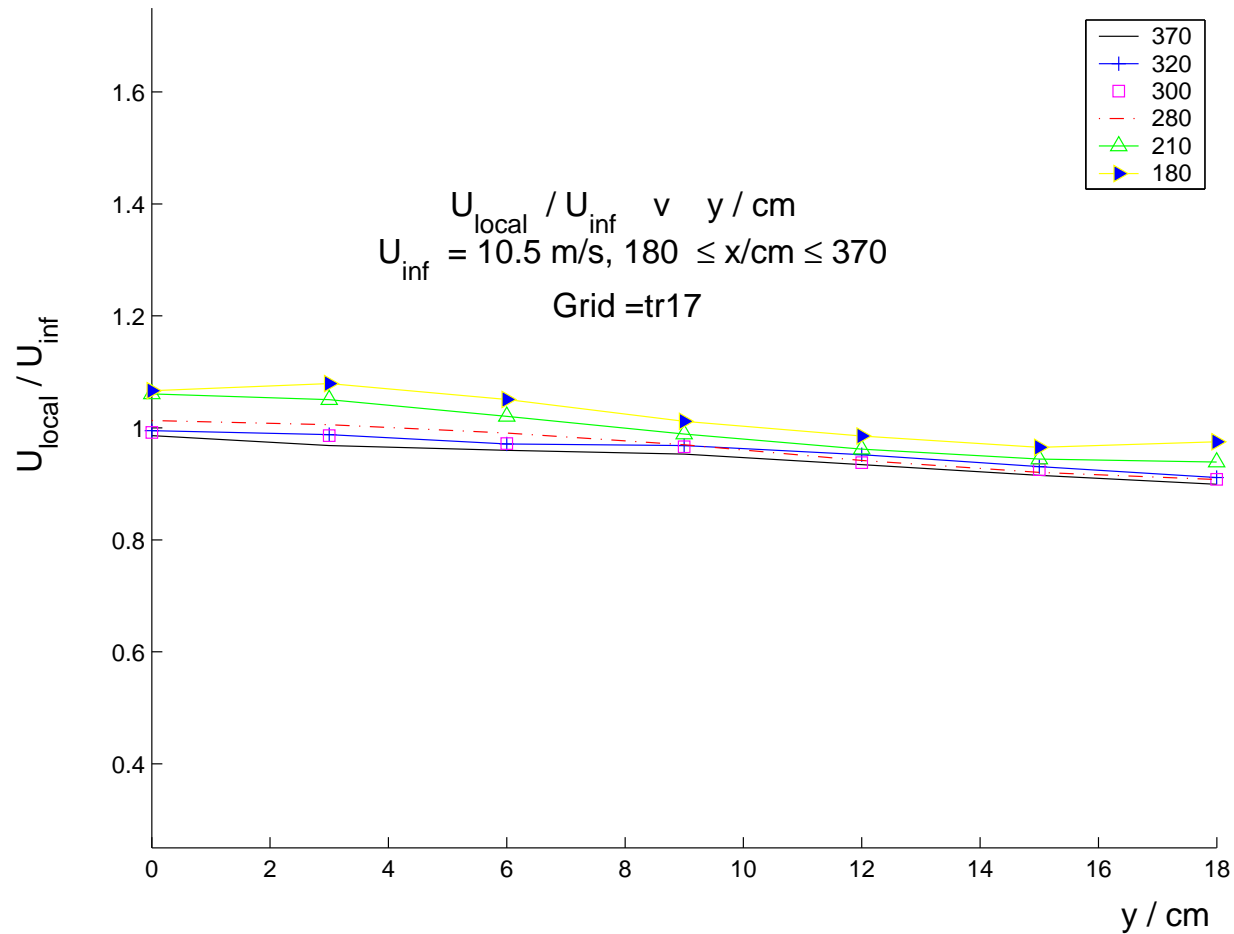


Mean flow and turbulence intensity profiles  
at  $x \approx 0.02x_*$  ( $x \approx 7M_{eff}$ ) and  $x \approx 0.15x_*$  ( $x \approx 53M_{eff}$ ).

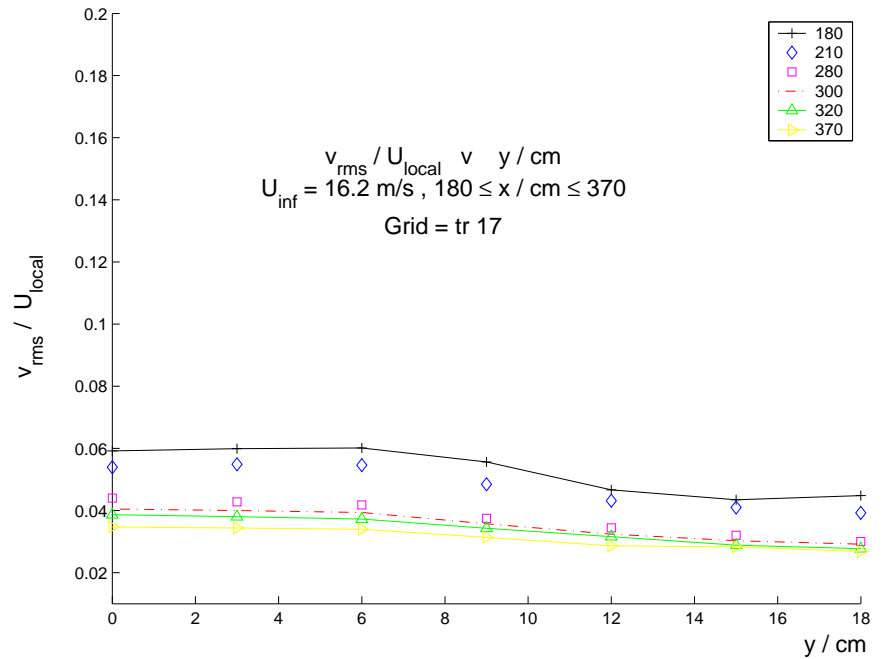
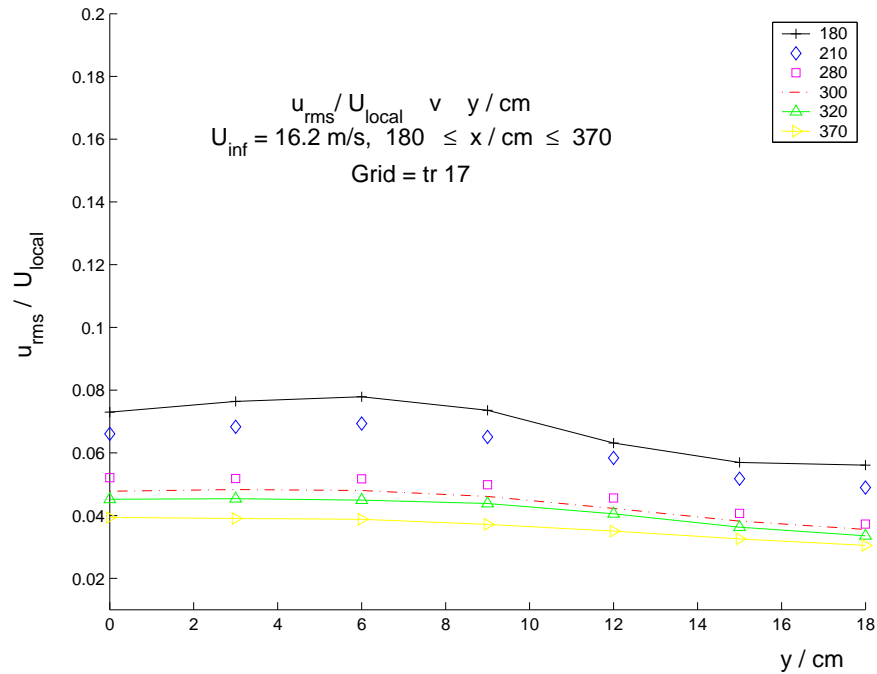
# From inhomogeneity to homogeneity



# Statistical homogeneity at $x > x_{peak}$

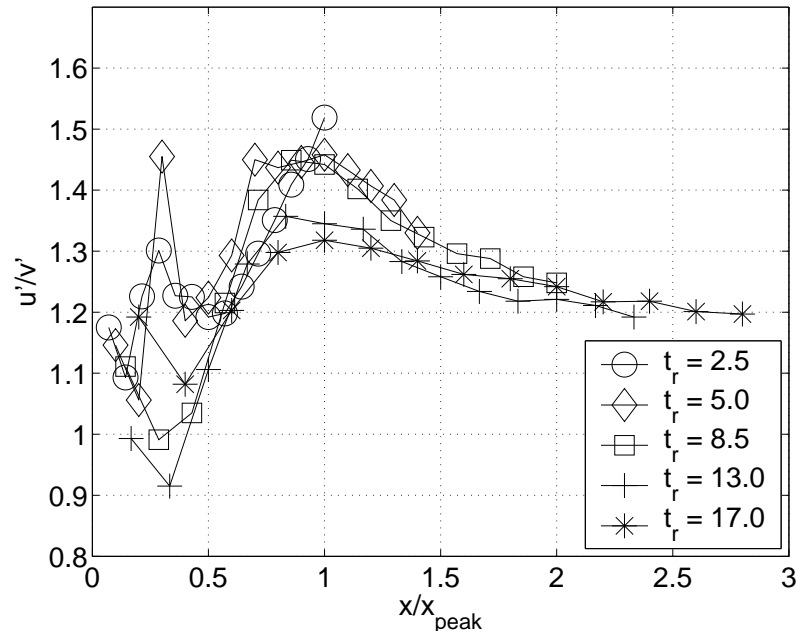
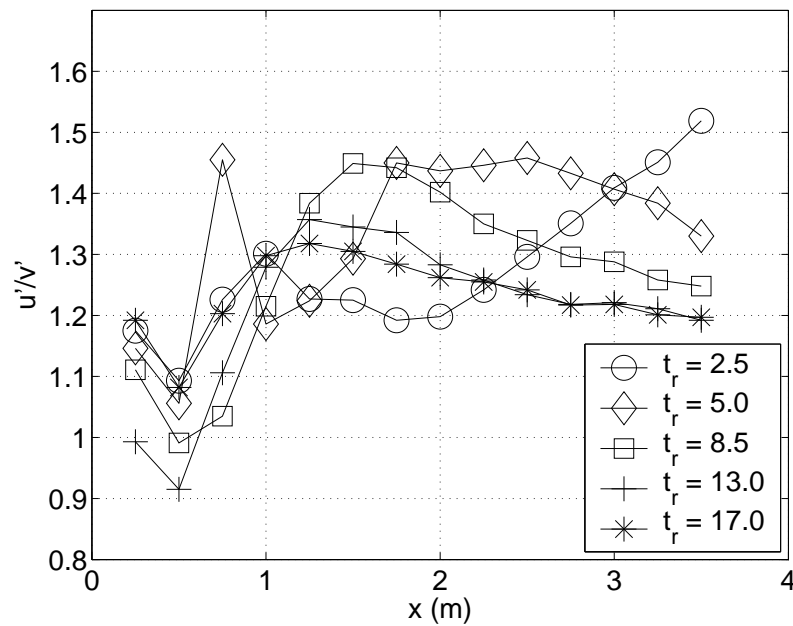


# Statistical homogeneity at $x > x_{peak}$



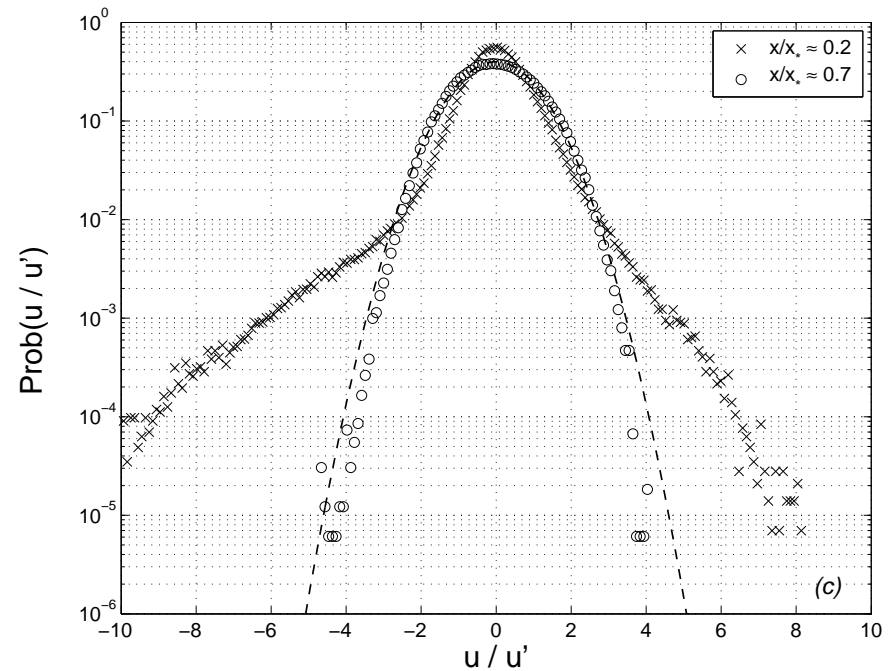
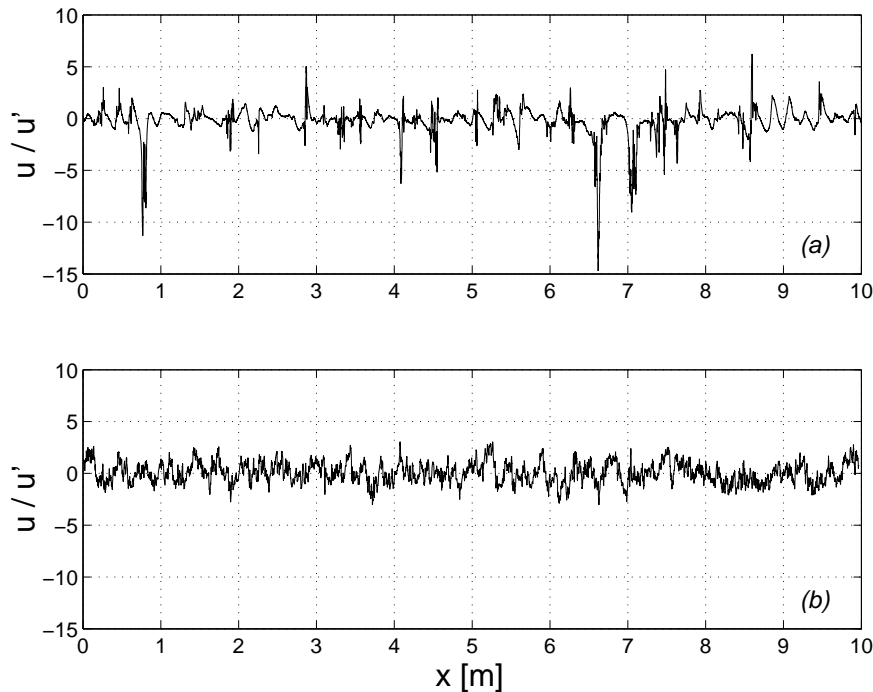
# From non-isotropy to near-isotropy

$x_{peak}$  helps collapse  $u'/v'$  as fct of  $x$



$T = 0.46m$  tunnel with  $U_{\infty} = 10m/s$ .

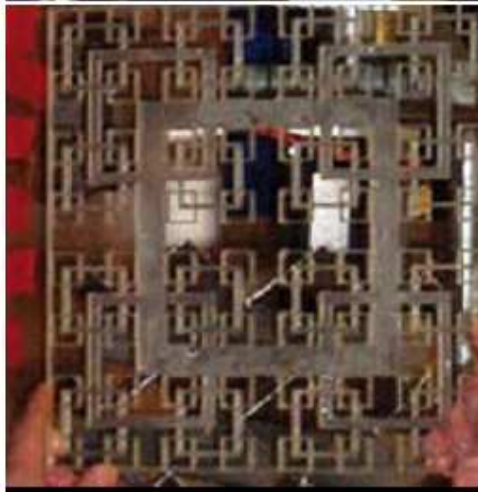
# From non-gaussianity to gaussianity



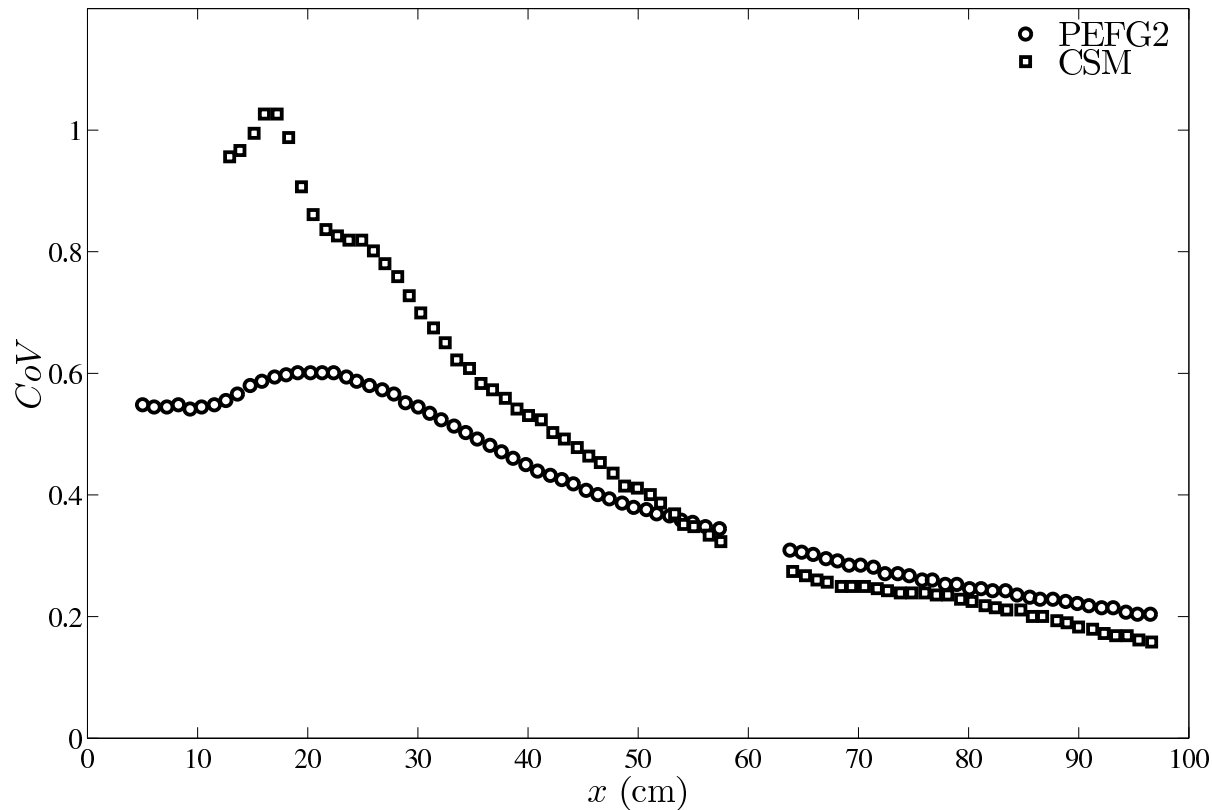
Note that  $S_u$  and  $F_u$  are close to 0 and 3 respectively at  $x > x_{peak}$ .



# Applications: mixing proof of concept



# Mixing proof of concept



Coffey, C.J., Hunt, G.R., Seoud, R.E. & V, Mixing effectiveness of fractal grids for inline static mixers. Proof of Concept Report. Imperial College London, 16 August 2007. Download from <http://www3.imperial.ac.uk/tmfc/papers/poc>

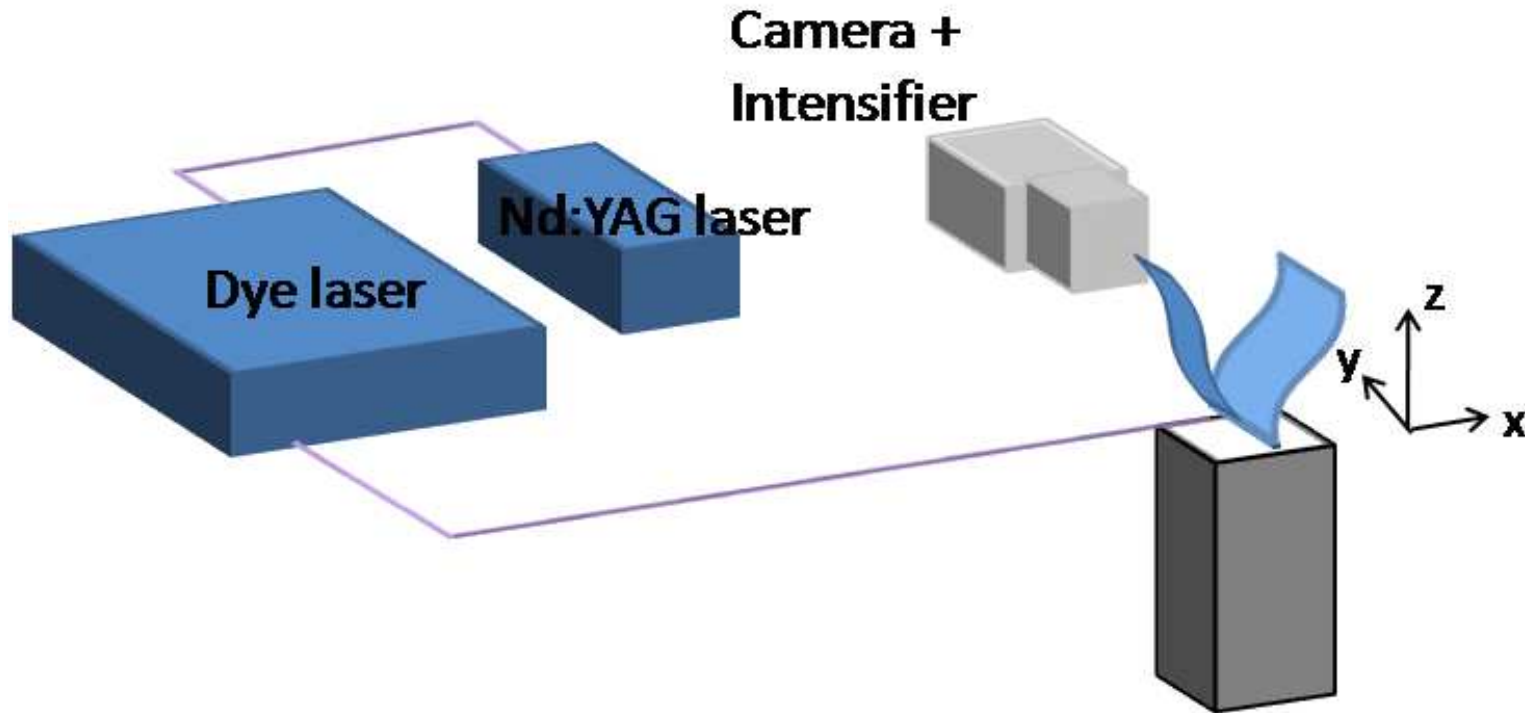
# Mixing proof of concept

Coffey, C.J., Hunt, G.R., Seoud, R.E. & Vassilicos, J.C.  
Mixing effectiveness of fractal grids for inline static mixers.  
Proof of Concept Report. ICL, 16/08/2007.

1. Importance of mode of scalar release vis-a-vis stirring element.
2. Confirmed that the CoV (Coeff of Variance of the scalar) decreases as  $t_r$  increases for fractal grids. Great sensitivity to small changes of grid geometry.
3. The combination fractal-grid with Sulzer static element returned the best mixing compared to fractal grids alone, Sulzer static alone and combinations fractal-fractal, Sulzer-Sulzer. (The CoV decreases very abruptly across the Sulzer element when a Pattern Enhanced fractal grid is placed upstream of the Sulzer and the source of dye is upstream of the fractal grid).

# Application: premixed combustion

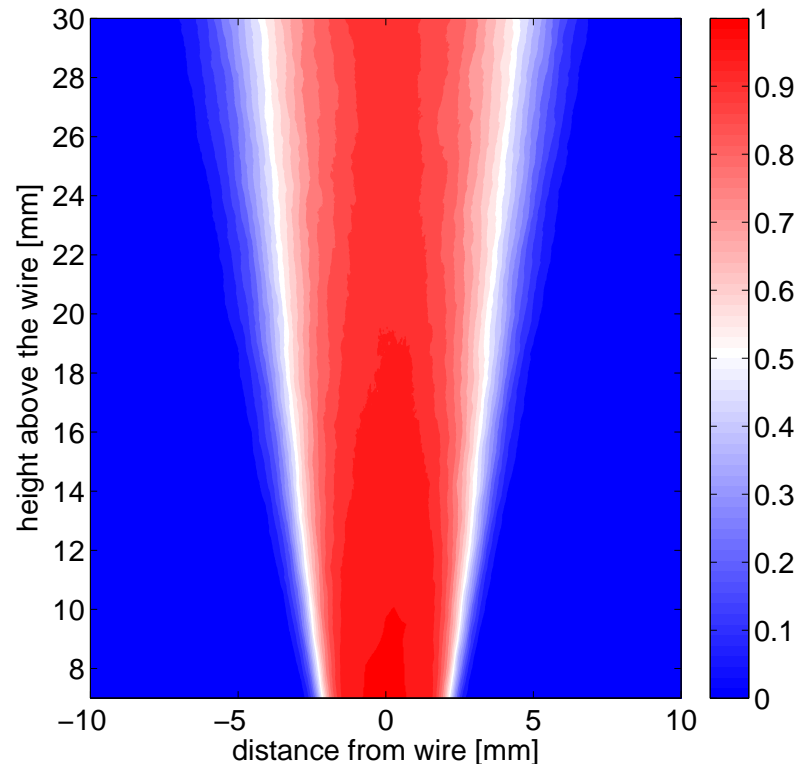
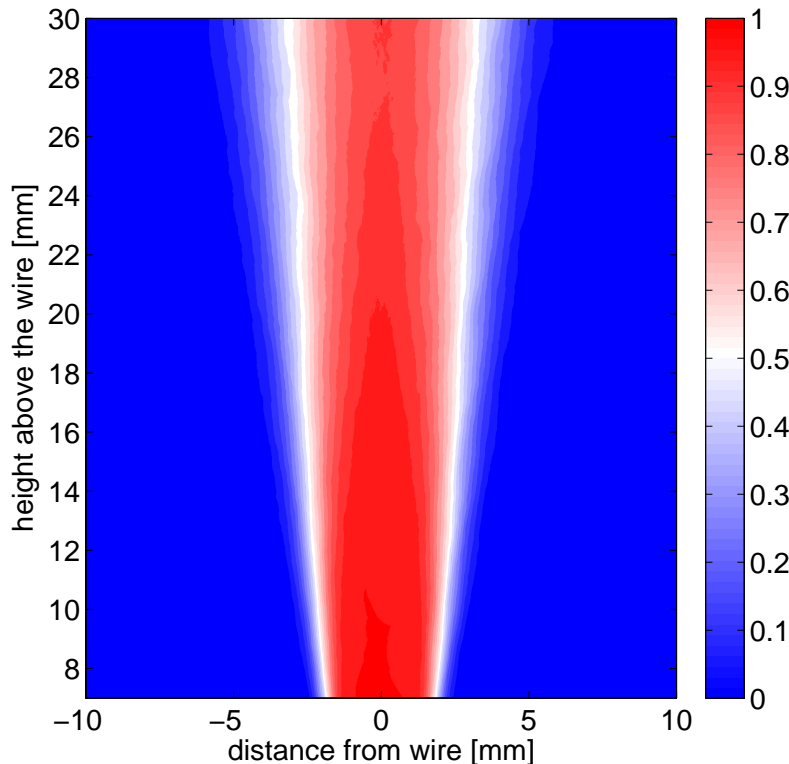
Experimental setup



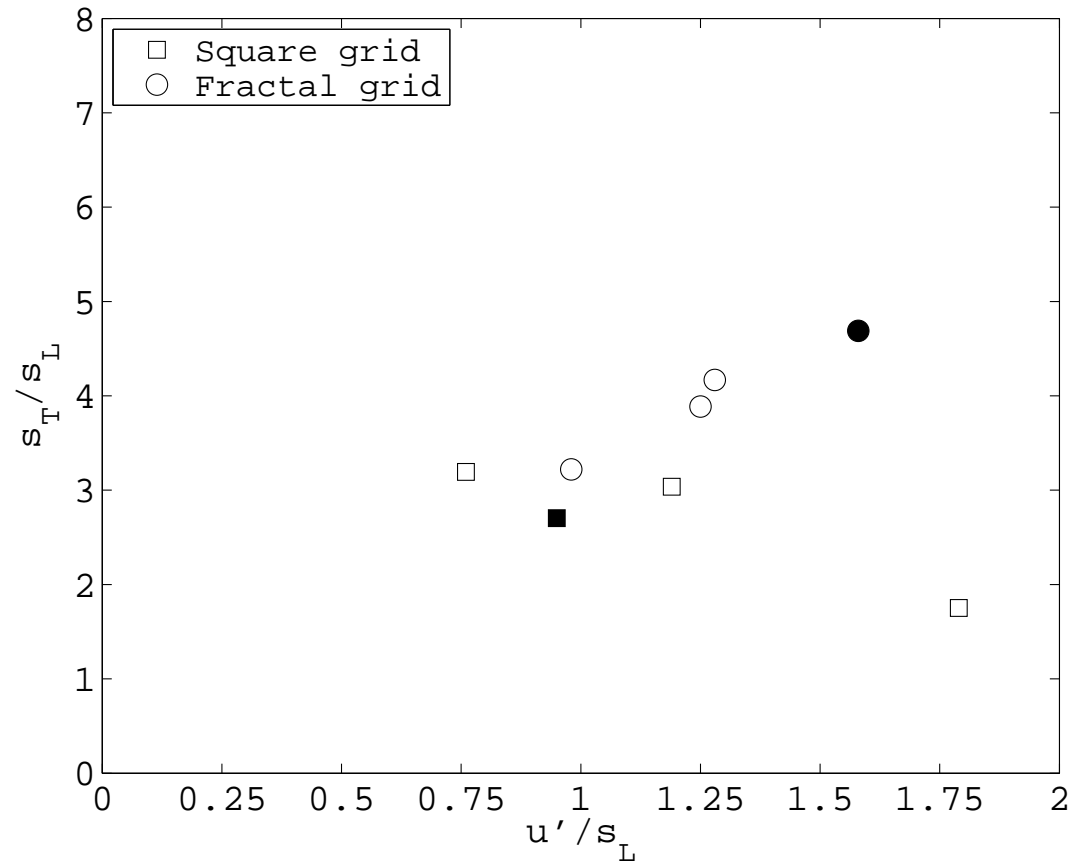
# Application: premixed combustion

Compare a regular grid (left) with a fractal square grid (right) of same blockage ratio and same  $M_{eff}$  placed upstream of the flame's anchoring wire.

Flame angle  $8^\circ$  (left),  $12^\circ$  (right), i.e. 50% increase in turbulent flame speed.



# Premixed combustion



Soulopoulos, N., Kerl, J., Sponfeldner, T., Beyrau, F., Hardalupas, Y., Taylor, A. & Vassilicos, J.C. Turbulent premixed flames on fractal-grid-generated turbulence. (2012, submitted).

# Collaboration with University of Poitiers

## Low Noise Fractal Spoilers



### The need

As a commercial aircraft comes into land, 26% of the total noise is due to the airframe. The spoilers that are deployed generate a low frequency noise that is less susceptible to atmospheric attenuation, hence are seen as a problem

### Aims

To reduce the noise generated by the outboard spoilers of an A320 aircraft, through means of large-scale fractal porosity, whilst maintaining lift and drag characteristics





# Collaboration with University of Poitiers

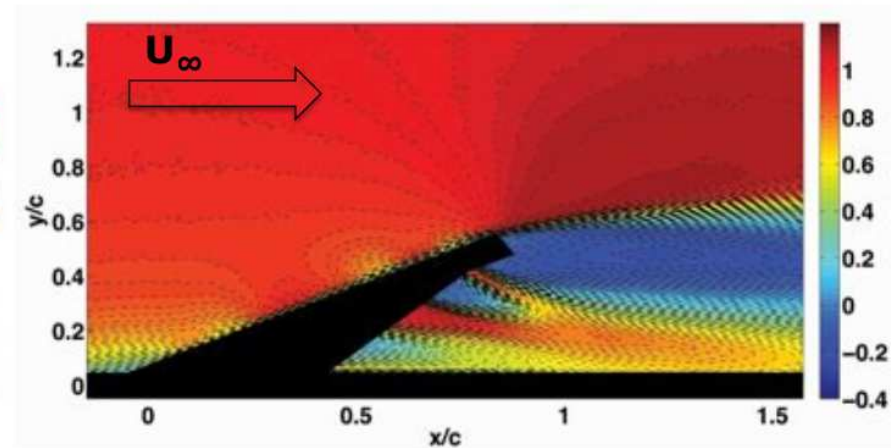
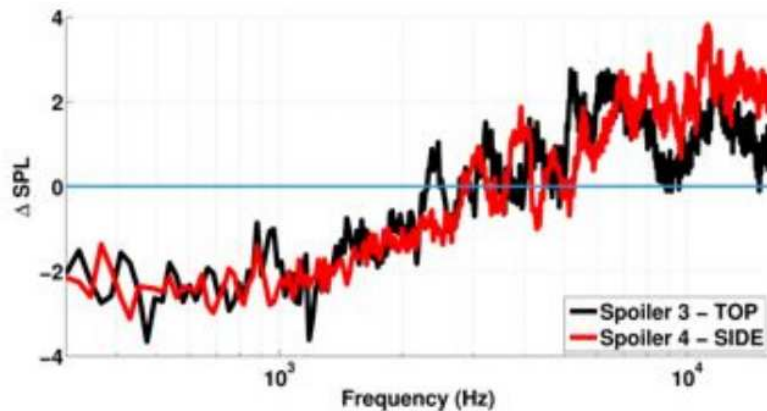
## Low Noise Fractal Spoilers



### Selected results

The fractal spoilers show a reduction of up to 2.5dB in the low frequency range.

This is achieved through an interaction with the re-circulating region behind the spoiler



On a wing section, the fractal spoilers also created a 0.03% increase in lift and a 4.70% decrease in drag compared to a current solid spoiler

**This makes it an ideal replacement for current aircraft spoilers**



# Collaboration with University of Poitiers

Nedic, J., Ganapathisubramani, B., Vassilicos, J.C., Boree, J., Brizzi, L.E., Spohn, A. Aeroacoustic performance of fractal spoilers. (AIAA Journal, 2012, to appear.)

And now back to fundamentals.

# Richardson-Kolmogorov cascade

in equilibrium turbulence.

Kolmogorov (1941):  $E(k) \approx C_K \epsilon^{2/3} k^{-5/3}$   
for  $1/L \ll k \ll 1/\eta$

assuming  $\epsilon$ , the K.E. dissipation rate per unit mass, to be (G.I. Taylor 1935)

$$\epsilon = C_\epsilon u'^3 / L$$

with  $C_K$  and  $C_\epsilon$  indep of  $Re_\lambda$  for  $Re_\lambda \gg 100$

Note:  $L/\eta \sim Re^{3/4}$ , i.e.  $L/\lambda \sim Re_\lambda$   
Richardson-Kolmogorov cascade for  
equilibrium turbulence

# One-point turbulence models

e.g. K- $\epsilon$  model (for HIT)

$$dK/dt = -\epsilon \text{ and } d\epsilon/dt = -\frac{\epsilon}{T_d}$$

where  $T_d \sim L/\sqrt{K}$  as  $Re_\lambda \rightarrow \infty$

using the cascade relation

$$\epsilon = C_\epsilon u'^3 / L$$

$$dK/dt = -\epsilon$$

$$d\epsilon/dt = -C_{\epsilon 2} \frac{\epsilon^2}{K}$$

$$C_{\epsilon 2} \sim C_\epsilon^{-1}.$$

Note:  $C_\epsilon = \text{const}$  means that the local  $\epsilon$  equals the local  $K$  divided by the time scale  $L/\sqrt{K}$  of the local energy containing eddies.

# LES modelling

Eddy viscosities in LES from  
Richardson-Kolmogorov cascade

$$\nu_t = \frac{2}{3} C_K^{-3/2} \epsilon^{1/3} k_c^{-4/3}$$

where  $\epsilon = C_\epsilon u'^3 / L$  with  $C_\epsilon$  indep of  $Re_\lambda$

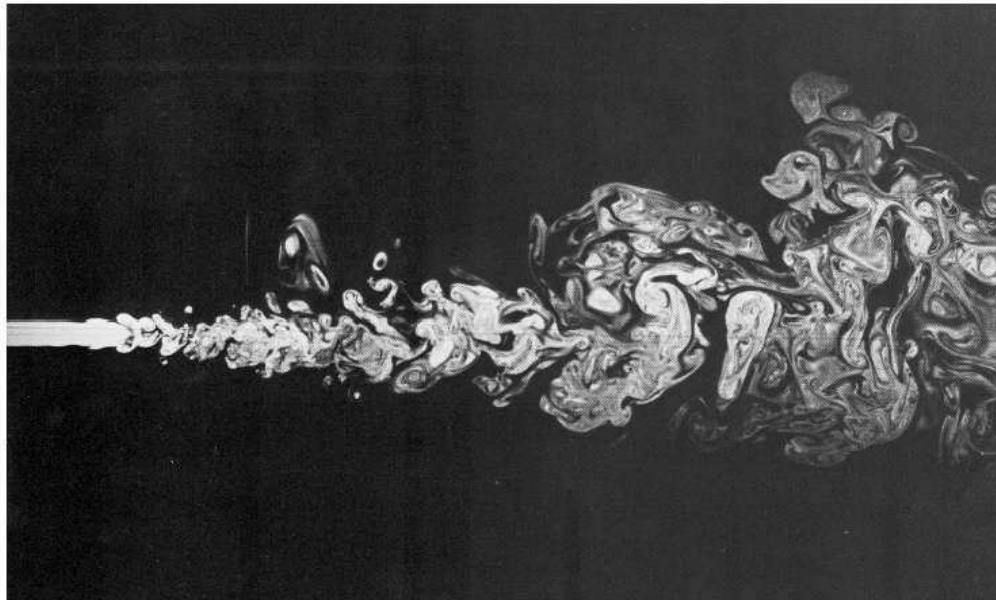
$$\nu_t = \frac{2}{3} C_K^{-3/2} C_\epsilon^{1/3} u' L (k_c L)^{-4/3}$$

with universal values of  $C_K$   
and  $C_\epsilon$ .

# Turbulent jets

(Picture from album of fluid motion)

Jets



# Turbulent wakes

(Picture downloaded from the web)

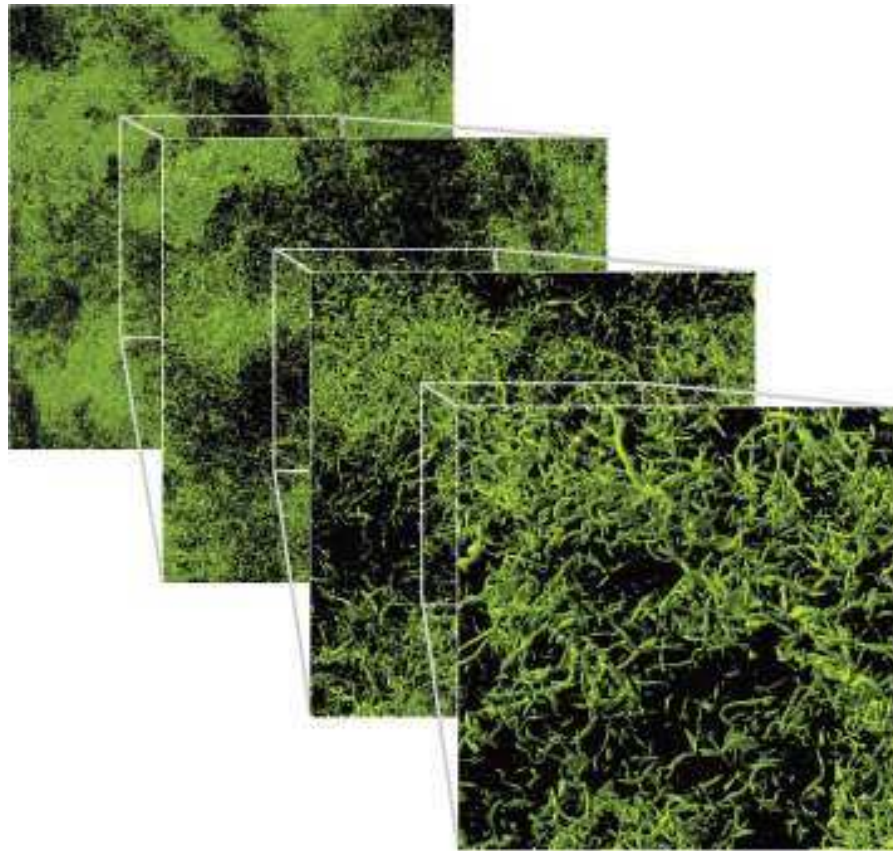


FIG. 1.



# Homogeneous turbulence

(from Ishihara et al, early/mid 2000s, Japan, Earth Simulator calculations)



# Some background

	<i>WT HT</i>	<i>Axisym Jet</i>	<i>Plane Jet</i>
$u'$	$U_\infty \left(\frac{x-x_0}{L_b}\right)^{-p}, 1/2 < p < 3/4$	$U_\infty \left(\frac{x-x_0}{L_b}\right)^{-1}$	$U_\infty \left(\frac{x-x_0}{L_b}\right)^{-1/2}$
$L_u$	$L_b \left(\frac{x-x_0}{L_b}\right)^q, 0 < q < 1/2$	$x - x_0$	$x - x_0$

	<i>Axisym Wake</i>	<i>Plane Wake</i>	<i>Mixing Layer</i>
$u'$	$U_\infty \left(\frac{x-x_0}{L_b}\right)^{-2/3}$	$U_\infty \left(\frac{x-x_0}{L_b}\right)^{-1/2}$	$U_\infty$
$L_u$	$L_b^{2/3} (x - x_0)^{1/3}$	$L_b^{1/2} (x - x_0)^{1/2}$	$(x - x_0)$

$L_b$ : characteristic cross-stream length-scale of inlet (e.g. mesh or nozzle or bluff body size...)

$U_\infty$ : characteristic inlet mean flow velocity or mean flow velocity cross-stream variation



# Some background

	<i>WT HT</i>	<i>Axisym Jet</i>	<i>Plane Jet</i>
$L_u/\lambda$	$Re_I^{1/2} \left(\frac{x-x_0}{L_b}\right)^{-p}$	$Re_I^{1/2} \left(\frac{x-x_0}{L_b}\right)^0$	$Re_I^{1/2} \left(\frac{x-x_0}{L_b}\right)^{1/4}$
$Re_\lambda$	$Re_I^{1/2} \left(\frac{x-x_0}{L_b}\right)^{-p}$	$Re_I^{1/2} \left(\frac{x-x_0}{L_b}\right)^0$	$Re_I^{1/2} \left(\frac{x-x_0}{L_b}\right)^{1/4}$

	<i>Axisym Wake</i>	<i>Plane Wake</i>	<i>Mixing Layer</i>
$L_u/\lambda$	$Re_I^{1/2} \left(\frac{x-x_0}{L_b}\right)^{-1/6}$	$Re_I^{1/2} \left(\frac{x-x_0}{L_b}\right)^0$	$Re_I^{1/2} \left(\frac{x-x_0}{L_b}\right)^{1/2}$
$Re_\lambda$	$Re_I^{1/2} \left(\frac{x-x_0}{L_b}\right)^{-1/6}$	$Re_I^{1/2} \left(\frac{x-x_0}{L_b}\right)^0$	$Re_I^{1/2} \left(\frac{x-x_0}{L_b}\right)^{1/2}$

if  $\lambda$  obtained from  $\epsilon \sim u'^3 / L_u \sim \nu u'^2 / \lambda^2$

then  $L_u/\lambda \sim Re_I^{1/2} f\left(\frac{x-x_0}{L_b}\right) \sim Re_\lambda$  in all cases

$Re_I \equiv \frac{U_\infty L_b}{\nu}$ : inlet Reynolds number

$$L/\lambda \sim C_\epsilon Re_\lambda$$

$$\epsilon \sim \nu u'^2 / \lambda^2 \text{ (Taylor 1935)}$$

$$\epsilon = C_\epsilon u'^3 / L \text{ (definition of } C_\epsilon \text{ introduced by Taylor 1935)}$$

These two relations imply  $L/\lambda \sim C_\epsilon Re_\lambda$ .

$$C_\epsilon = Const \text{ IFF } L/\lambda \sim Re_\lambda$$

in which case,

$$\text{if } Re_\lambda \sim Re_I^{1/2} f\left(\frac{x-x_0}{L_b}\right)$$

$$\text{then } L/\lambda \sim Re_I^{1/2} f\left(\frac{x-x_0}{L_b}\right).$$

$$C_\epsilon = \epsilon L / u'^3 \text{ indep of } u', L \text{ and } \nu$$

at high enough Reynolds numbers means that  $C_\epsilon$  is indep of  $Re_\lambda$  if  $Re_\lambda$  is varied by varying  $Re_I$  or if  $Re_\lambda$  is varied by varying streamwise position  $x$ .

This implies that  $L/\lambda$  and  $Re_\lambda$  have the same dependencies on  $Re_I$  and  $(x - x_0)/L_b$  even though the dependence on  $(x - x_0)/L_b$  varies from flow to flow:

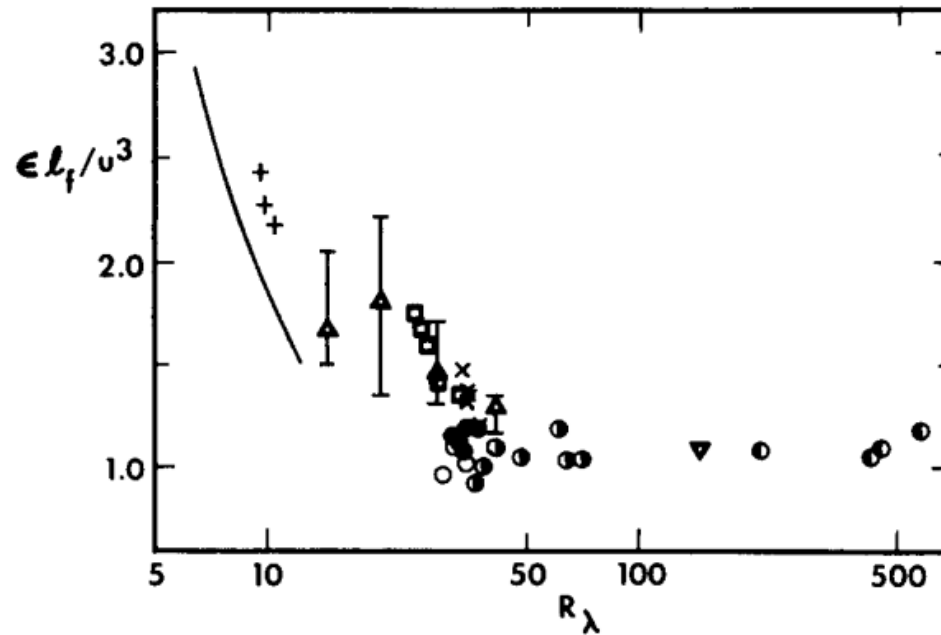
$$L_u/\lambda \sim Re_I^{1/2} \left( \frac{x-x_0}{L_b} \right)^m$$

$$Re_\lambda \sim Re_I^{1/2} \left( \frac{x-x_0}{L_b} \right)^m$$

where  $m = 0$  for axisym jet,  $m = 1/4$  for plane jet,  $m = -1/6$  for axisym wake,  $m = 0$  for plane wake,  $m = 1/2$  for mixing layer, etc...

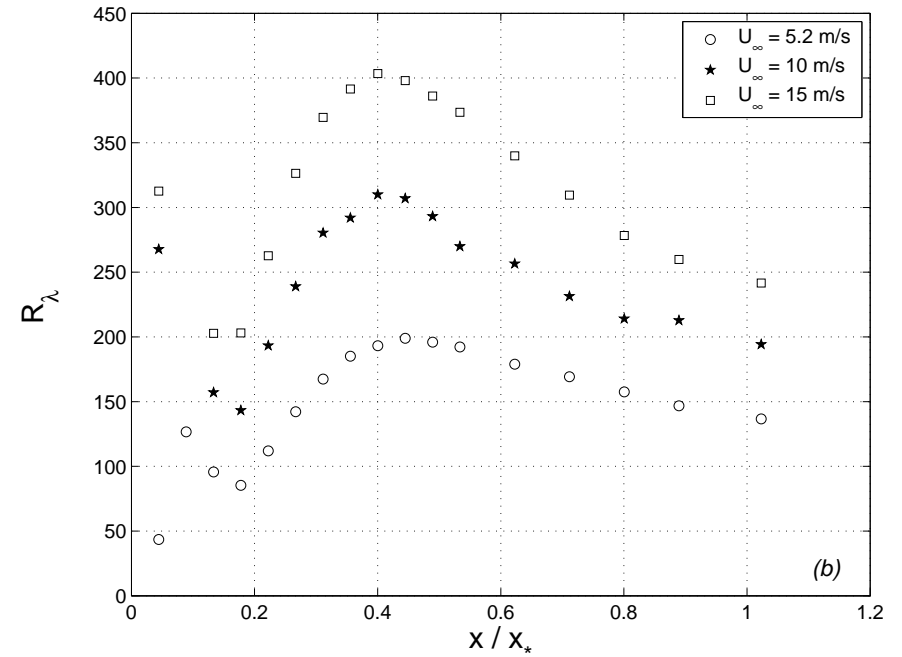
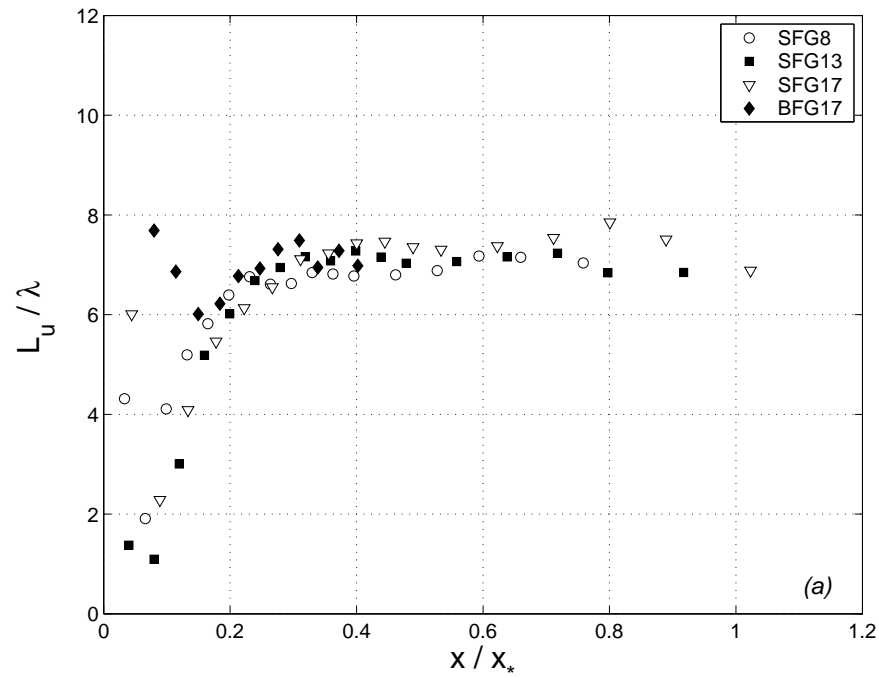
$L/\lambda \sim Re_\lambda$  is basic Richardson-Kolmogorov phenomenology for equilibrium turbulence

$$C_\epsilon = \epsilon L / u'^3 \text{ indep of } u', L \text{ and } \nu$$

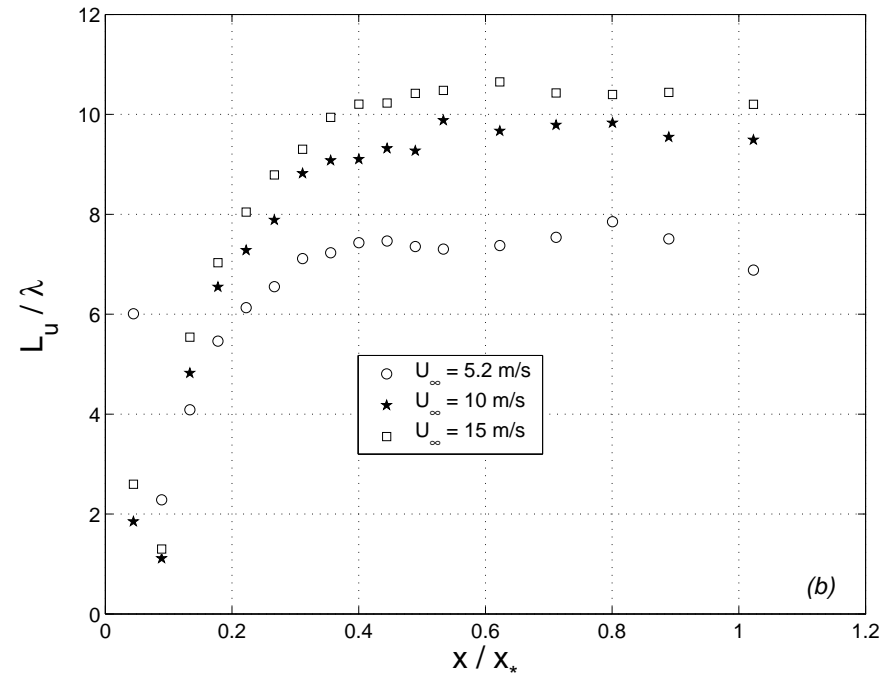
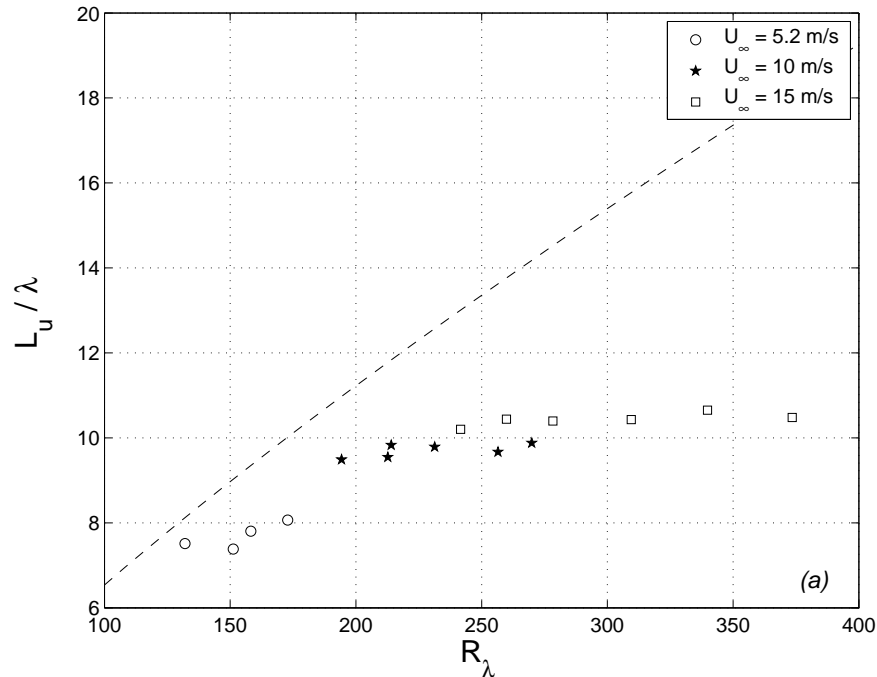


Plot from Sreenivasan (1984): 4 highest  $Re_\lambda$  points are obtained by Kistler & Vebralovich (1966) at same point  $x$  by varying  $Re_I$ . 4 points at and below  $Re_\lambda = 50$  and 3 points between  $Re_\lambda = 50$  and 100 are obtained by Comte-Bellot & Corrsin (1971) at constant  $Re_I$  but moving along  $x$ .

# $L_u/\lambda$ and $Re_\lambda$ in FSG turbulence

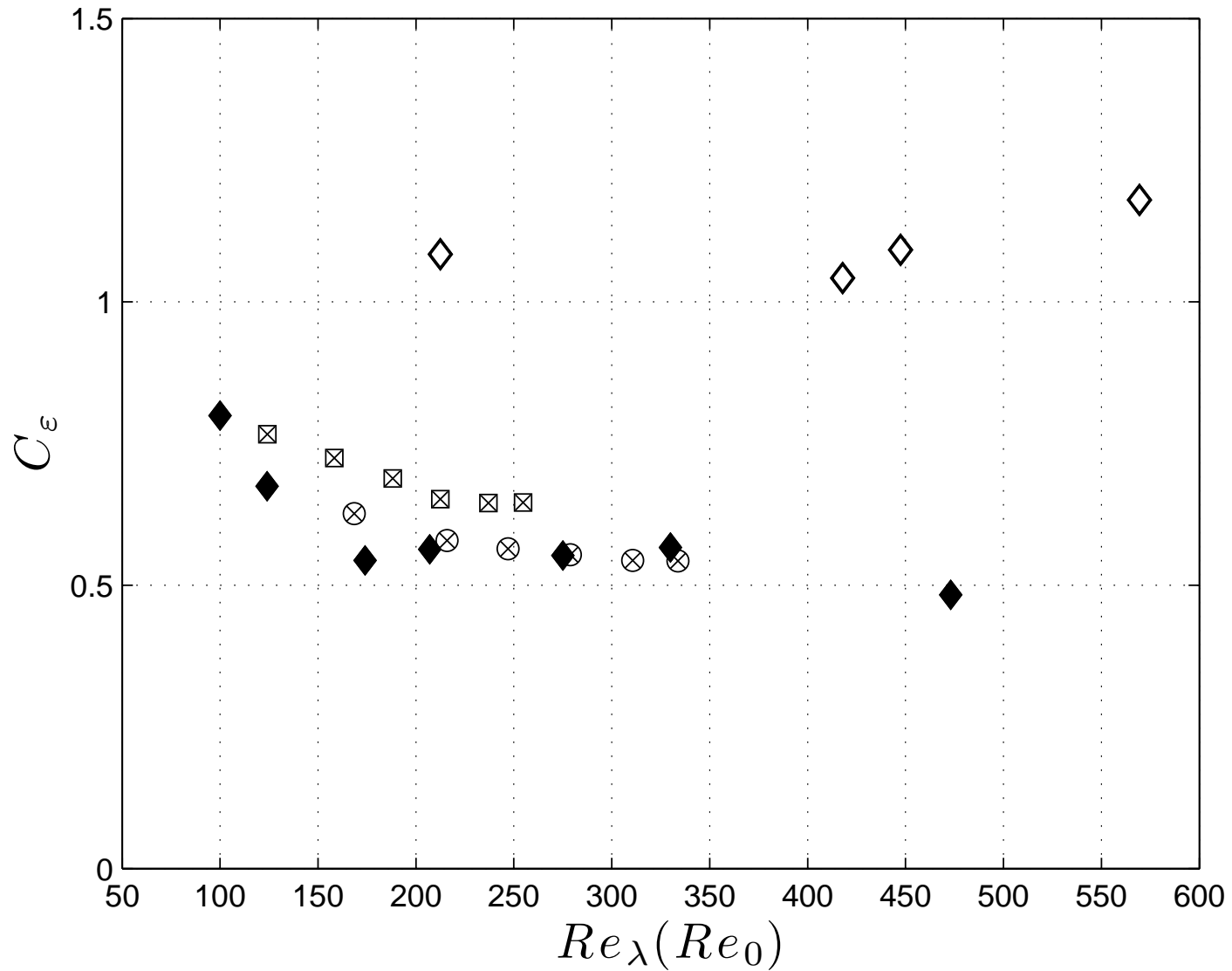


# $L_u/\lambda$ versus $Re_\lambda$ and $Re_I$

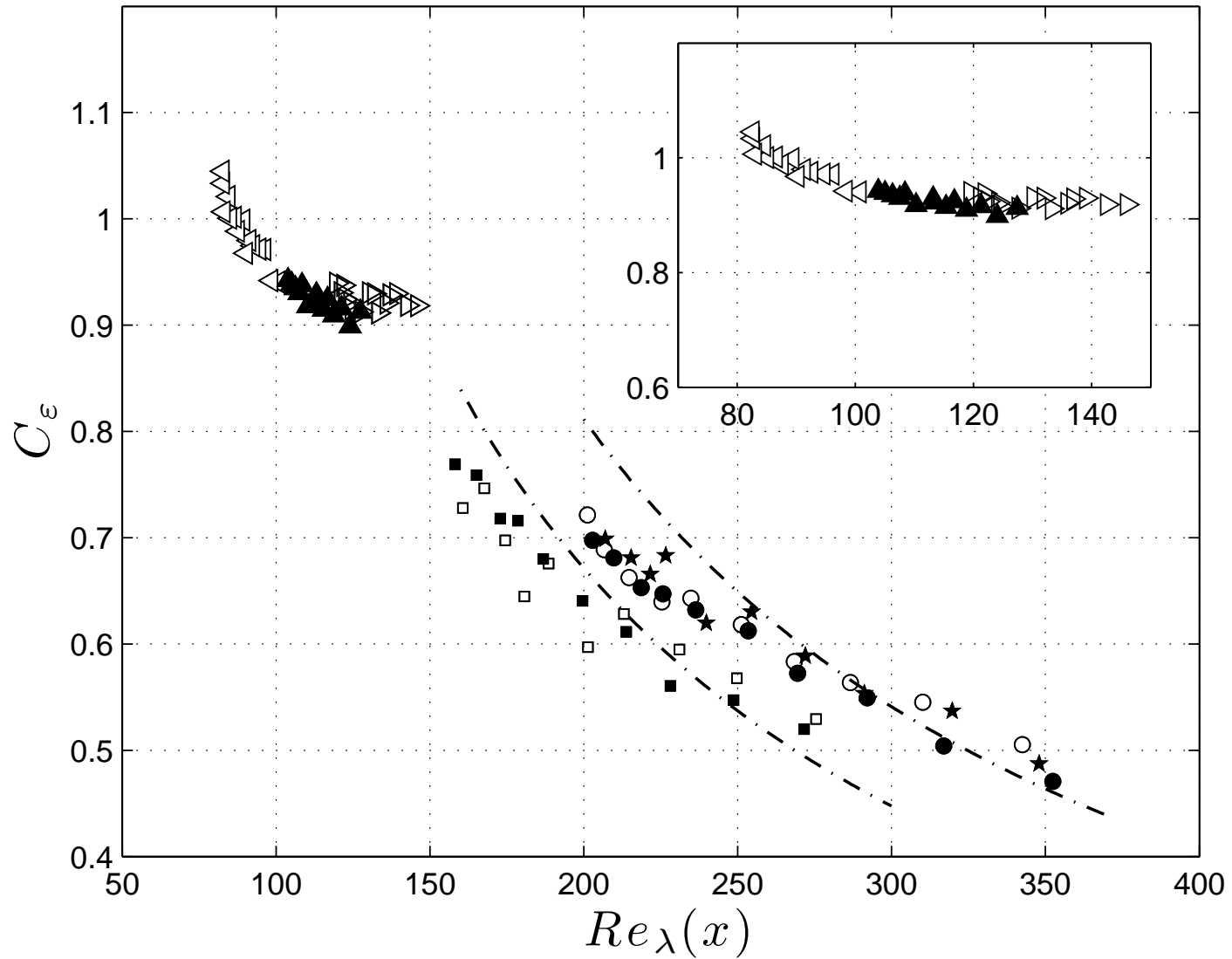


$L_u/\lambda$  indep of  $Re_\lambda$  but  $L_u/\lambda$  is increasing fct of  $Re_I$ , e.g.  
 $L_u/\lambda \propto Re_I^\gamma$ ,  $\gamma > 0$ , (e.g.  $\gamma = 1/2$ ?)  $L_u/\lambda \sim C_\epsilon Re_\lambda \propto Re_I^\gamma$   
 indep of  $x$  means  $C_\epsilon \sim \frac{Re_I^\gamma}{Re_\lambda}$ .

# $C_\epsilon$ versus $Re_\lambda(Re_0)$



# $C_\epsilon$ versus $Re_\lambda(x)$





# Qualitative extrapolating summary

$$C_\epsilon \sim Re_I / Re_L = U_\infty L_b / (u' L)$$

(This functional dependence is not exact, just indicative)

$$\text{i.e. } \epsilon \sim u'^2 / T$$

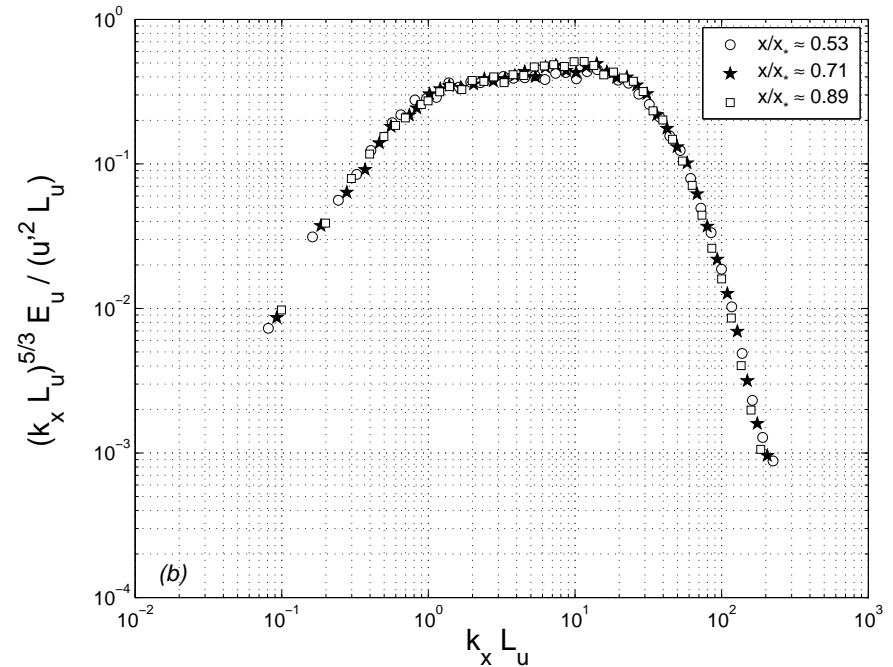
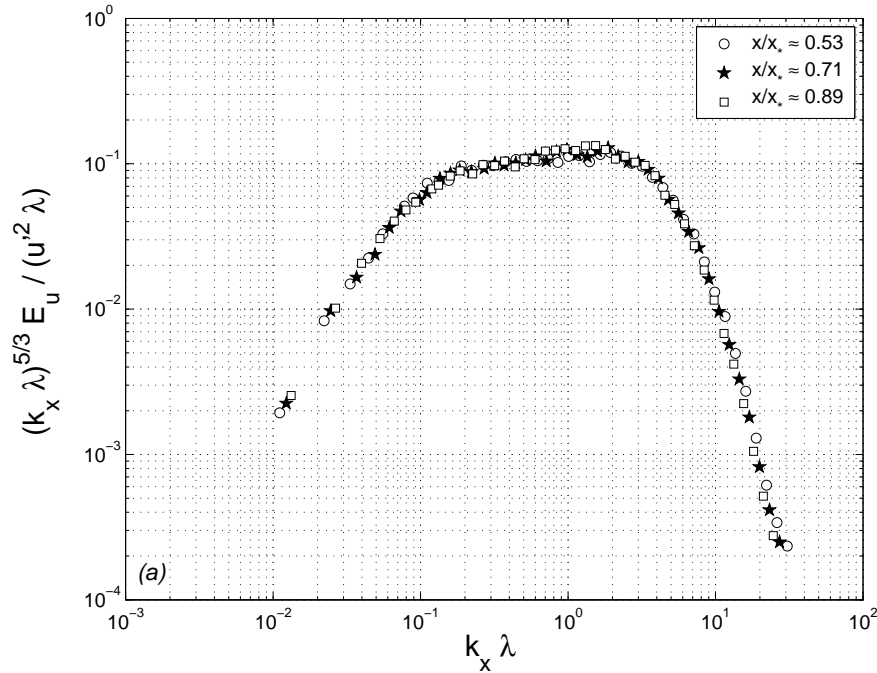
where  $T = L^2 / (U_\infty L_b)$

instead of  $T = L / u'$ .

Note:  $L^2 / (U_\infty L_b) < L / u'$  downstream.

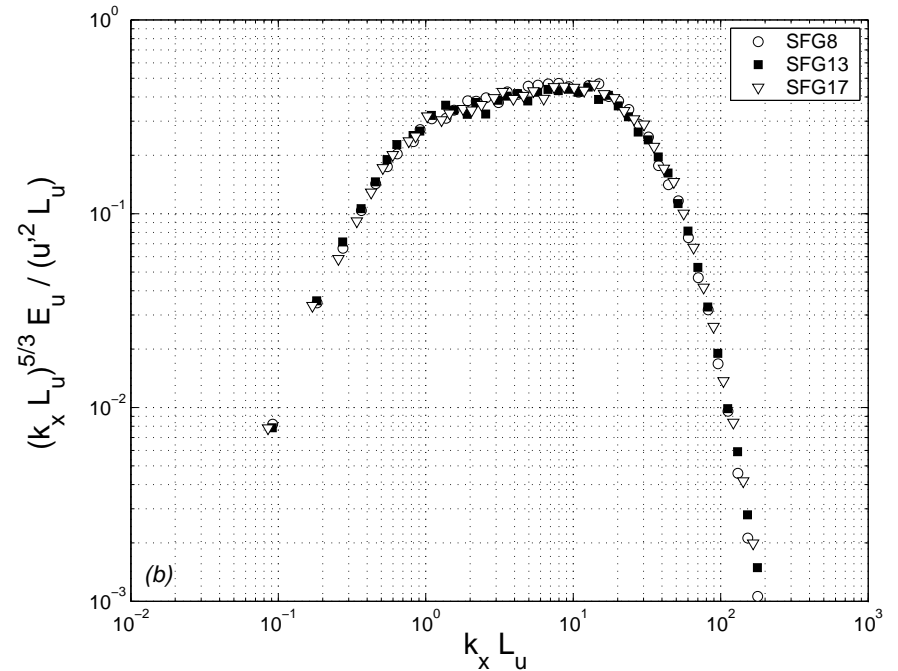
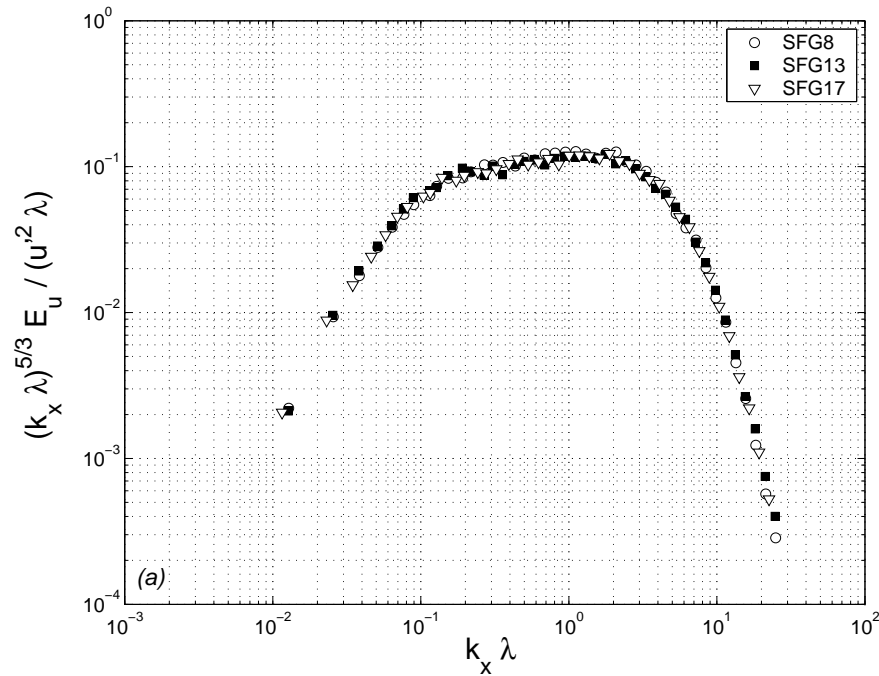
# Self-preserving energy spectrum

$$E_u(k_x, x) = u'^2(x) L_u f(k_x L_u, Re_I)$$



One fractal square grid and three different  $x$  positions

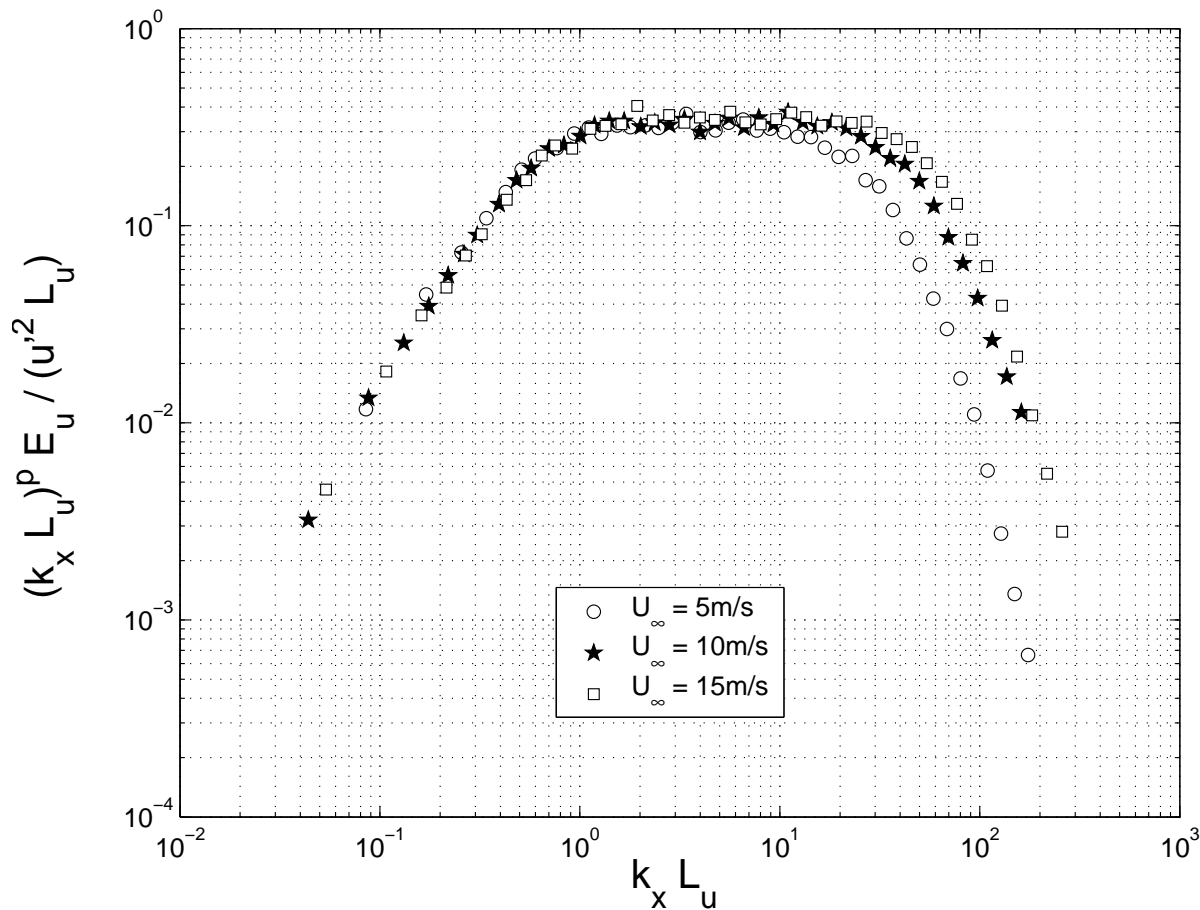
# Self-preserving energy spectrum



One  $x/x_*$  position and three different fractal square grids

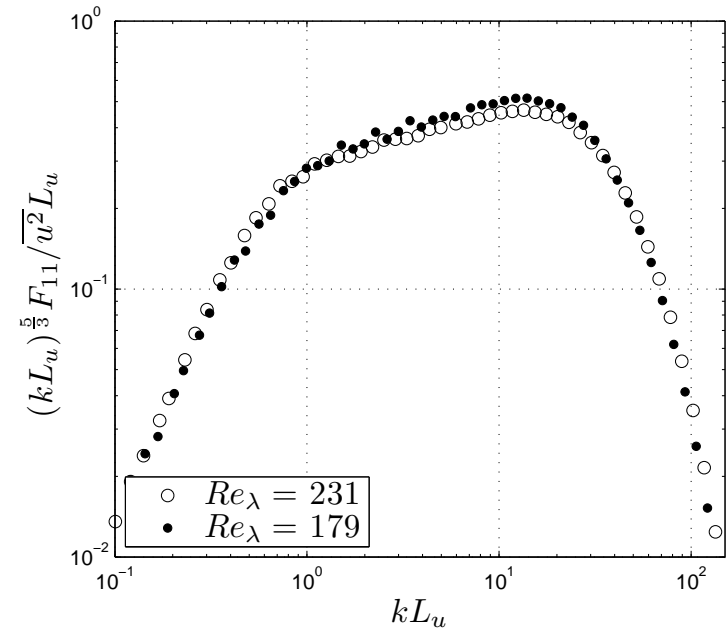
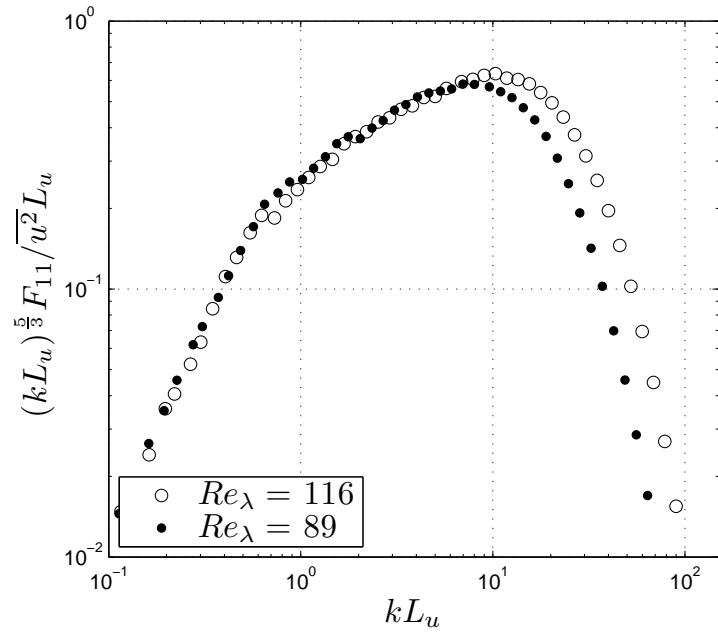
# Energy spectrum's $Re_I$ dependence

$$E_u(k_x, x) = u'^2(x) L_u (k_x L_u)^{-p} \text{ for } 1 < k_x L_u < Re_I^{3/4}$$



One  $x/x_*$  position, one fractal square grid, three different  $Re_I$   
 $p$  increases with  $Re_0$ , perhaps towards  $5/3$

# Two classes of small-scale turbulence?



# Two classes of small-scale turbulence?

A self-preserving/single-scale class where (assuming 5/3)

- (i)  $E_u(k_x) \sim \left(\frac{u'^3}{L_u}\right)^{2/3} k_x^{-5/3}$  for  $1 \ll k_x L_u \ll Re_I^{3/4}$
- (ii)  $L_u/\lambda \propto Re_I^{1/2}$  but independent of  $x$  in the decay region where  $Re_\lambda$  decays fast. Decoupling between  $L_u/\lambda$  and  $Re_\lambda$ .
- (iii)  $C_\epsilon \sim (u'/U_\infty)^{-1} (L/L_b)^{-1}$  indicatively.

And the K41 class where (assuming asymptotic 5/3)

- (i)  $E_u(k_x) \sim \left(\frac{u'^3}{L_u}\right)^{2/3} k_x^{-5/3} \sim \epsilon^{2/3} k_x^{-5/3}$  for  $1 \ll k_x L_u \ll Re_\lambda^{3/2}$ .
- (ii)  $L_u/\lambda \sim Re_\lambda$  locally at every  $x$  in the decay region.
- (iii)  $C_\epsilon = const$

# Turbulence decay $u'^2 \sim (x - x_0)^{-n}$

$$\frac{3}{2}U \frac{d}{dx} u'^2 = -\epsilon = -C_\epsilon u'^3 / L$$

with  $C_\epsilon$  **Const** if  $L/\lambda \sim Re_\lambda$  or  $C_\epsilon \sim Re_\lambda^{-1}$  if  $L/\lambda$  **Const**.

Additional input:  $u'^2 L^{M+1} = \text{const}$  during decay

$$n = \frac{2(M+1)}{M+3} \text{ if } C_\epsilon \text{ Const}$$

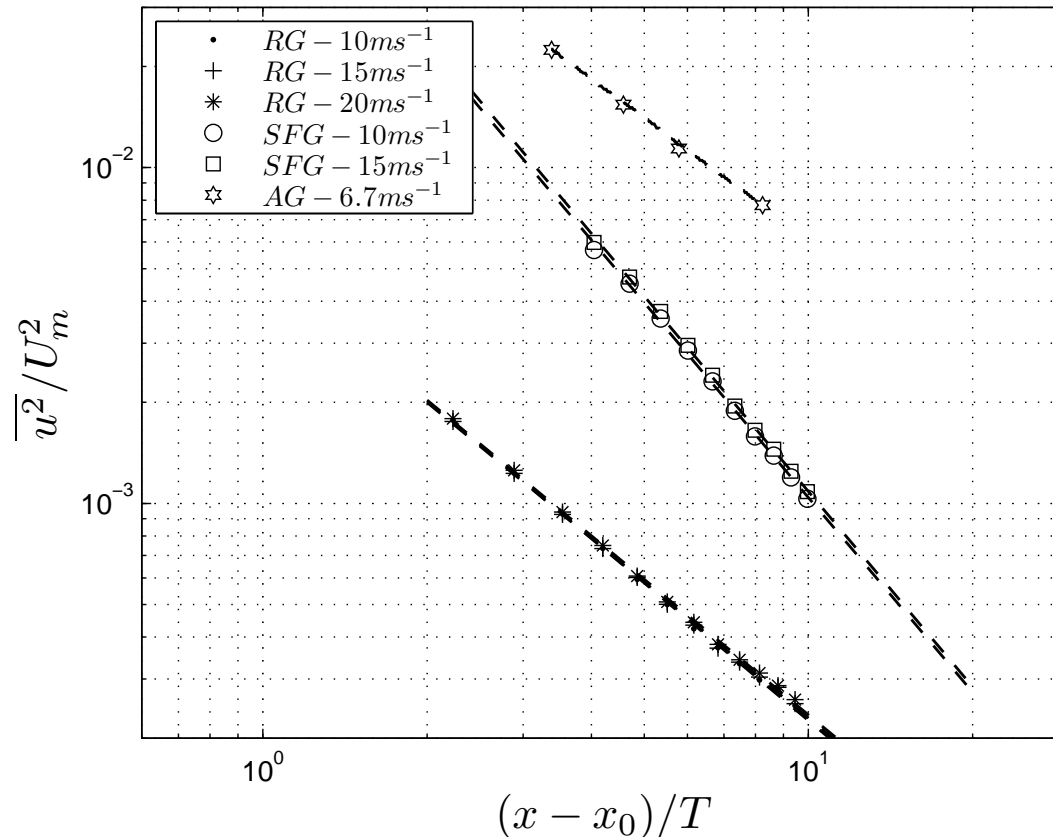
$$n = \frac{M+1}{2} \text{ if } C_\epsilon \sim Re_\lambda^{-1}$$

**Much larger exponent  $n$  when  $L/\lambda$  Const**

Note: we are not referring to the final period of decay but to decaying turbulence with  $Re_\lambda$  well above 100 (up to about 400 here) and a decade of power-law energy spectrum.

# Turbulence decay $u'^2 \sim (x - x_0)^{-n}$

Streamwise fetch for FSG:  $0.5 < x/x_* < 1.5$



Decay exponents: from 1.21 to 1.72 for RG and AG (Mydlarski & Warhaft '96); from 2.36 to 2.57 for FSG by various ways to fit



# TKE equation on the centreline

$$(1) \quad \frac{U}{2} \frac{\partial \overline{q^2}}{\partial x} = \mathcal{P} + \mathcal{T} + \Pi + \mathcal{D}_\nu - \epsilon$$

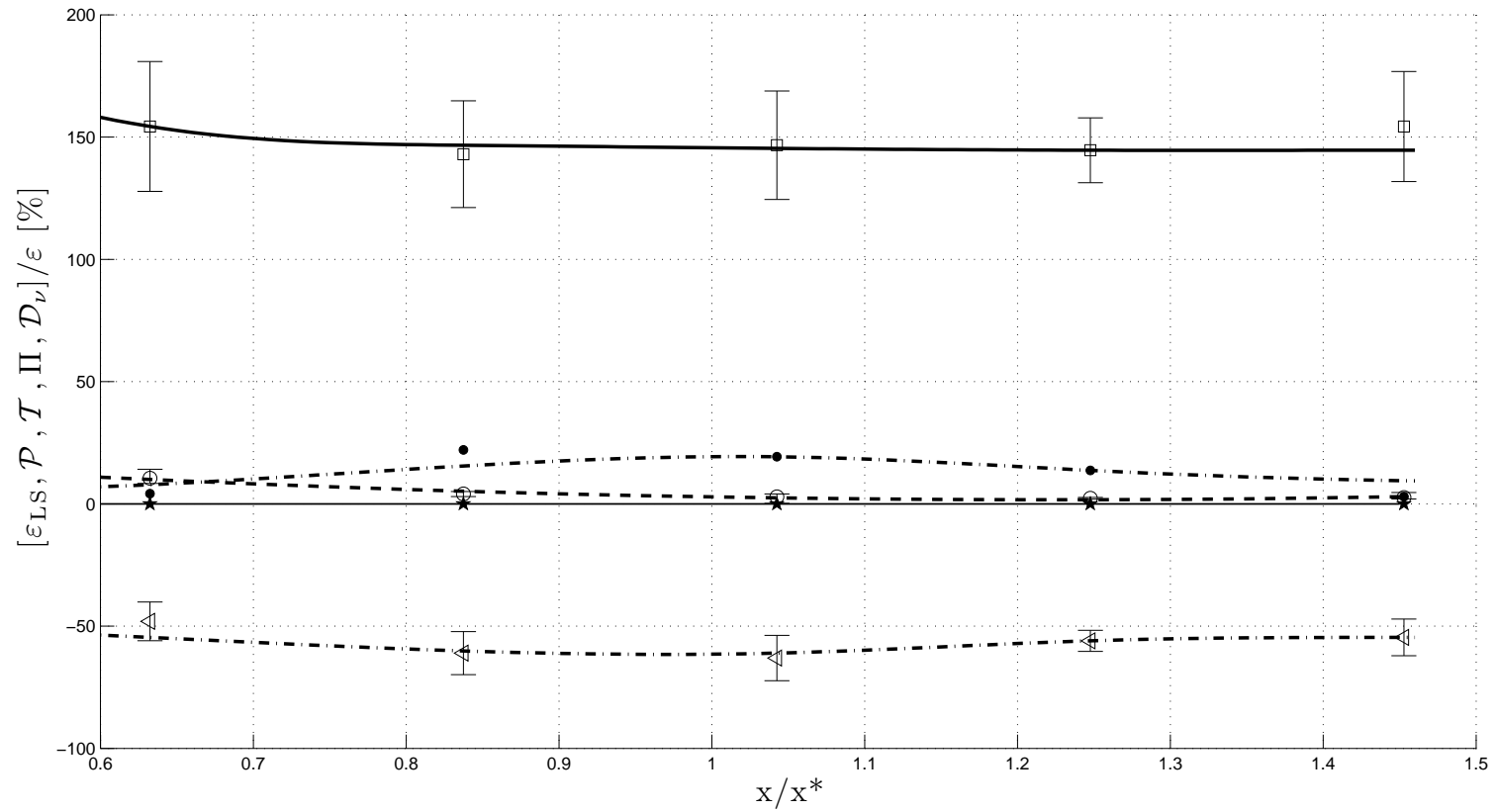
$$\text{where } \mathcal{P} = -\overline{u^2} \frac{\partial U}{\partial x} - 2\overline{uv} \frac{\partial U}{\partial y}$$

$$\text{where } \mathcal{T} = -\frac{\partial}{\partial x} \frac{\overline{uq^2}}{2} - 2\frac{\partial}{\partial y} \frac{\overline{vq^2}}{2}$$

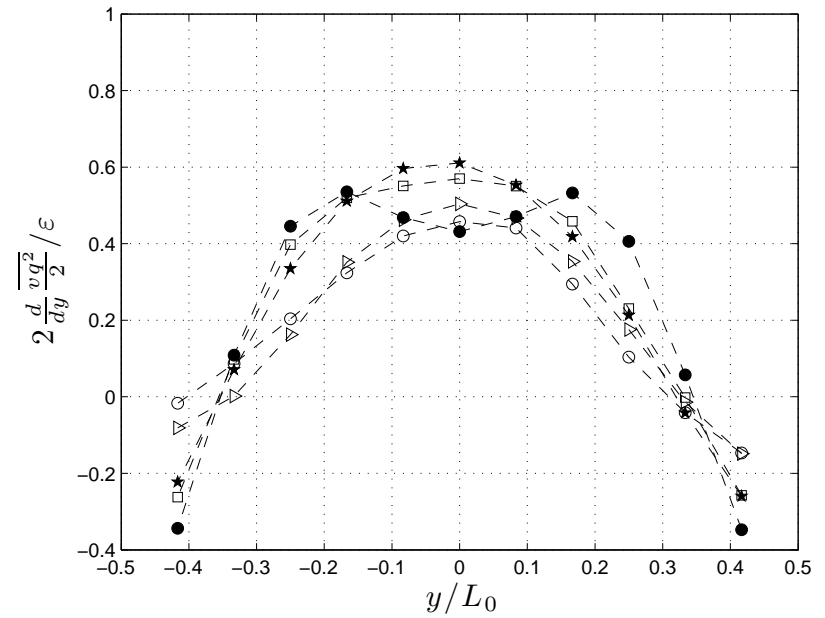
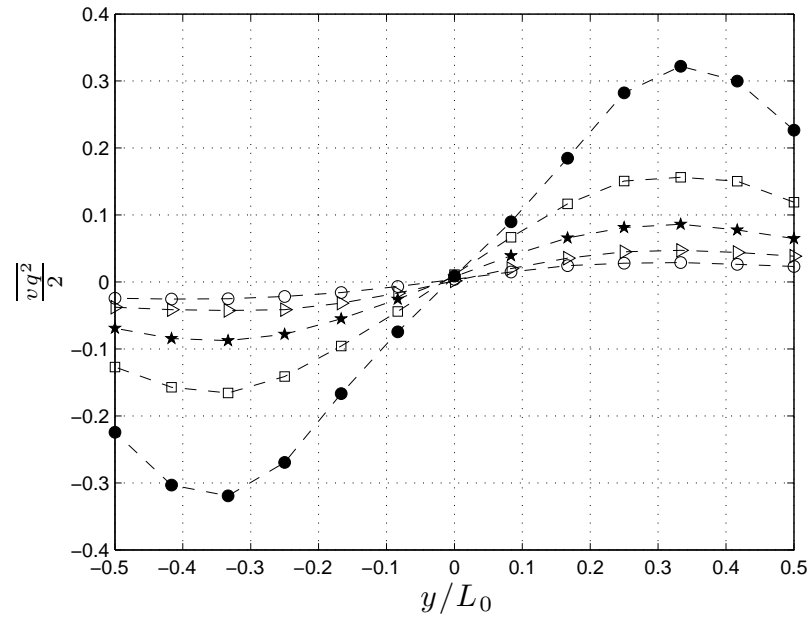
$$\text{where } \Pi = -\frac{\partial}{\partial x} \frac{\overline{up}}{\rho} - 2\frac{\partial}{\partial y} \frac{\overline{vp}}{\rho}$$

$$\text{and where } \mathcal{D}_\nu = \frac{\nu}{2} \left( \frac{\partial^2 \overline{q^2}}{\partial x^2} + 2\frac{\partial^2 \overline{q^2}}{\partial y^2} \right)$$

# Homogeneity but for transverse transport



# Transverse turbulent transport of TKE



# Non-negligible transverse transport

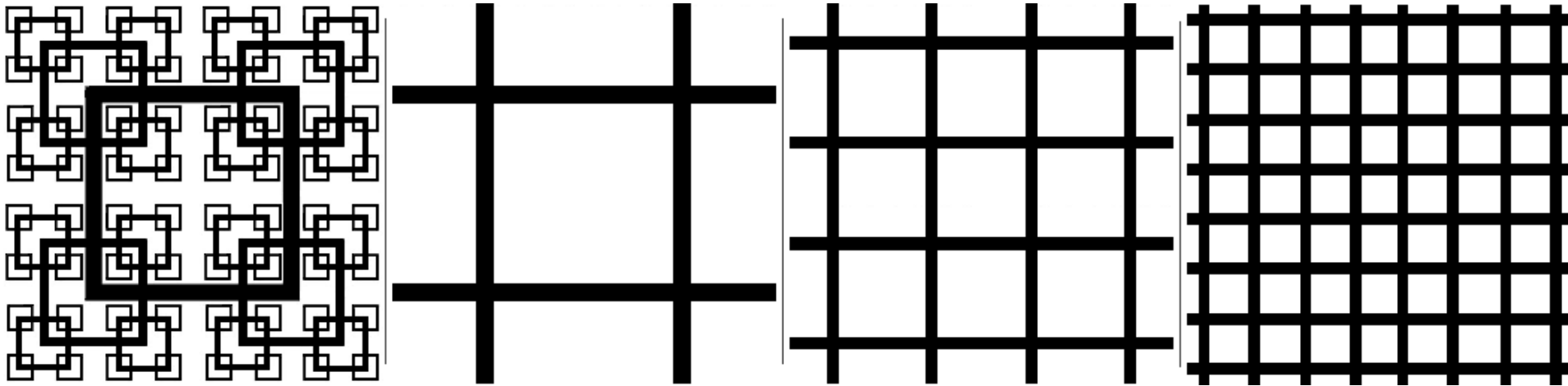
Note that in fact,  $\frac{3}{2}U \frac{d}{dx} u'^2 = -\epsilon$  does not hold true in the region where we measure (up to  $x/x_* \approx 1.5$ ) as there is no homogeneity of third order moments.

In fact  $\frac{3}{2}U \frac{d}{dx} u'^2 = -\epsilon - 2 \frac{\partial}{\partial y} \langle \frac{vq^2}{2} \rangle + \Pi$  where  $\Pi$  is the pressure transport.

However,  $[\frac{\partial}{\partial y} \langle vq^2 \rangle - \Pi]/\epsilon \approx 0.5$  throughout the decay region, so that we can write  $\frac{3}{2}U \frac{d}{dx} u'^2 \approx -\frac{3}{2}\epsilon$ .

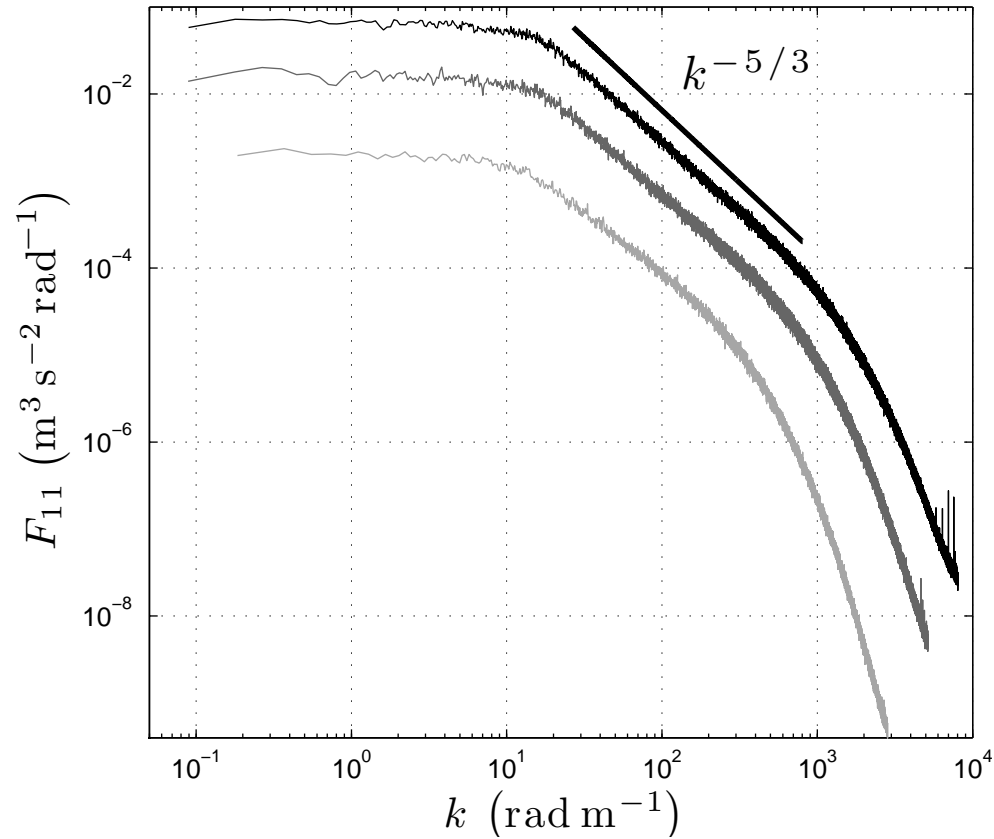
So conclusions on turbulence decay remain unchanged

# How universal is $L/\lambda$ indep of $Re_\lambda$ ?



$L_u/\lambda$  is independent of  $Re_\lambda$  and an increasing function of  $Re_I$  in the near decay region of regular grid turbulence too, a region which had been mostly neglected till now. The trick was to apply to regular grid turbulence the scaling of downstream distance based on  $x_*$  and find the equivalent region where  $C_\epsilon \sim Re_\lambda^{-1}$  for regular grids appropriately designed to be able to detect this region.

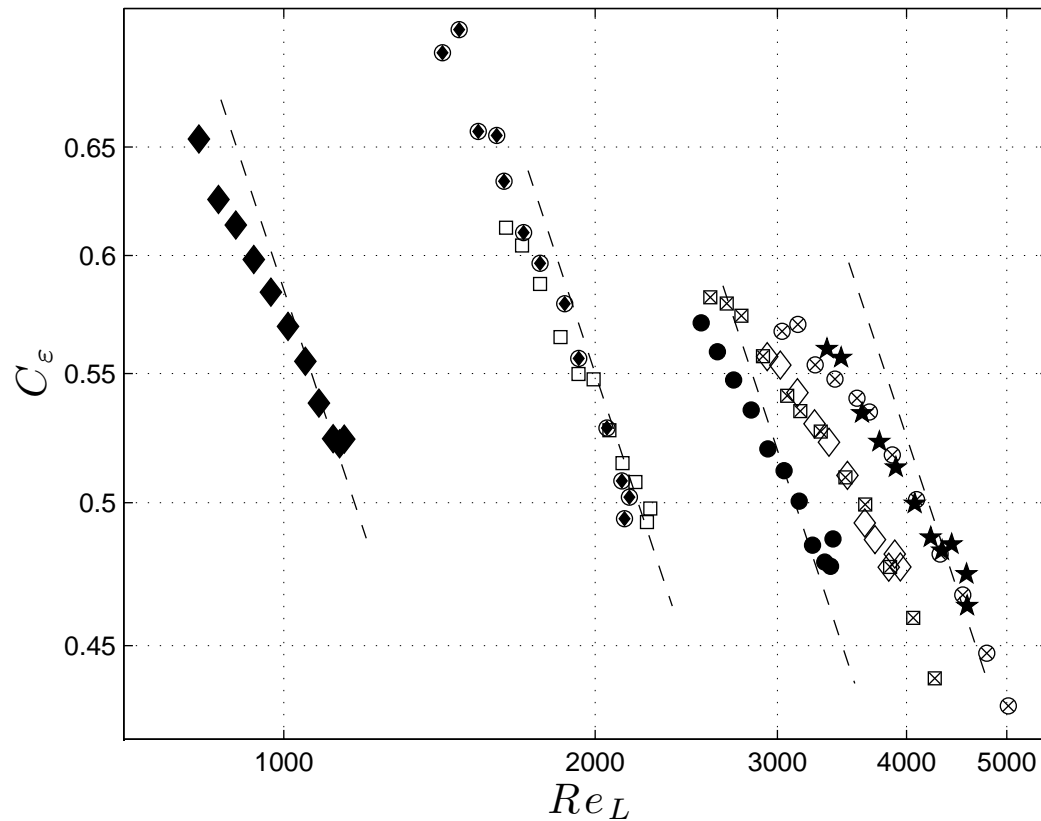
$$x = 0.64x_* \approx 7.4M, \quad x = 1.19x_* \approx 13.8M$$



$$U_{\infty} = 20 \text{ m/s}, 10 \text{ m/s}, 5 \text{ m/s}$$

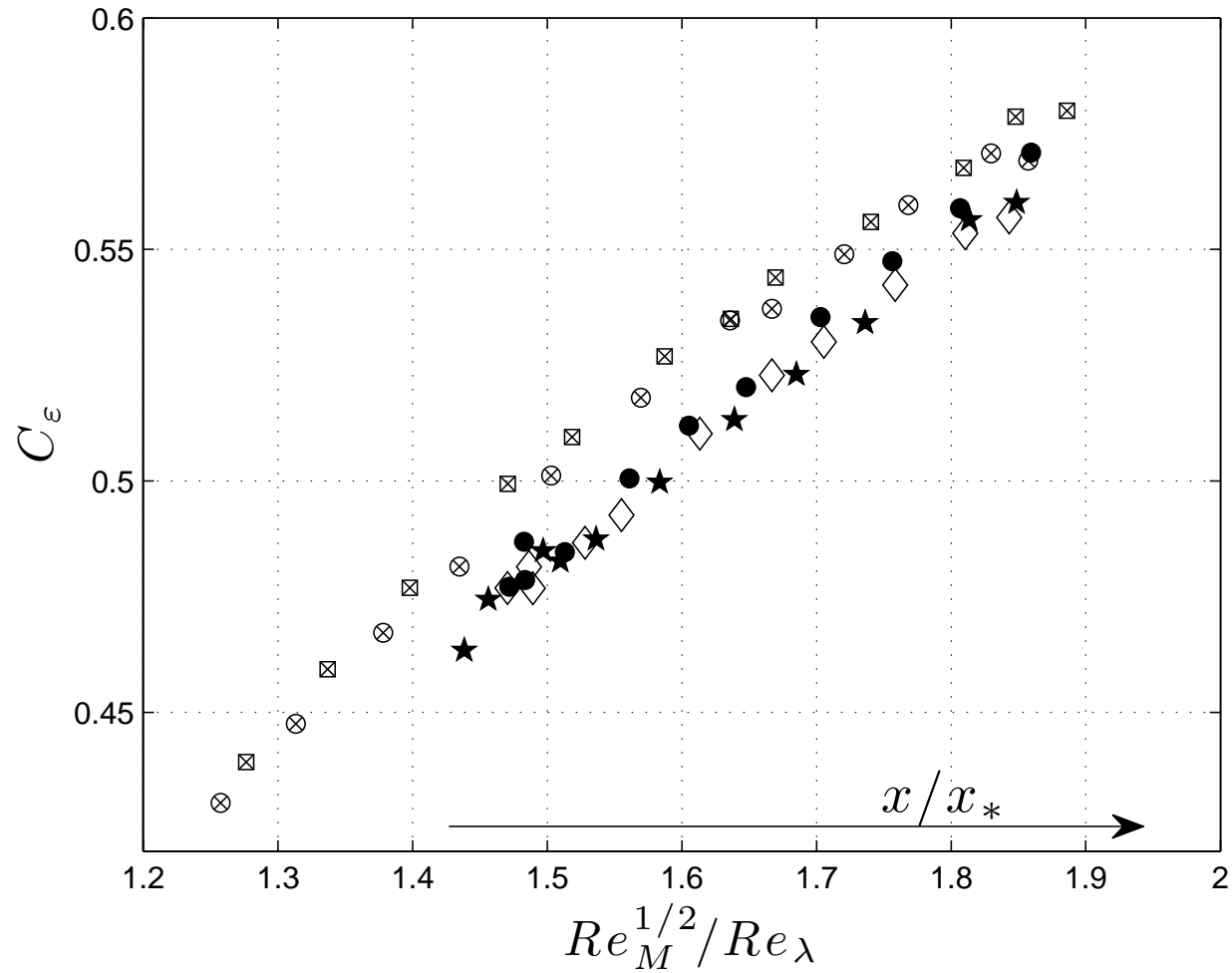
# $C_\epsilon$ vs $Re_L$ for RGs and FSG17

Each set of points: one grid and one inflow Reynolds number  $Re_I \equiv U_\infty L_b / \nu$  where  $L_b$  is the largest mesh size.



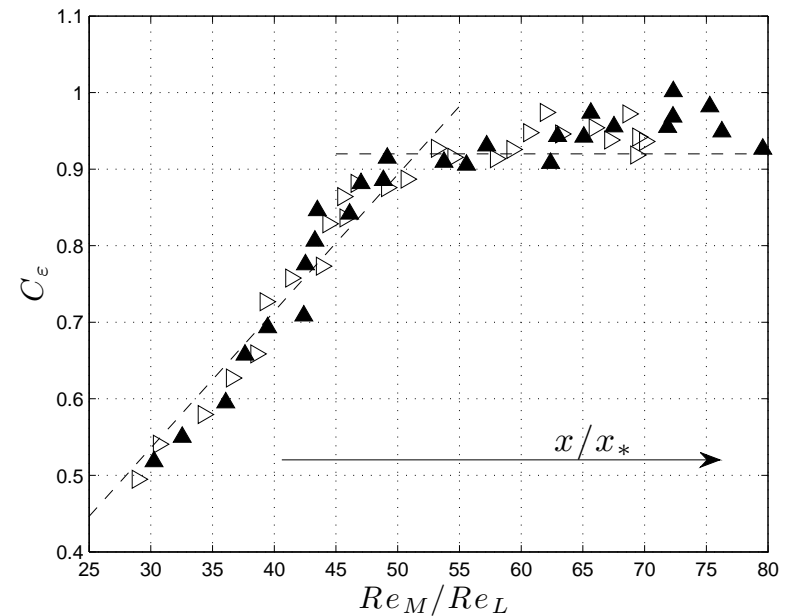
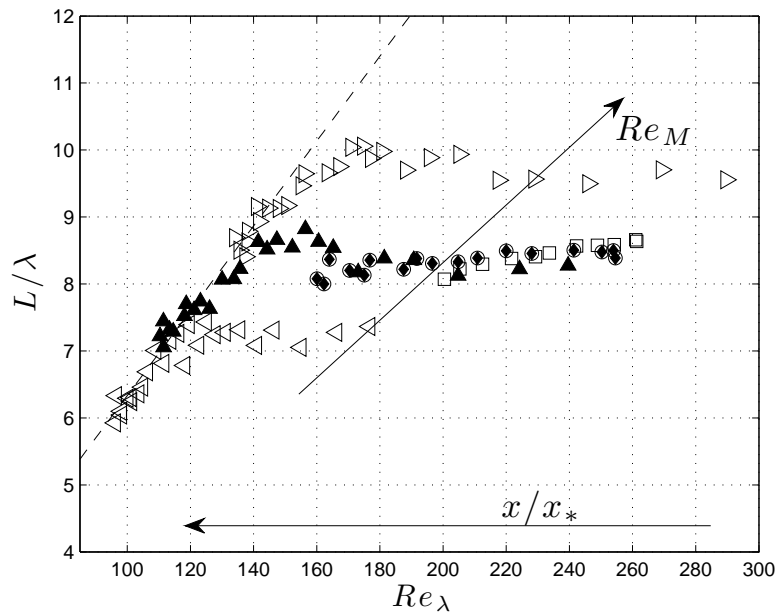
$Re_\lambda$  values range from 140 to 420.

$$C_\epsilon \propto Re_I / Re_L \propto Re_I^{1/2} / Re_\lambda$$





# Further downstream, $x > 2x_*$ for RG60



$C_\epsilon \sim Re_I^\gamma / Re_\lambda \sim Re_I^{2\gamma} / Re_L$  ( $\gamma = 1/2$  in plots above) in the high- $Re_L$  decay region followed by  $C_\epsilon \sim const$  in the further downstream low- $Re_L$  decay region

For the rest of the talk, consider  $C_\epsilon \sim Re_I^\beta / Re_L^\alpha$  for more generality and greater sweep of concepts.

# Batchelor (1953) and $C_\epsilon \sim Re_I^\beta / Re_L^\alpha$

Batchelor (1953) provides evidence from grid-generated turbulence which seems to suggest that  $C_\epsilon$  is independent of both  $Re_I$  and streamwise distance  $x$ , i.e. local turbulence Reynolds number  $Re_L \equiv u'L/\nu$ . Hence  $\beta = \alpha = 0$ .

He interprets this observation as being a “**demonstration that changes in  $\nu$ , which will be accompanied by changes in the motion associated with the dissipation range of wave-numbers, have no effect on the rate of transfer of energy from the lower wavenumbers**”.

$$C_\epsilon \sim Re_I^\beta / Re_L^\alpha$$

Batchelor's (1953) comment implies that if  $\alpha - \beta$  is different from 0 then viscosity has an effect on the rate of energy transfer. We now look closer into this by a re-examination of  $\langle \delta u^3(r) \rangle \approx -\frac{4}{5}\epsilon r$  in homogeneous isotropic turbulence.

Quoting Batchelor (1953): “the statistical quantities determined by the equilibrium range are independent of the properties of the large-scale components of the turbulence and do not require the turbulence to be accurately homogeneous.”

$$\langle \delta u^3(r) \rangle \approx -\frac{4}{5}\epsilon r$$

Derivations of this relation in the inertial range of scales  $r$  have been proposed for

(i) statistically stationary homogeneous isotropic turbulence forced at the large scales by a number of authors, e.g.

Frisch (1995), under the assumption that  $C_\epsilon = const$ , specifically  $\alpha = \beta = 0$

(ii) decaying homogeneous isotropic turbulence by Lundgren (PoF 2002, 2003) under the assumption that

$C_\epsilon = const$ , specifically  $\alpha = \beta = 0$

(iii) decaying homogeneous isotropic turbulence by Tchoufag, Sagaut & Cambon (PoF 2012) under the

assumption that the spectral transfer term  $T(k) \approx 0$  in the assumed inertial range.

$$\langle \delta u^3(r) \rangle \approx -\frac{4}{5}\epsilon r$$

It is possible to derive  $T(k) \approx 0$  in an intermediate range of scales for decaying homogeneous isotropic turbulence under the assumption that energy and its time derivative are finite and various forms of assumption on dissipation, one of them being that  $C_\epsilon \sim Re_L(0)^\beta / Re_L^\alpha$  with  $\alpha < 1$ .

It is then also possible to rigorously use the following relation of Tchoufag, Sagaut & Cambon (2012) to derive  $\langle \delta u^3(r) \rangle \approx -\frac{4}{5}\epsilon r$  in a rigorously defined sufficient intermediate range of scales  $r$ :

$$\langle \delta u^3(r) \rangle = 12r \int_0^{+\infty} g_5(kr) T(k) dk$$

where  $g_5(kr) = \frac{3(\sin kr - kr \cos kr) - (kr)^3 \sin kr}{(kr)^5}$

# Decaying HIT

Lin (1949) equation:

$$\frac{\partial}{\partial t} E(k, t) = T(k, t) - 2\nu k^2 E(k, t)$$

**ASSUMPTION 1:** An outer length-scale  $L(t)$  exists such that

$$\int_0^{k'} E(k, t) \approx \frac{3}{2} u'^2 \quad \& \quad \frac{d}{dt} \int_0^{k'} E(k, t) \approx \epsilon$$

for  $k'L \gg 1$ .

Integrate the Lin equation from 0 to  $k'$  and apply assumption 1 to get:

$$-\epsilon \approx \int_0^{k'} T(k, t) dk - 2\nu \int_0^{k'} k^2 E(k, t) dk$$

Next, non-dimensionalise with  $u'(t)$  and  $L(t)$  using  $\epsilon = C_\epsilon u'^3 / L$  as definition of  $C_\epsilon$  (no assumptions).

# Non-dimensional approximate Lin eq.

$$-C_\epsilon \approx \int_0^{k'L} \tau(\kappa, t) d\kappa - \frac{2}{Re_L} \int_0^{k'L} \kappa^2 e(\kappa, t) d\kappa$$

where  $\kappa \equiv kL$ ,  $\tau(\kappa, t) \equiv \frac{T(k, t)}{u'^3(t)}$ ,  $e(\kappa, t) \equiv \frac{E(k, t)}{u'^2(t)L(t)}$  and  $Re_L \equiv u'L/\nu$ .

A sufficient condition for  $-C_\epsilon \approx \int_0^{k'L} \tau(\kappa, t) d\kappa$ ,  $k'L \gg 1$  is

$$C_\epsilon \gg \frac{2}{Re_L} (k'L)^2 \int_0^{k'L} e(\kappa, t) d\kappa$$

because  $(k'L)^2 \int_0^{k'L} e(\kappa, t) d\kappa > \int_0^{k'L} \kappa^2 e(\kappa, t) d\kappa$ , which is the neglected viscous term.

Using assumption 1, the sufficient condition for

$$-C_\epsilon \approx \int_0^{k'L} \tau(\kappa, t) d\kappa \text{ at } k'L \gg 1$$

is  $C_\epsilon \gg \frac{3}{Re_L} (k'L)^2$

# An assumption on dissipation

A sufficient range where  $-\epsilon \approx \int_0^{k'} T(k, t) dk$  is

$$L^{-1} \ll k' \ll L^{-1} \left( \frac{C_\epsilon Re_L}{3} \right)^{1/2} \sim \lambda^{-1}$$

Now chose an assumption on dissipation, for example

$$C_\epsilon \sim \frac{Re_L(0)^\beta}{Re_L^\alpha}.$$

The sufficient range becomes

$$L^{-1} \ll k' \ll L^{-1} Re_L(0)^\beta Re_L^{(1-\alpha)/2}$$

This is a sufficient range of wavenumbers where the

interscale energy flux  $\int_0^{k'} T(k, t) dk$  is independent of  $k'$ ,

hence  $T(k', t) \approx 0$ . One can then obtain  $\langle \delta u^3(r) \rangle \approx -\frac{4}{5} \epsilon r$

in a well-defined sufficient range of length-scales  $r$ .



$$L^{-1} \ll k' \ll L^{-1} Re_L(0)^\beta Re_L^{(1-\alpha)/2}$$

This is not a range, however, where the interscale energy flux is independent of viscosity except in the particular case where  $\alpha = \beta$  because of the ansatz  $C_\epsilon \sim \frac{Re_L(0)^\beta}{Re_L^\alpha}$ .

So, except if  $\beta = \alpha$ , the K41-type arguments which require  $\epsilon$  to be independent of  $\nu$  to yield  $\langle \delta u^n(r) \rangle \sim (\epsilon r)^{n/3}$  in an appropriate intermediate range cannot be used. Nevertheless,  $\langle \delta u^3(r) \rangle \sim \epsilon r$  ( $n = 3$ ).

However, one can always argue that  $E(k)$  can only depend on  $k$  and interscale energy flux, thus leading to  $E(k) \sim \epsilon^{2/3} k^{-5/3}$ , and therefore  $\langle \delta u^2(r) \rangle \sim (\epsilon r)^{2/3}$  in the appropriate ranges. But this energy flux and  $\epsilon$  can now depend on viscosity.

$$L^{-1} \ll k' \ll L^{-1} Re_L(0)^\beta Re_L^{(1-\alpha)/2} \sim \lambda^{-1}$$

Sufficient condition range for  $\int_0^{k'} T(k, t) dk = -\epsilon$  under assumption 1 and  $C_\epsilon \sim \frac{Re_L(0)^\beta}{Re_L^\alpha}$

Note 1: This range decreases with time if  $Re_L$  decreases with time and  $\alpha < 1$ .

Note 2:  $\alpha = 1$  is special as the range  $L^{-1}$  to  $\lambda^{-1}$  remains constant during turbulence decay in that case.

Note 3: The range where  $\int_0^{k'} T(k, t) dk = -\epsilon$  may in fact be wider as the range we found is only sufficient, not necessary.

And Note 4: Assumption  $\frac{d}{dt} \int_0^{k'} E(k, t) \approx \epsilon$  may be wrong: non-equilibrium

# Vorticity and strain

In homogeneous isotropic turbulence,

$$\frac{\langle \boldsymbol{\omega} \cdot \mathbf{s} \boldsymbol{\omega} \rangle}{\langle \boldsymbol{\omega}^2 \rangle} = \frac{\int_0^\infty k^2 T(k) dk}{\left( \int_0^\infty k^2 E(k) dk \right)^{3/2}}$$

In general  $\mathbf{u} = \langle \mathbf{u} \rangle + \mathbf{u}'$  and

$$\frac{\partial}{\partial t} \mathbf{u}' + \mathbf{u}' \cdot \nabla \mathbf{u}' = -\nabla p' / \rho + \nu \nabla^2 \mathbf{u}' + \frac{1}{\rho} \mathbf{f}$$

where

$$\frac{1}{\rho} \mathbf{f} = \mathbf{u}' \cdot \nabla \langle \mathbf{u} \rangle + \frac{\partial}{\partial x_k} \langle u'_k \mathbf{u}' \rangle - \langle \mathbf{u} \rangle \cdot \nabla \mathbf{u}'$$

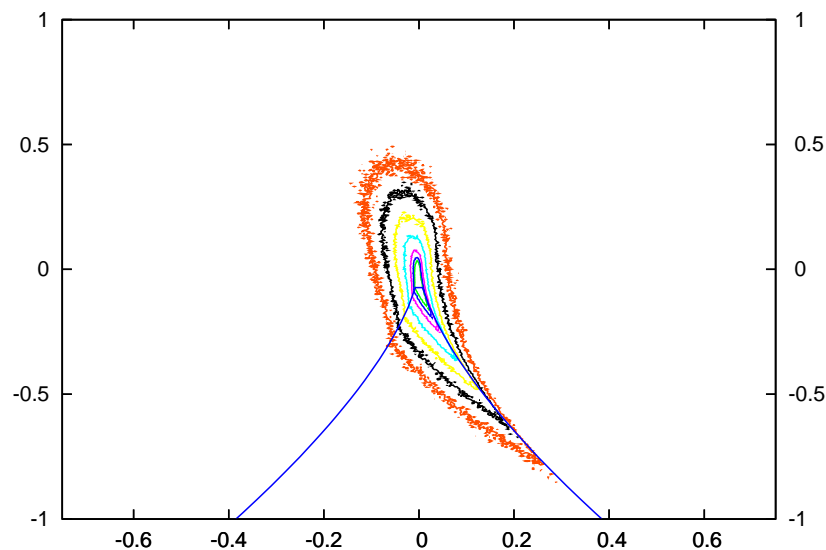
Vorticity and strain rate of fluctuating velocity:

$$\boldsymbol{\omega} \equiv \nabla \times \mathbf{u}' \text{ and } s_{ij} \equiv \frac{1}{2} \left( \frac{\partial}{\partial x_i} u'_j + \frac{\partial}{\partial x_j} u'_i \right)$$

# $Q - R$ diagram

$$Q \equiv \frac{1}{4}(\omega^2 - 2s_{ij}s_{ji}) \text{ and } R \equiv -\frac{1}{3}(s_{ij}s_{jk}s_{ki} + \frac{3}{4}\omega_i s_{ij} \omega_j)$$

The  $Q$ - $R$  diagram (below for periodic DNS turbulence, courtesy of Ryo Onishi) has this tear-drop shape in many turbulent flows: turbulent boundary layers, mixing layers, grid turbulence, jet turbulence (see Tsinober 2009). For homogeneous/periodic turbulence it can be proved that  $\langle Q \rangle = 0$ ,  $\langle R \rangle = 0$ .



# Direct Numerical Simulations

We use Incompact3D which originates from Eric Lamballais (Poitiers) and his coworkers: solves incompressible Navier-Stokes on a cartesian mesh with 6th-order compact finite difference schemes for spatial discretization, 3rd-order Adams-Bashforth for time advancement and a fractional step method for incompressibility which involves solving the Poisson pressure equation in spectral space and use of the concept of modified wave number.

Immersed Boundary Method for modelling the grid in the flow.

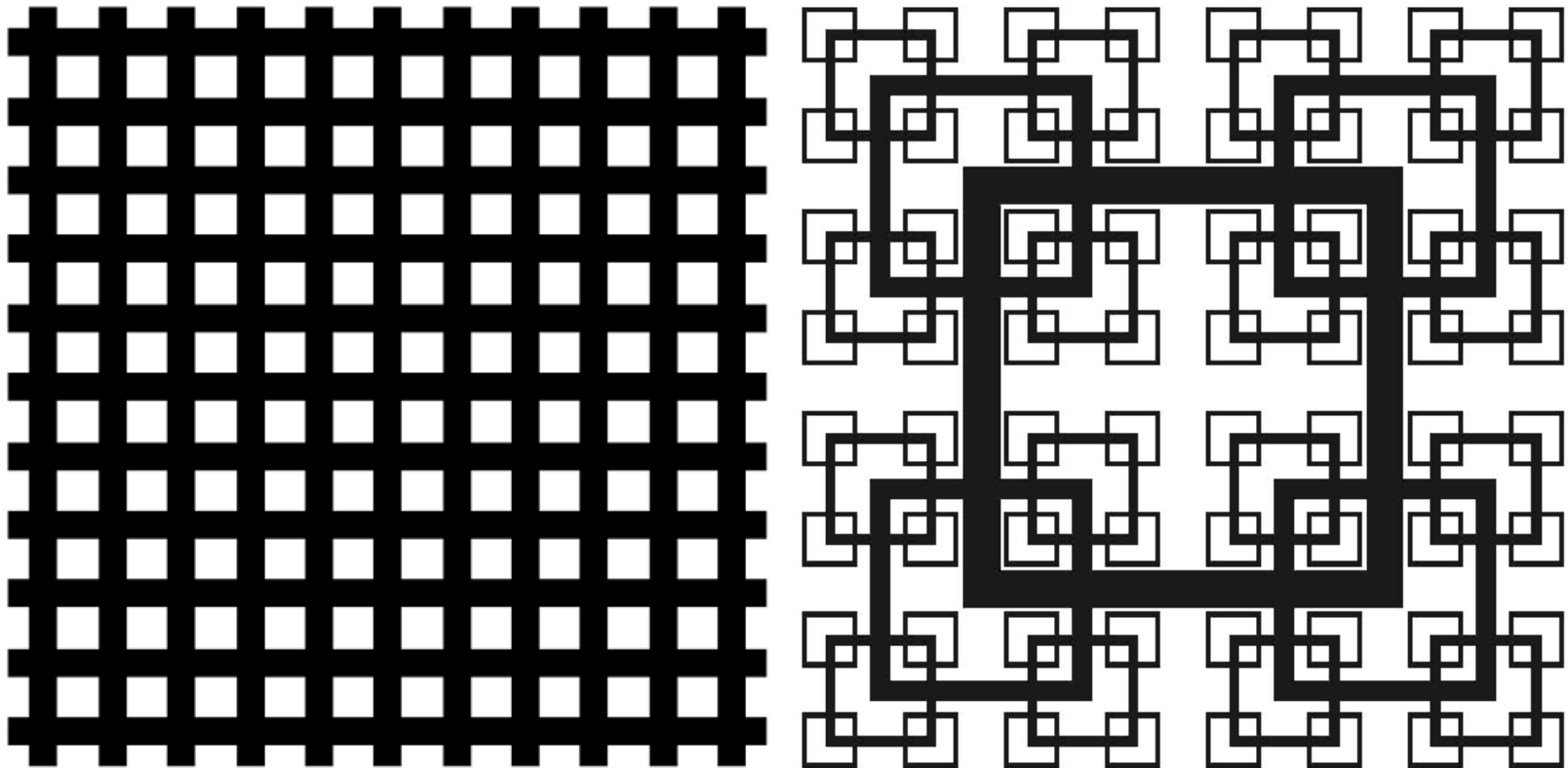
Inflow/outflow boundary conditions in the streamwise direction, periodic boundary conditions in the lateral directions.

# Grids with same $\sigma = 50\%$

same  $M_{eff} \equiv \frac{4T^2}{P} \sqrt{1 - \sigma}$  and  $U_\infty M_{eff} / \nu$ .

Fractal grid:  $D_f = 2$ ,  $N = 4$ ,  $t_r = 8.5$

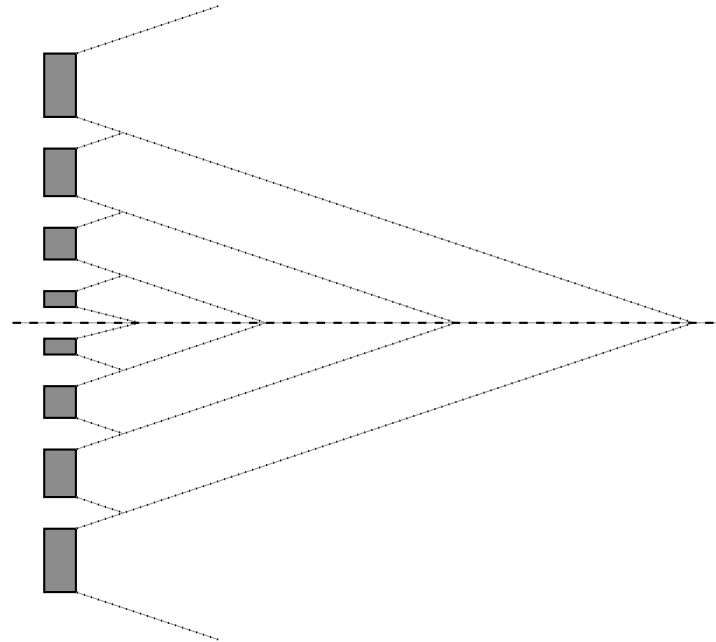
Regular grid:  $b = 2t_{min}$



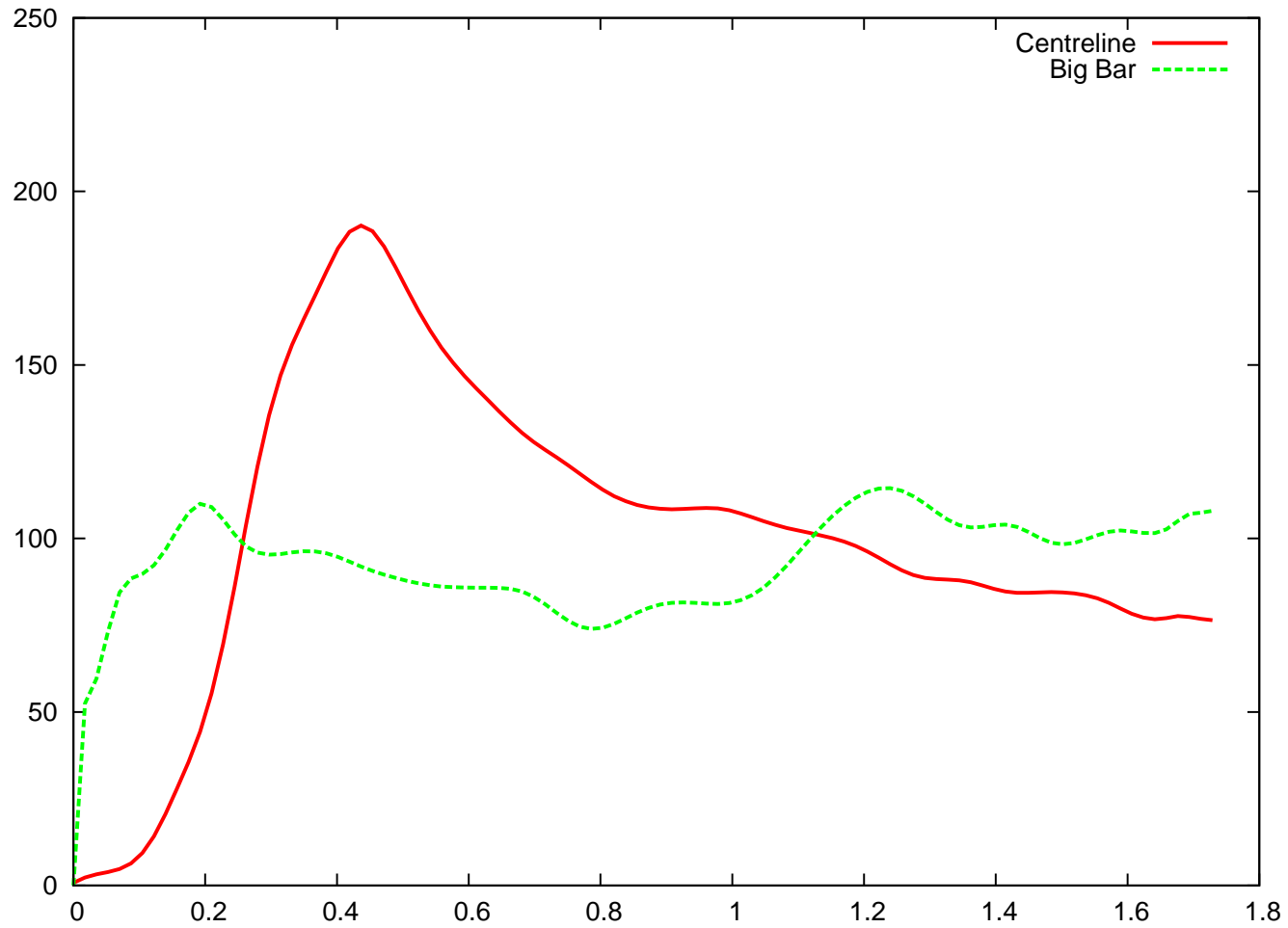
# Wake-interaction length-scales

Regular grid:  $\frac{1}{2}M^2/b$

Fractal grid:  $\frac{1}{2}L_3^2/t_3 \approx 6.25M_{eff} < \frac{1}{2}L_2^2/t_2 \approx 12.255M_{eff} < \frac{1}{2}L_1^2/t_1 \approx 24M_{eff} < \frac{1}{2}L_0^2/t_0 \approx 47M_{eff} = \frac{1}{2}x_*$



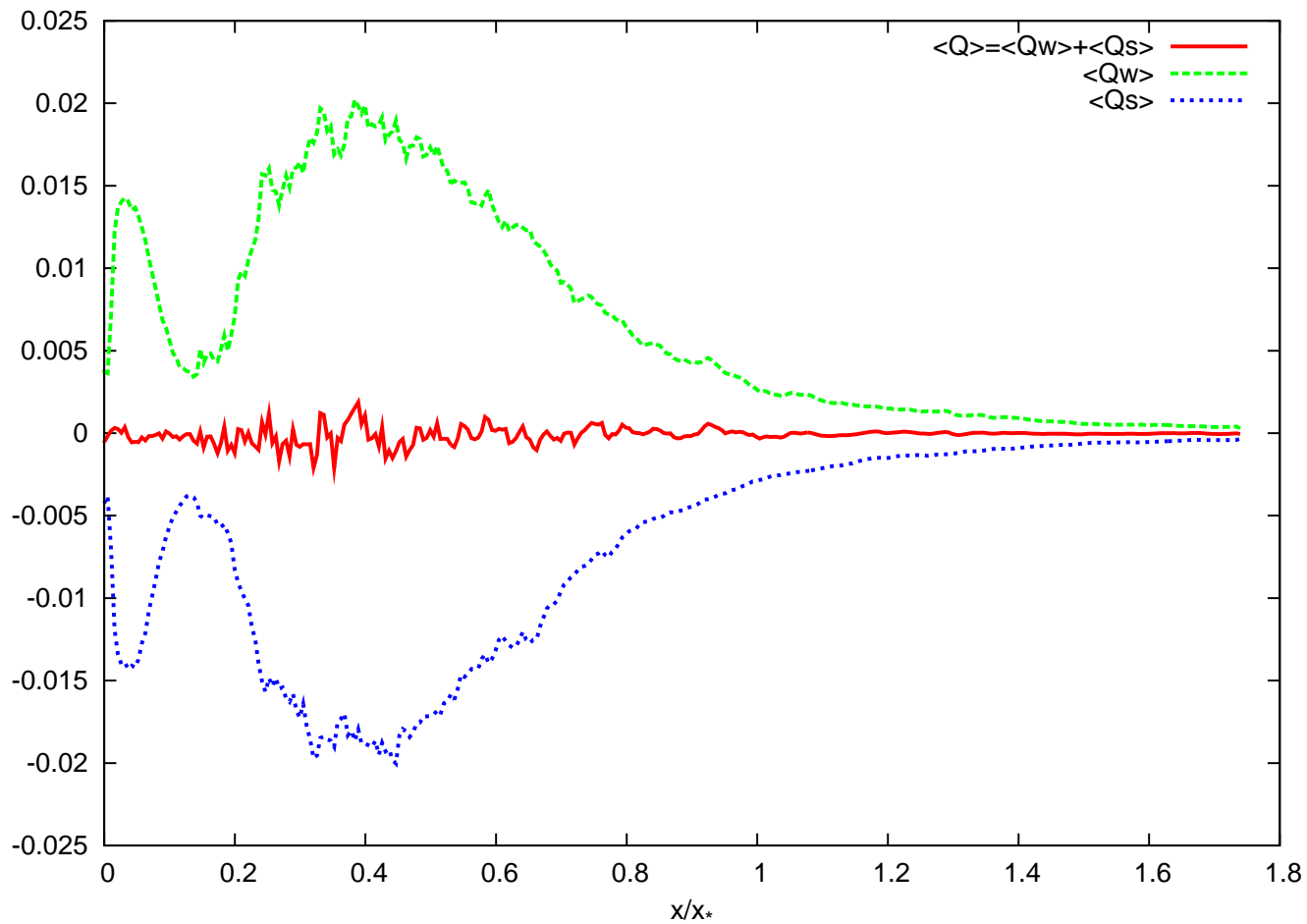
# $Re_\lambda$ as fct of $x/x_*$





$$Q_w \equiv \frac{1}{4}\omega^2 \quad \text{and} \quad Q_s \equiv -\frac{1}{2}s_{ij}s_{ij}$$

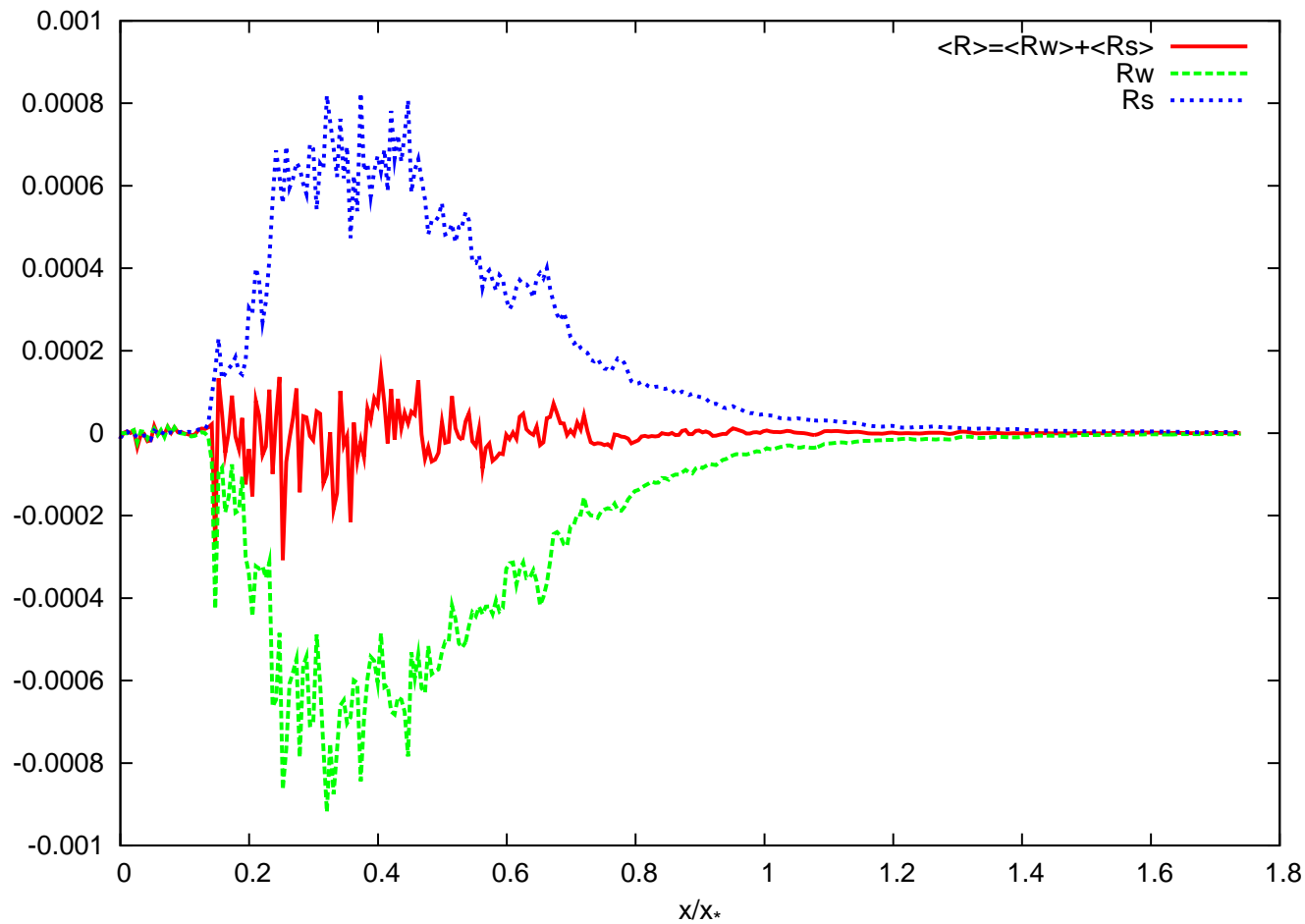
$\langle Q_w \rangle$  and  $\langle Q_s \rangle$  as fcts of  $x/x_*$  along the centerline



$$Q = Q_w + Q_s$$

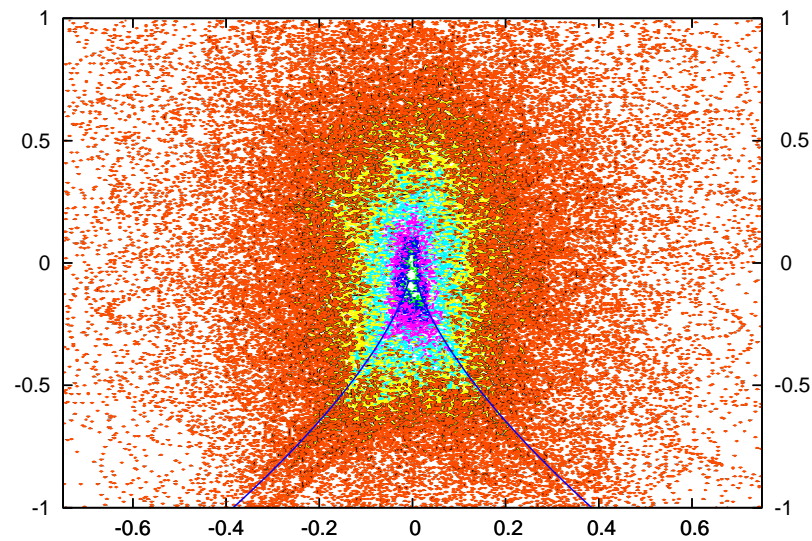
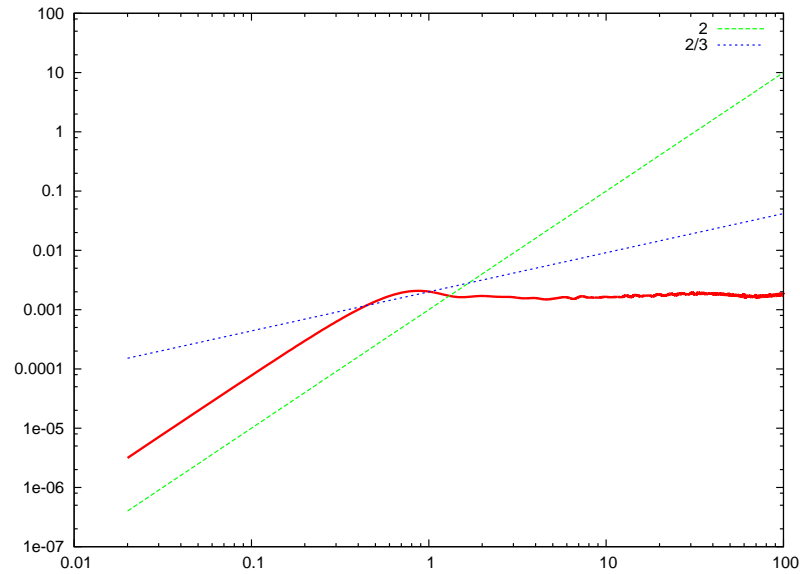
$$R_w \equiv -\frac{1}{4}\omega_i\omega_j s_{ij} \quad \mathbf{and} \quad R_s \equiv -\frac{1}{3}s_{ij}s_{jk}s_{ki}$$

$\langle R_w \rangle$  and  $\langle R_s \rangle$  as fcts of  $x/x_*$  along the centerline

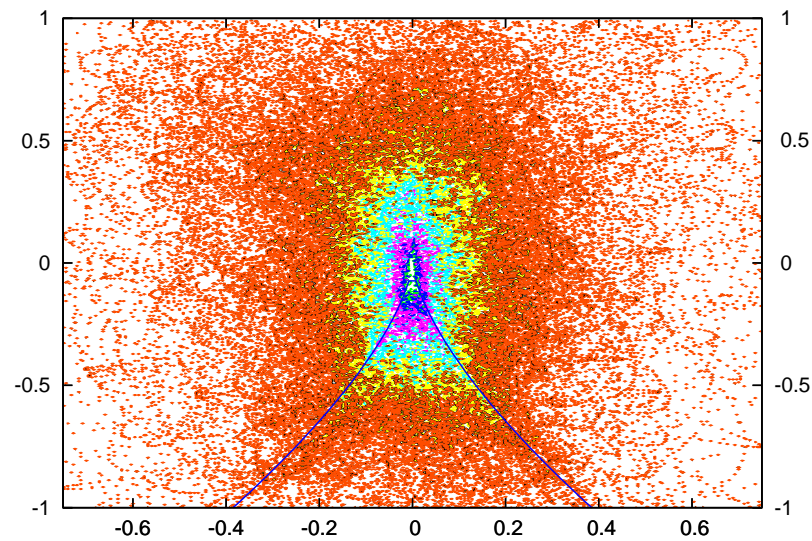
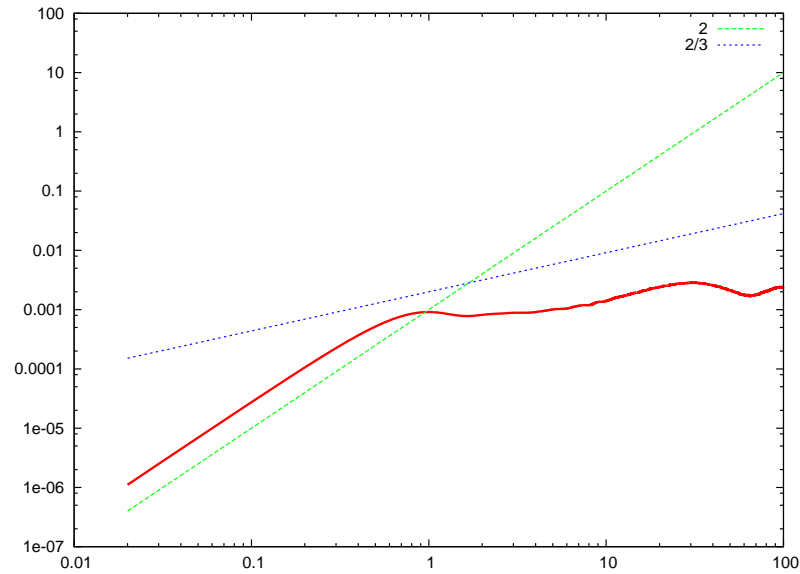


$$R = R_w + R_s$$

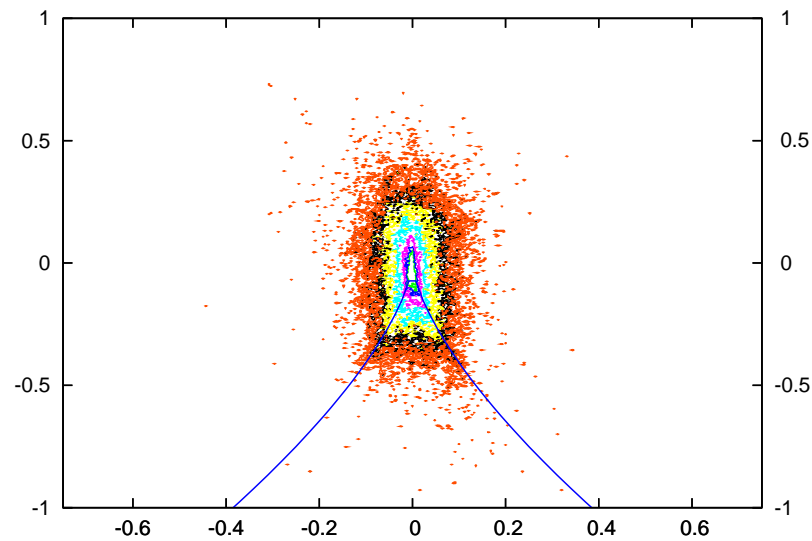
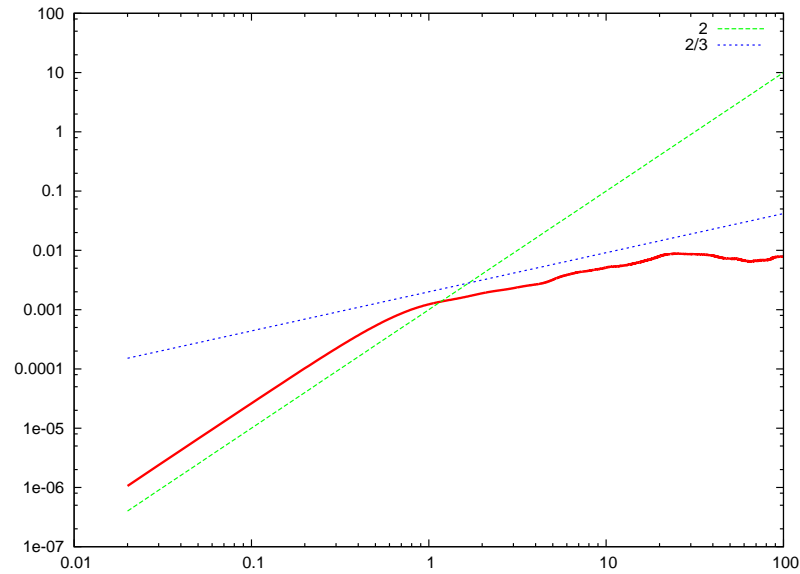
# $\langle \delta u^2(\tau) \rangle$ and $Q - R$ at $x/x_* = 0.052$



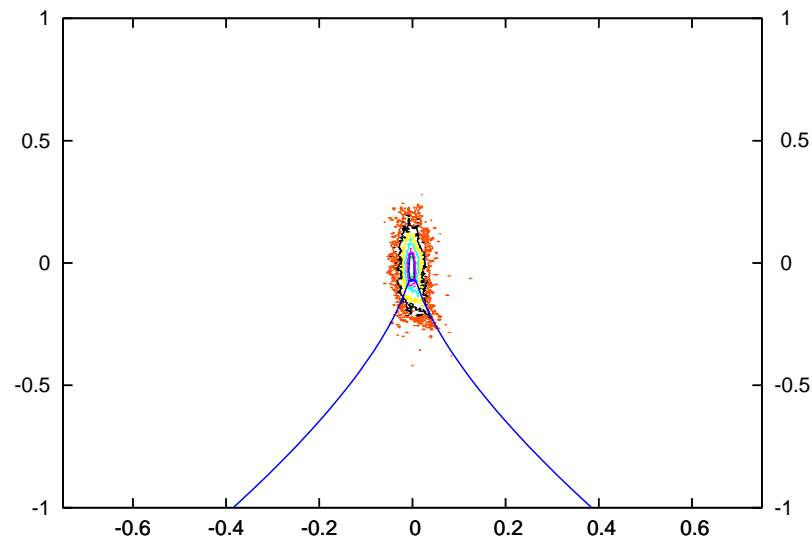
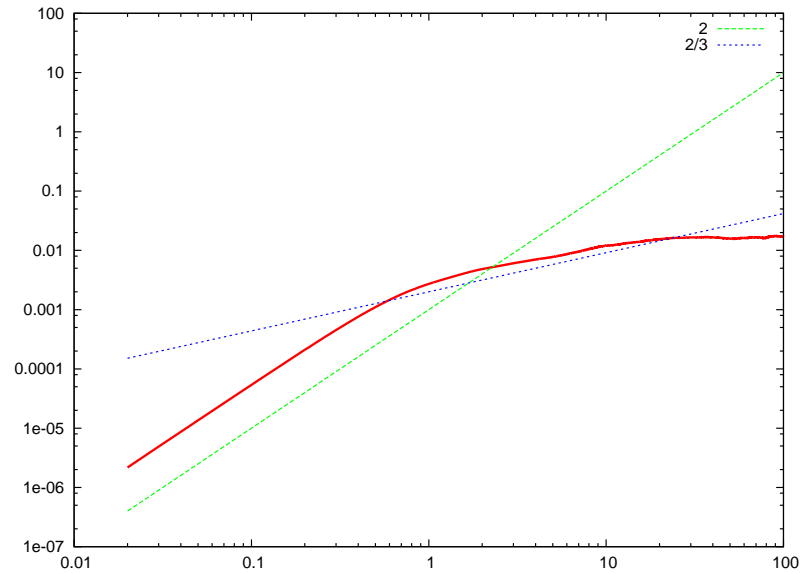
# $\langle \delta u^2(\tau) \rangle$ and $Q - R$ at $x/x_* = 0.105$



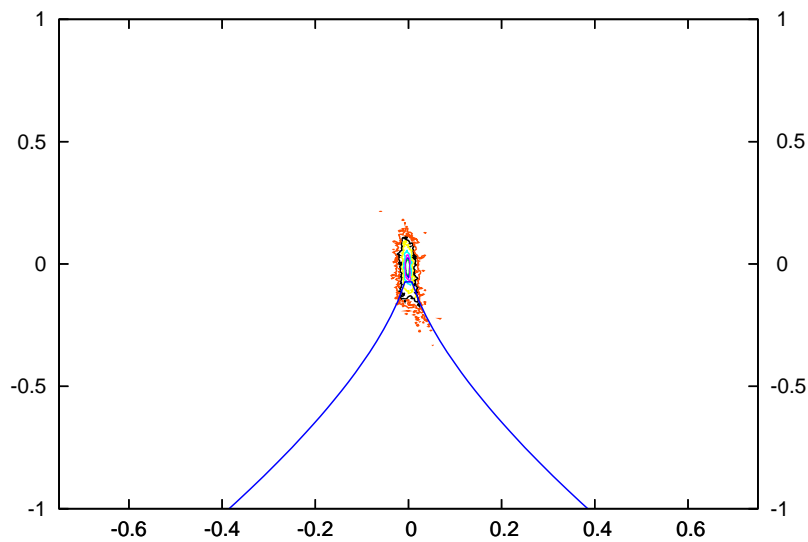
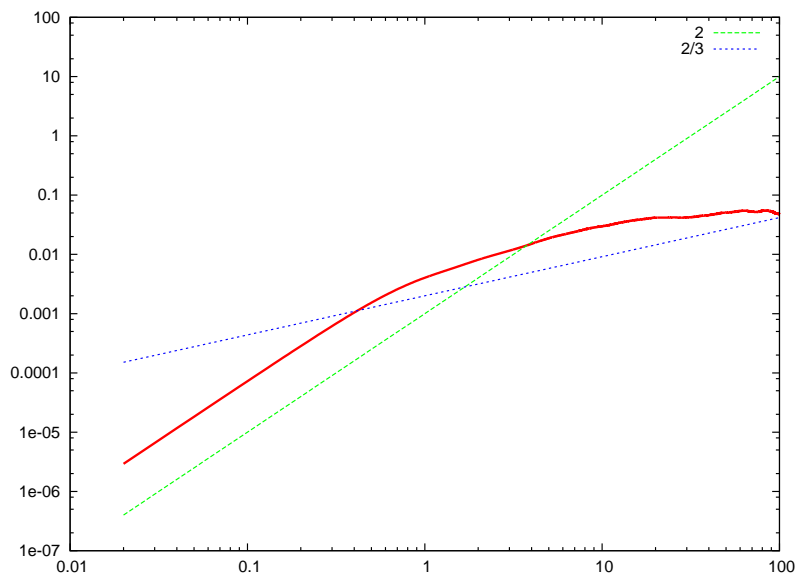
# $\langle \delta u^2(\tau) \rangle$ and $Q - R$ at $x/x_* = 0.157$



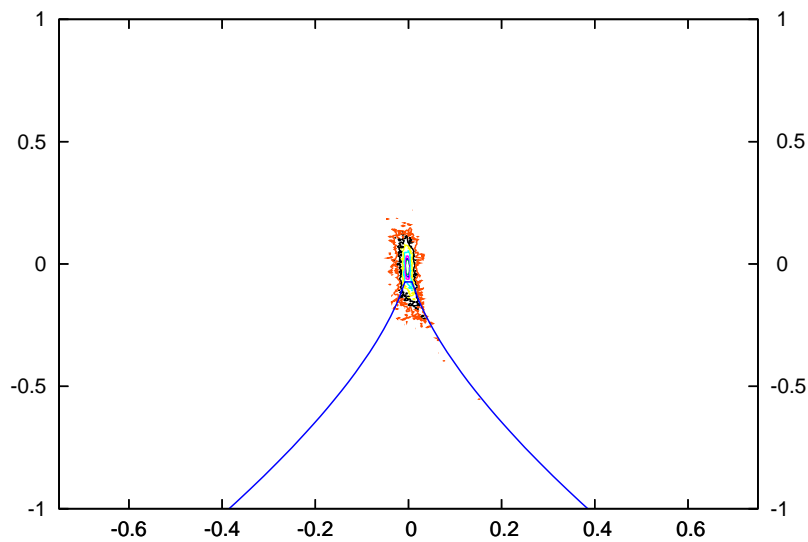
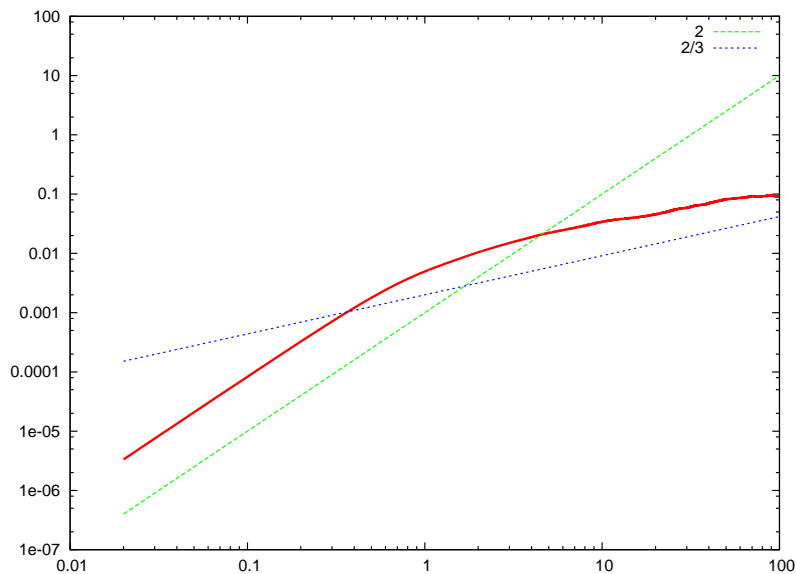
# $\langle \delta u^2(\tau) \rangle$ and $Q - R$ at $x/x_* = 0.210$



$\langle \delta u^2(\tau) \rangle$  and  $Q - R$  at  $x/x_* = 0.262$

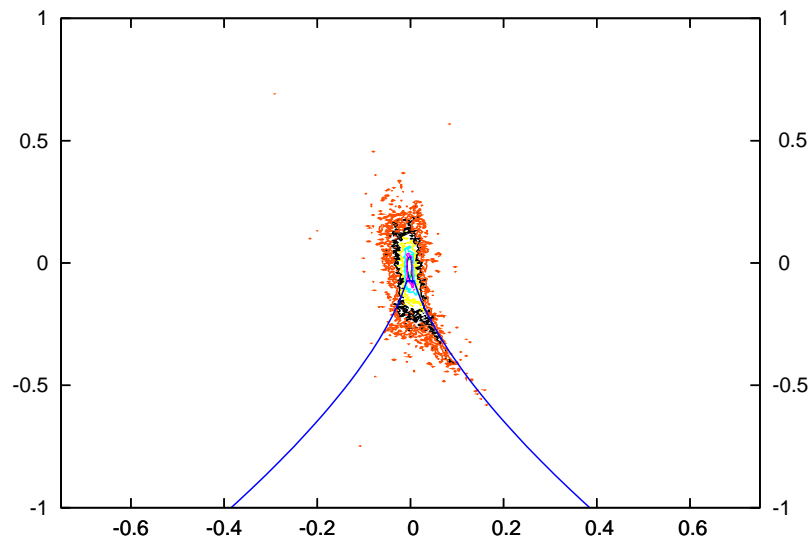
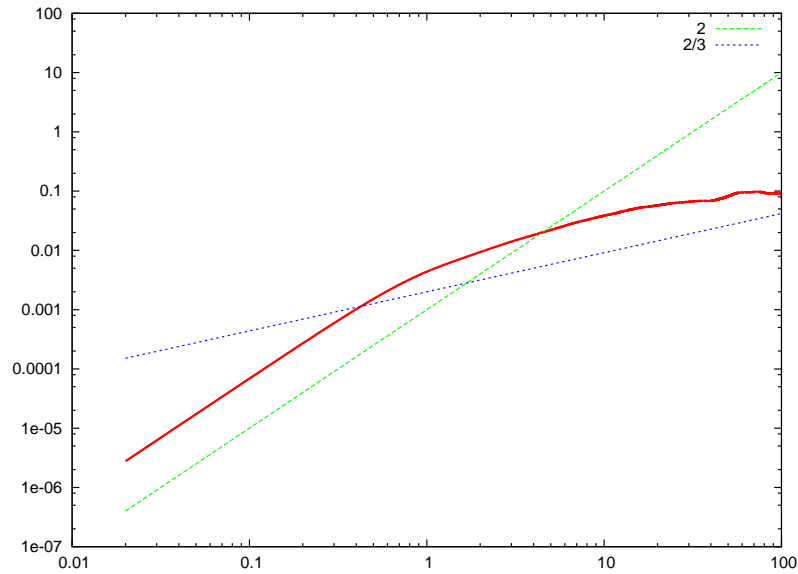


# $\langle \delta u^2(\tau) \rangle$ and $Q - R$ at $x/x_* = 0.315$

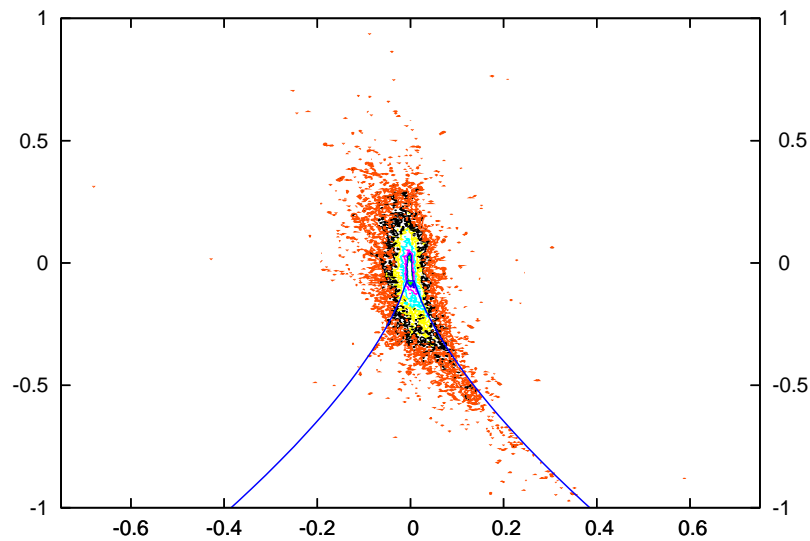
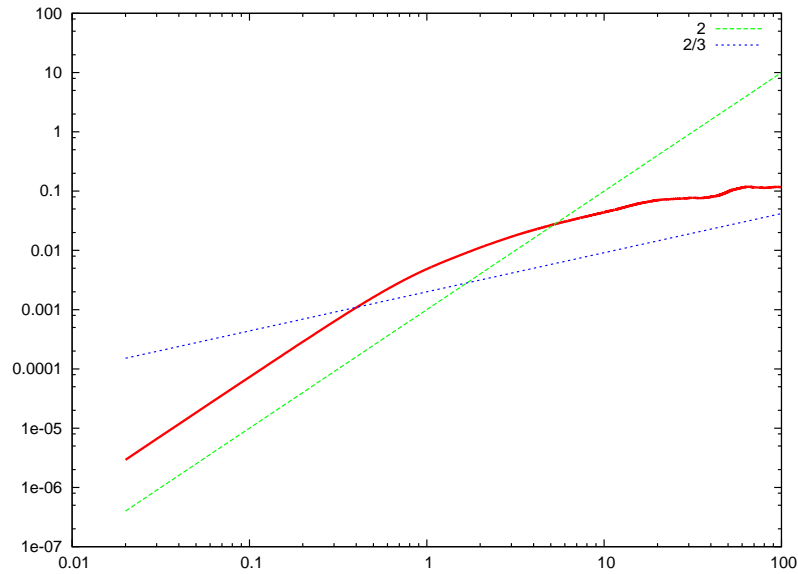




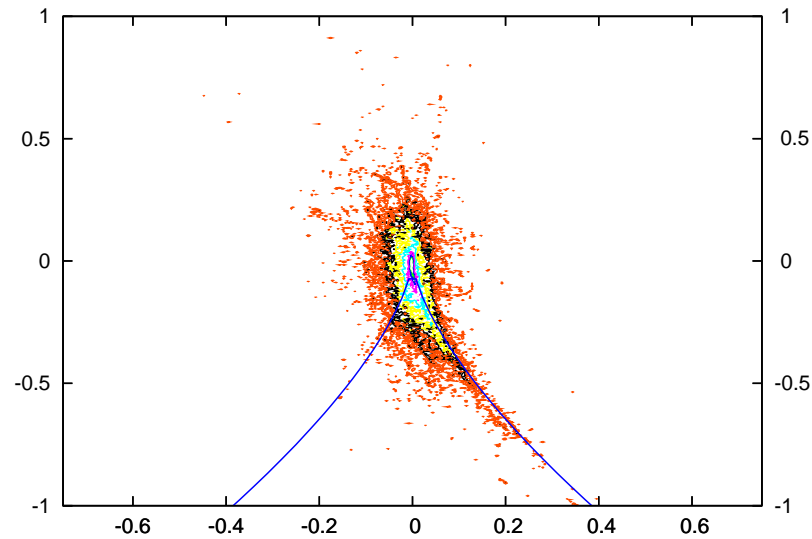
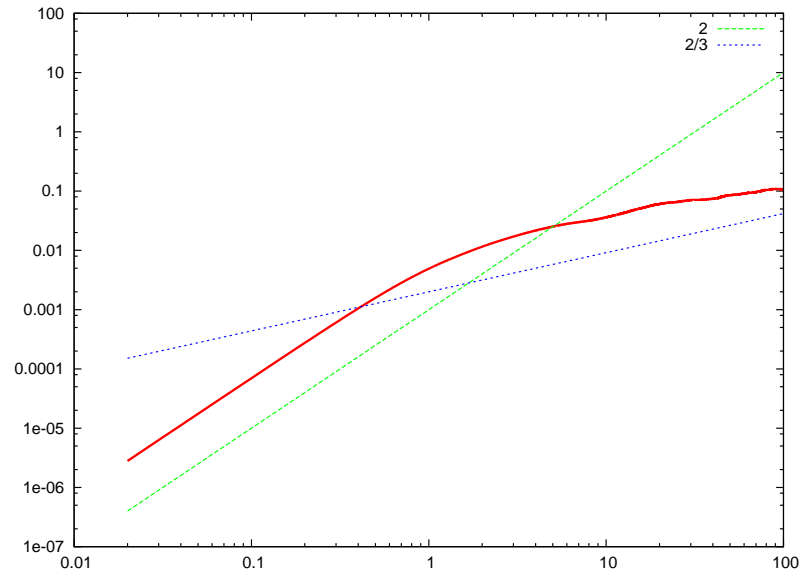
# $\langle \delta u^2(\tau) \rangle$ and $Q - R$ at $x/x_* = 0.367$



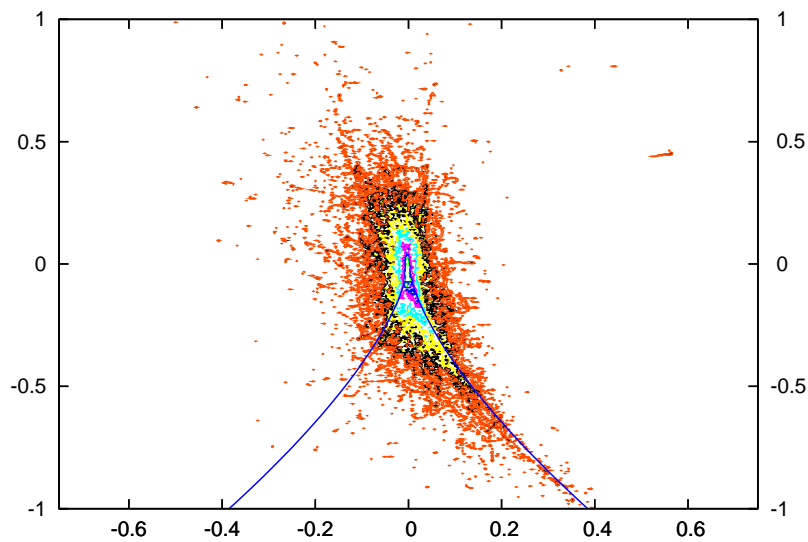
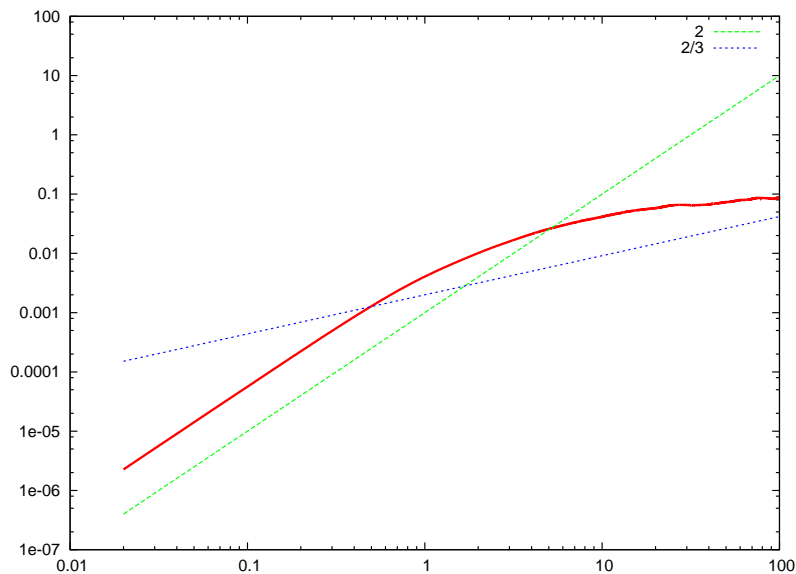
# $\langle \delta u^2(\tau) \rangle$ and $Q - R$ at $x/x_* = 0.420$



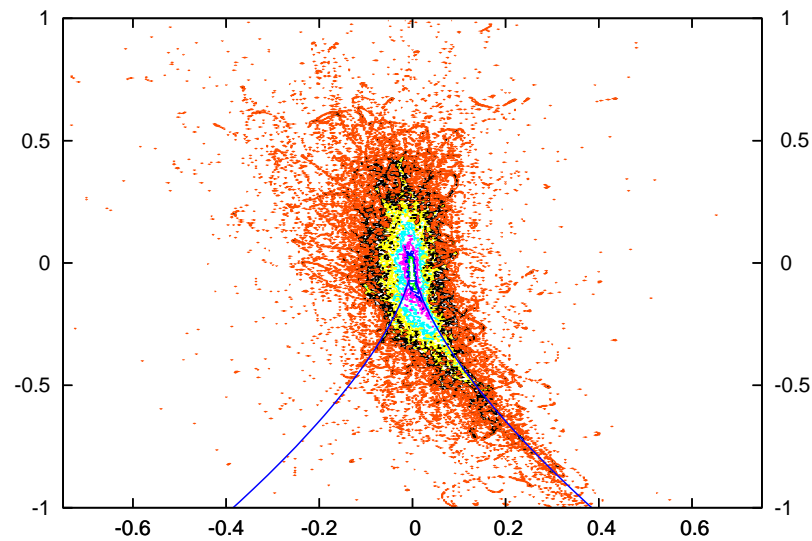
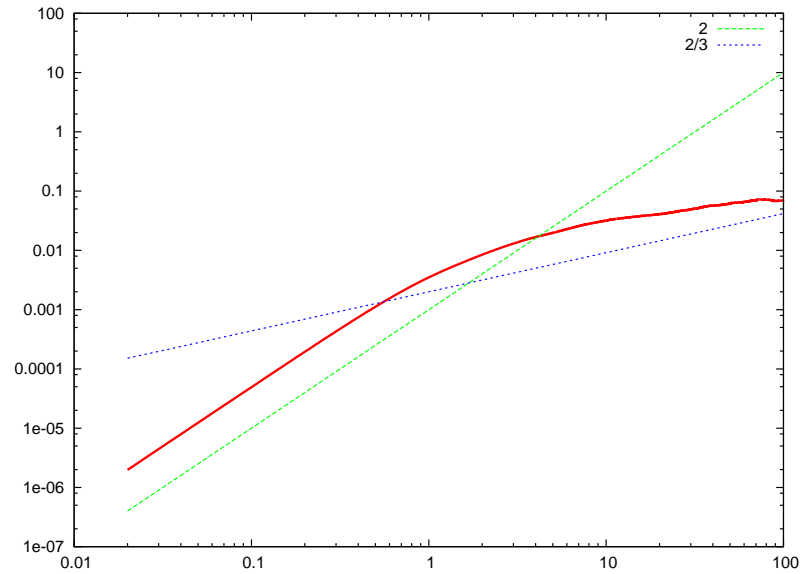
# $\langle \delta u^2(\tau) \rangle$ and $Q - R$ at $x/x_* = 0.472$



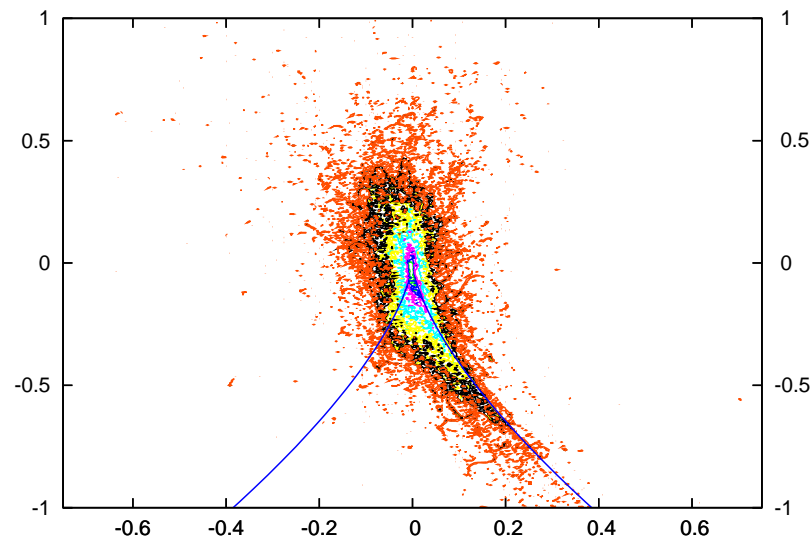
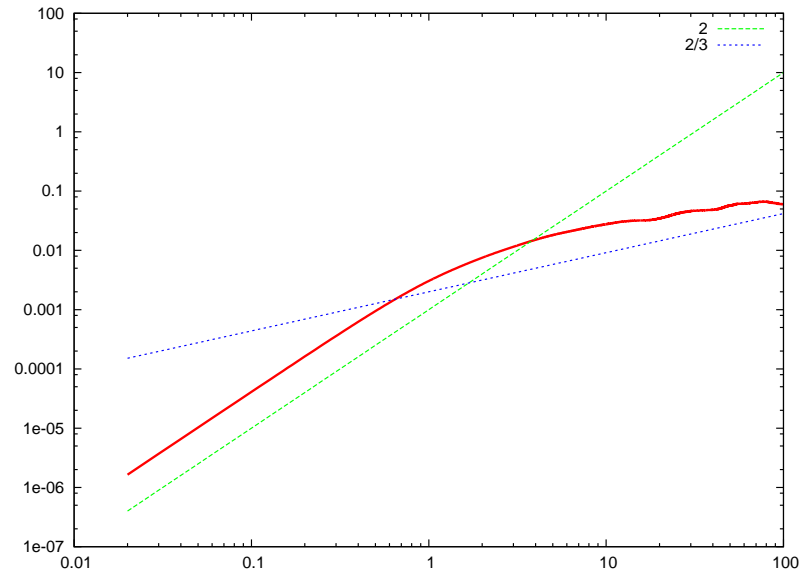
# $\langle \delta u^2(\tau) \rangle$ and $Q - R$ at $x/x_* = 0.525$



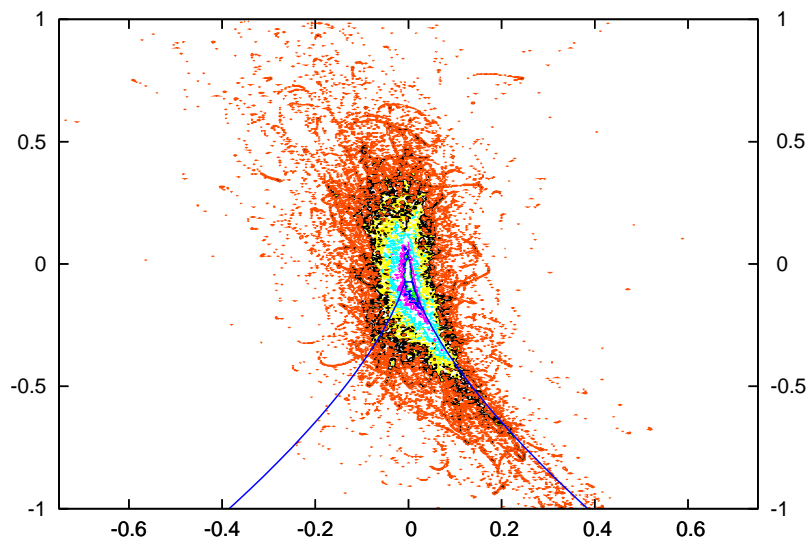
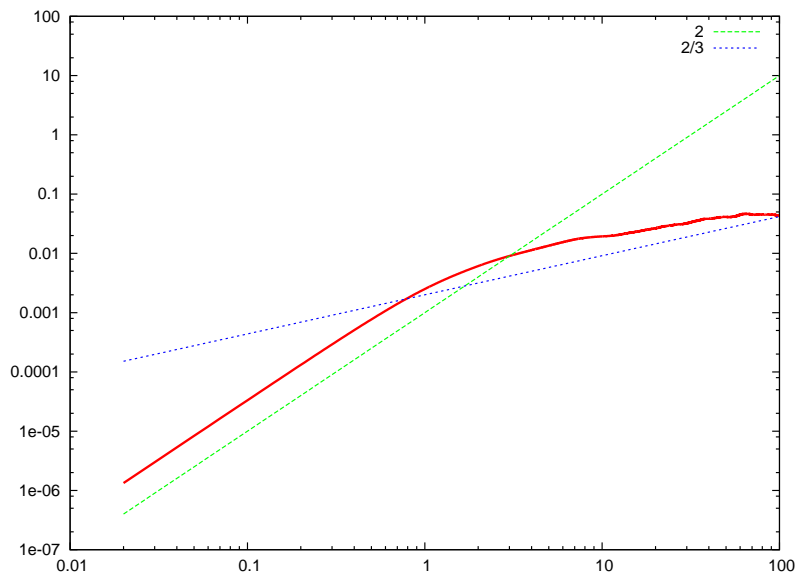
# $\langle \delta u^2(\tau) \rangle$ and $Q - R$ at $x/x_* = 0.577$



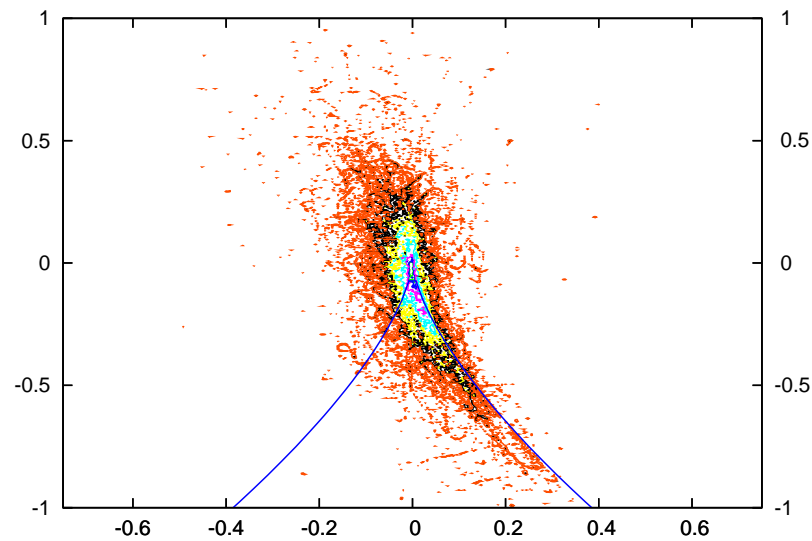
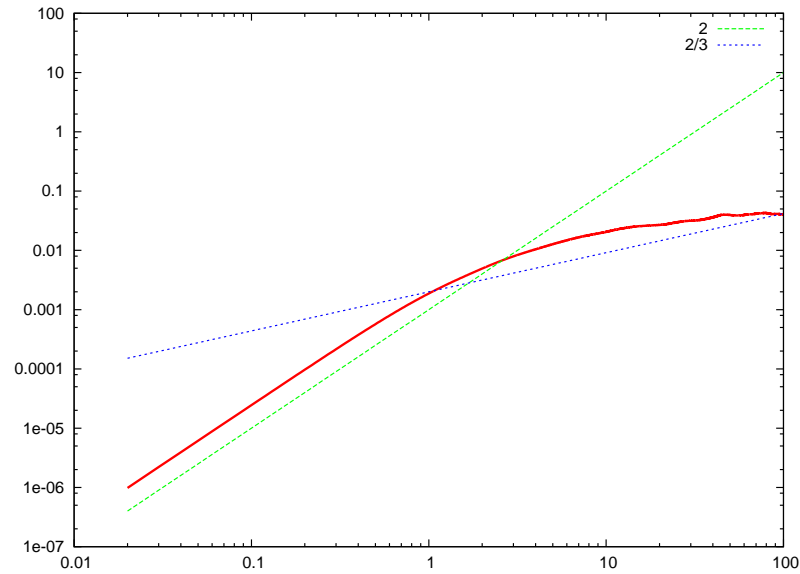
# $\langle \delta u^2(\tau) \rangle$ and $Q - R$ at $x/x_* = 0.630$



# $\langle \delta u^2(\tau) \rangle$ and $Q - R$ at $x/x_* = 0.683$

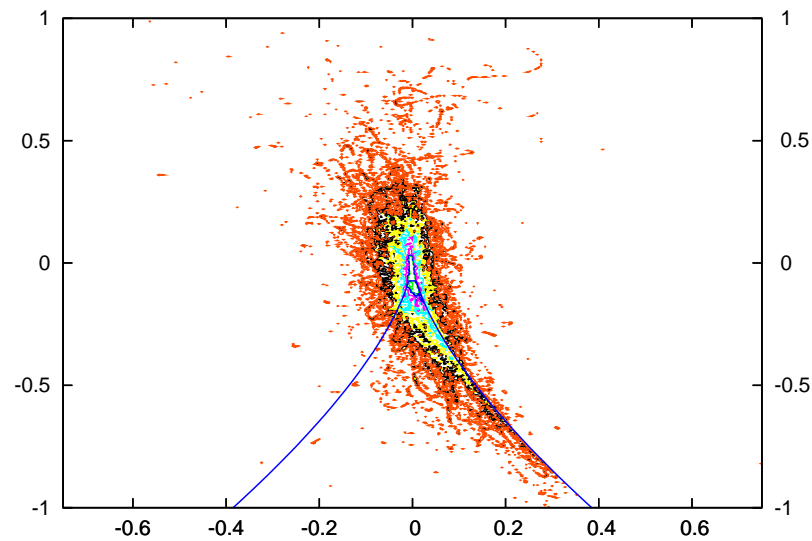
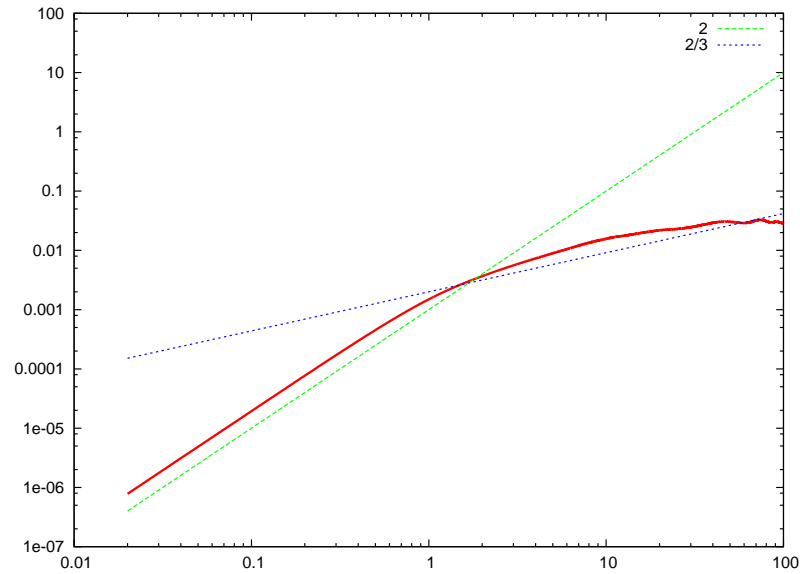


# $\langle \delta u^2(\tau) \rangle$ and $Q - R$ at $x/x_* = 0.735$

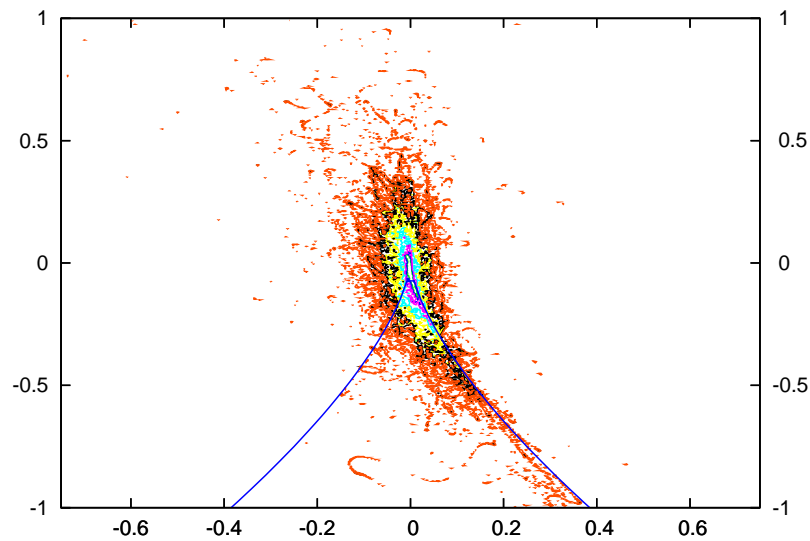
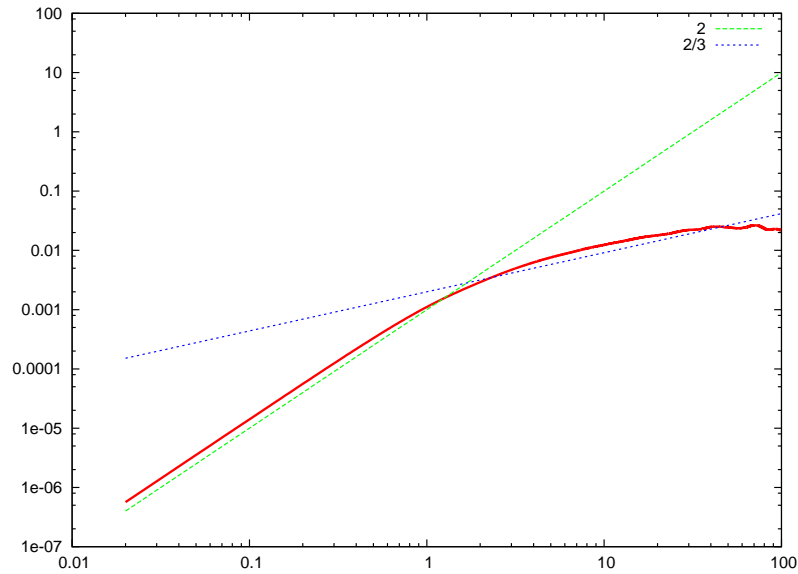




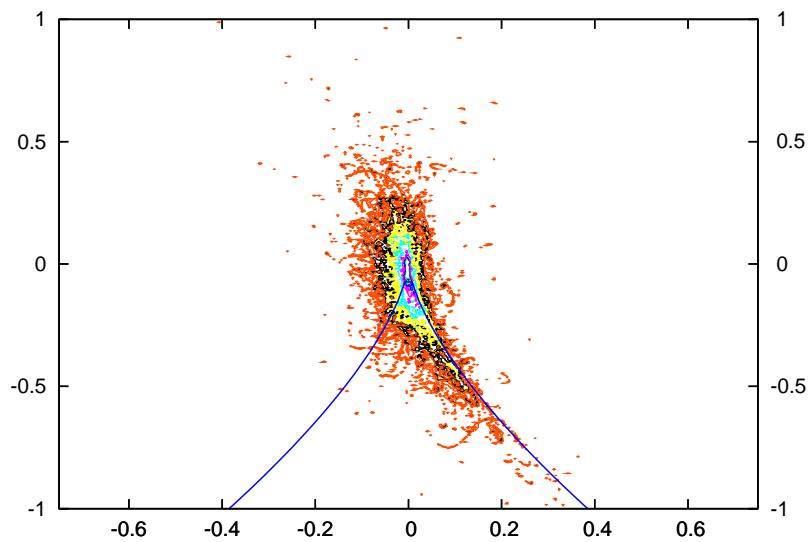
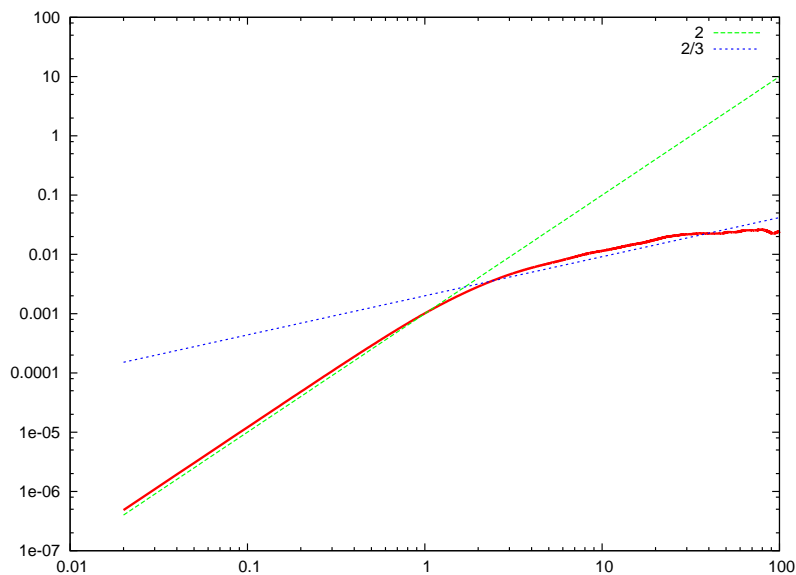
# $\langle \delta u^2(\tau) \rangle$ and $Q - R$ at $x/x_* = 0.788$



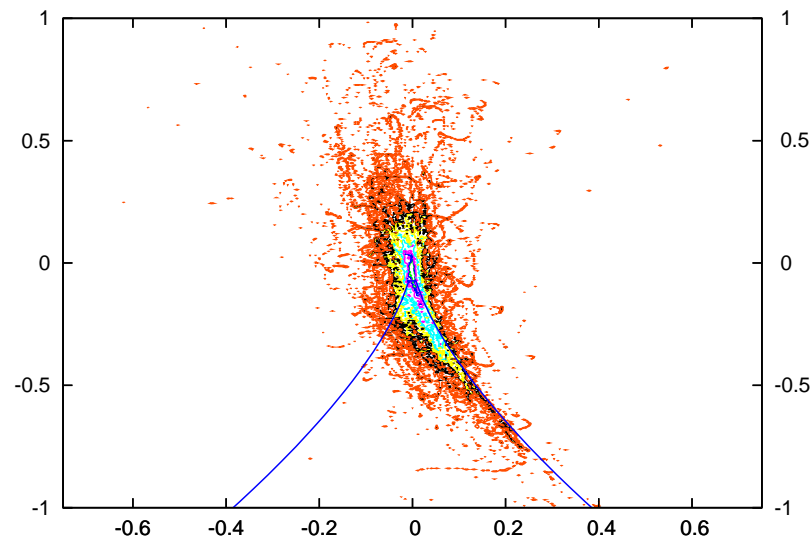
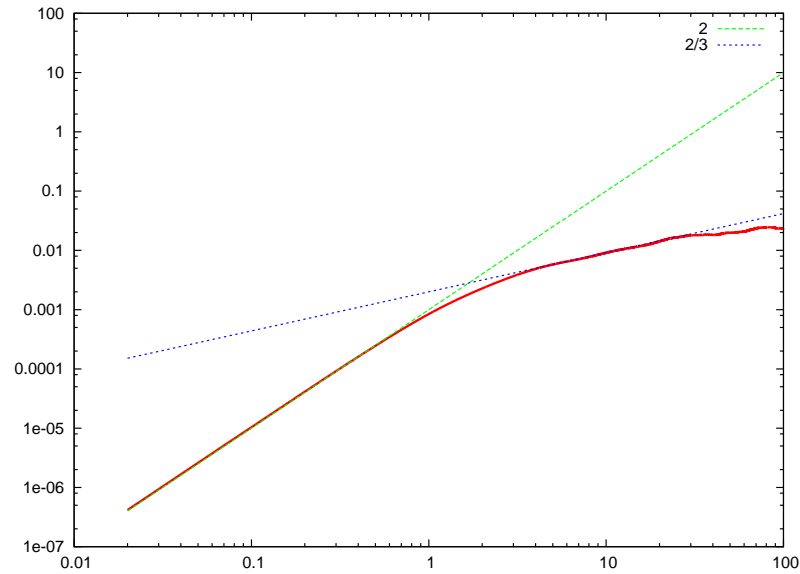
# $\langle \delta u^2(\tau) \rangle$ and $Q - R$ at $x/x_* = 0.840$



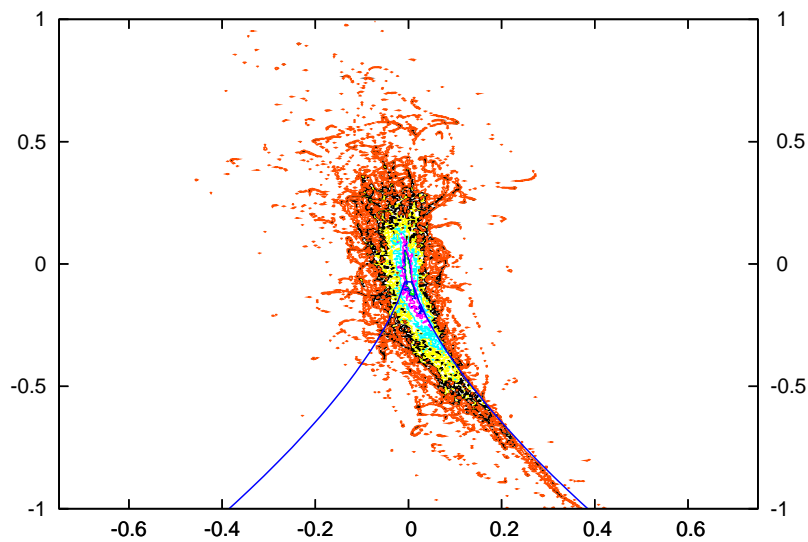
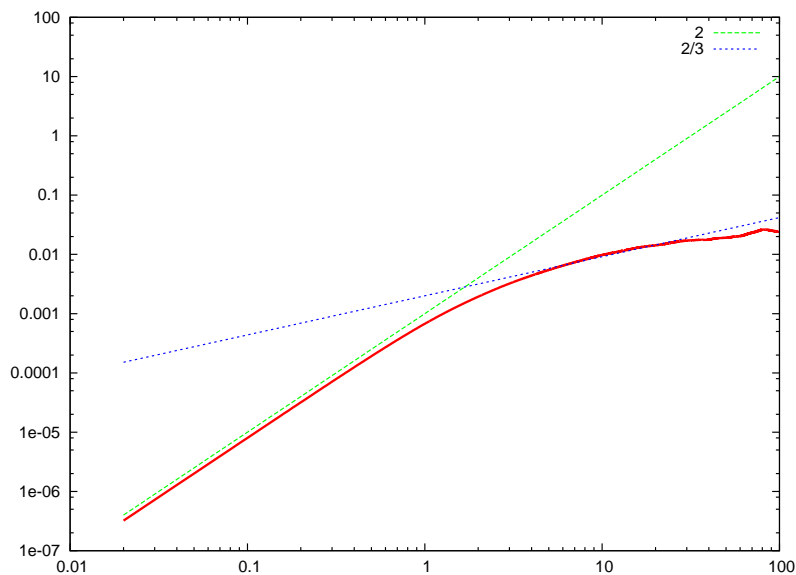
# $\langle \delta u^2(\tau) \rangle$ and $Q - R$ at $x/x_* = 0.893$



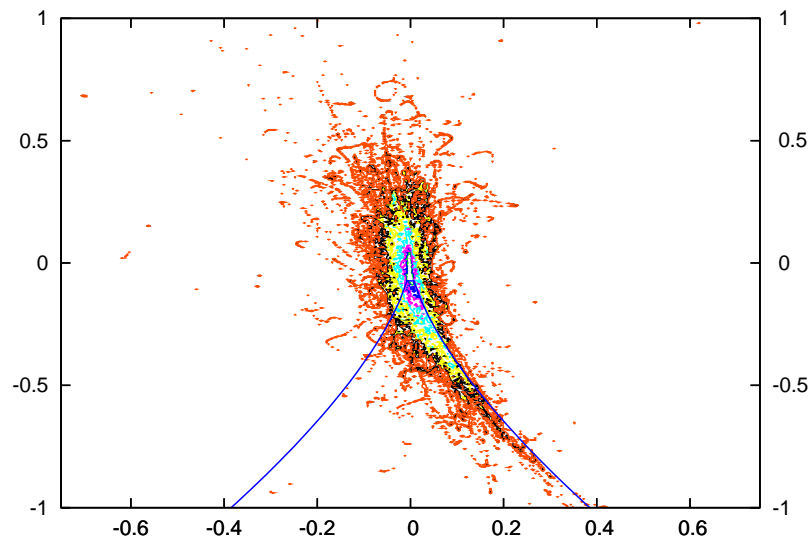
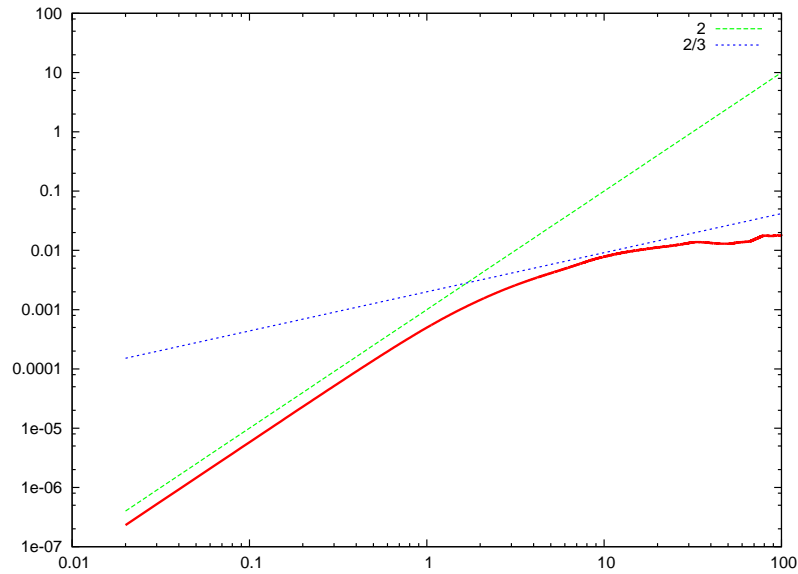
# $\langle \delta u^2(\tau) \rangle$ and $Q - R$ at $x/x_* = 0.945$



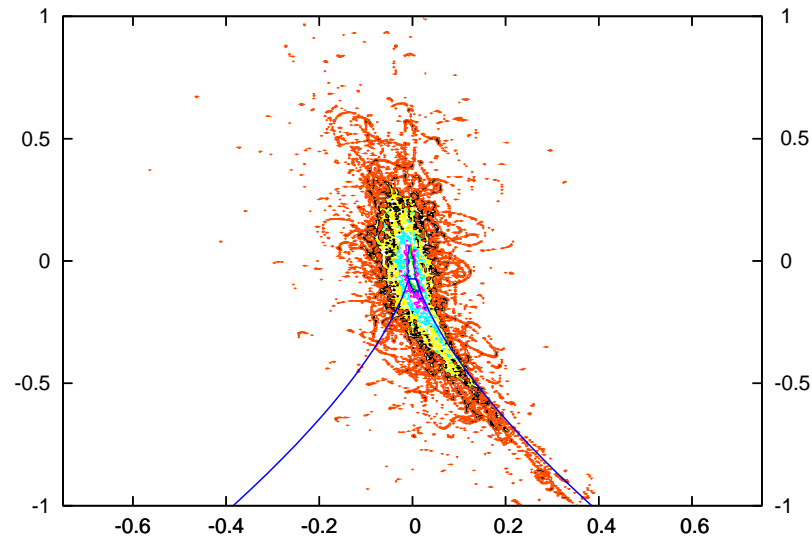
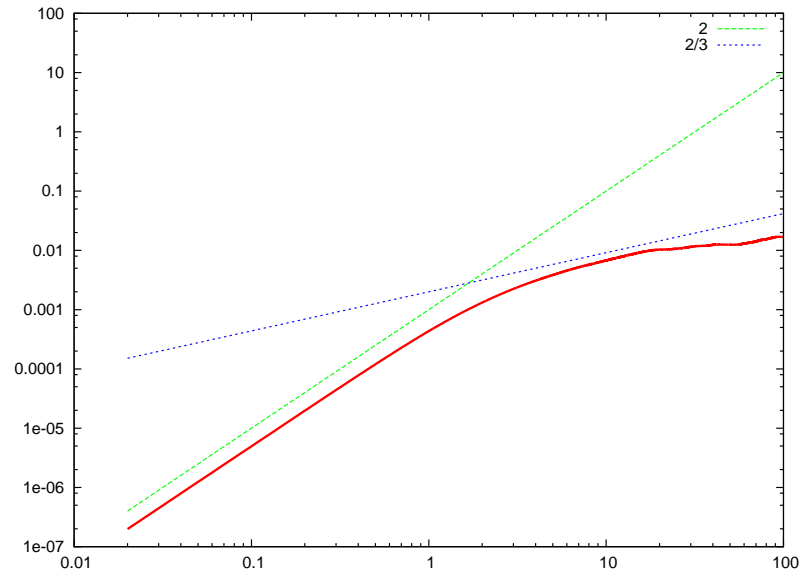
$\langle \delta u^2(\tau) \rangle$  and  $Q - R$  at  $x/x_* = 0.998$



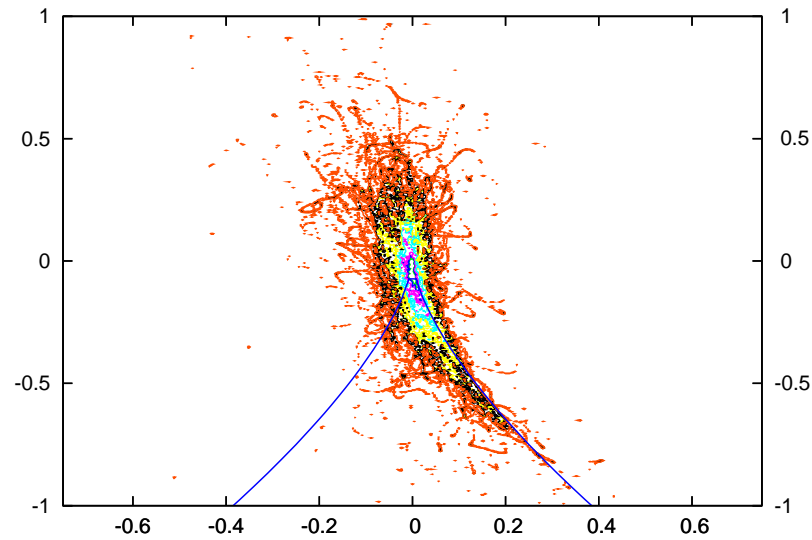
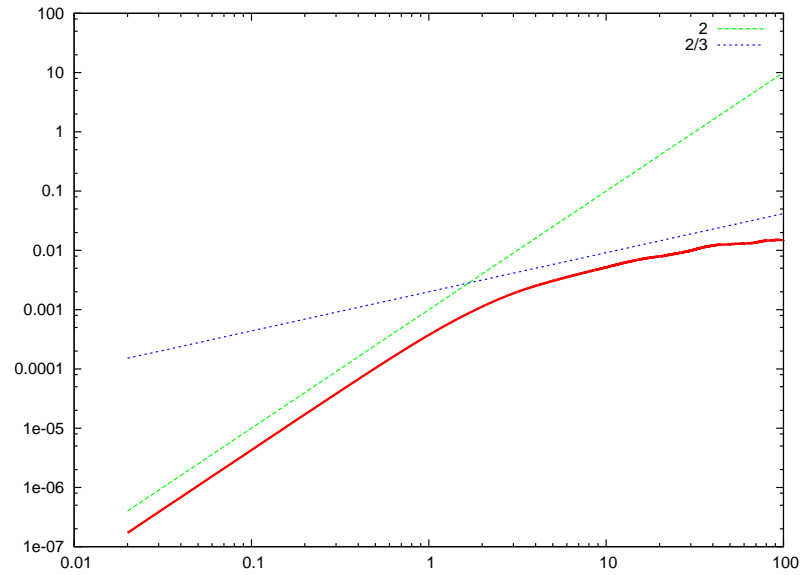
# $\langle \delta u^2(\tau) \rangle$ and $Q - R$ at $x/x_* = 1.050$



$\langle \delta u^2(\tau) \rangle$  and  $Q - R$  at  $x/x_* = 1.103$

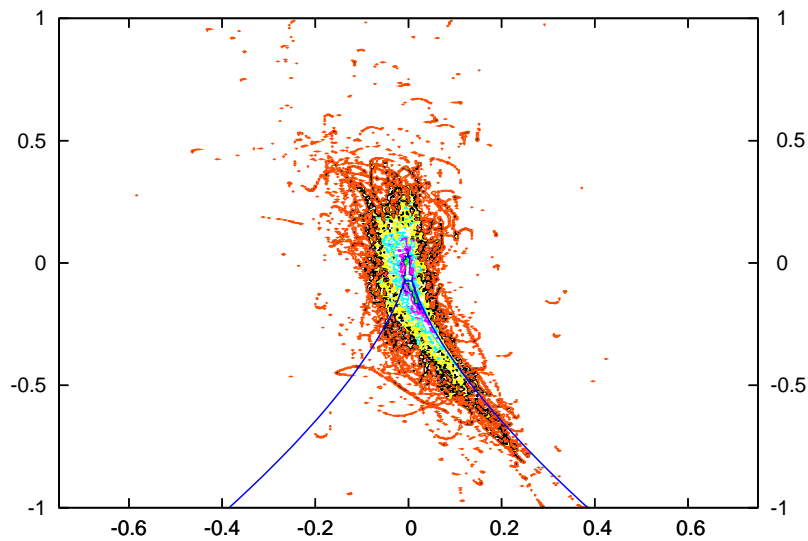
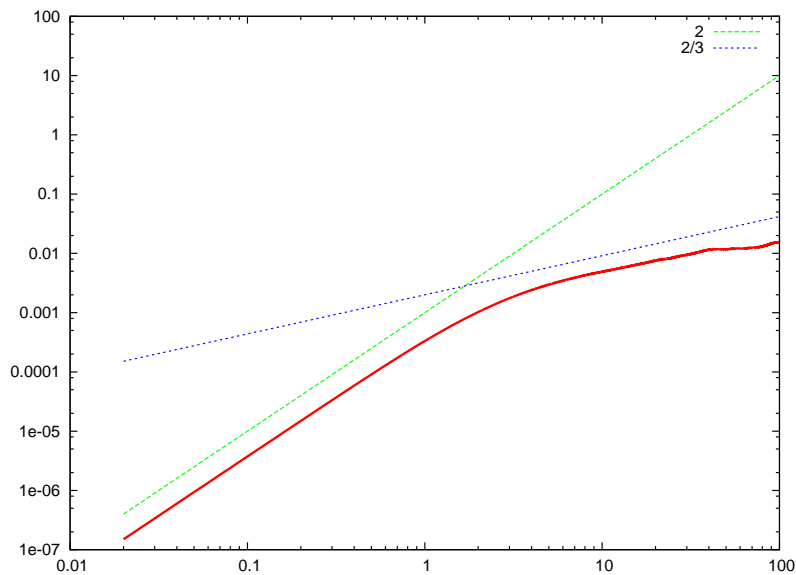


$\langle \delta u^2(\tau) \rangle$  and  $Q - R$  at  $x/x_* = 1.155$

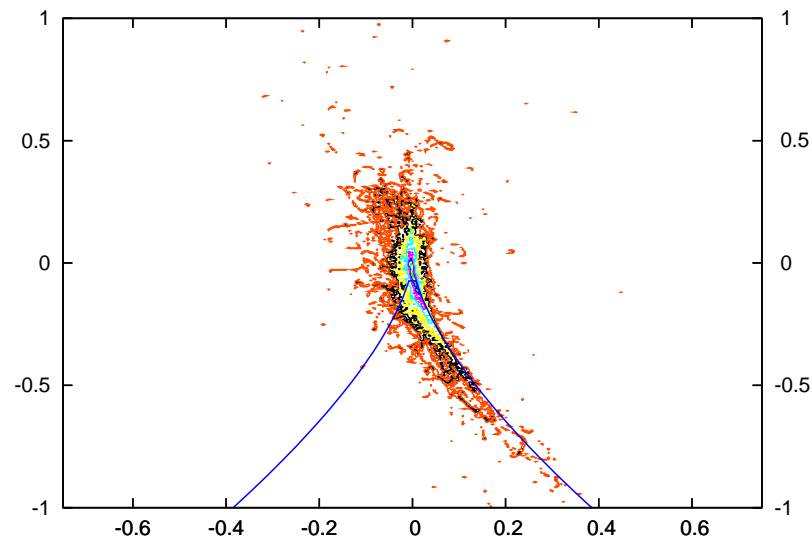
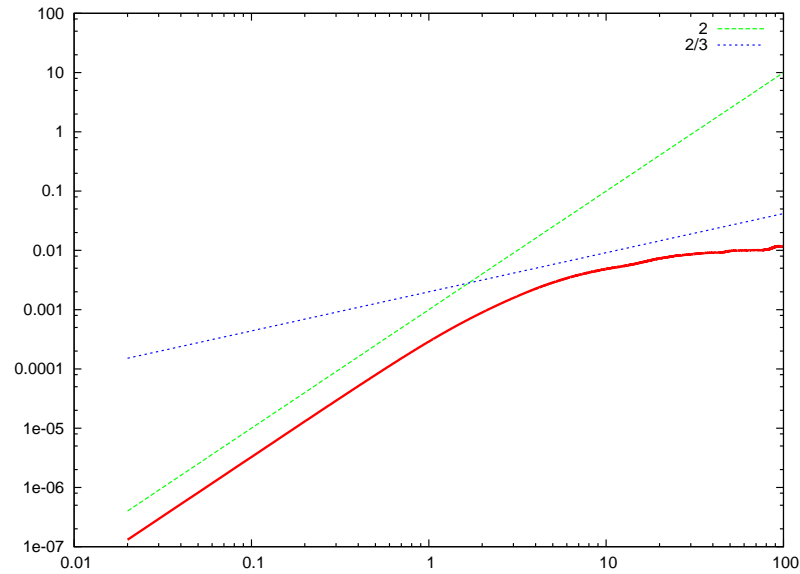




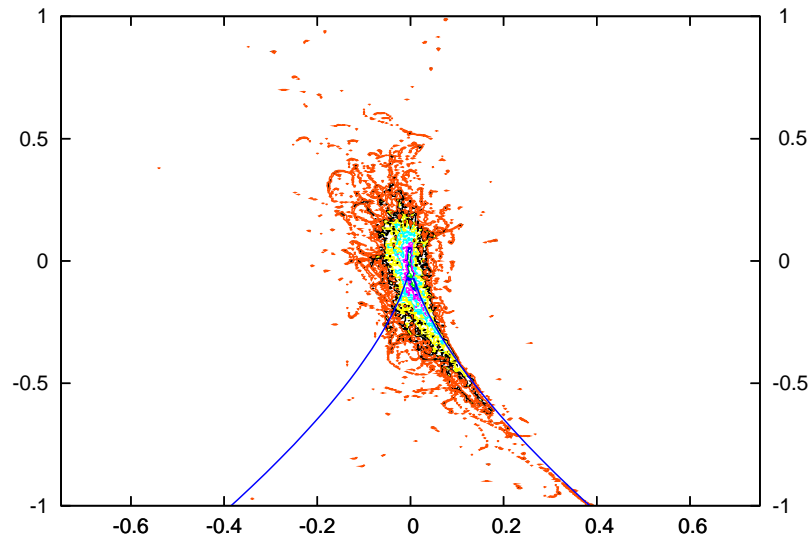
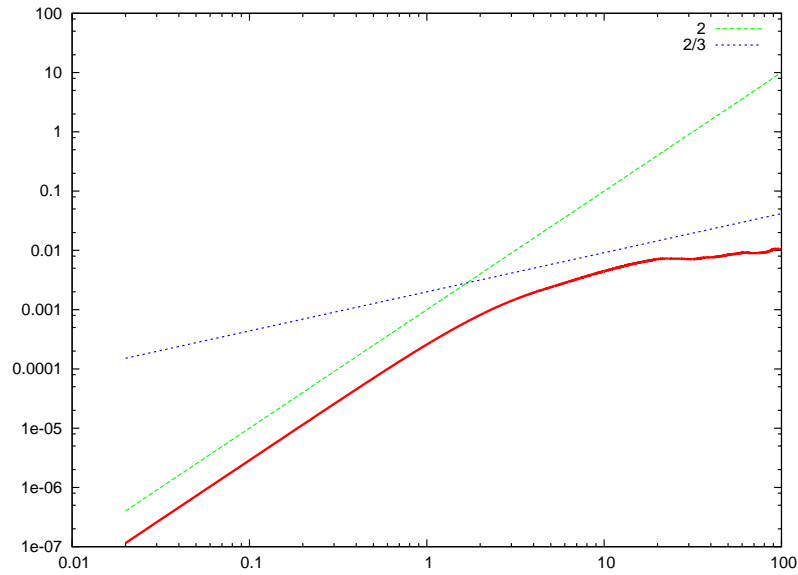
$\langle \delta u^2(\tau) \rangle$  and  $Q - R$  at  $x/x_* = 1.208$



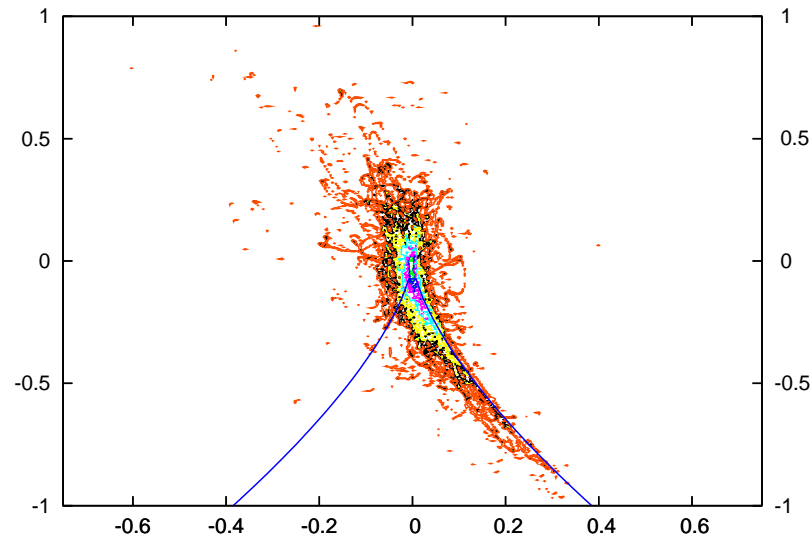
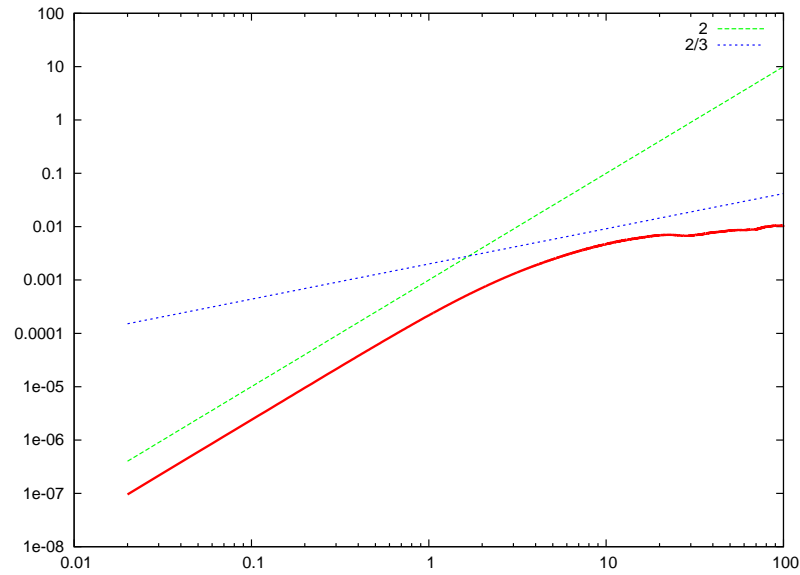
$\langle \delta u^2(\tau) \rangle$  and  $Q - R$  at  $x/x_* = 1.261$



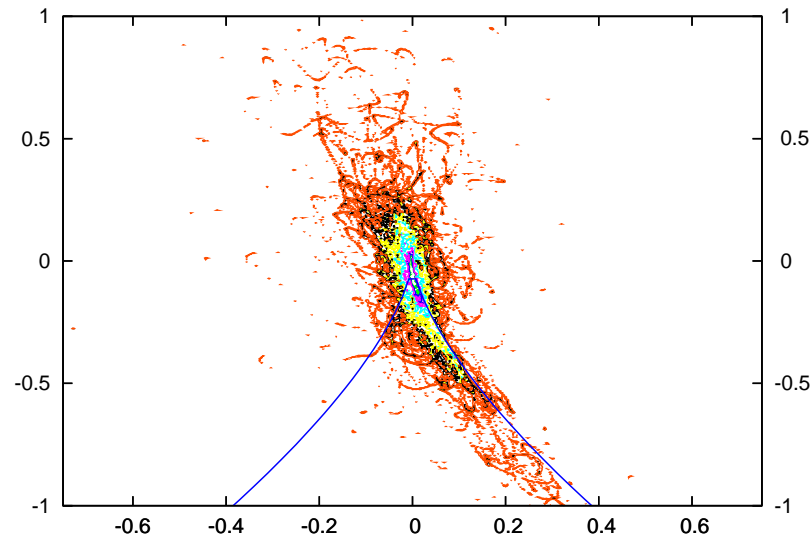
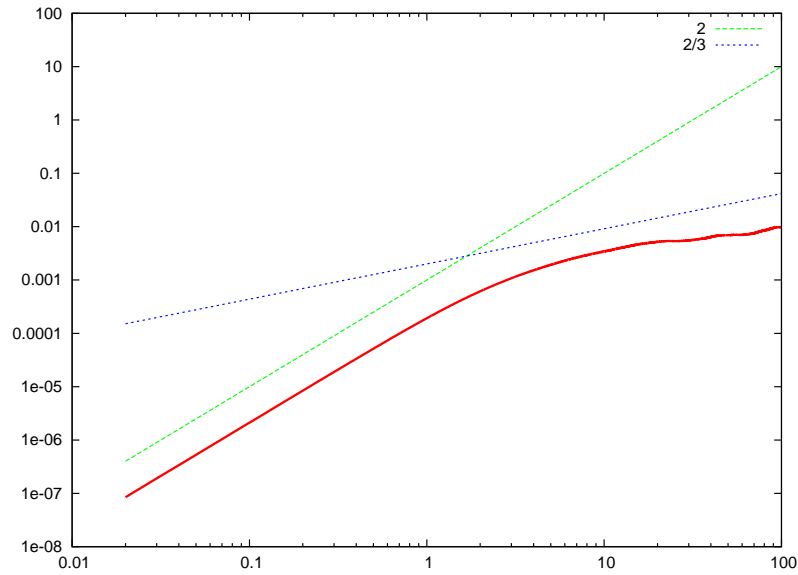
# $\langle \delta u^2(\tau) \rangle$ and $Q - R$ at $x/x_* = 1.313$



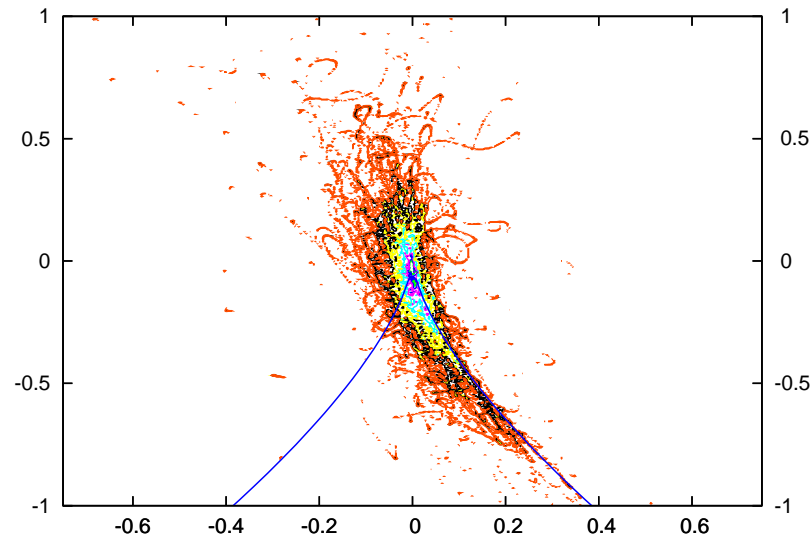
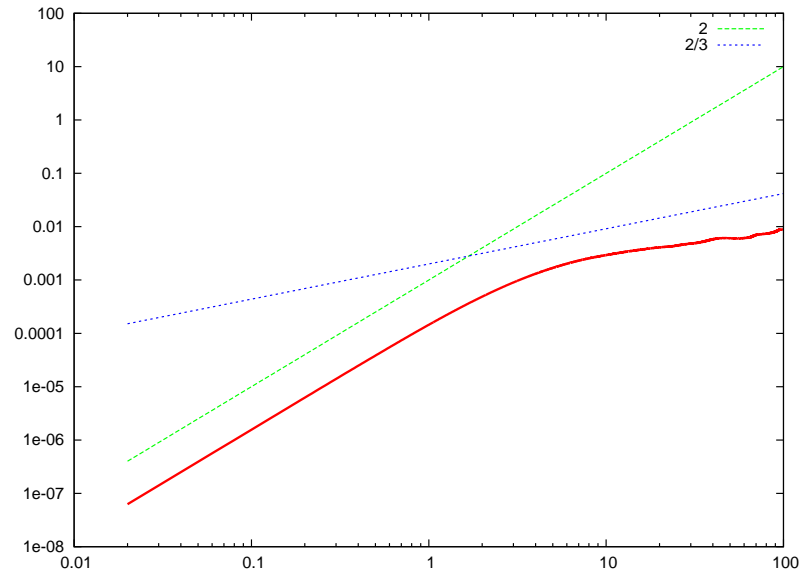
$\langle \delta u^2(\tau) \rangle$  and  $Q - R$  at  $x/x_* = 1.366$



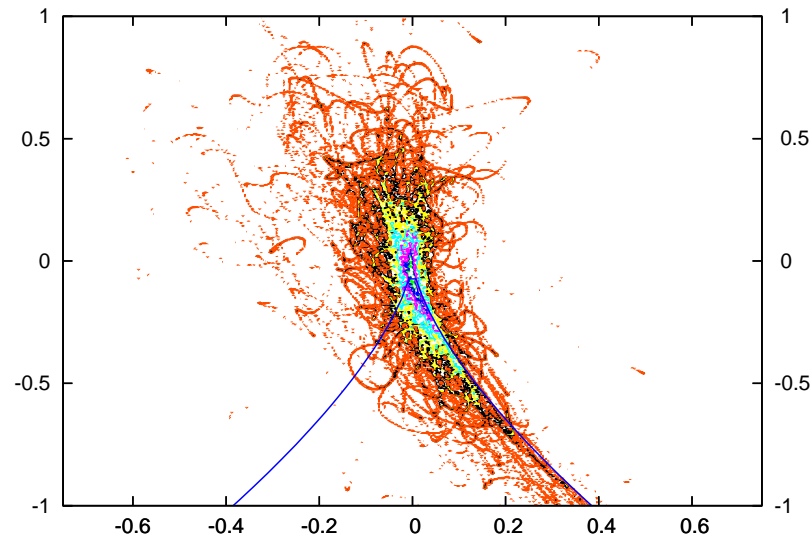
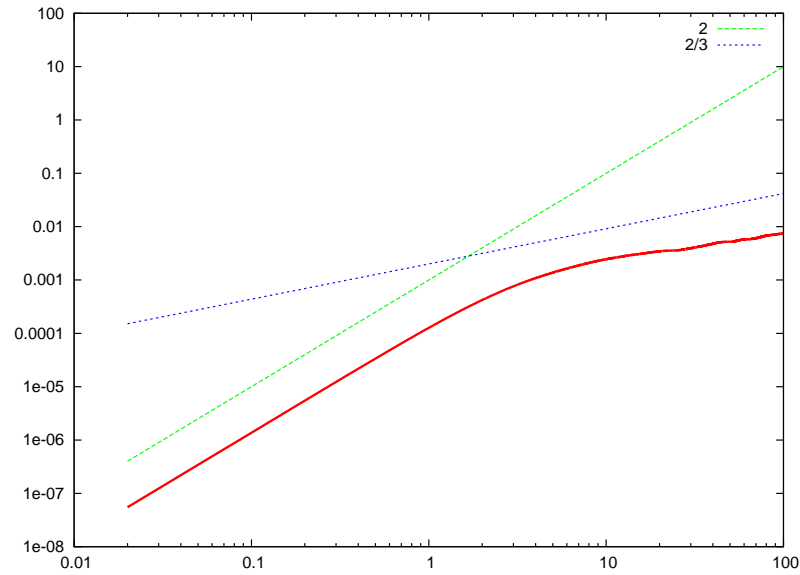
# $\langle \delta u^2(\tau) \rangle$ and $Q - R$ at $x/x_* = 1.418$



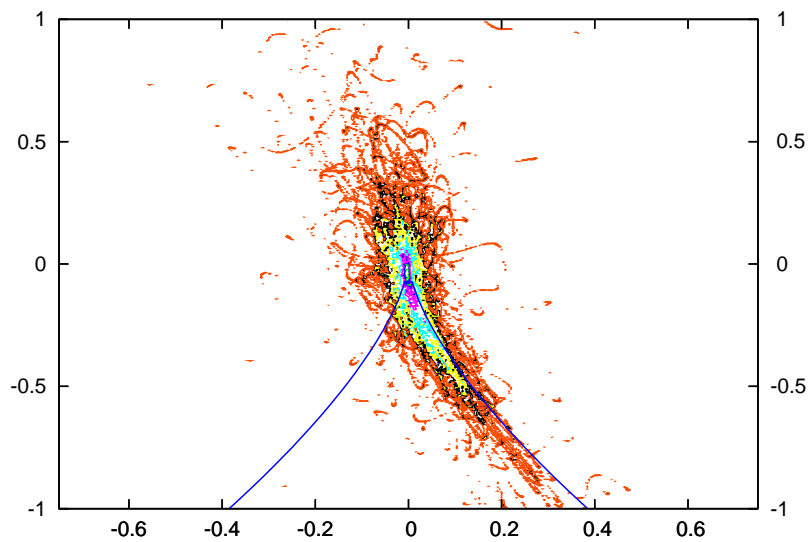
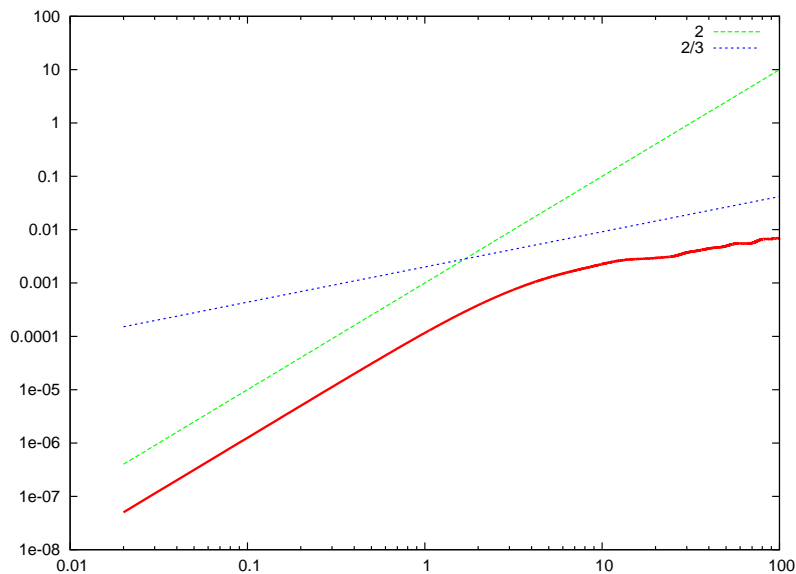
# $\langle \delta u^2(\tau) \rangle$ and $Q - R$ at $x/x_* = 1.471$



# $\langle \delta u^2(\tau) \rangle$ and $Q - R$ at $x/x_* = 1.523$

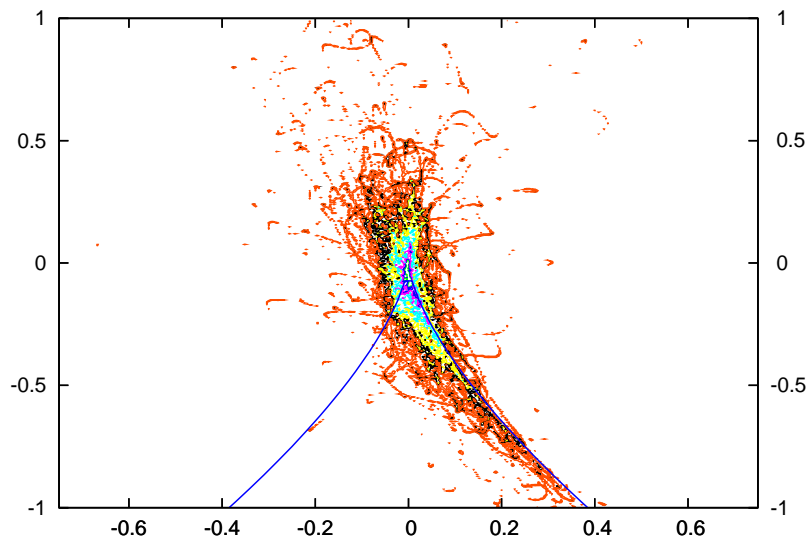
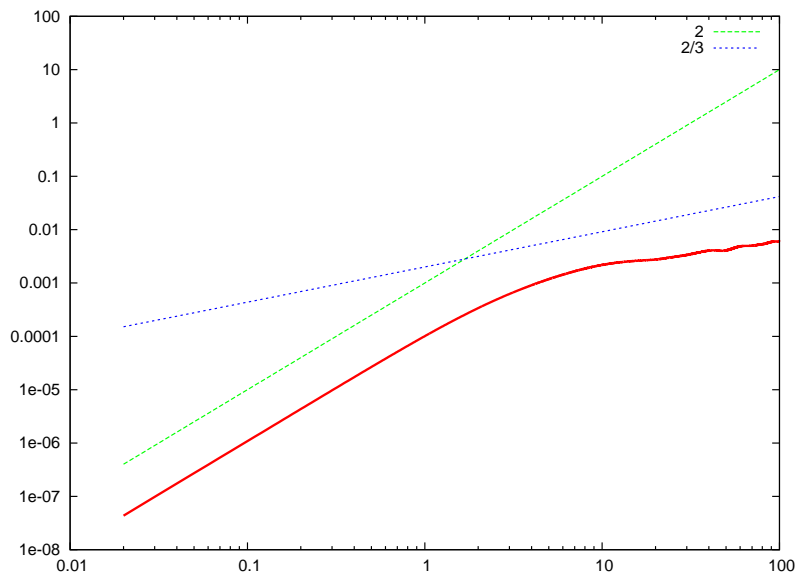


# $\langle \delta u^2(\tau) \rangle$ and $Q - R$ at $x/x_* = 1.576$

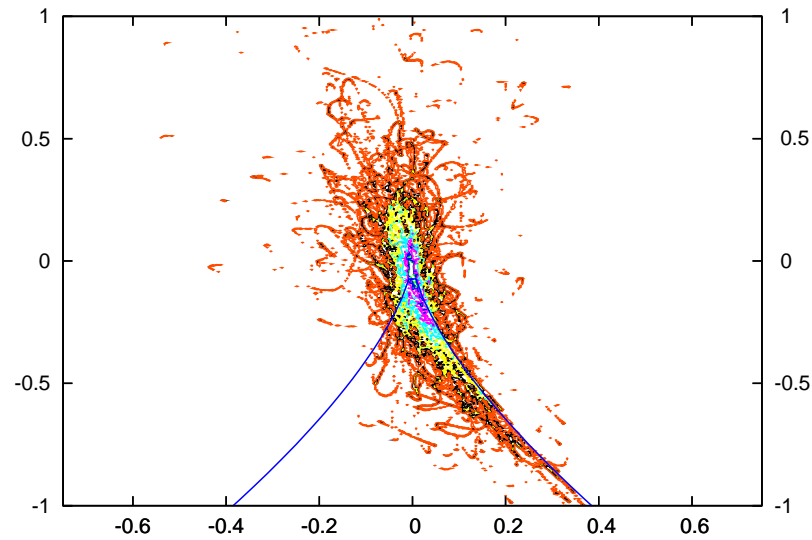
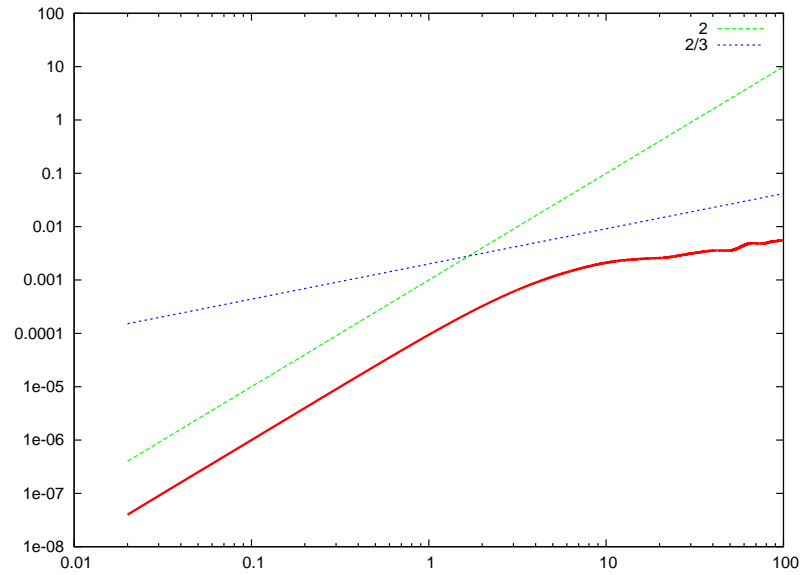




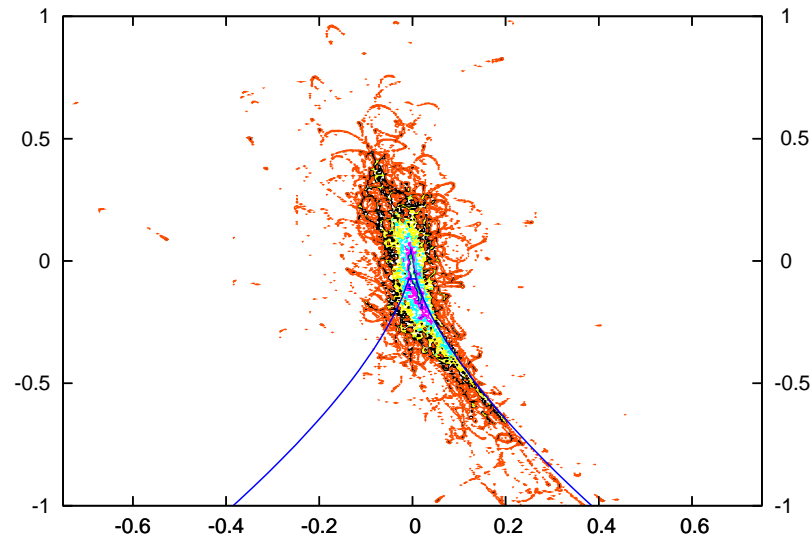
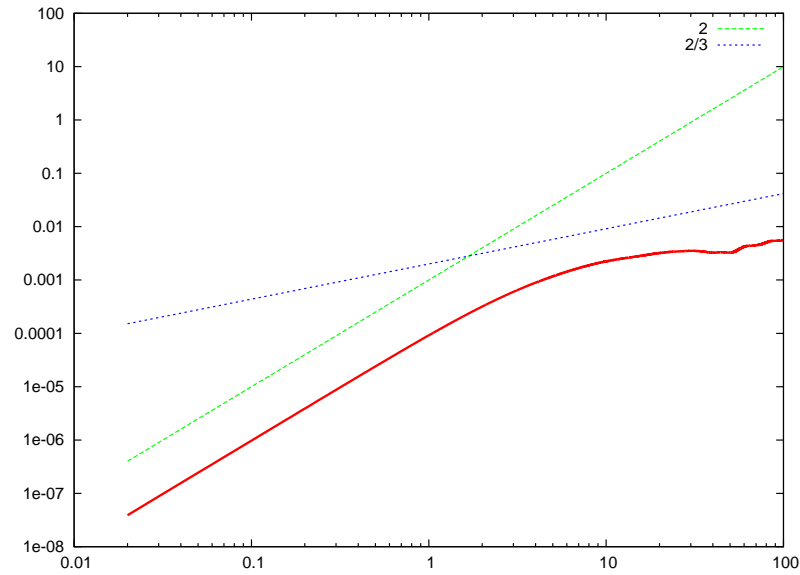
$\langle \delta u^2(\tau) \rangle$  and  $Q - R$  at  $x/x_* = 1.628$



# $\langle \delta u^2(\tau) \rangle$ and $Q - R$ at $x/x_* = 1.681$

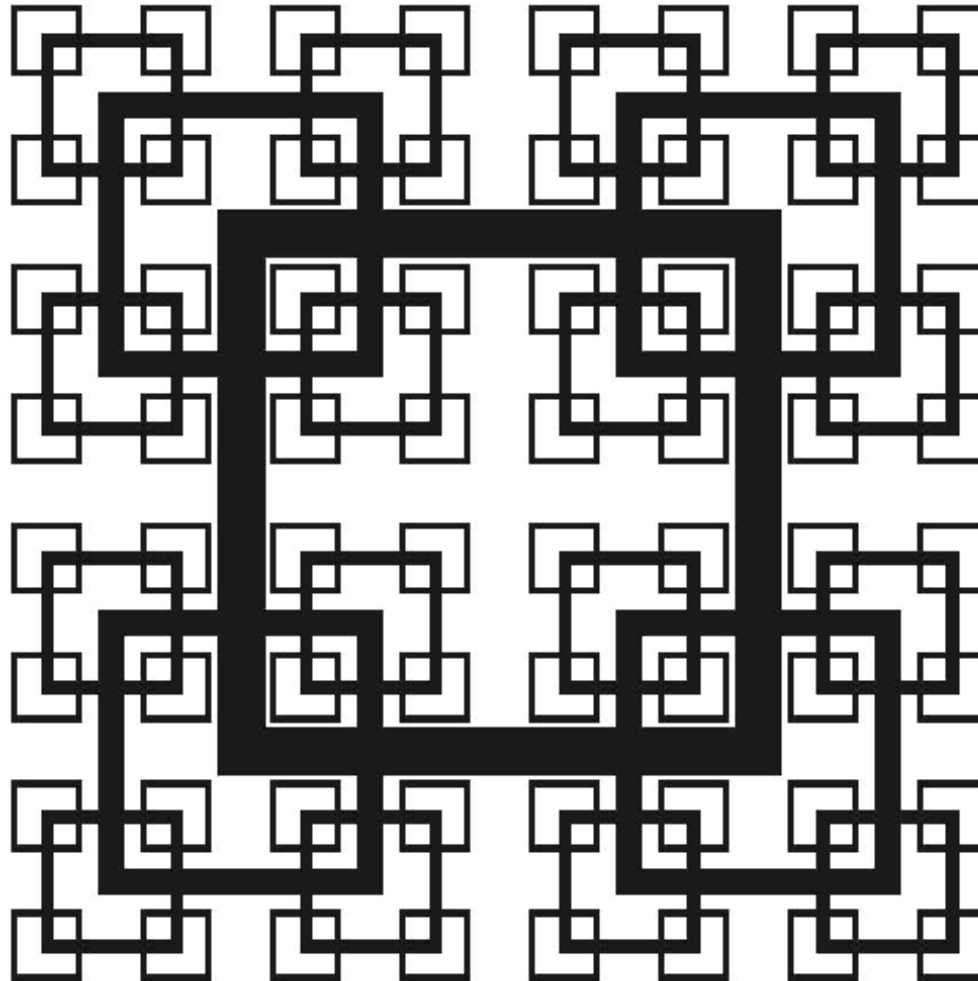


# $\langle \delta u^2(\tau) \rangle$ and $Q - R$ at $x/x_* = 1.733$

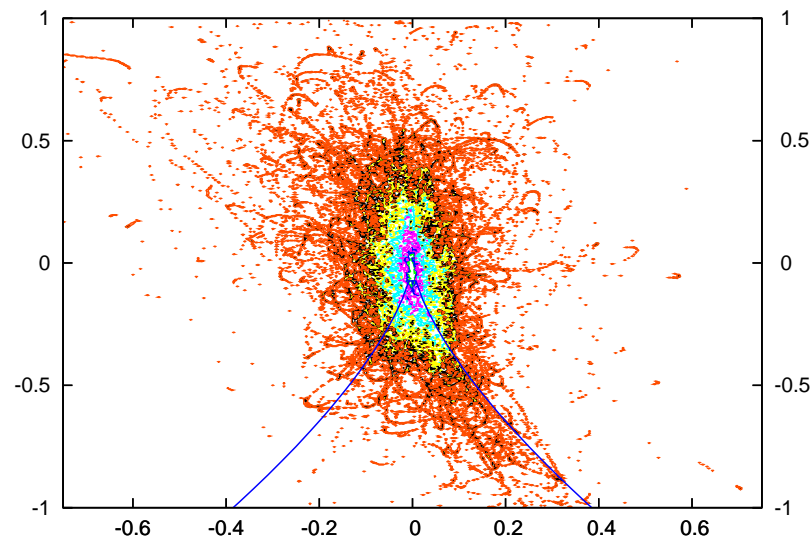
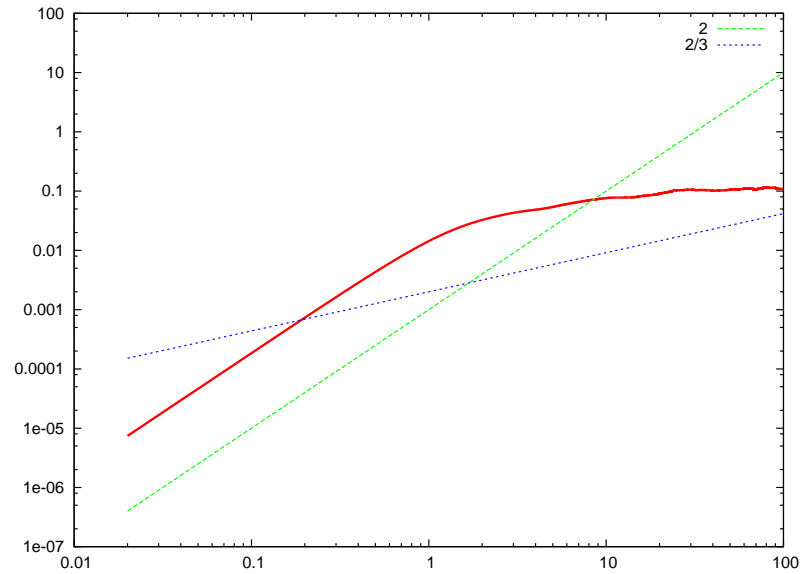


# Next inside wake of big bars

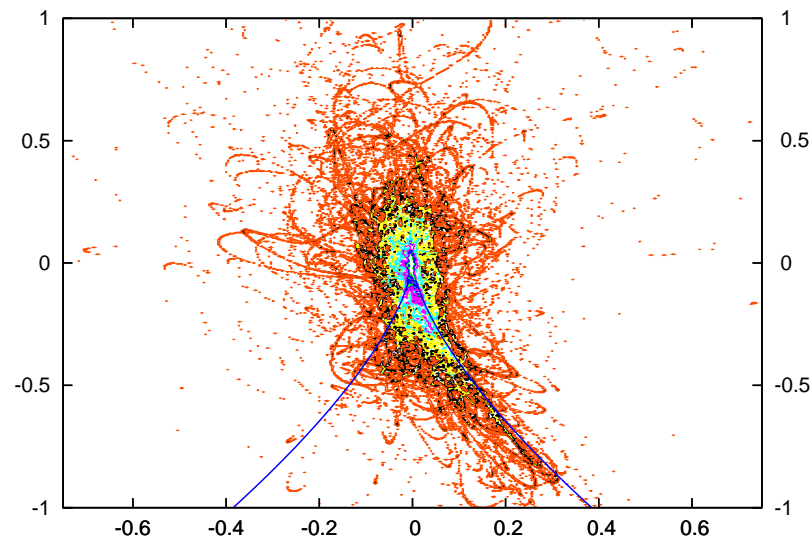
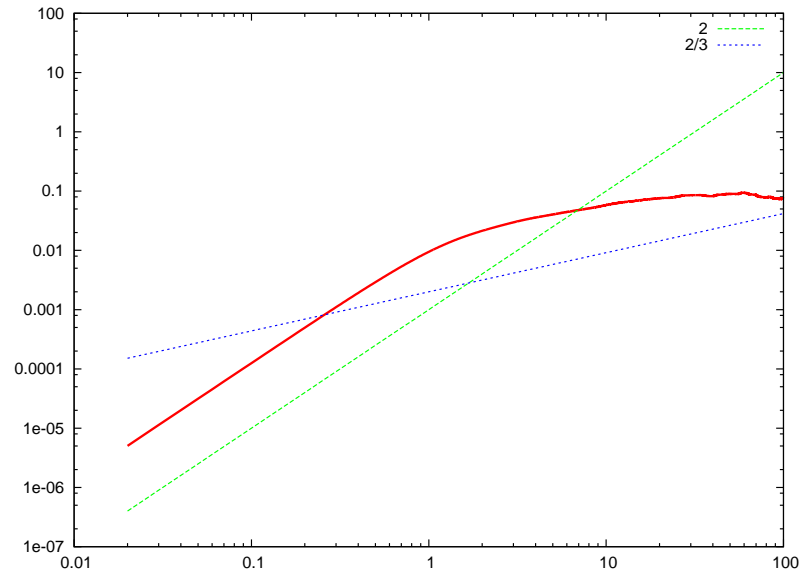
Previous plots were taken along the centreline.  
Next plots are taken along the line normal to the grid and  
crossing a biggest bar at the middle.



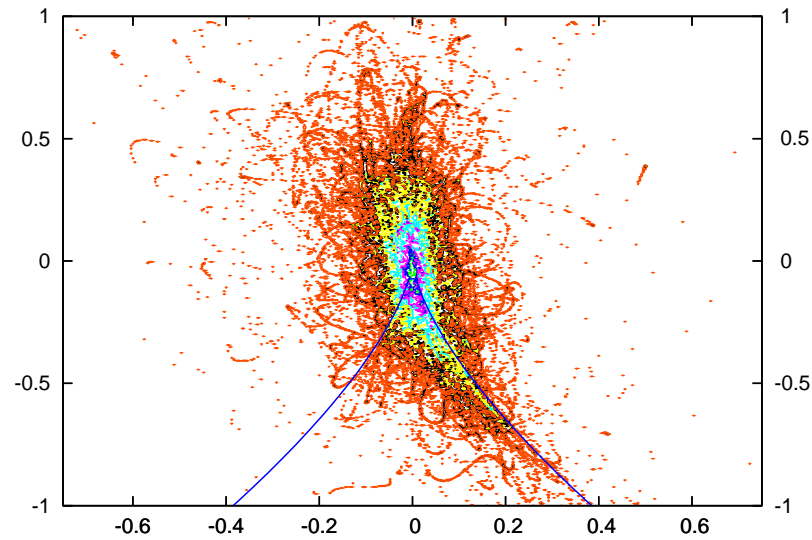
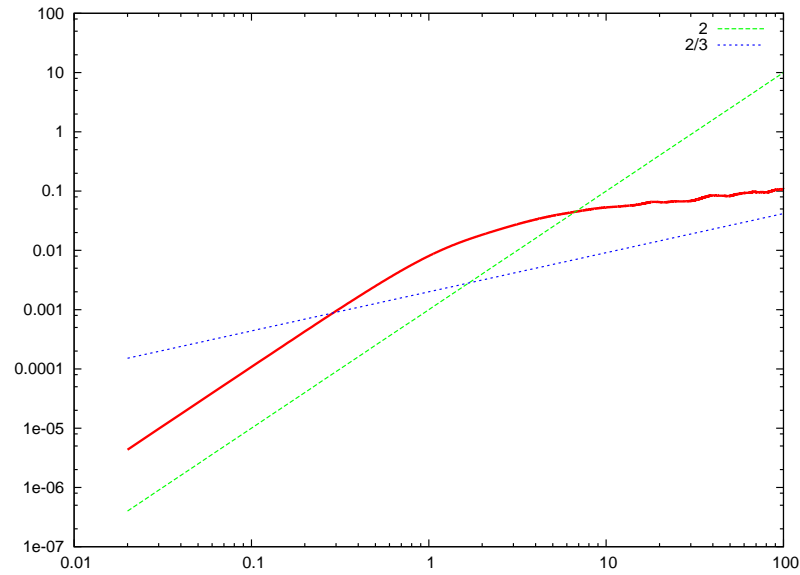
$\langle \delta u^2(\tau) \rangle$  and  $Q - R$  at  $x/x_* = 0.052$



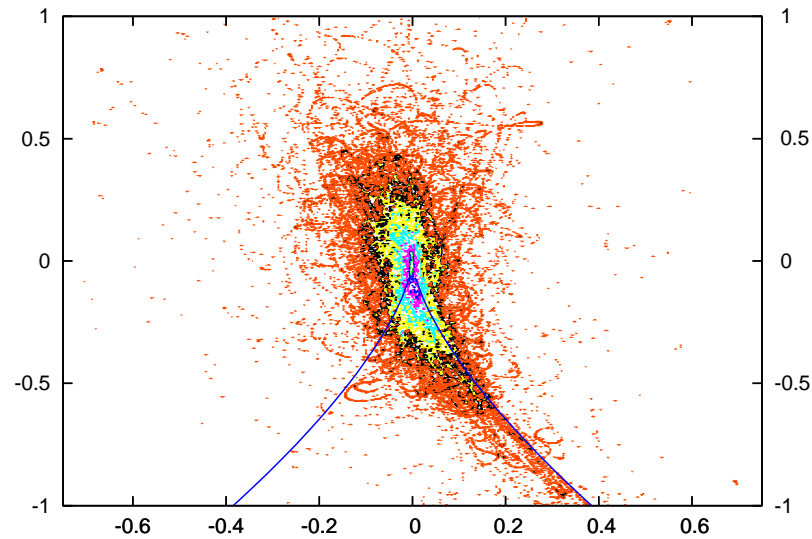
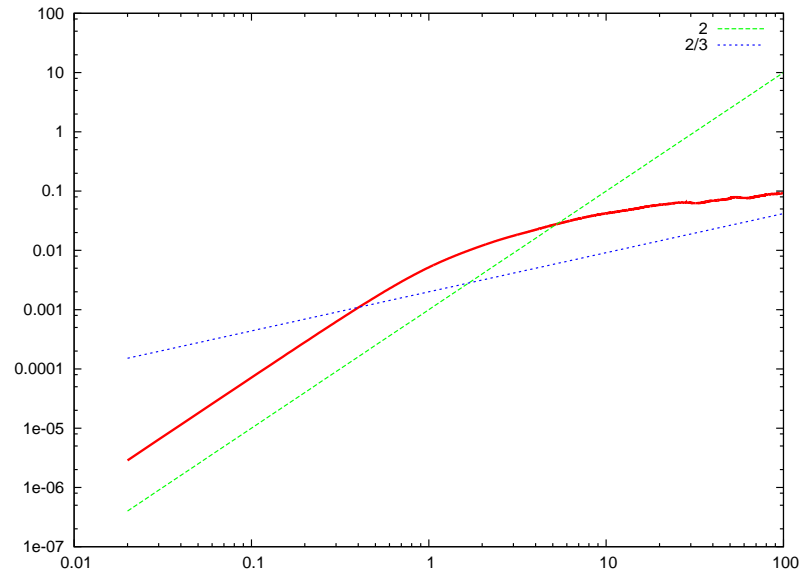
# $\langle \delta u^2(\tau) \rangle$ and $Q - R$ at $x/x_* = 0.105$



$\langle \delta u^2(\tau) \rangle$  and  $Q - R$  at  $x/x_* = 0.157$

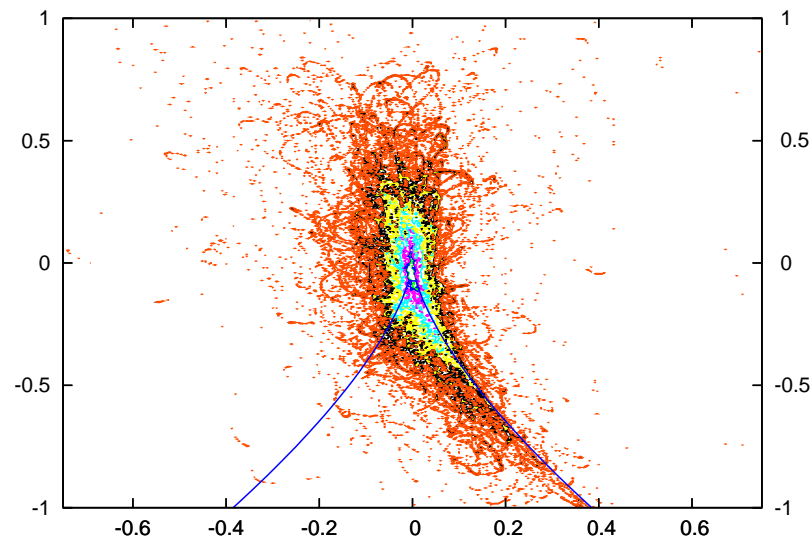
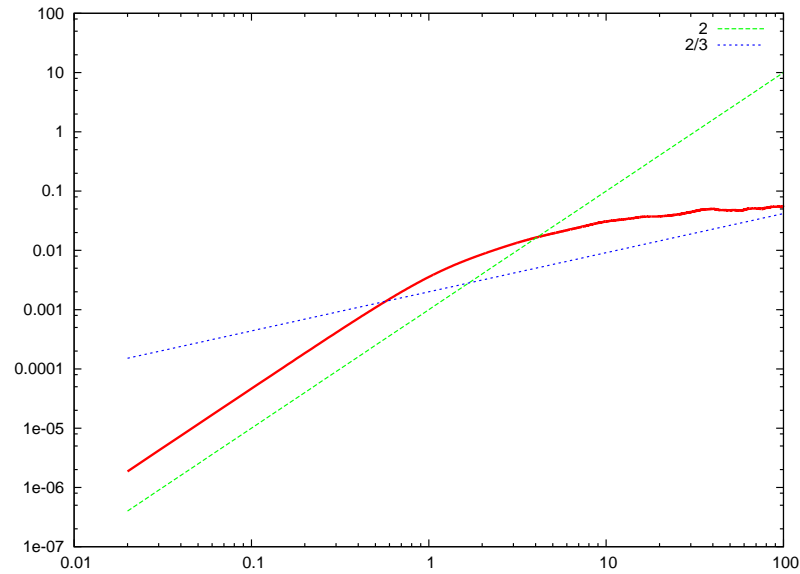


# $\langle \delta u^2(\tau) \rangle$ and $Q - R$ at $x/x_* = 0.210$

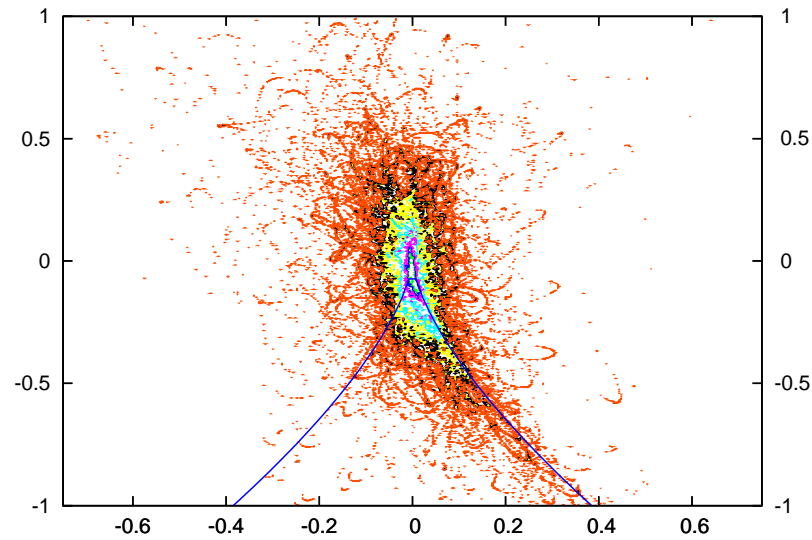
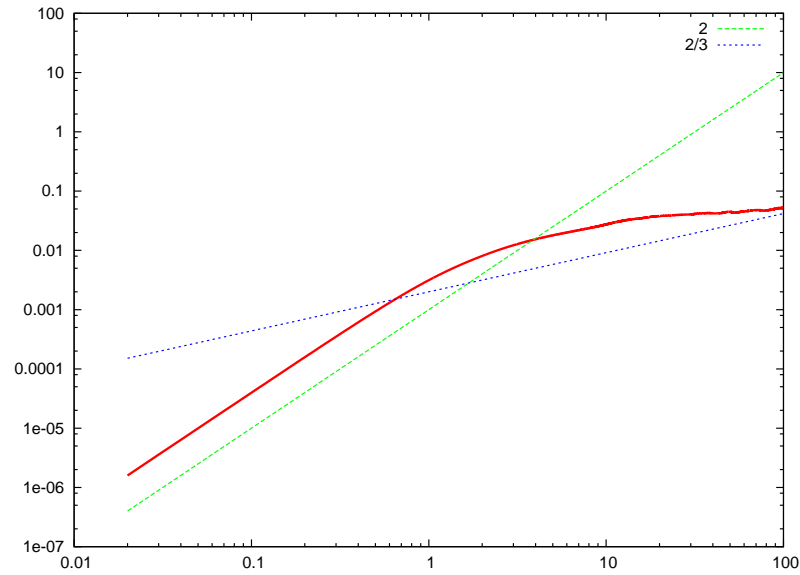




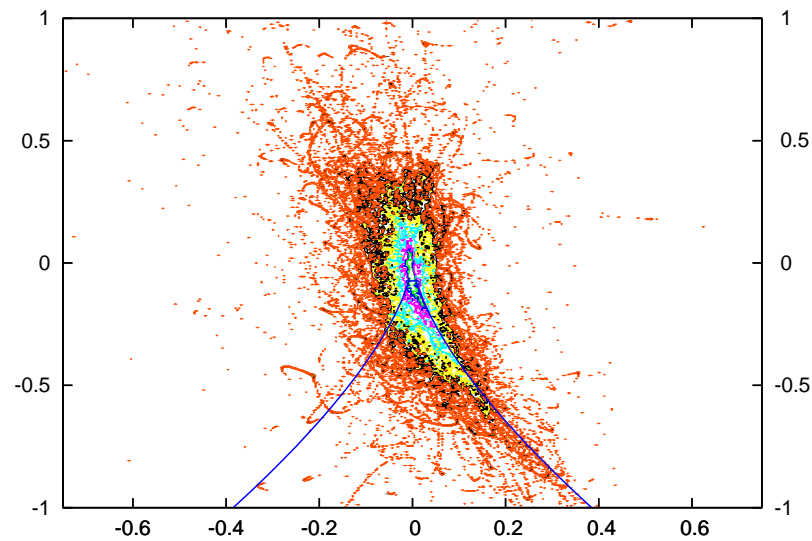
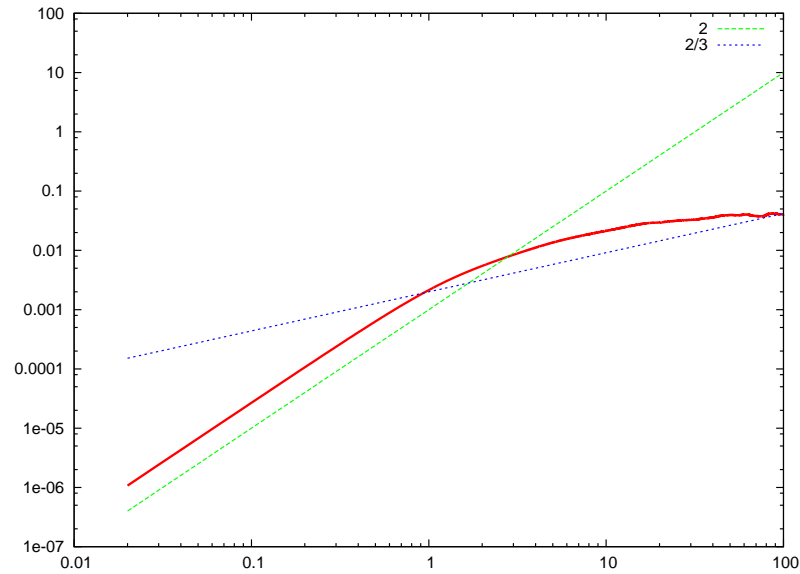
$\langle \delta u^2(\tau) \rangle$  and  $Q - R$  at  $x/x_* = 0.262$



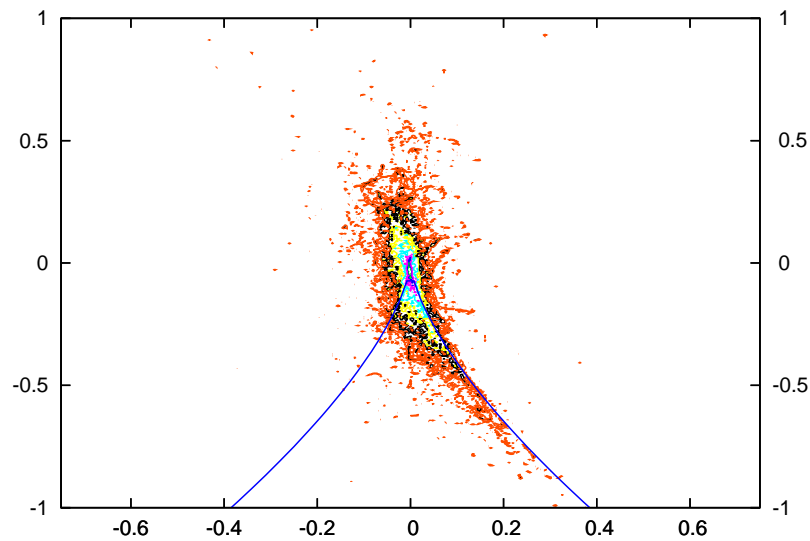
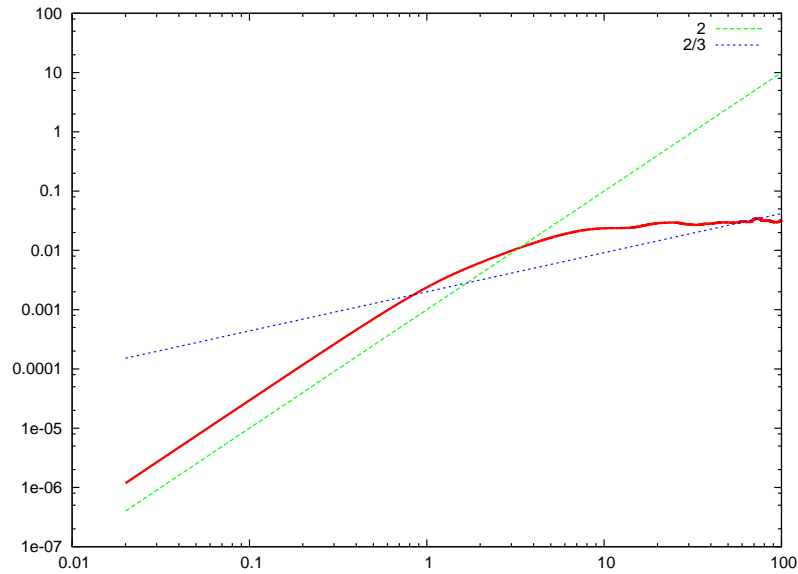
# $\langle \delta u^2(\tau) \rangle$ and $Q - R$ at $x/x_* = 0.315$



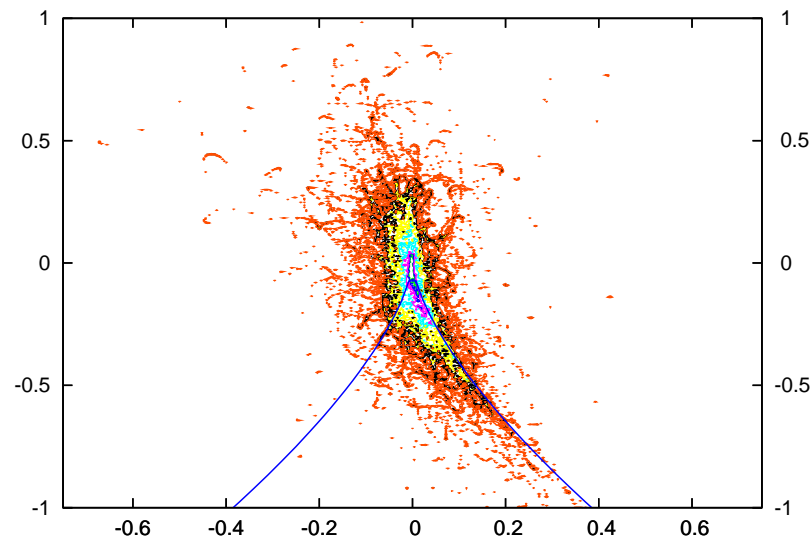
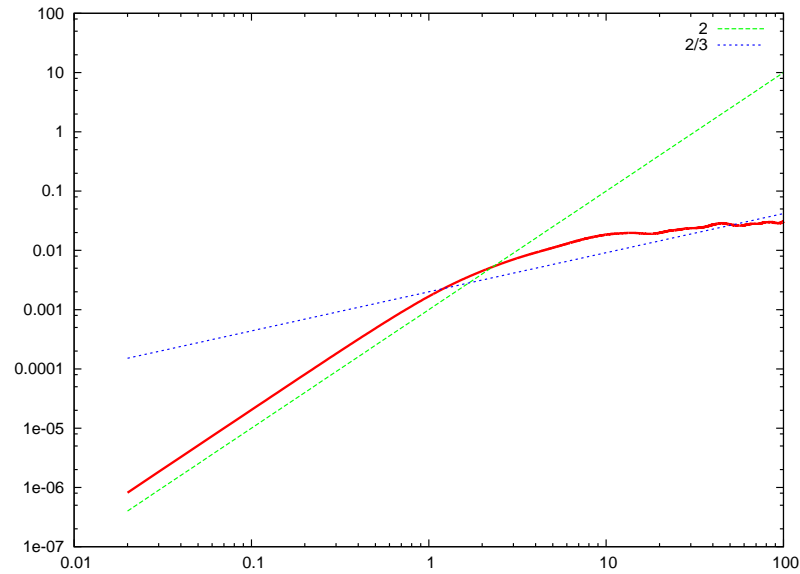
# $\langle \delta u^2(\tau) \rangle$ and $Q - R$ at $x/x_* = 0.367$



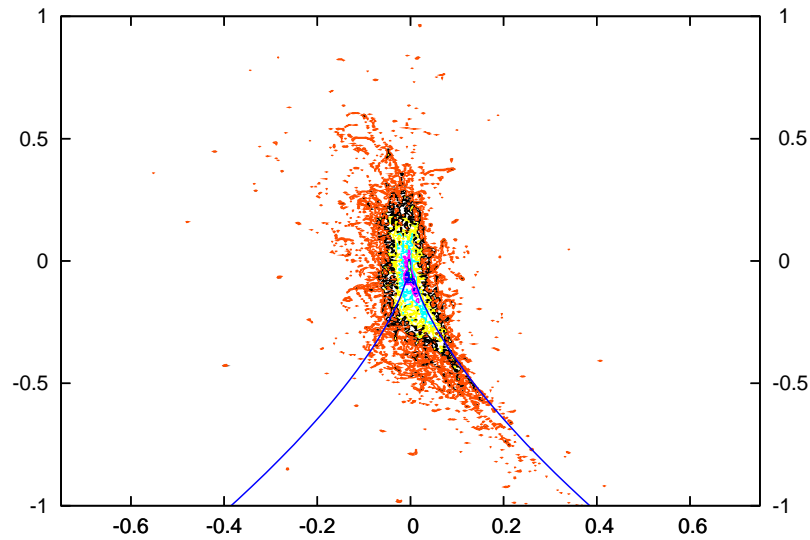
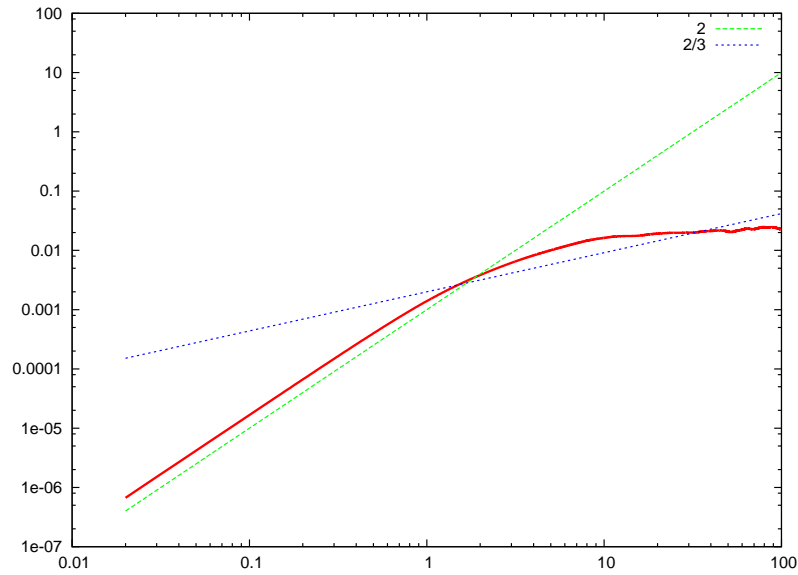
# $\langle \delta u^2(\tau) \rangle$ and $Q - R$ at $x/x_* = 0.420$



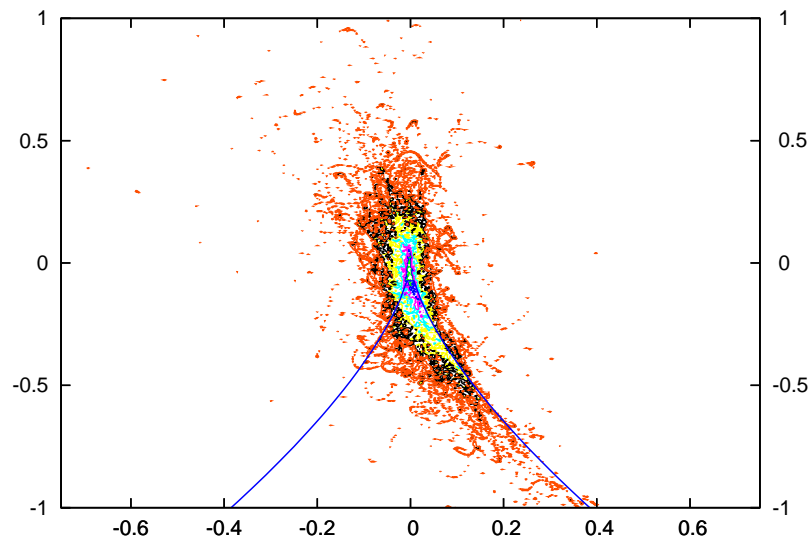
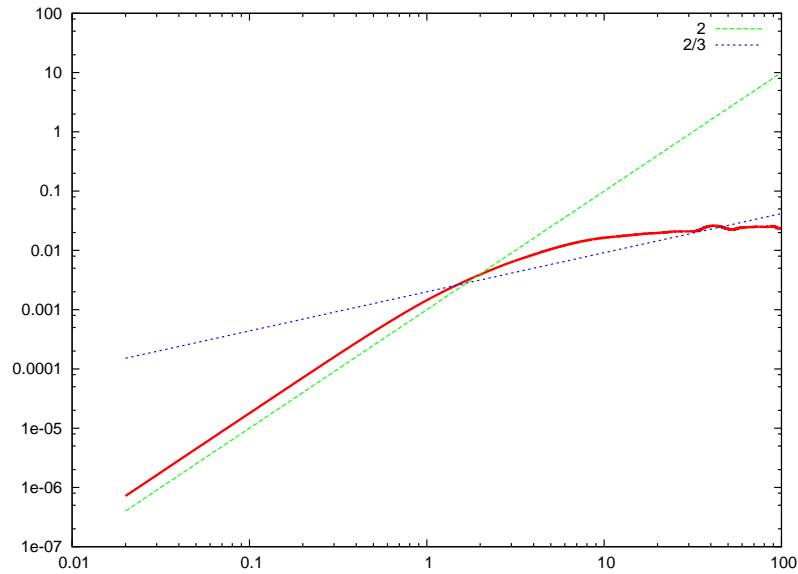
# $\langle \delta u^2(\tau) \rangle$ and $Q - R$ at $x/x_* = 0.472$



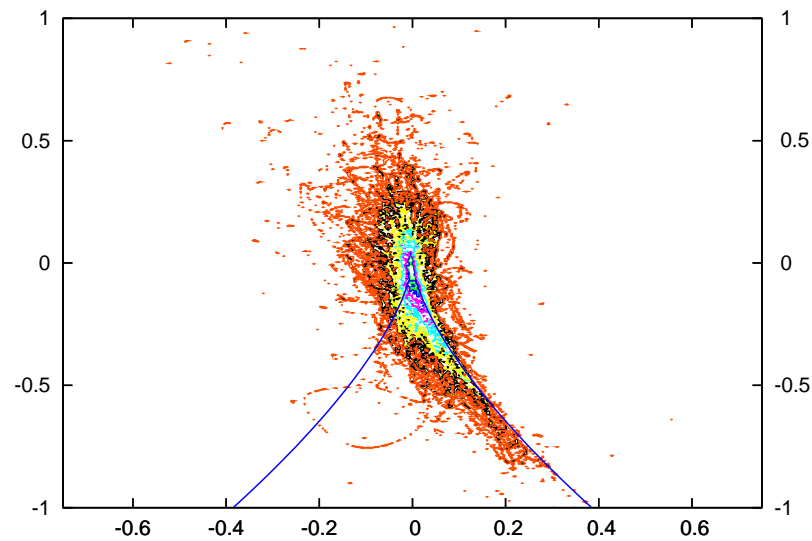
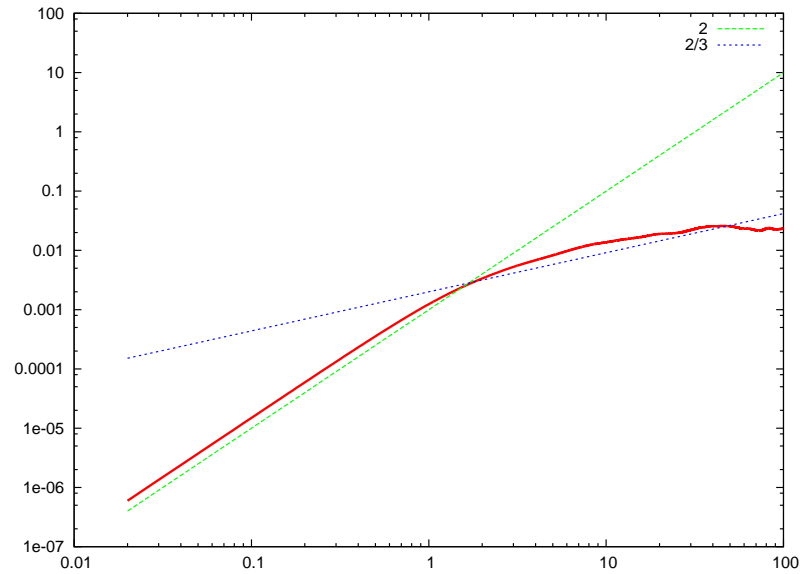
# $\langle \delta u^2(\tau) \rangle$ and $Q - R$ at $x/x_* = 0.525$



# $\langle \delta u^2(\tau) \rangle$ and $Q - R$ at $x/x_* = 0.577$

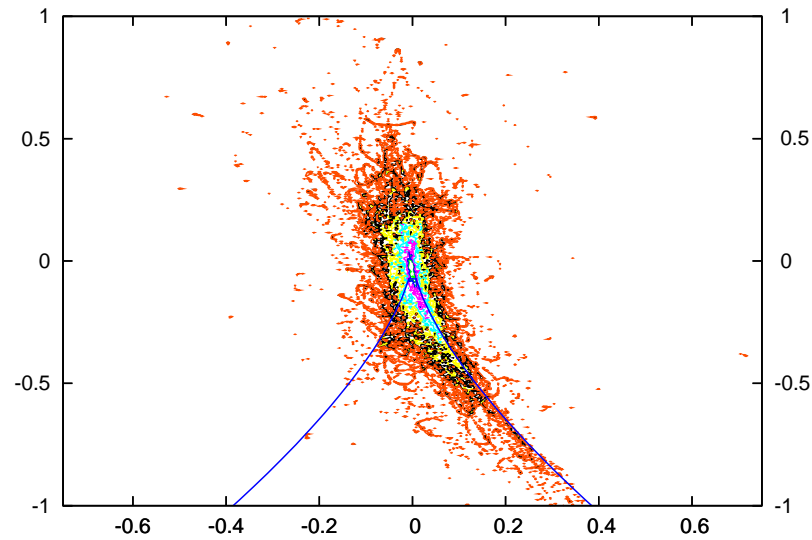
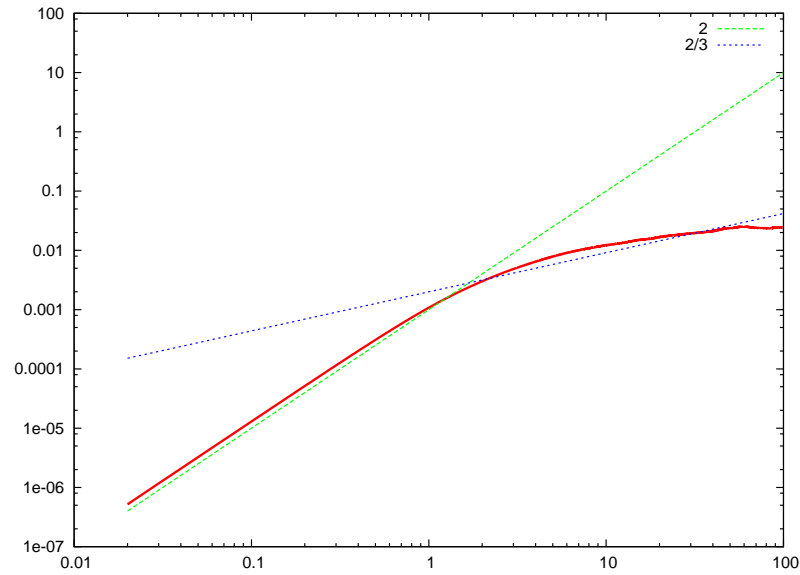


# $\langle \delta u^2(\tau) \rangle$ and $Q - R$ at $x/x_* = 0.630$

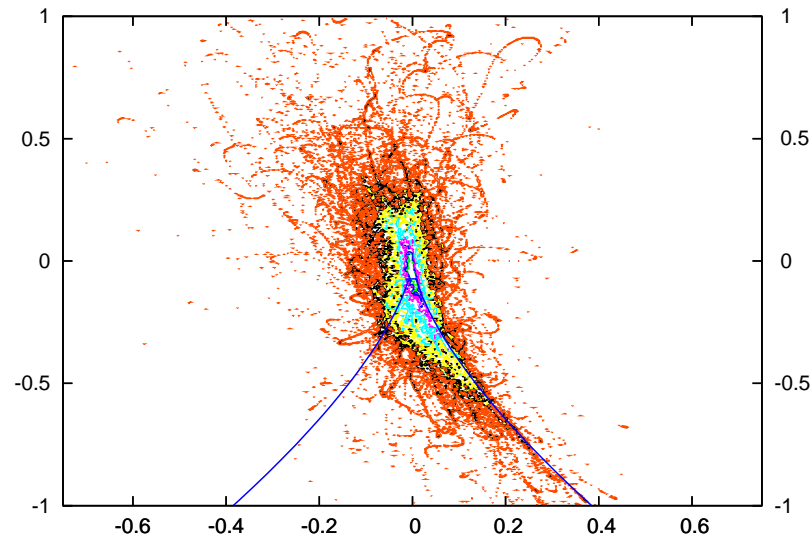
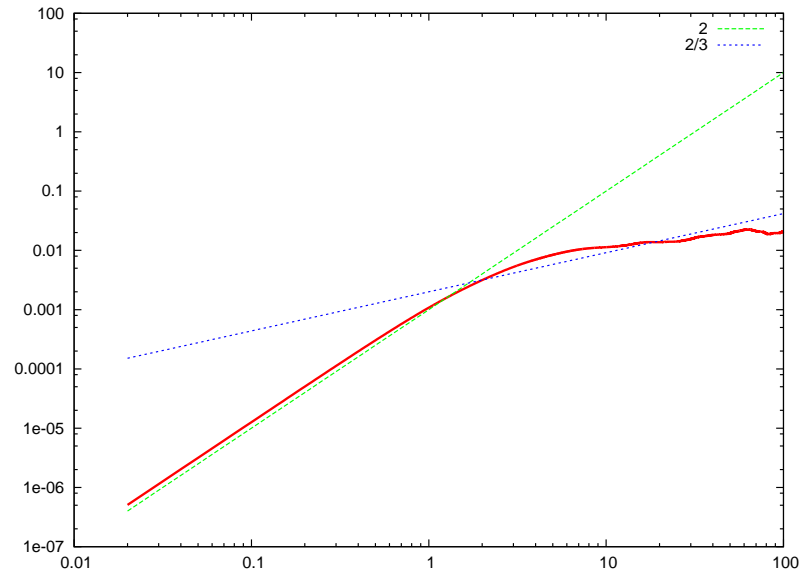




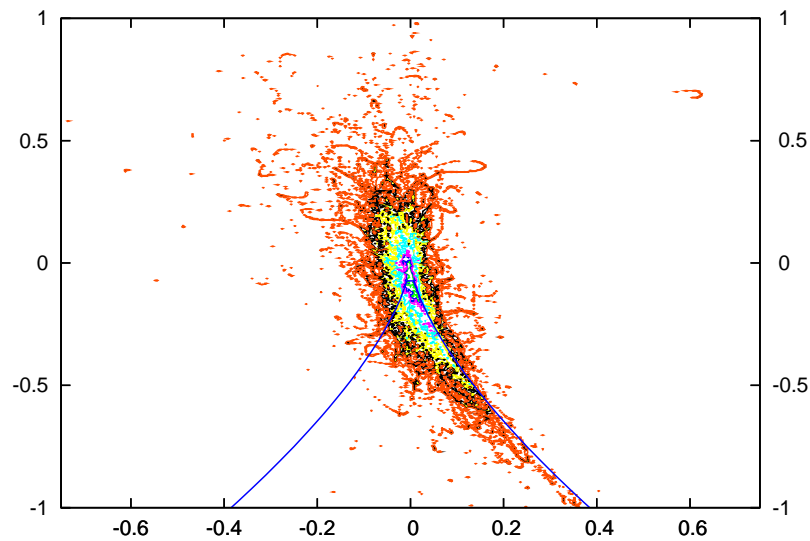
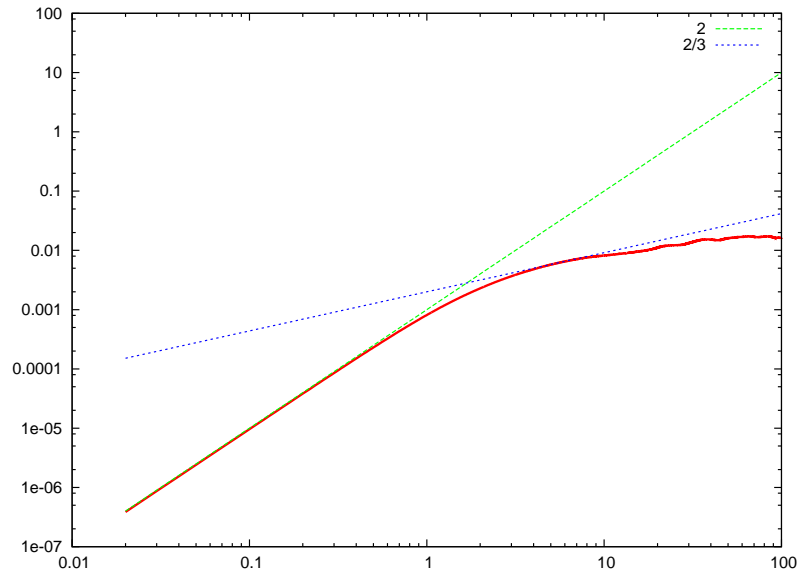
$\langle \delta u^2(\tau) \rangle$  and  $Q - R$  at  $x/x_* = 0.683$



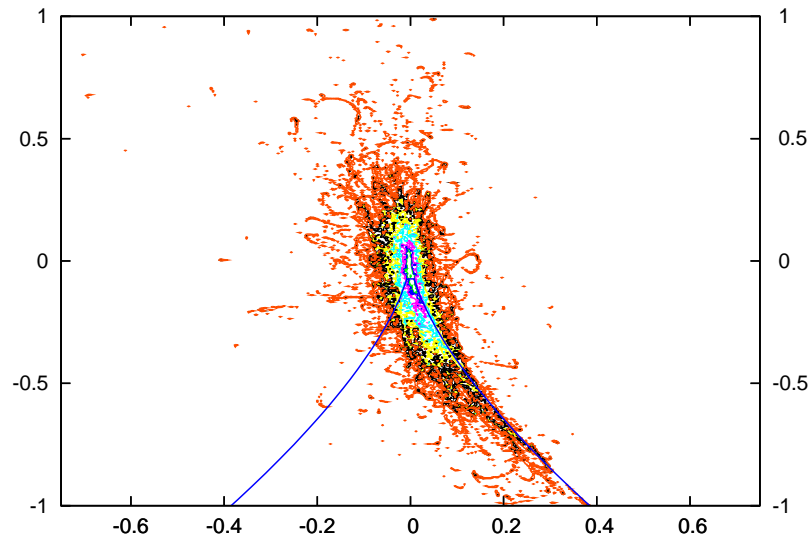
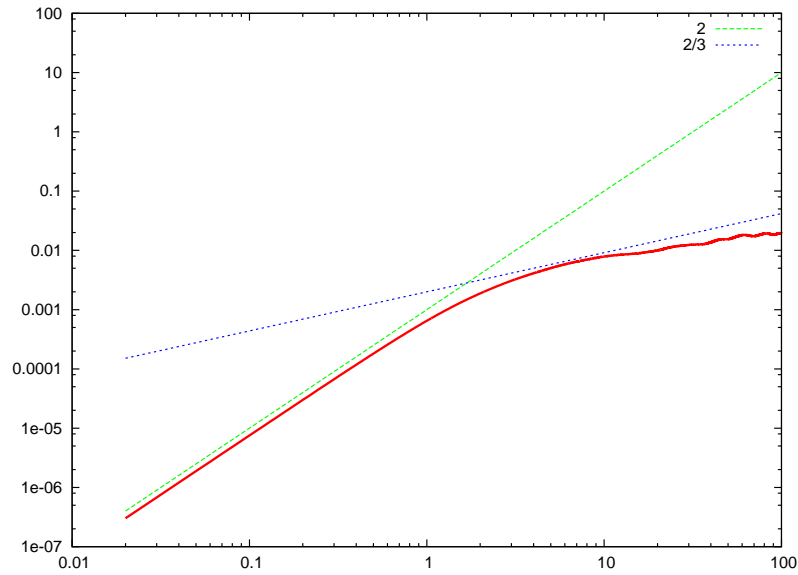
$\langle \delta u^2(\tau) \rangle$  and  $Q - R$  at  $x/x_* = 0.735$



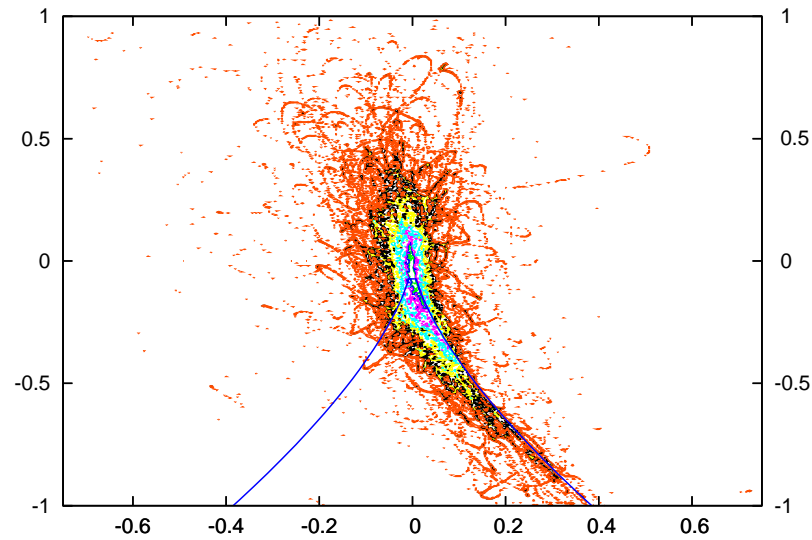
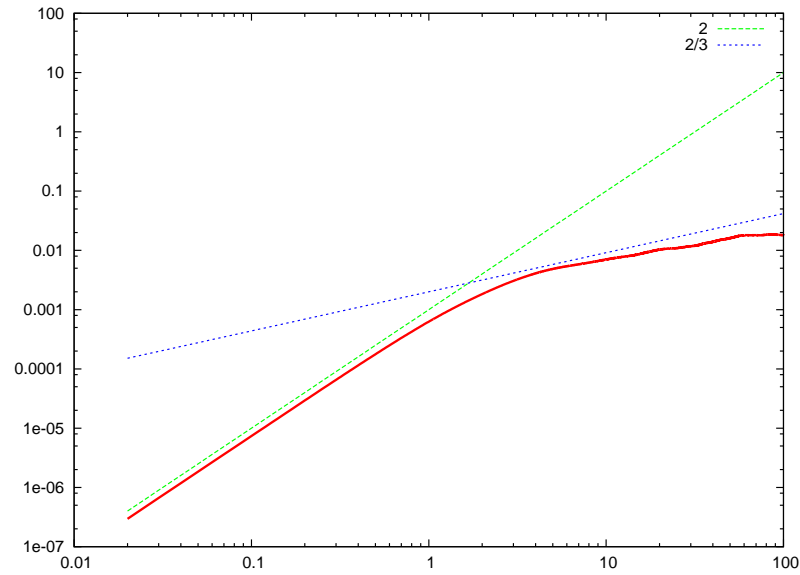
# $\langle \delta u^2(\tau) \rangle$ and $Q - R$ at $x/x_* = 0.788$



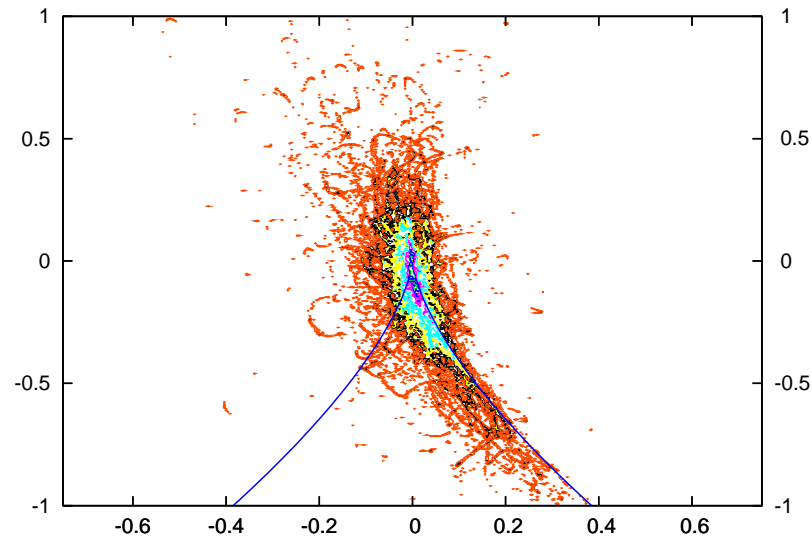
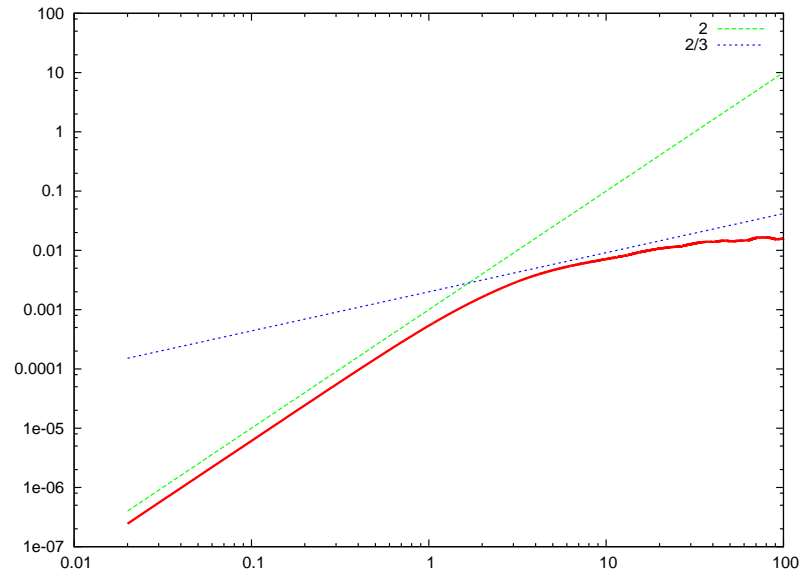
$\langle \delta u^2(\tau) \rangle$  and  $Q - R$  at  $x/x_* = 0.840$



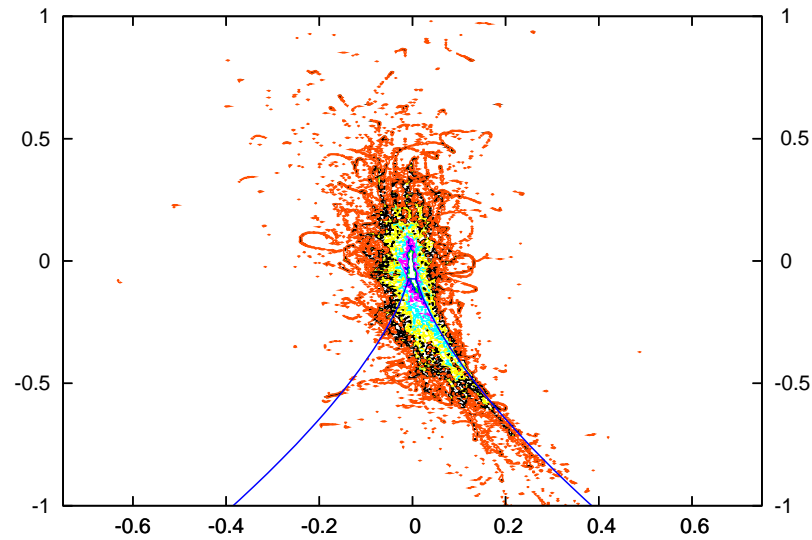
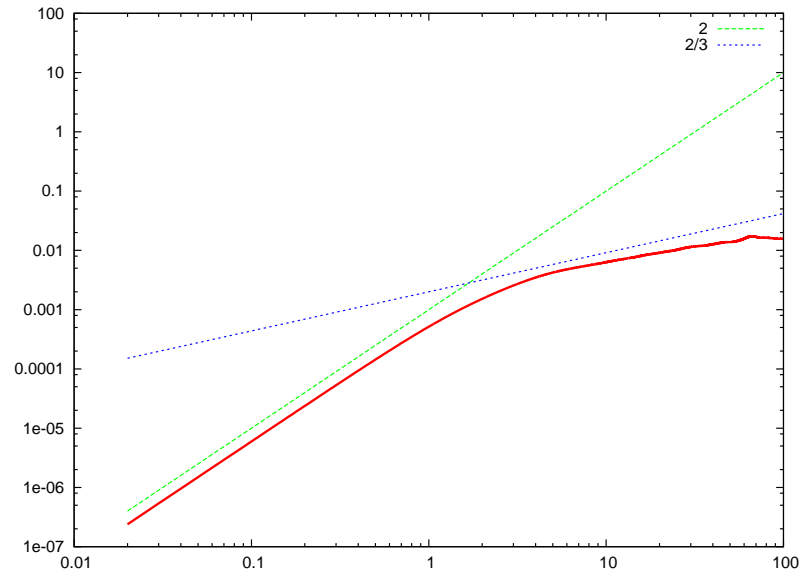
# $\langle \delta u^2(\tau) \rangle$ and $Q - R$ at $x/x_* = 0.893$



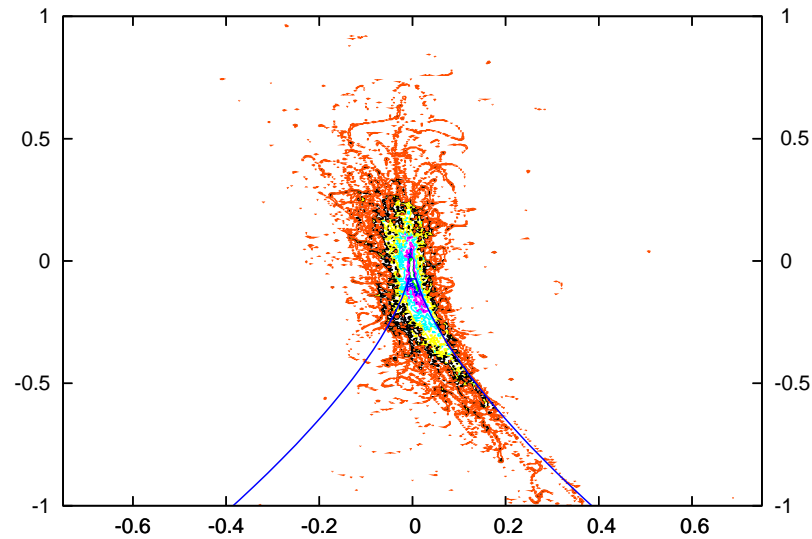
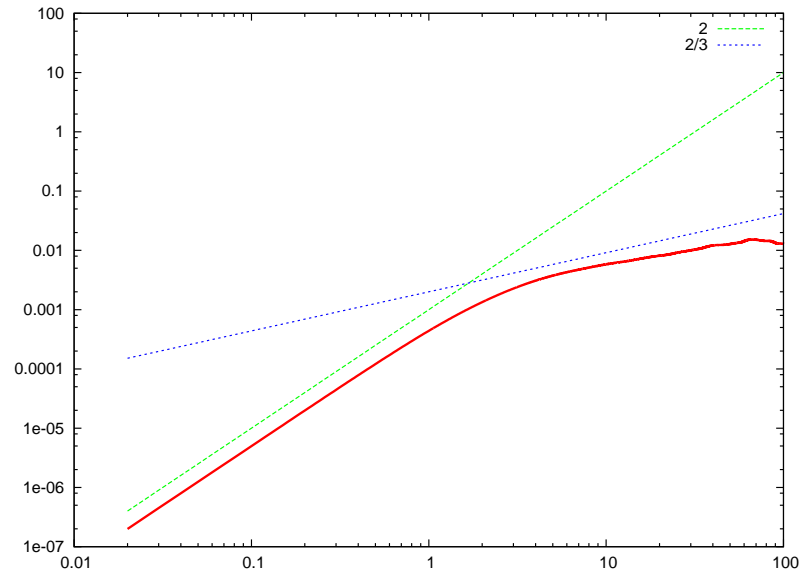
$\langle \delta u^2(\tau) \rangle$  and  $Q - R$  at  $x/x_* = 0.945$



# $\langle \delta u^2(\tau) \rangle$ and $Q - R$ at $x/x_* = 0.998$

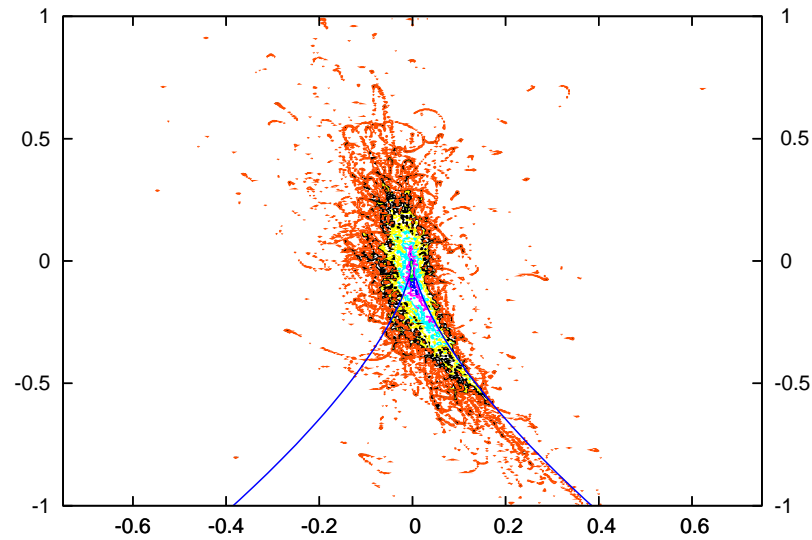
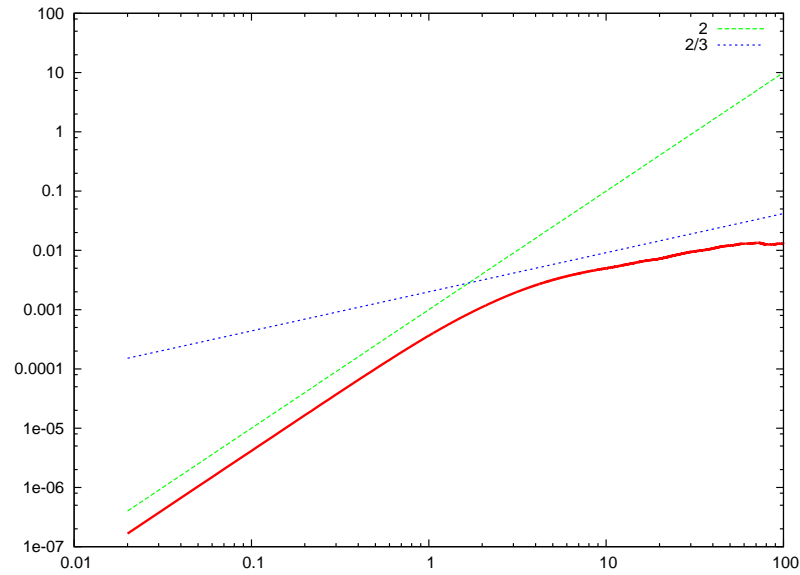


$\langle \delta u^2(\tau) \rangle$  and  $Q - R$  at  $x/x_* = 1.050$

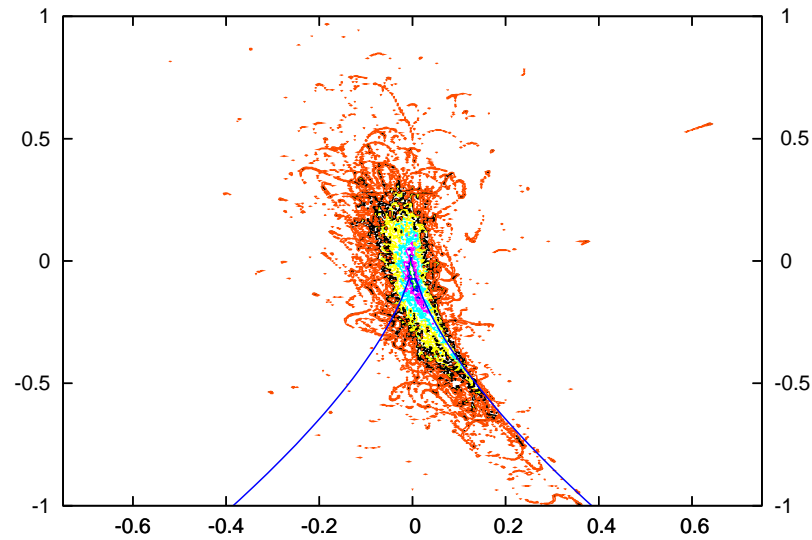
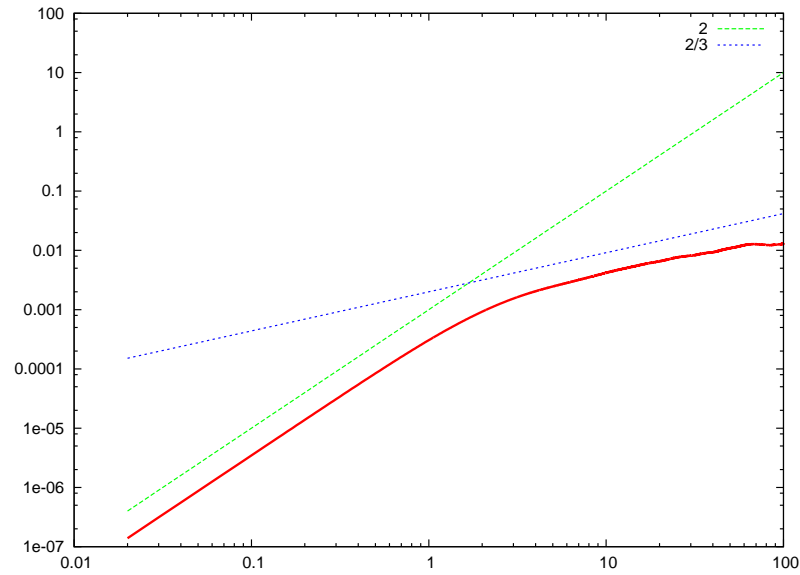




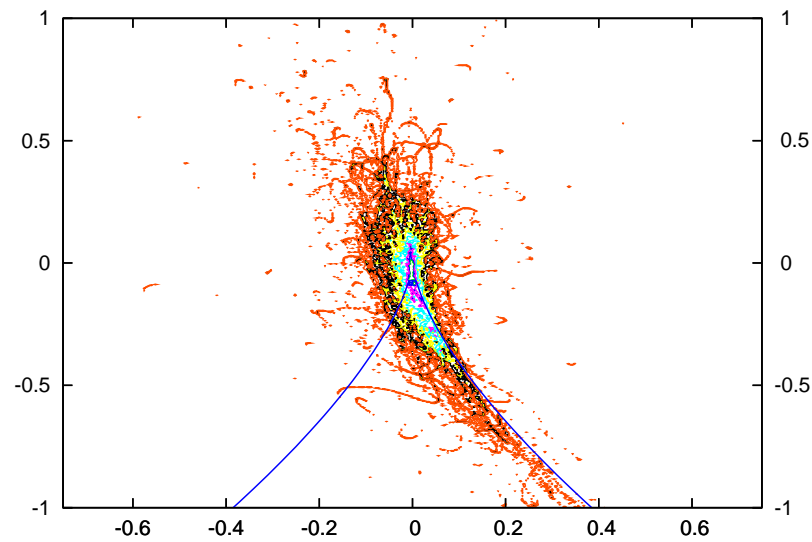
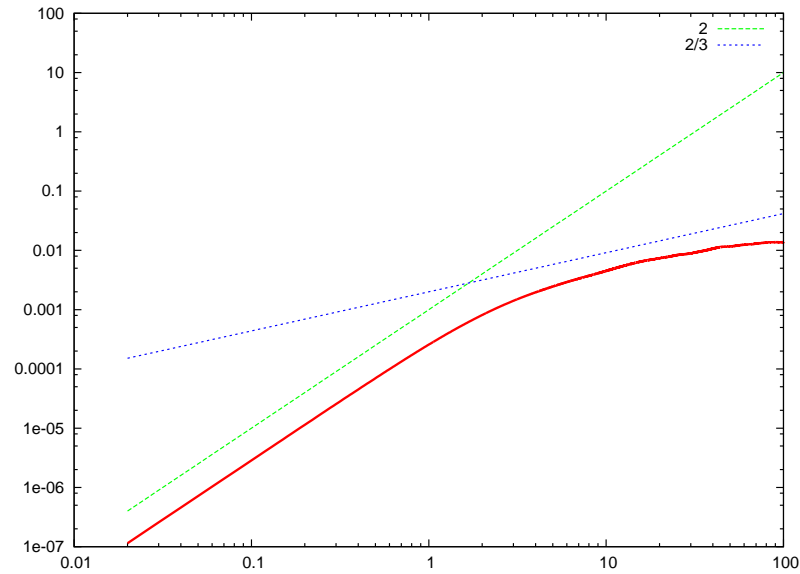
$\langle \delta u^2(\tau) \rangle$  and  $Q - R$  at  $x/x_* = 1.103$



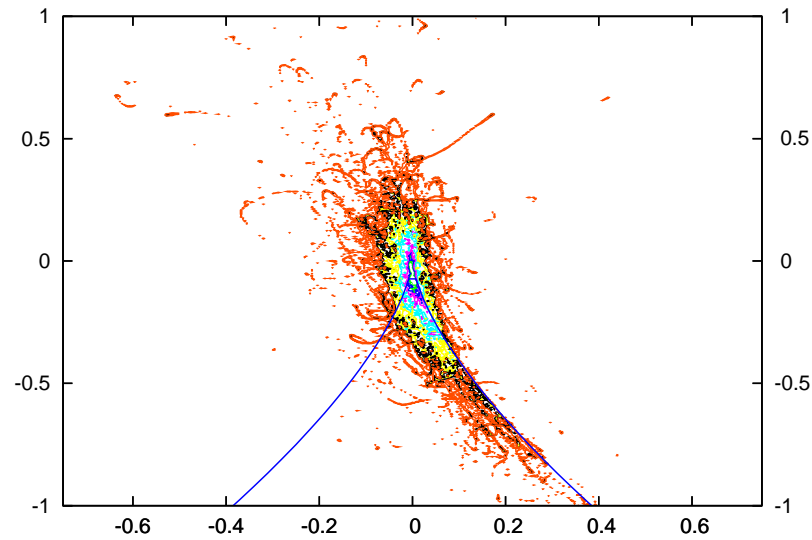
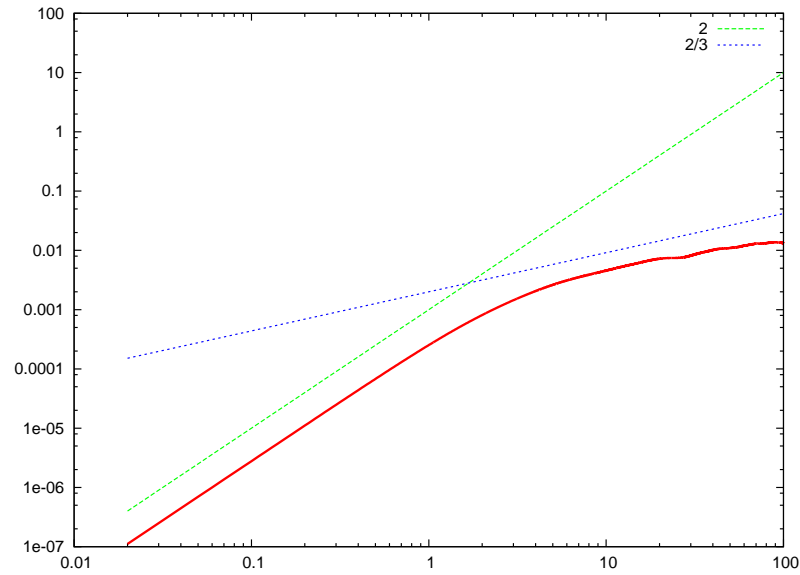
$\langle \delta u^2(\tau) \rangle$  and  $Q - R$  at  $x/x_* = 1.155$



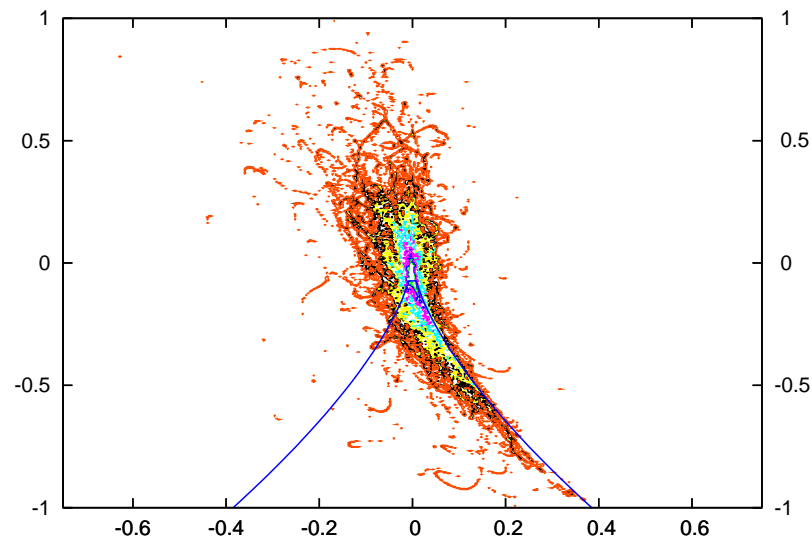
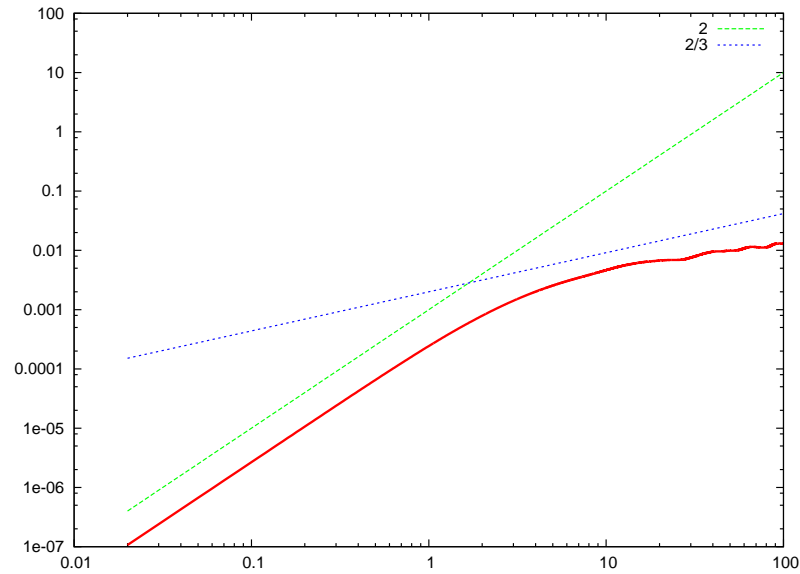
$\langle \delta u^2(\tau) \rangle$  and  $Q - R$  at  $x/x_* = 1.208$



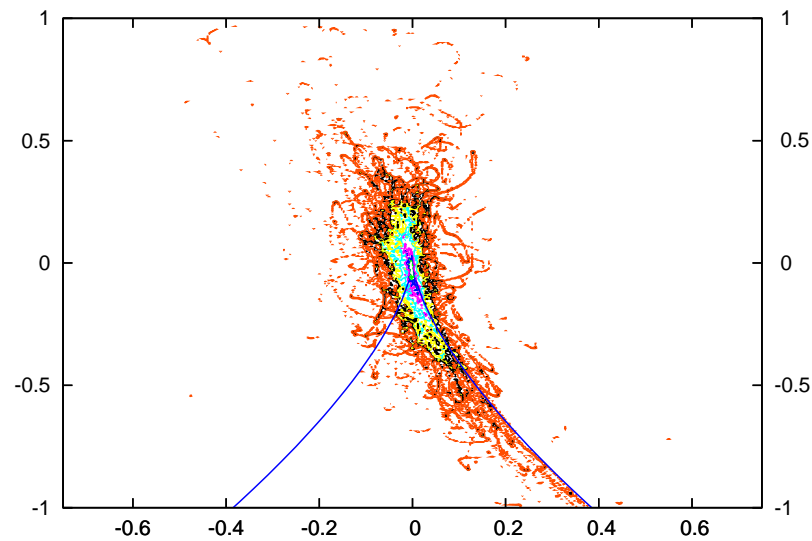
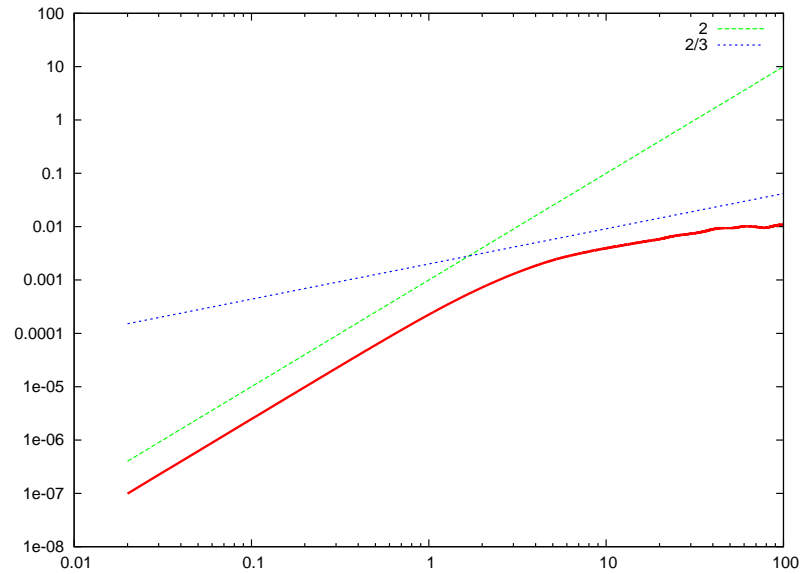
$\langle \delta u^2(\tau) \rangle$  and  $Q - R$  at  $x/x_* = 1.261$



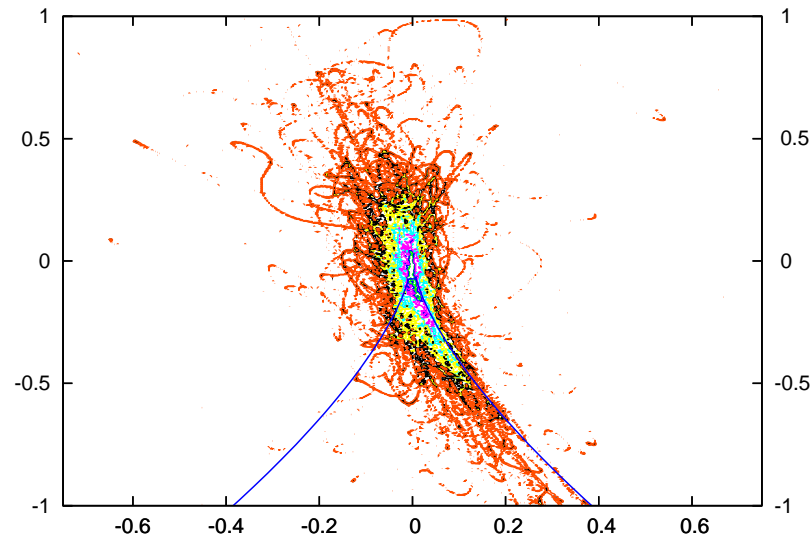
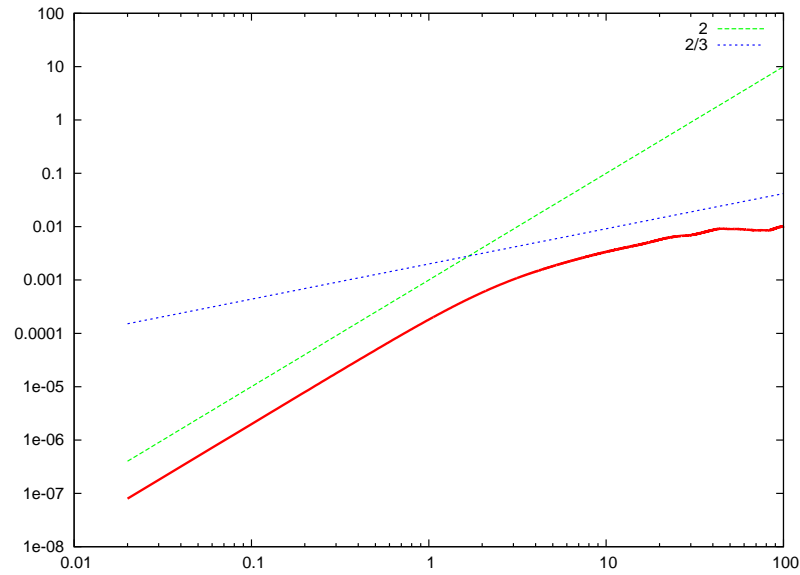
# $\langle \delta u^2(\tau) \rangle$ and $Q - R$ at $x/x_* = 1.313$



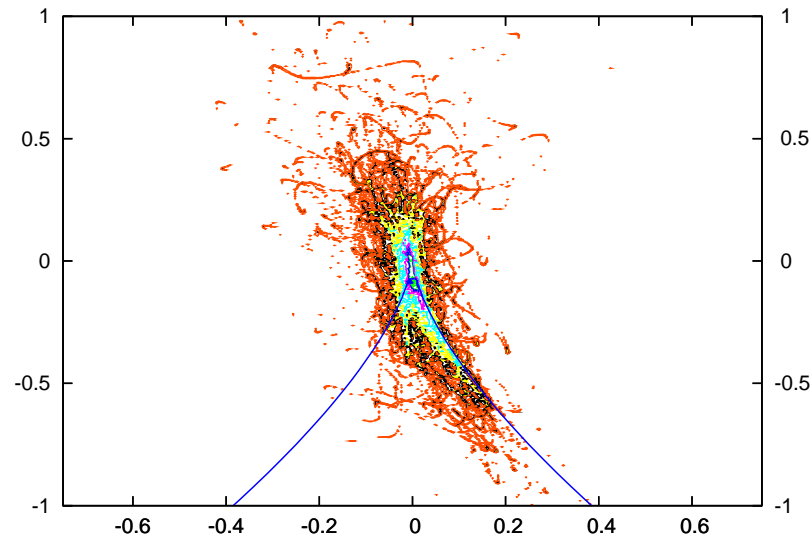
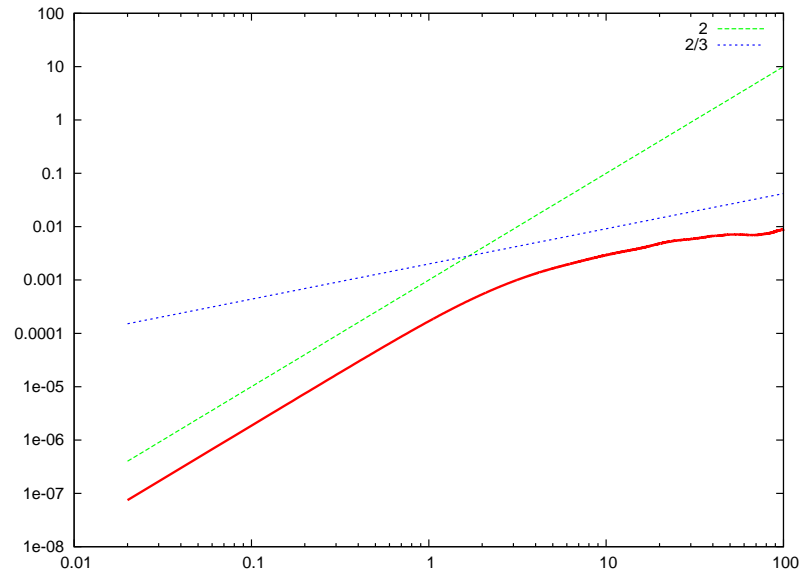
# $\langle \delta u^2(\tau) \rangle$ and $Q - R$ at $x/x_* = 1.366$



# $\langle \delta u^2(\tau) \rangle$ and $Q - R$ at $x/x_* = 1.418$

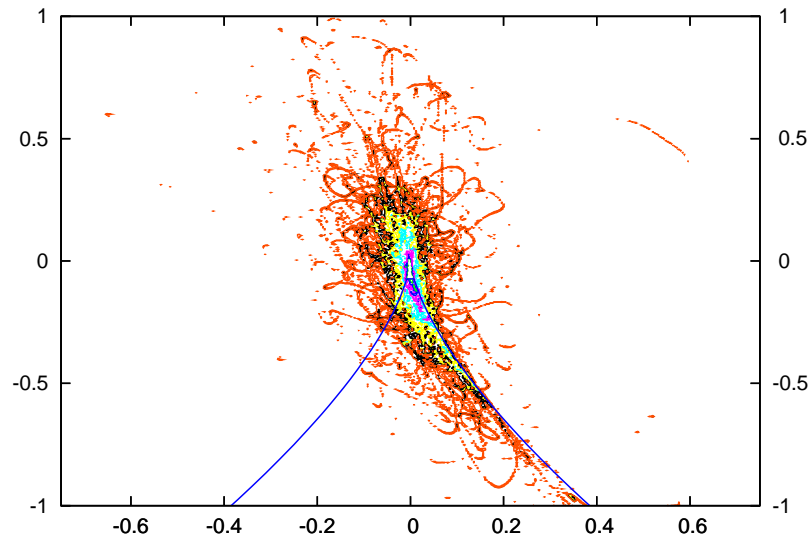
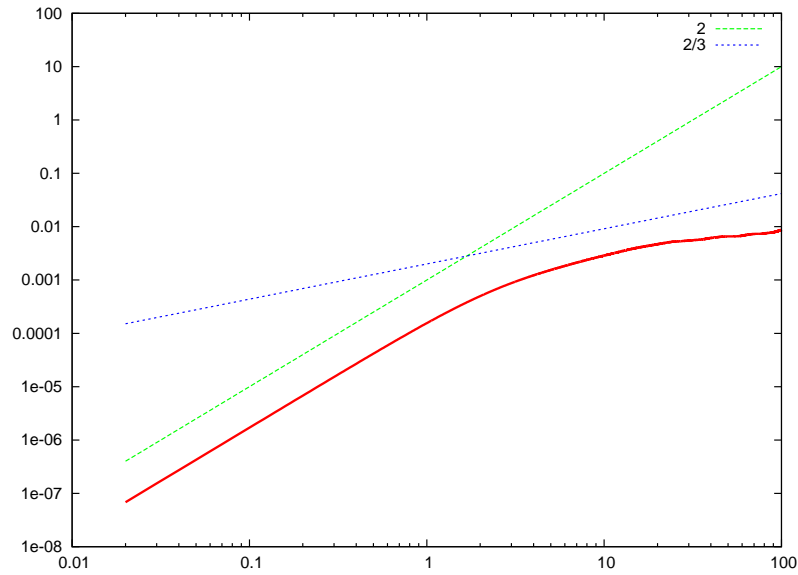


# $\langle \delta u^2(\tau) \rangle$ and $Q - R$ at $x/x_* = 1.471$

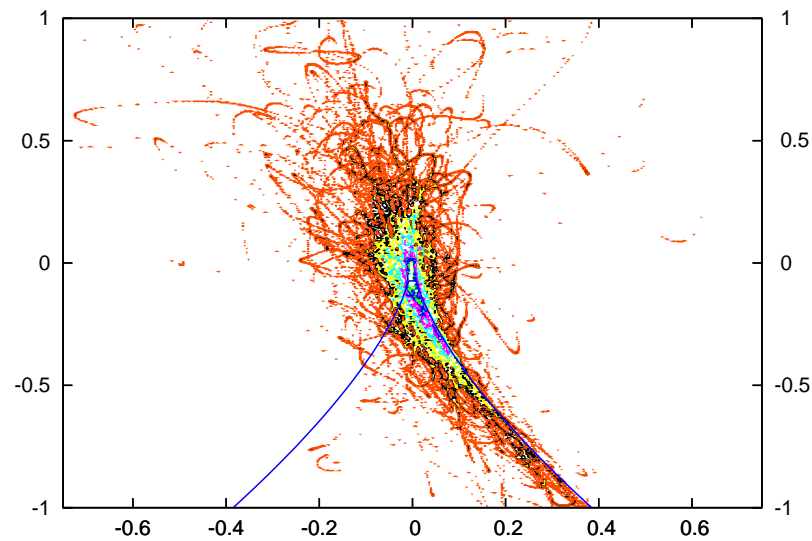
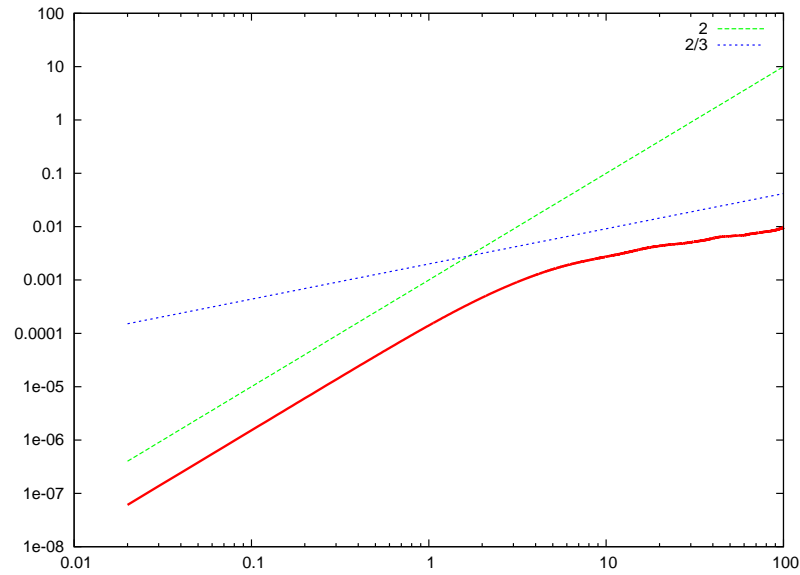




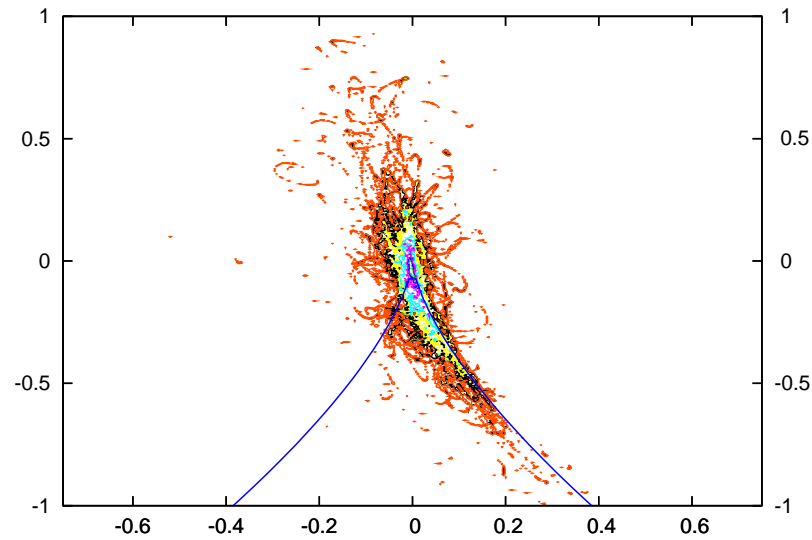
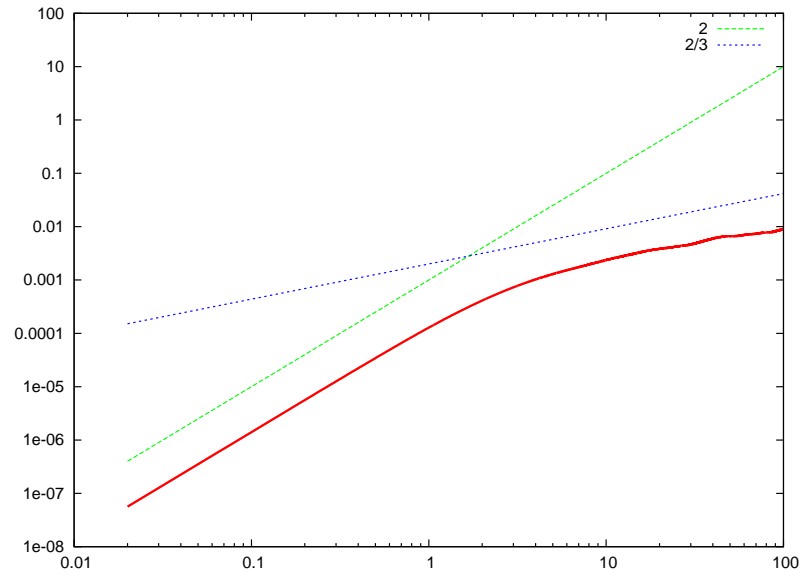
# $\langle \delta u^2(\tau) \rangle$ and $Q - R$ at $x/x_* = 1.523$



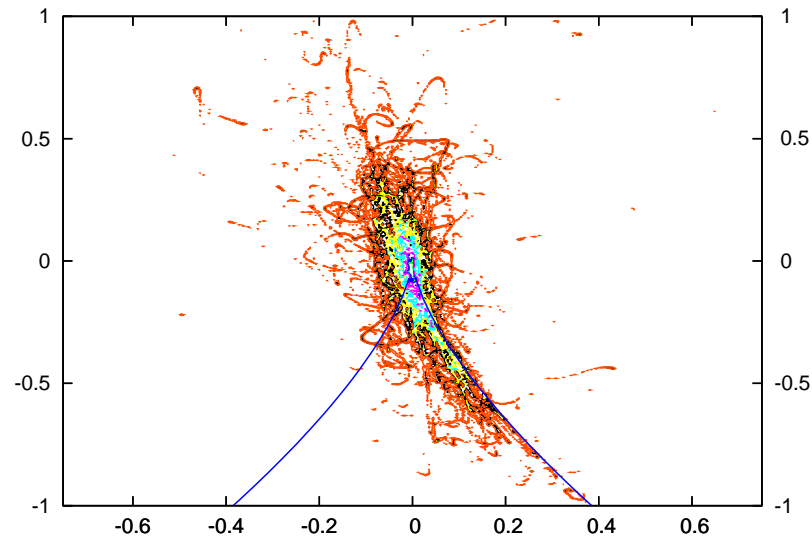
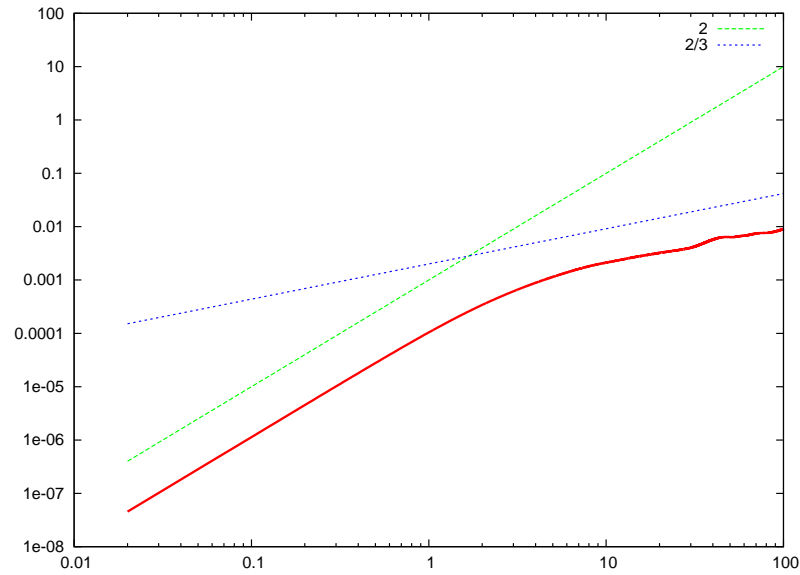
# $\langle \delta u^2(\tau) \rangle$ and $Q - R$ at $x/x_* = 1.576$



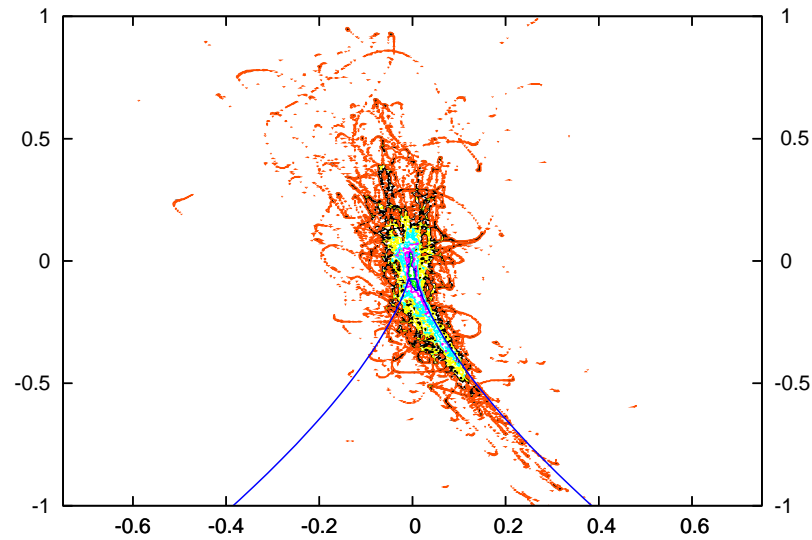
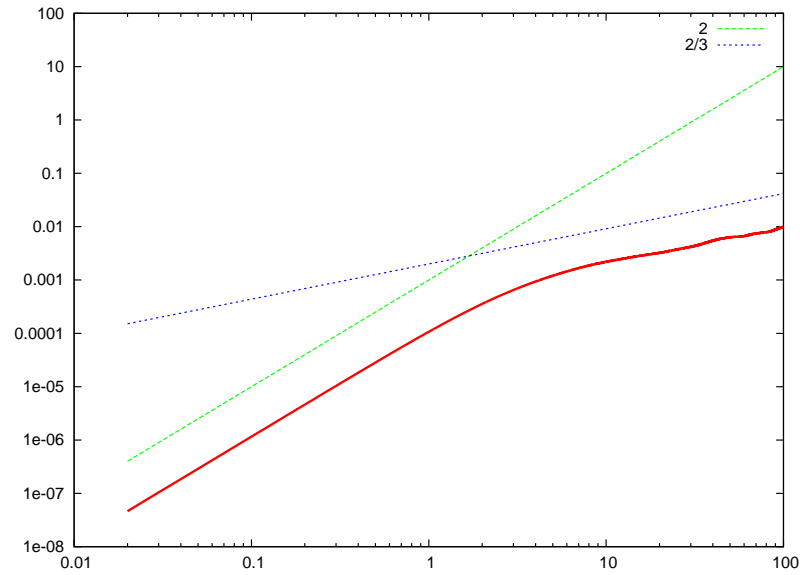
# $\langle \delta u^2(\tau) \rangle$ and $Q - R$ at $x/x_* = 1.628$



# $\langle \delta u^2(\tau) \rangle$ and $Q - R$ at $x/x_* = 1.681$

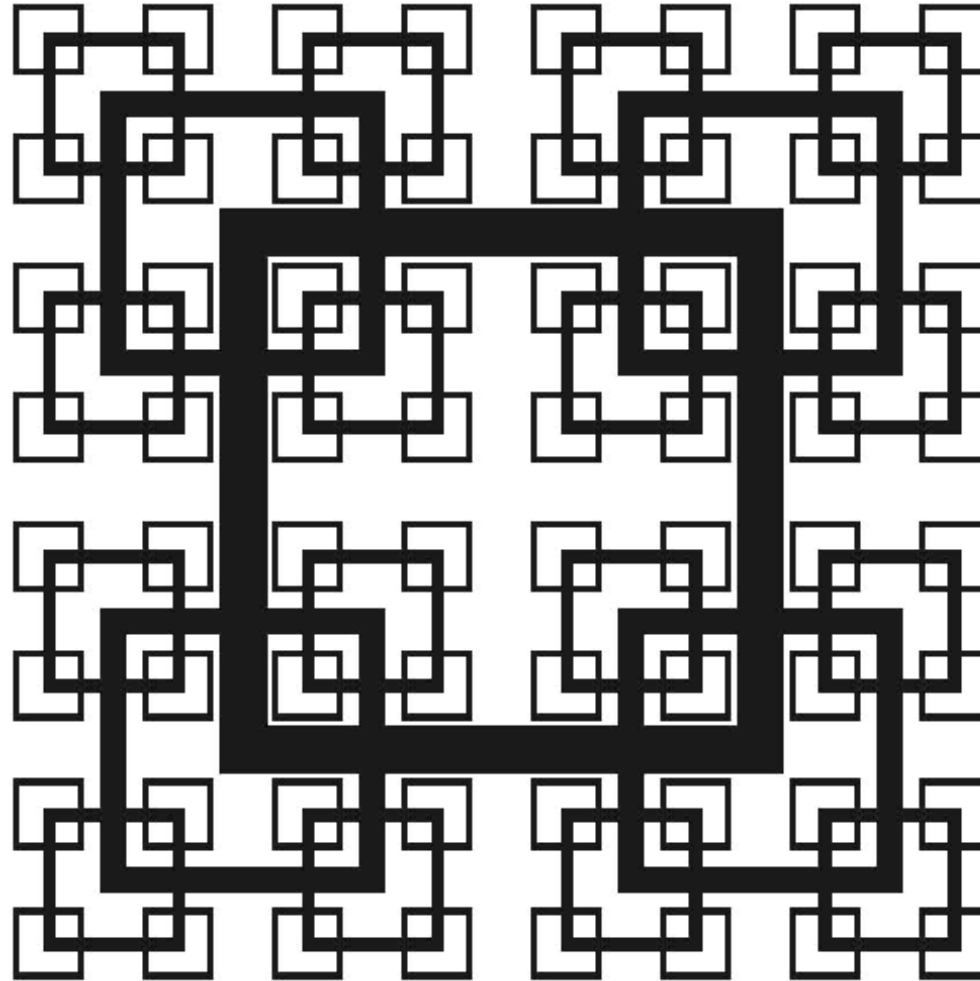


# $\langle \delta u^2(\tau) \rangle$ and $Q - R$ at $x/x_* = 1.733$

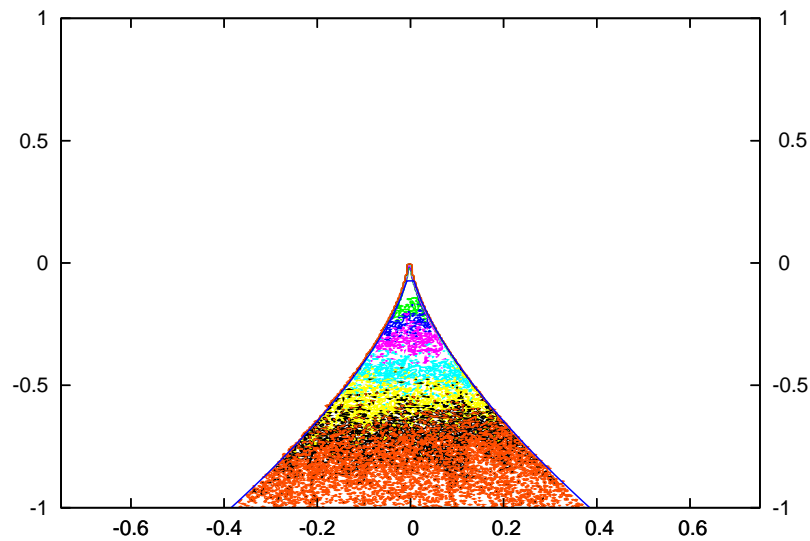
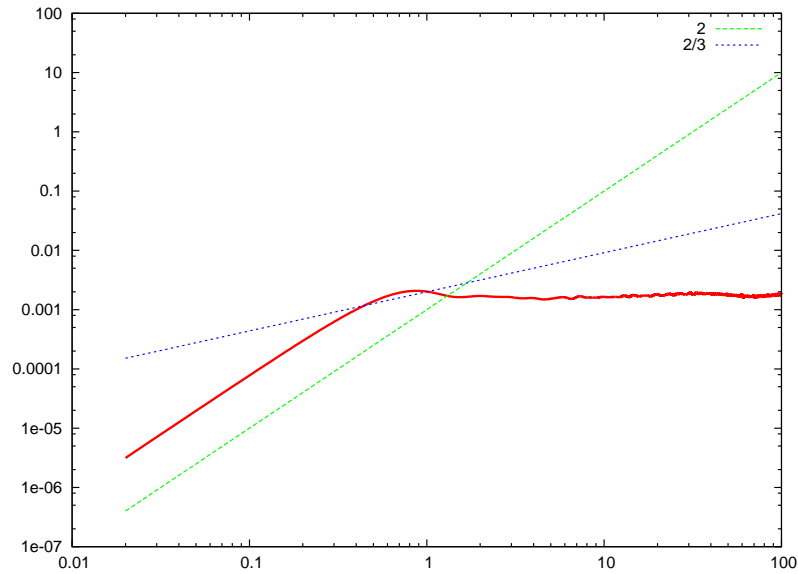


# Back along centerline

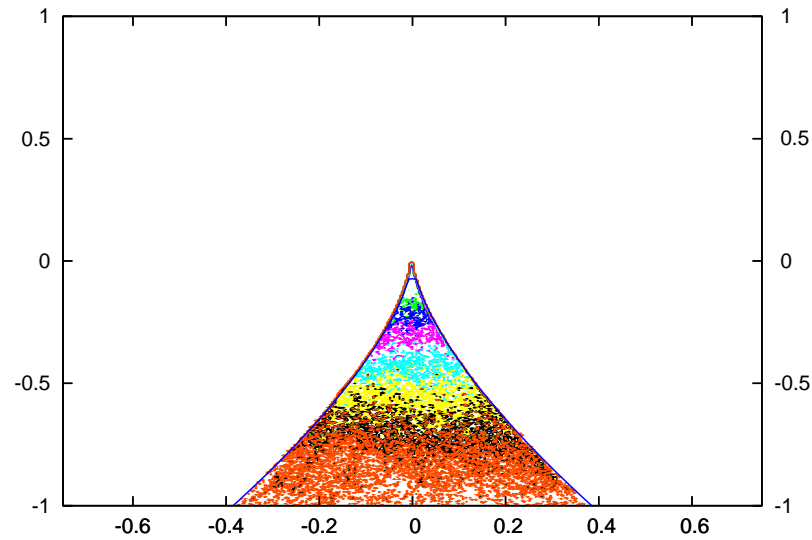
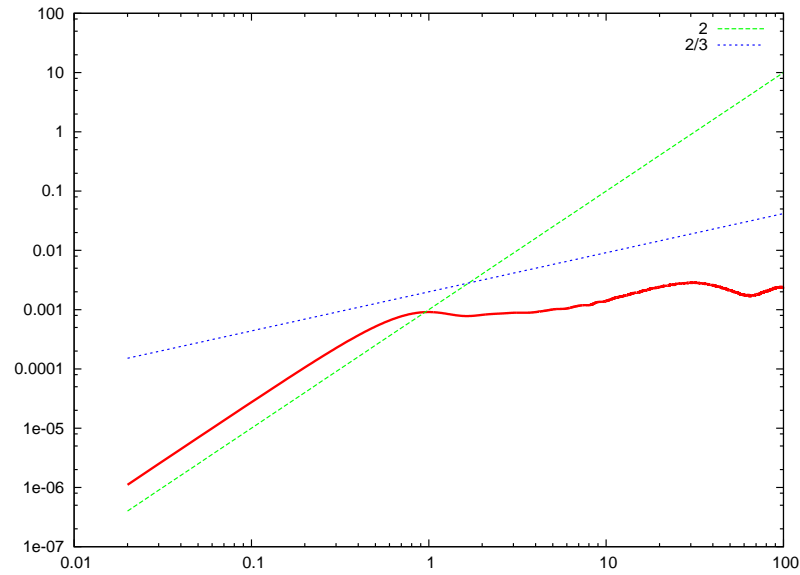
But now  $Q_s - R_s$  plots along the centreline.



# $\langle \delta u^2(\tau) \rangle$ and $Q_s - R_s$ at $x/x_* = 0.052$

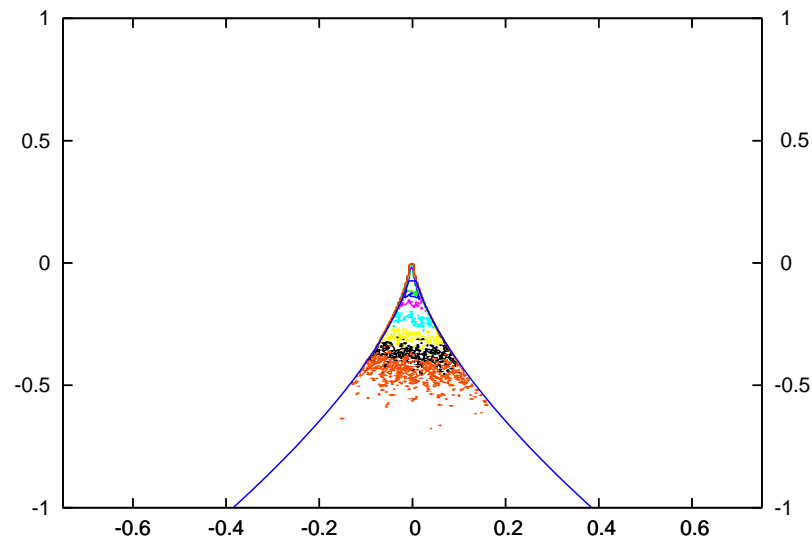
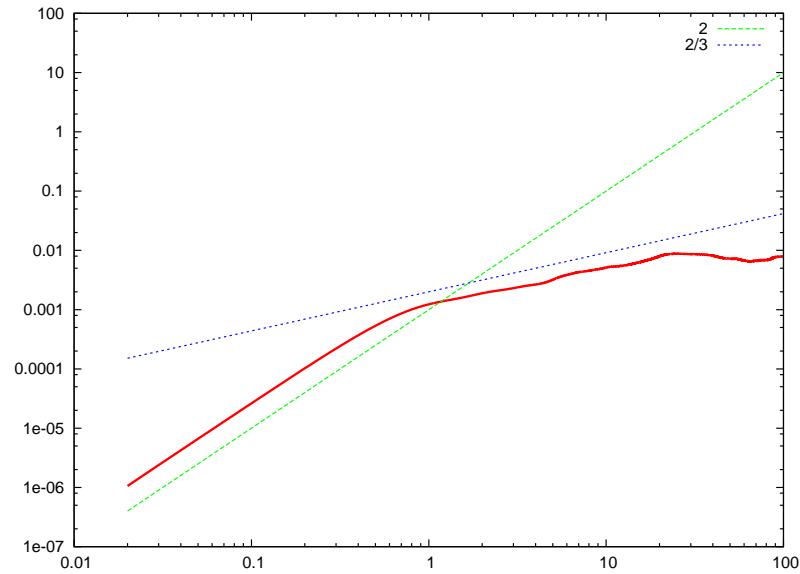


# $\langle \delta u^2(\tau) \rangle$ and $Q_s - R_s$ at $x/x_* = 0.105$

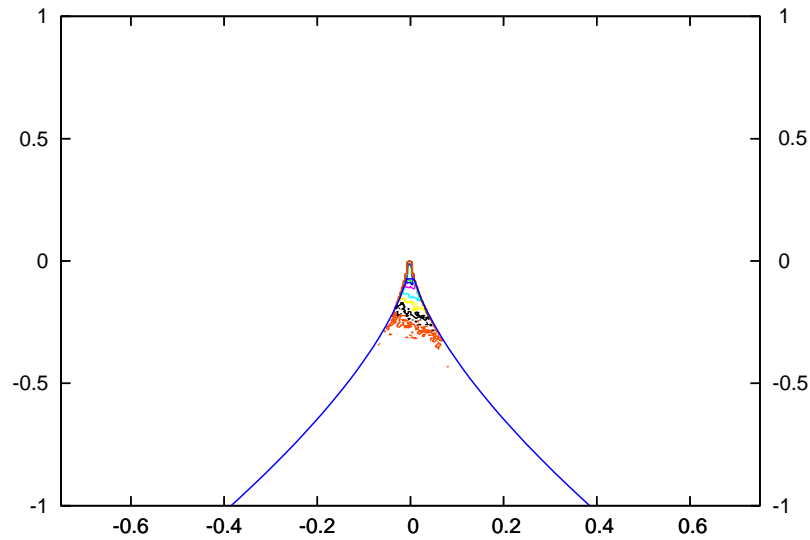
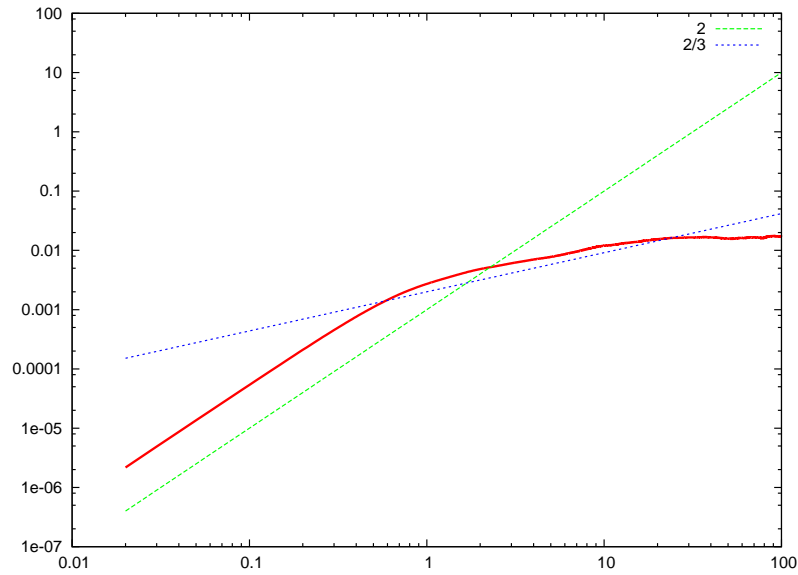




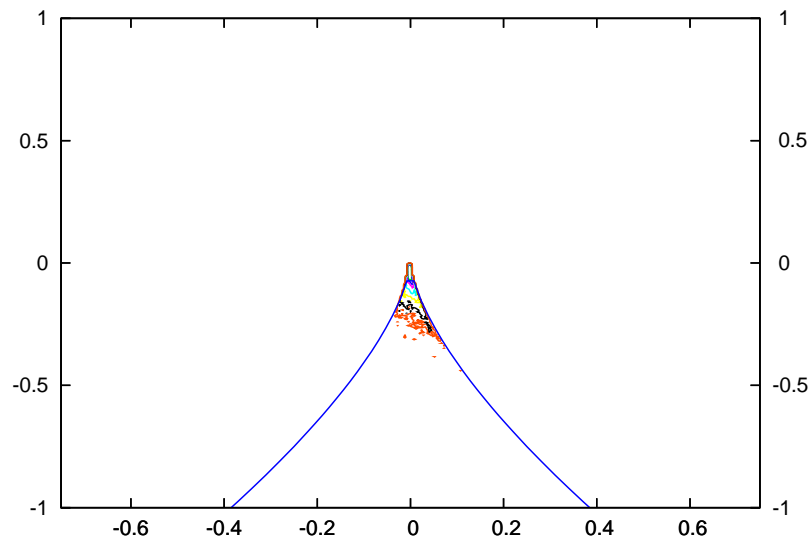
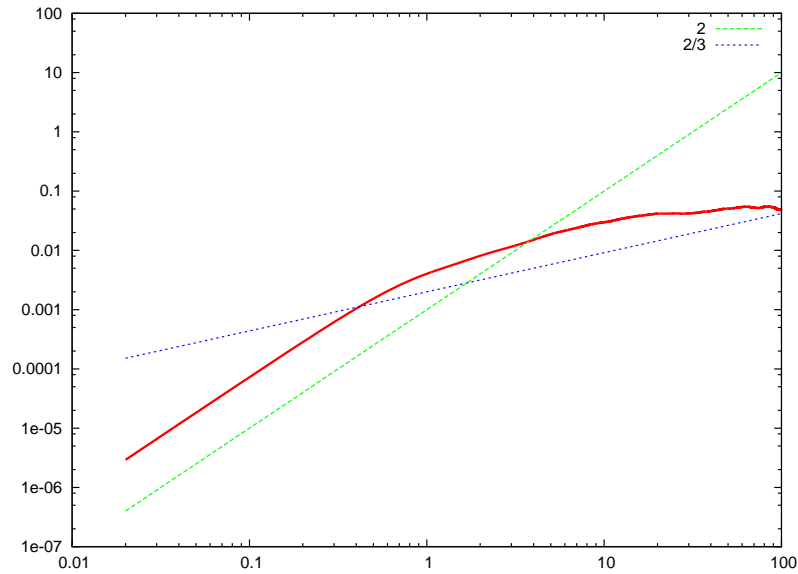
# $\langle \delta u^2(\tau) \rangle$ and $Q_s - R_s$ at $x/x_* = 0.157$



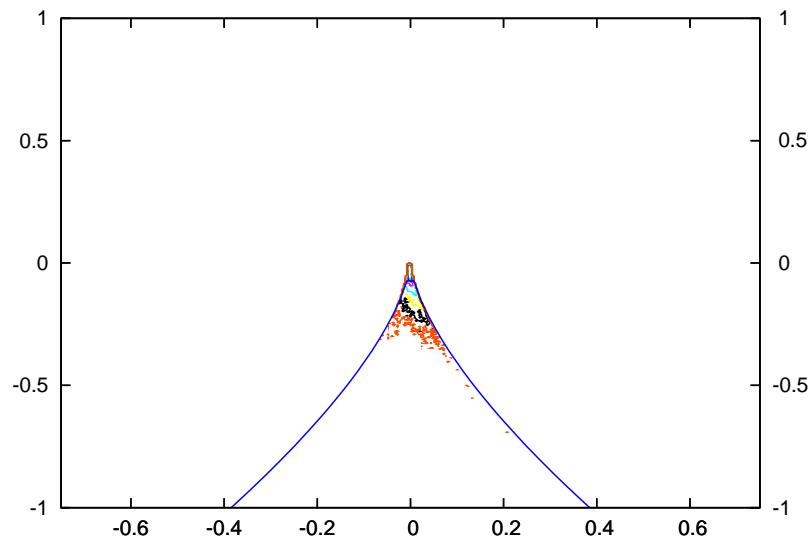
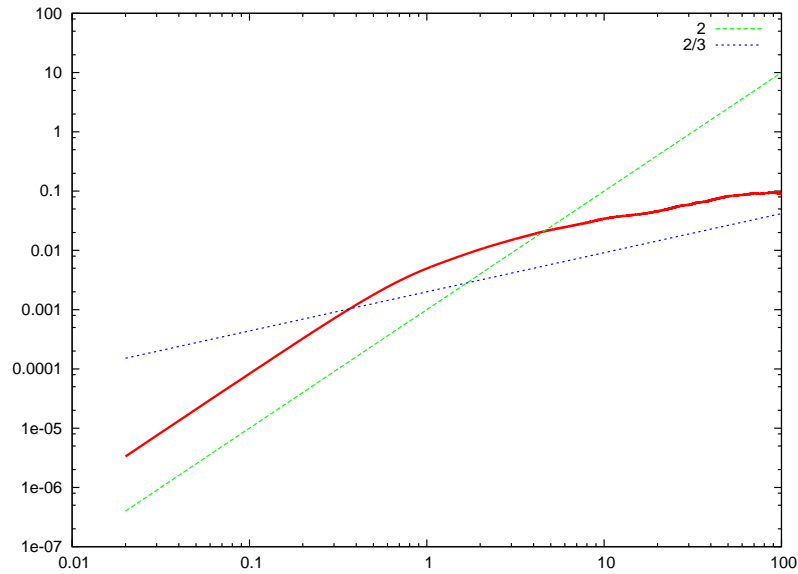
# $\langle \delta u^2(\tau) \rangle$ and $Q_s - R_s$ at $x/x_* = 0.210$



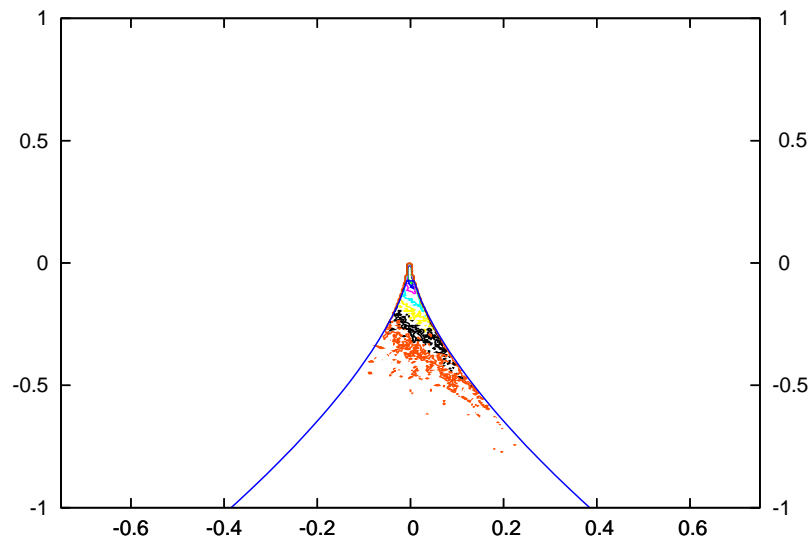
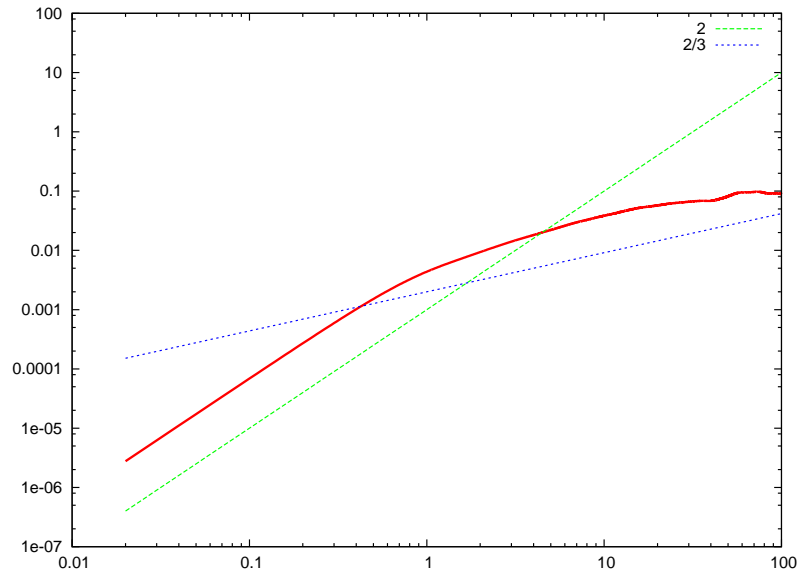
# $\langle \delta u^2(\tau) \rangle$ and $Q_s - R_s$ at $x/x_* = 0.262$



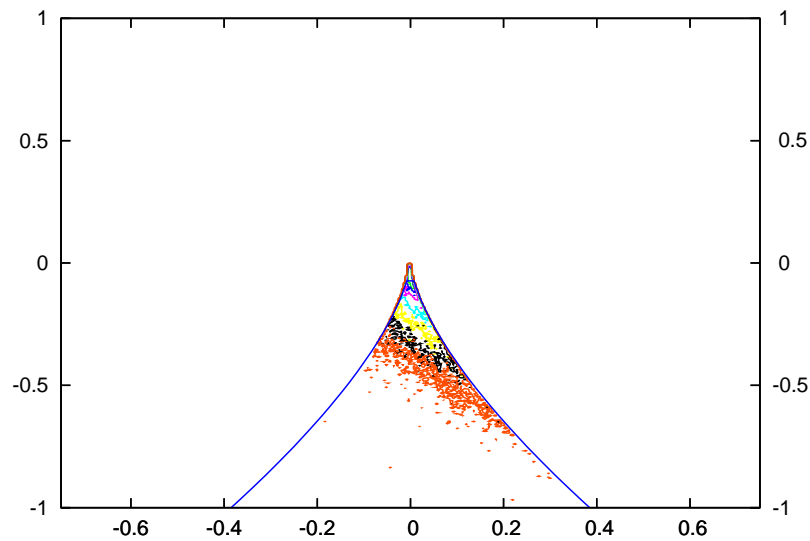
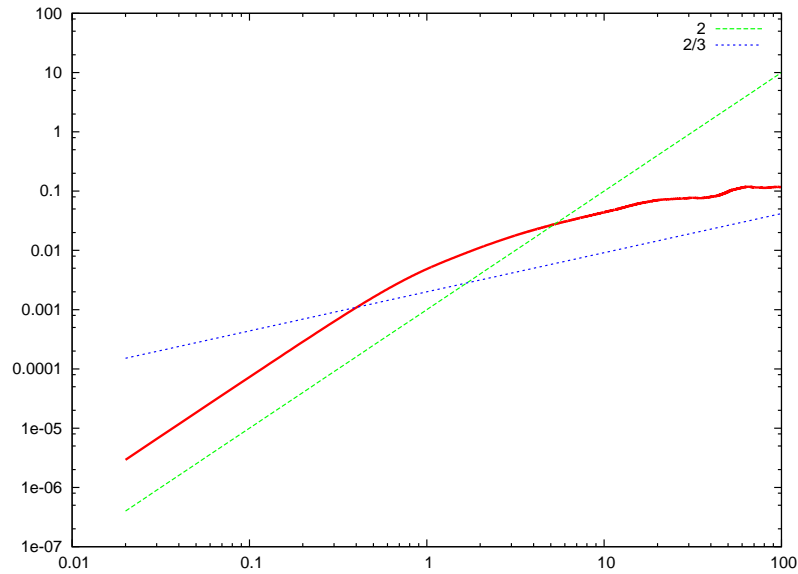
# $\langle \delta u^2(\tau) \rangle$ and $Q_s - R_s$ at $x/x_* = 0.315$



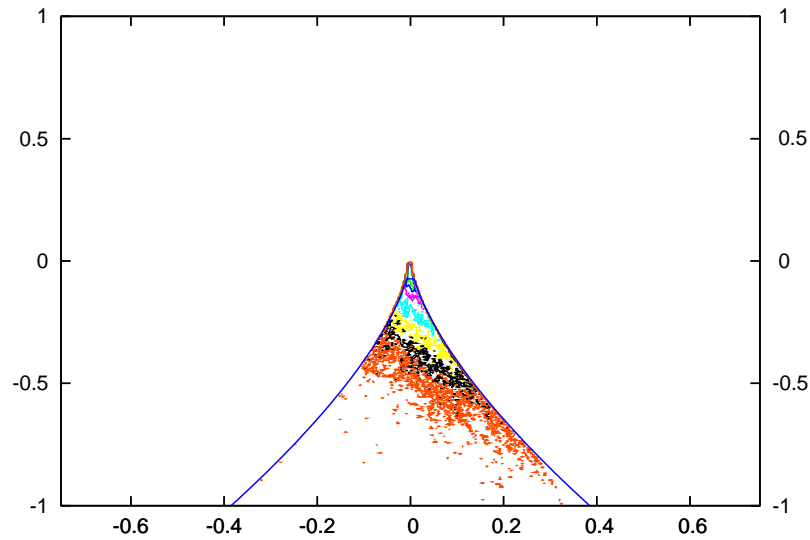
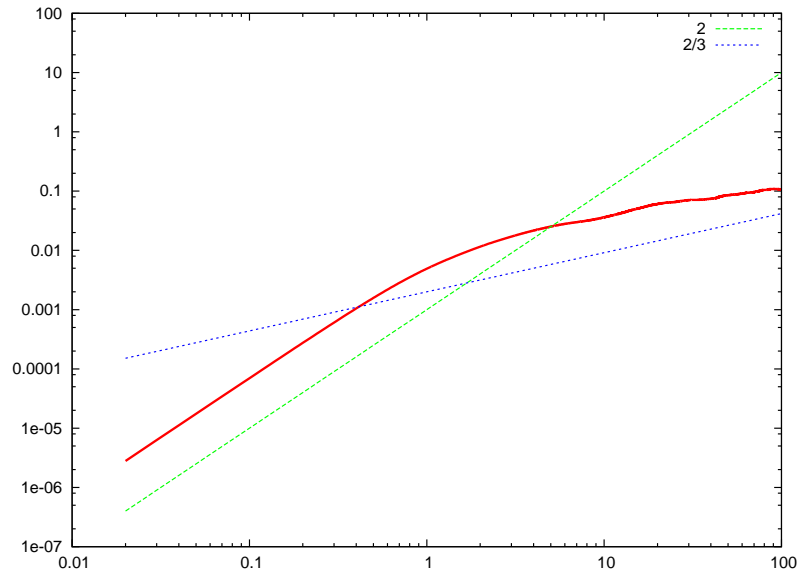
# $\langle \delta u^2(\tau) \rangle$ and $Q_s - R_s$ at $x/x_* = 0.367$



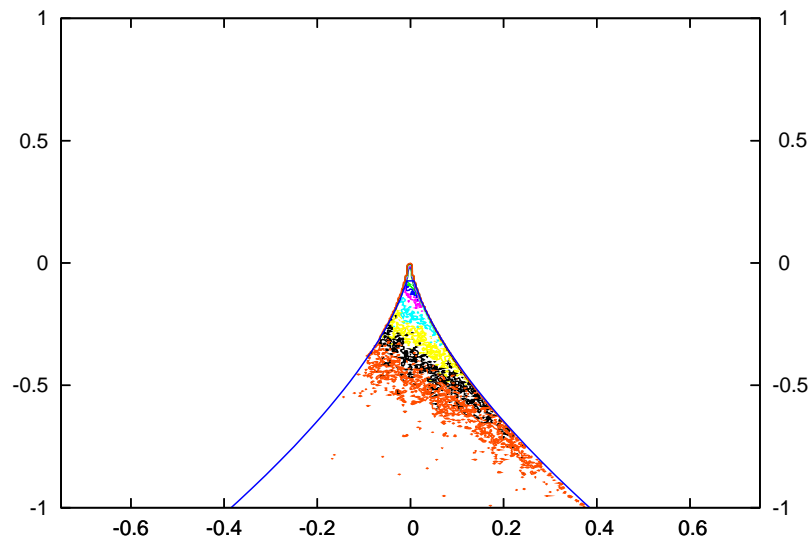
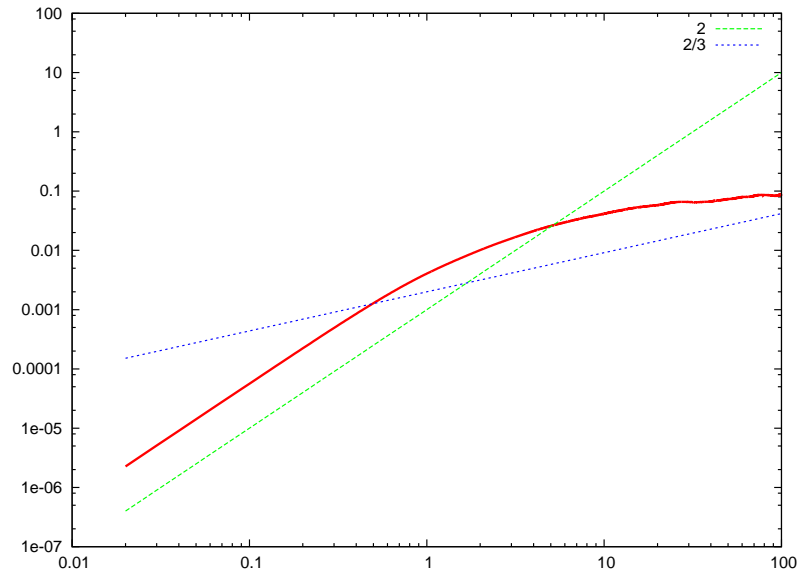
# $\langle \delta u^2(\tau) \rangle$ and $Q_s - R_s$ at $x/x_* = 0.420$



# $\langle \delta u^2(\tau) \rangle$ and $Q_s - R_s$ at $x/x_* = 0.472$

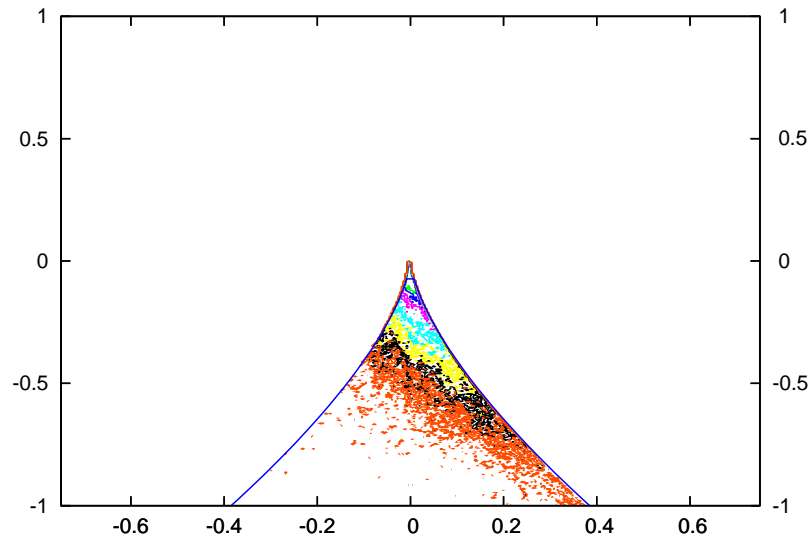
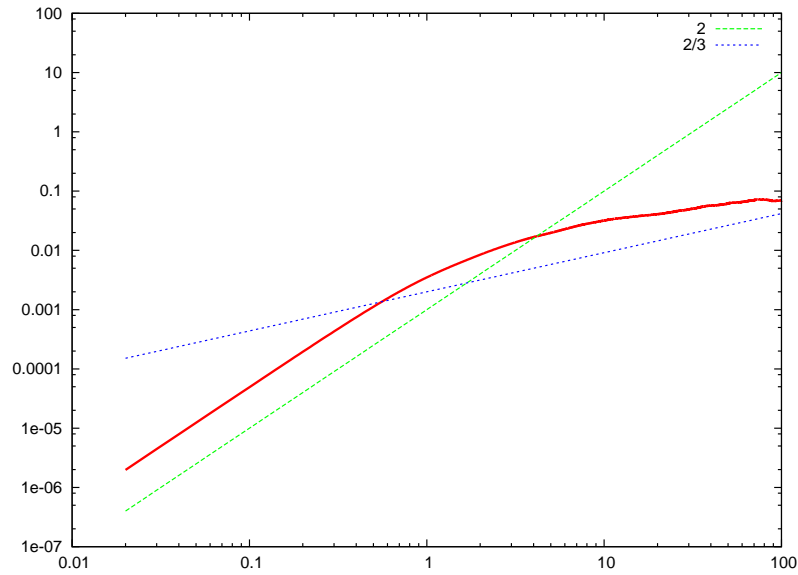


# $\langle \delta u^2(\tau) \rangle$ and $Q_s - R_s$ at $x/x_* = 0.525$

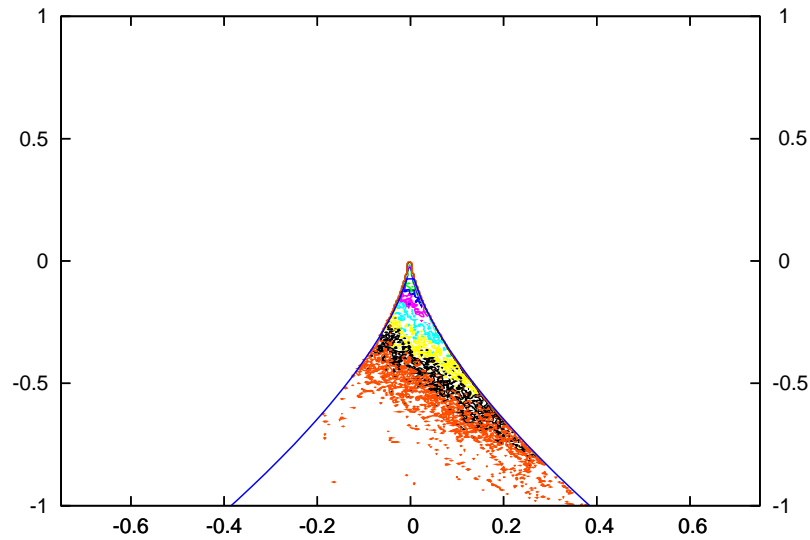
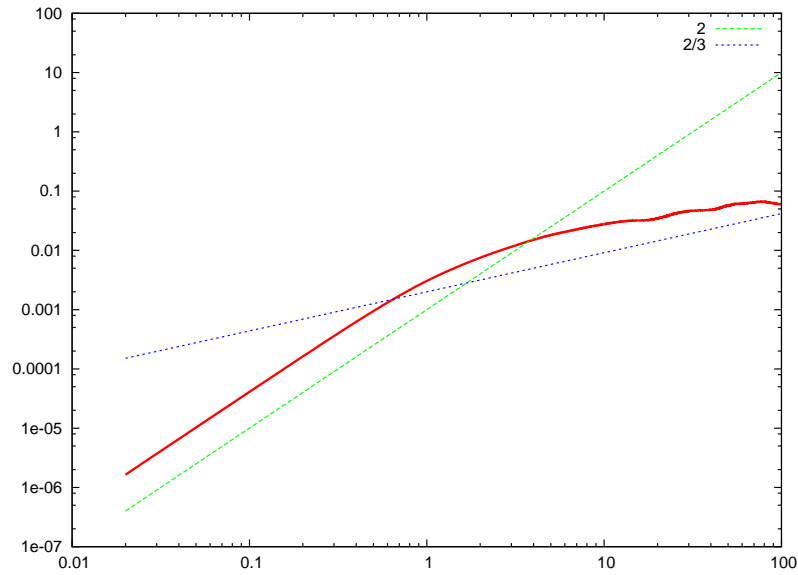




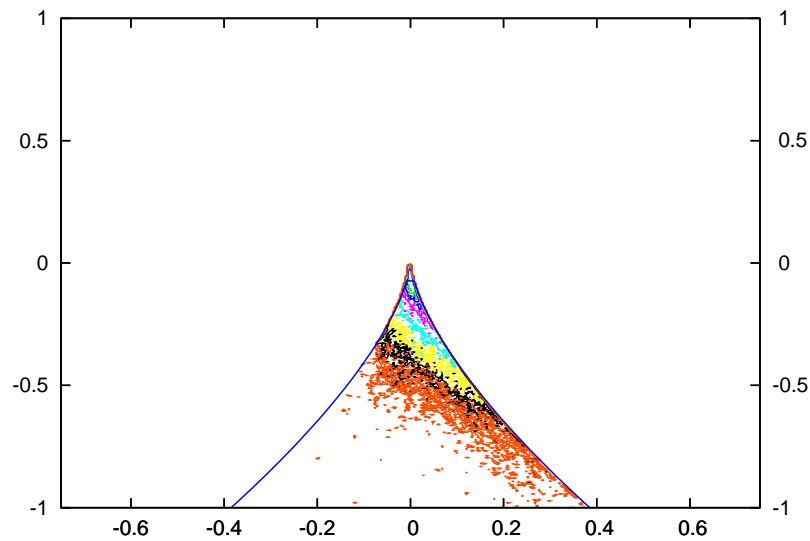
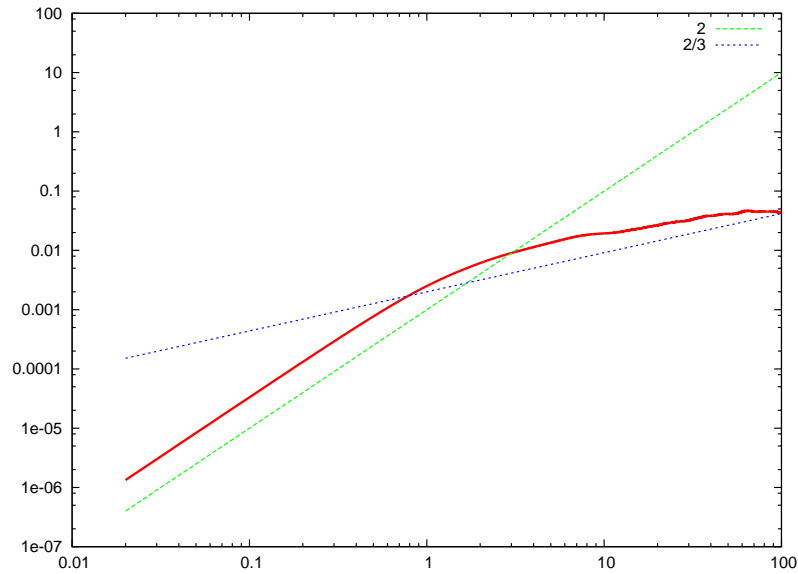
# $\langle \delta u^2(\tau) \rangle$ and $Q_s - R_s$ at $x/x_* = 0.577$



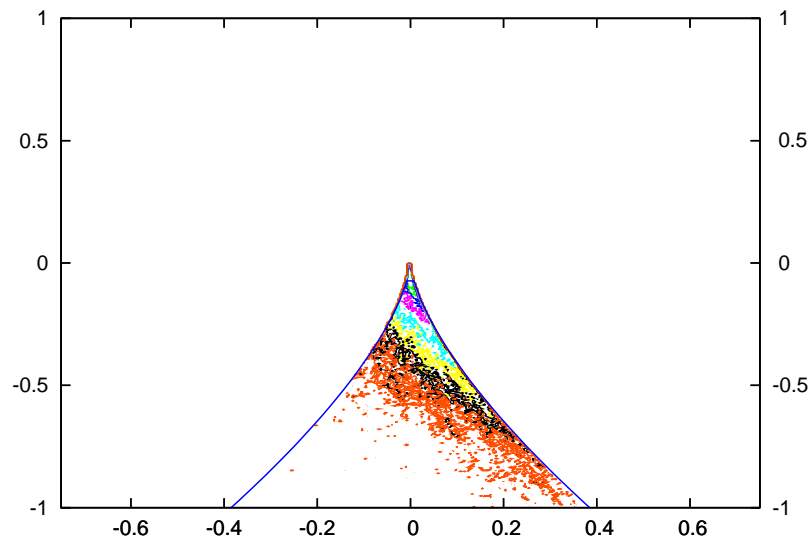
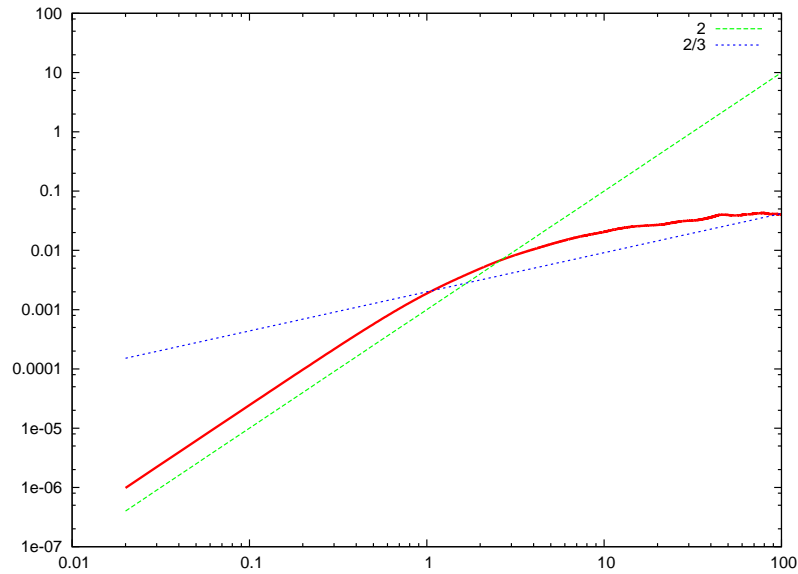
# $\langle \delta u^2(\tau) \rangle$ and $Q_s - R_s$ at $x/x_* = 0.630$



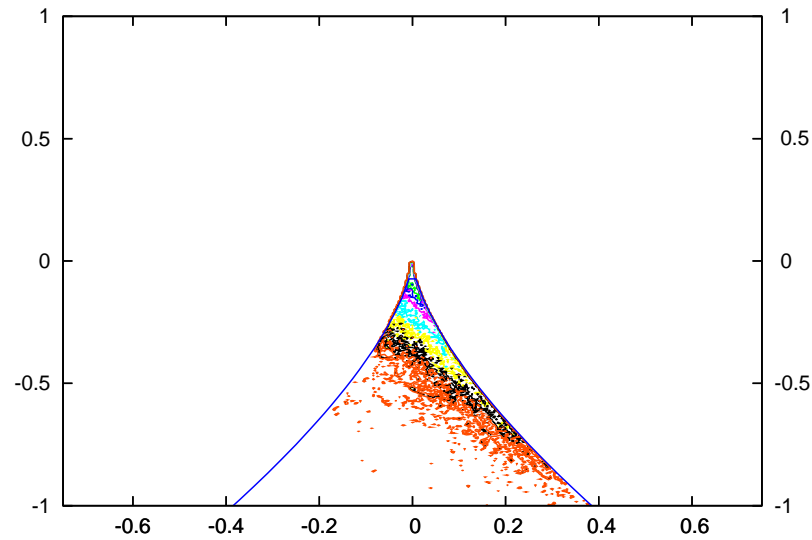
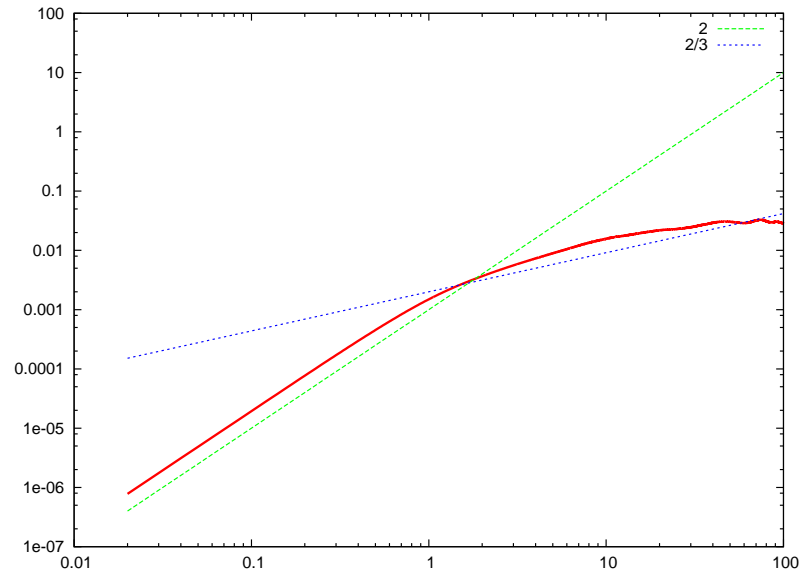
# $\langle \delta u^2(\tau) \rangle$ and $Q_s - R_s$ at $x/x_* = 0.683$



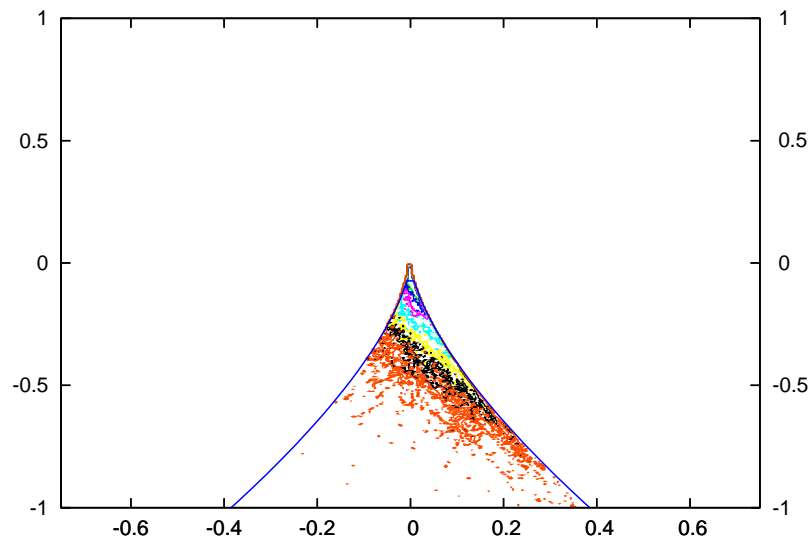
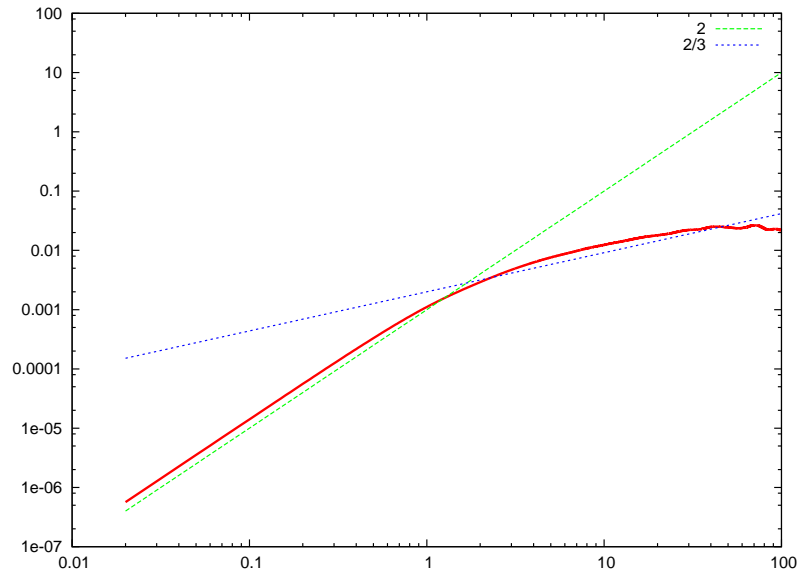
# $\langle \delta u^2(\tau) \rangle$ and $Q_s - R_s$ at $x/x_* = 0.735$



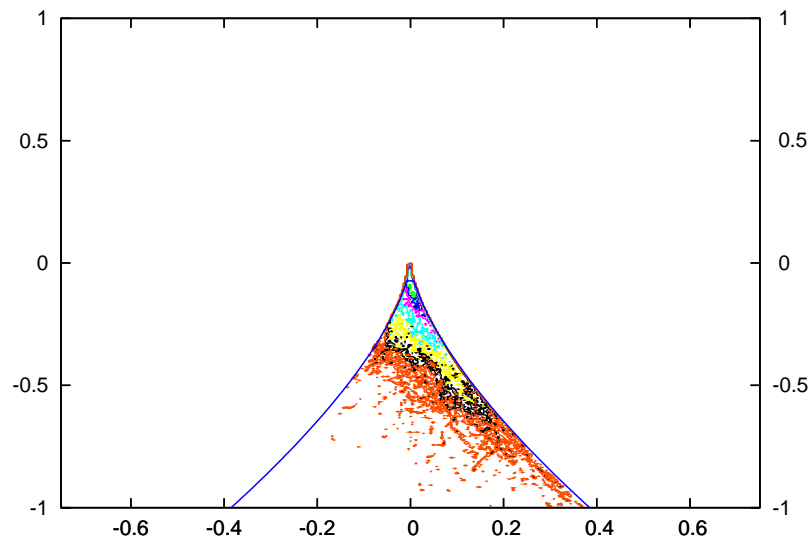
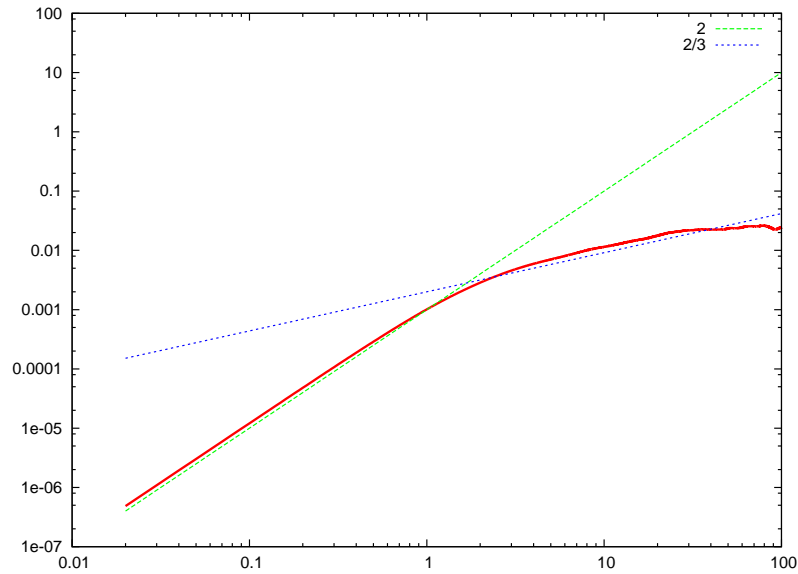
# $\langle \delta u^2(\tau) \rangle$ and $Q_s - R_s$ at $x/x_* = 0.788$



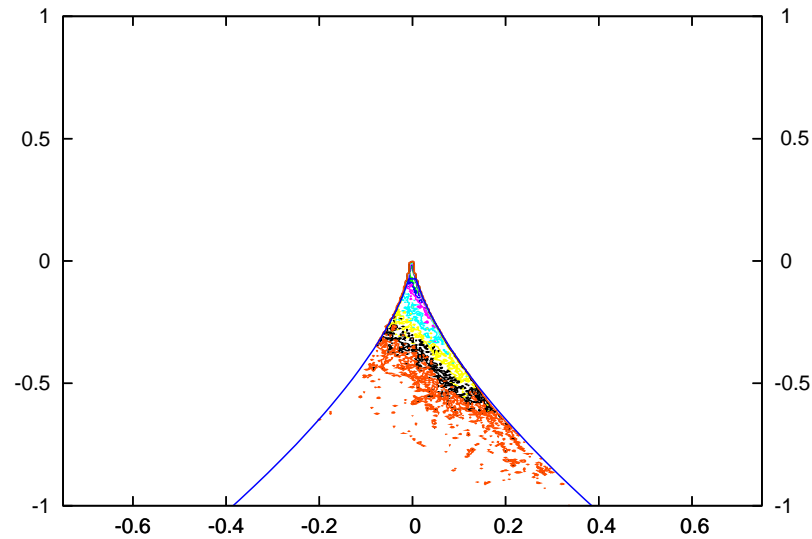
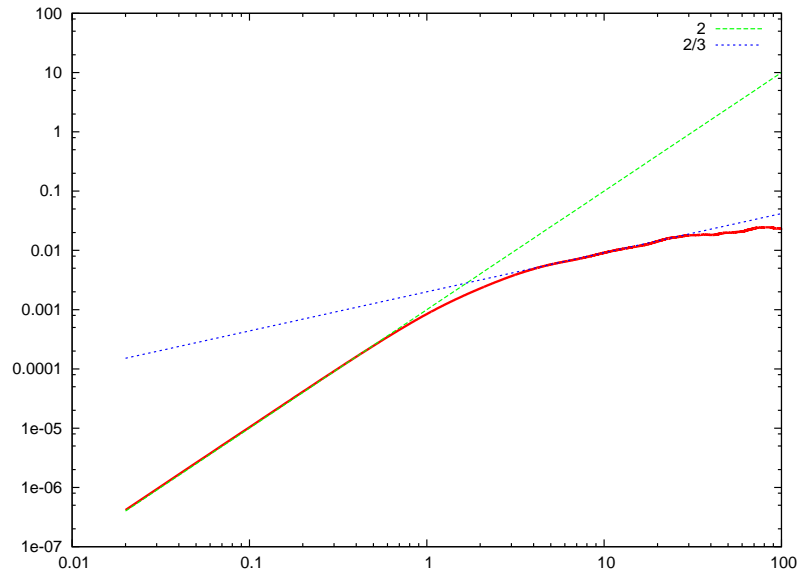
# $\langle \delta u^2(\tau) \rangle$ and $Q_s - R_s$ at $x/x_* = 0.840$



# $\langle \delta u^2(\tau) \rangle$ and $Q_s - R_s$ at $x/x_* = 0.893$

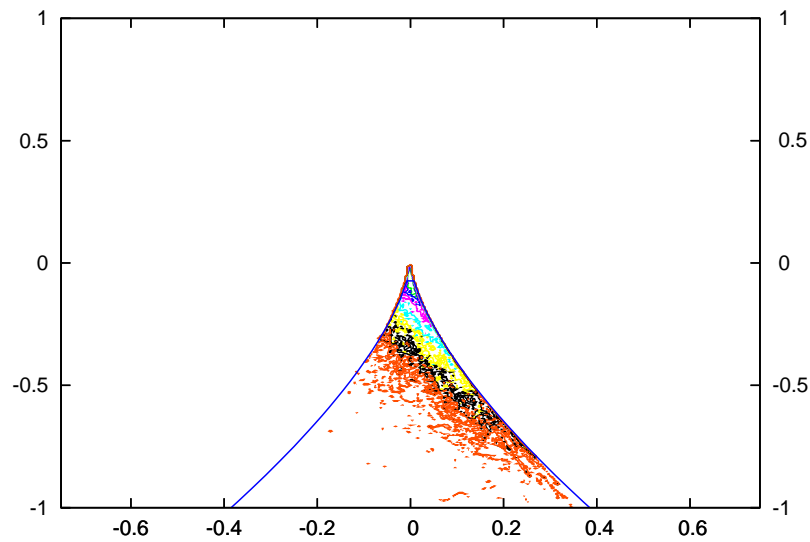
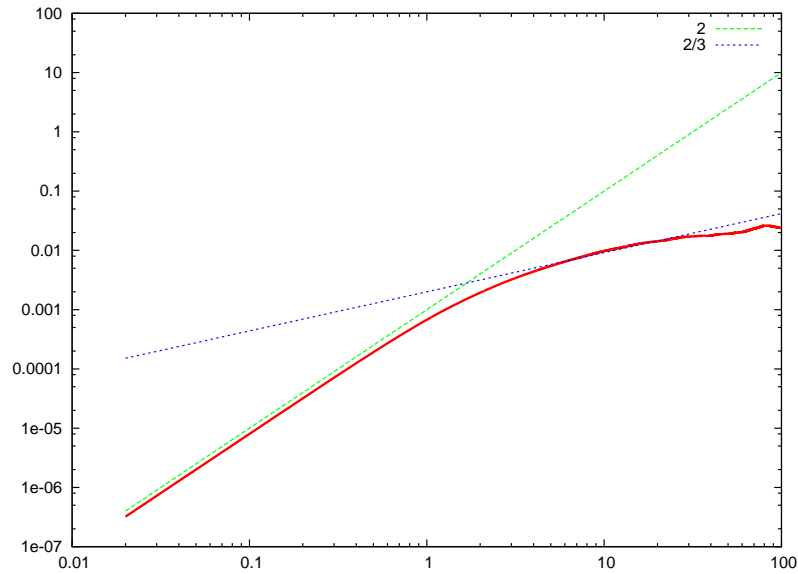


# $\langle \delta u^2(\tau) \rangle$ and $Q_s - R_s$ at $x/x_* = 0.945$

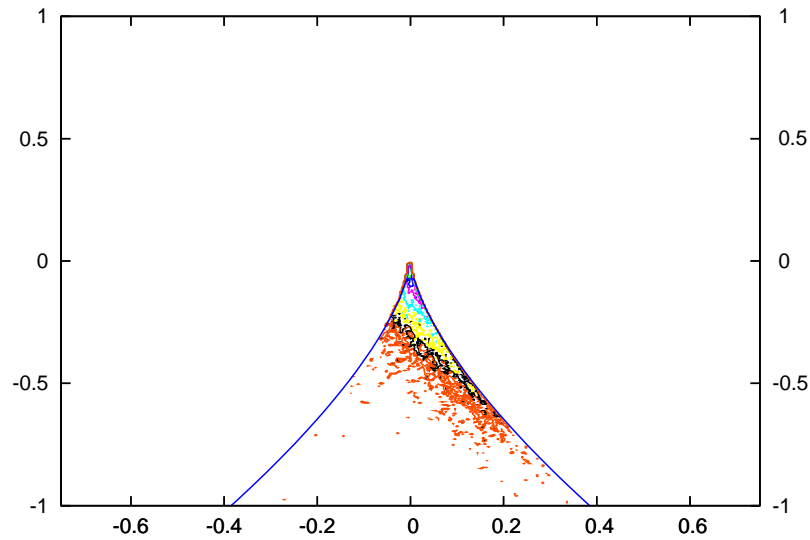
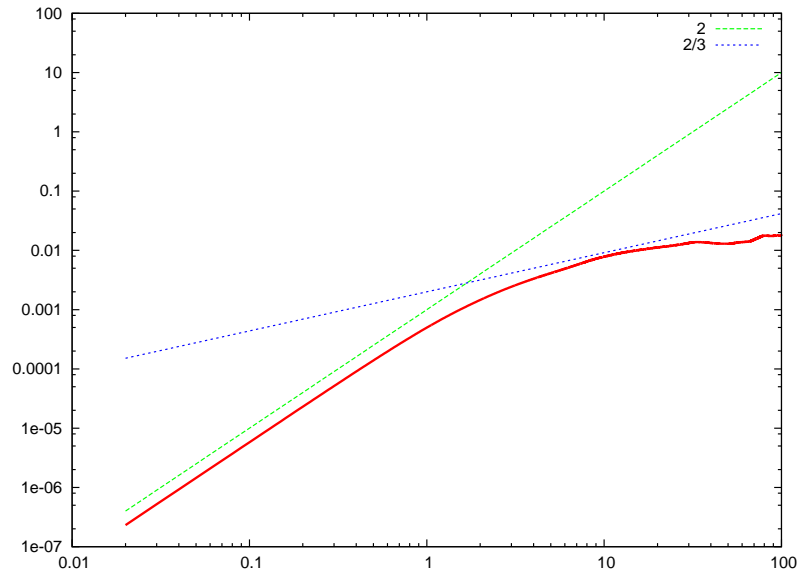




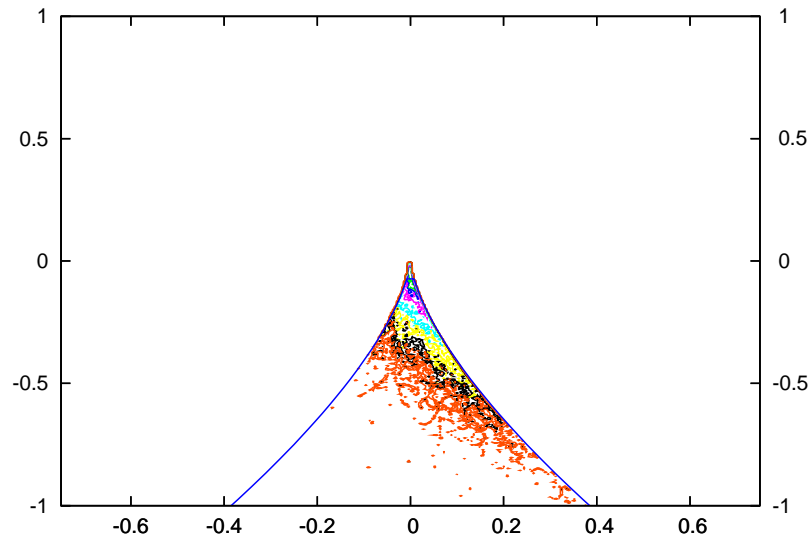
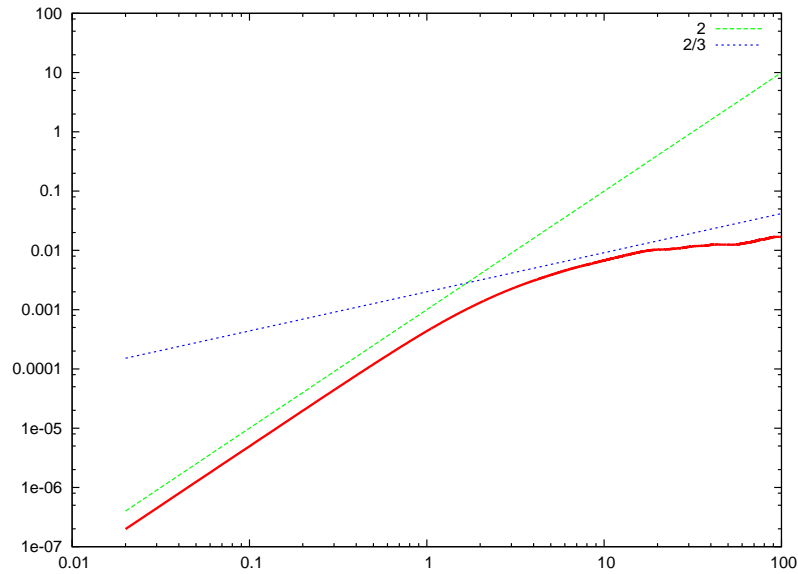
# $\langle \delta u^2(\tau) \rangle$ and $Q_s - R_s$ at $x/x_* = 0.998$



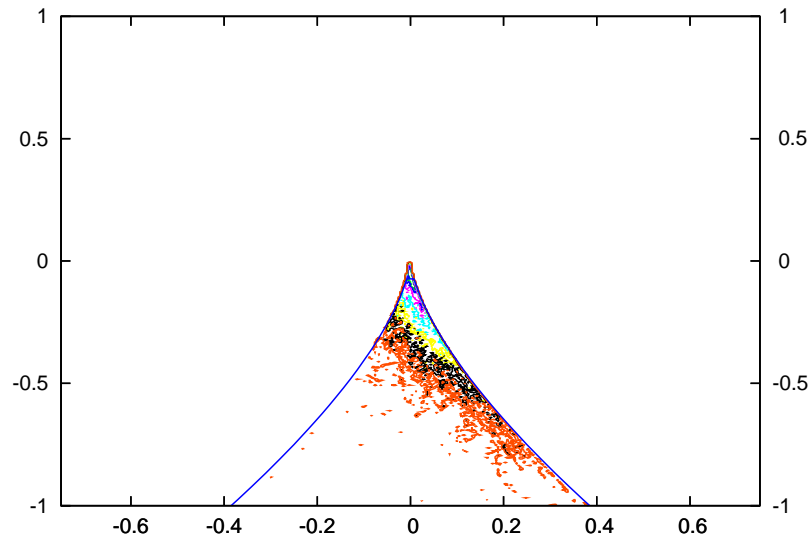
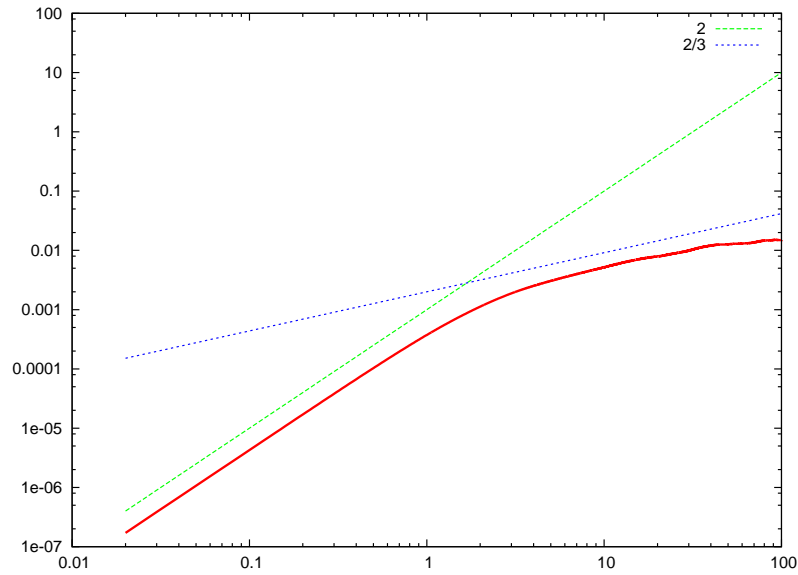
# $\langle \delta u^2(\tau) \rangle$ and $Q_s - R_s$ at $x/x_* = 1.050$



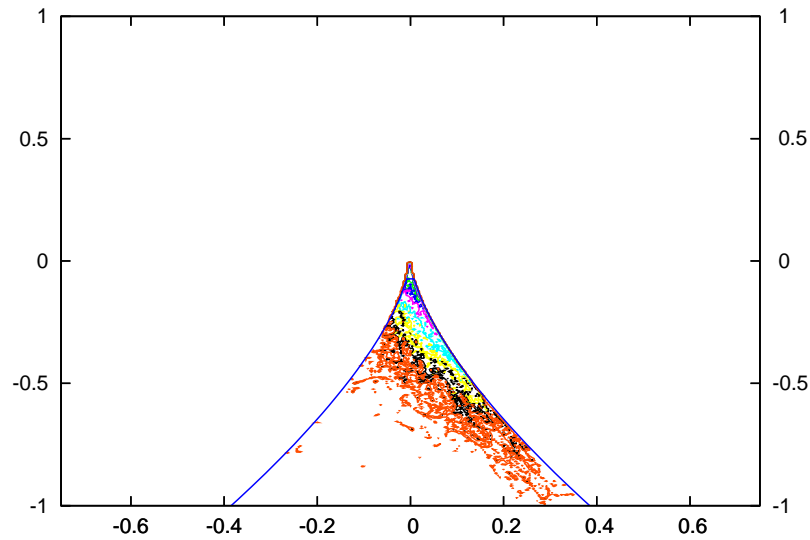
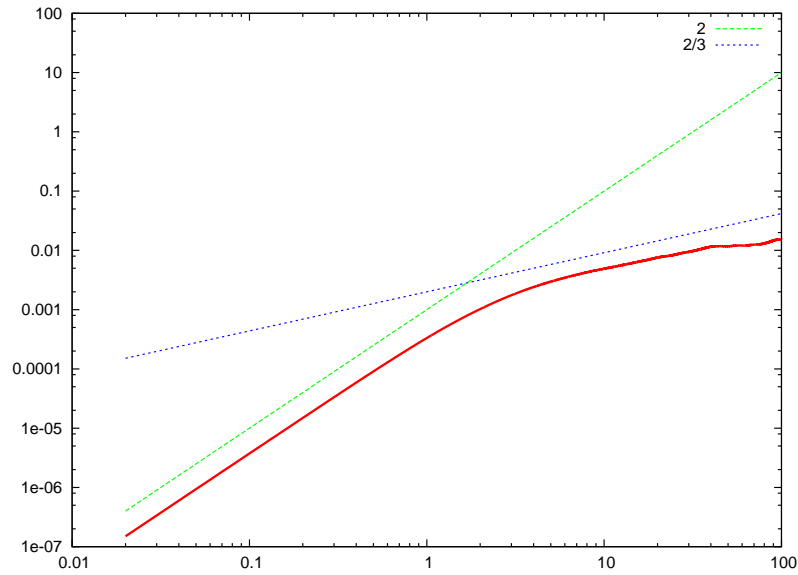
# $\langle \delta u^2(\tau) \rangle$ and $Q_s - R_s$ at $x/x_* = 1.103$



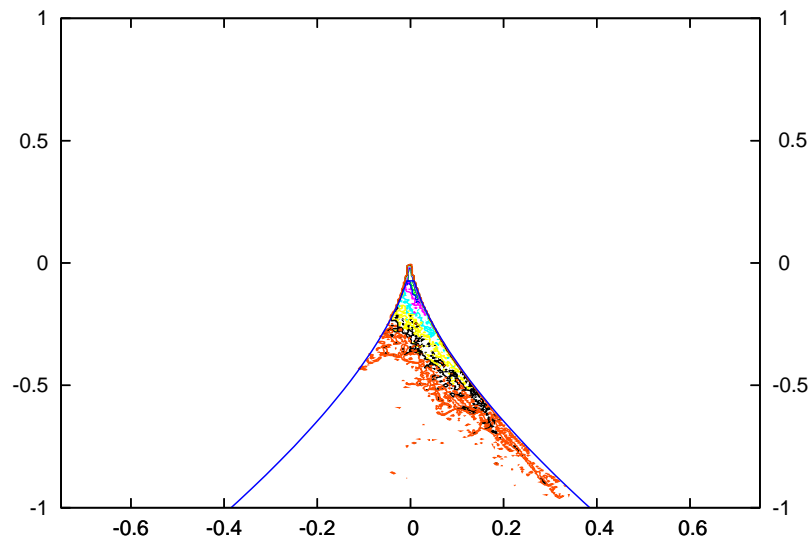
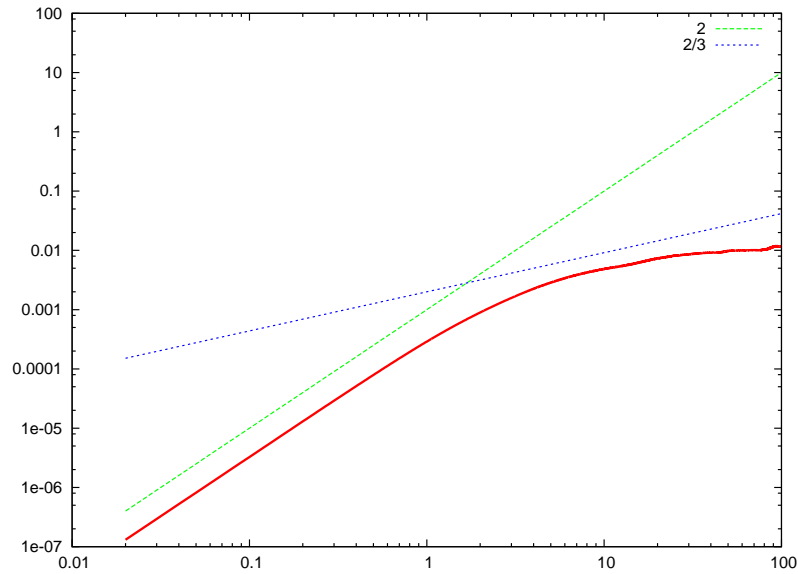
# $\langle \delta u^2(\tau) \rangle$ and $Q_s - R_s$ at $x/x_* = 1.155$



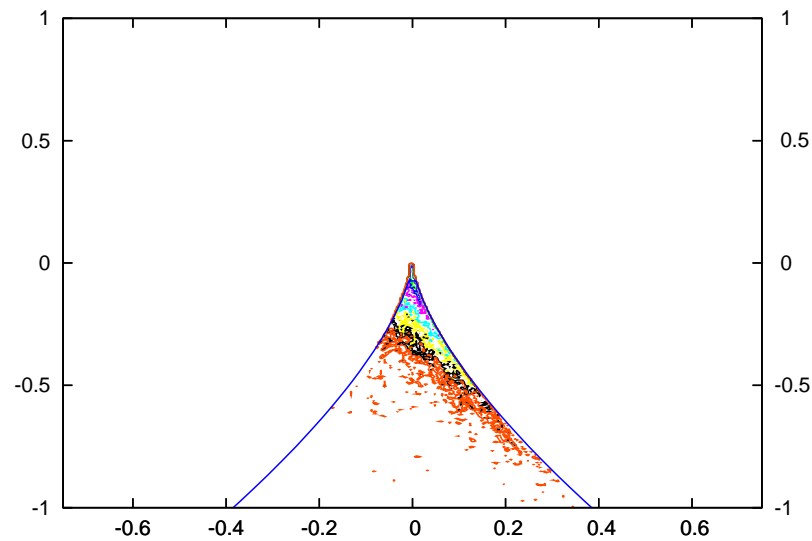
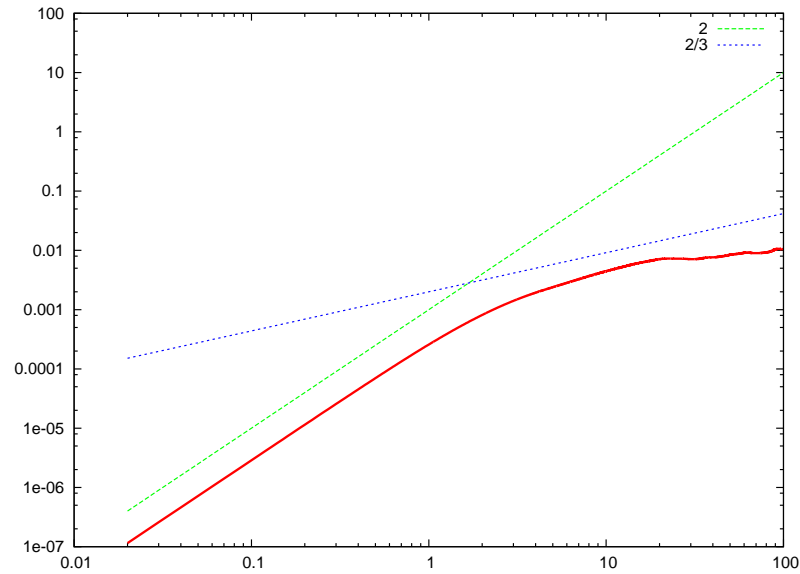
# $\langle \delta u^2(\tau) \rangle$ and $Q_s - R_s$ at $x/x_* = 1.208$



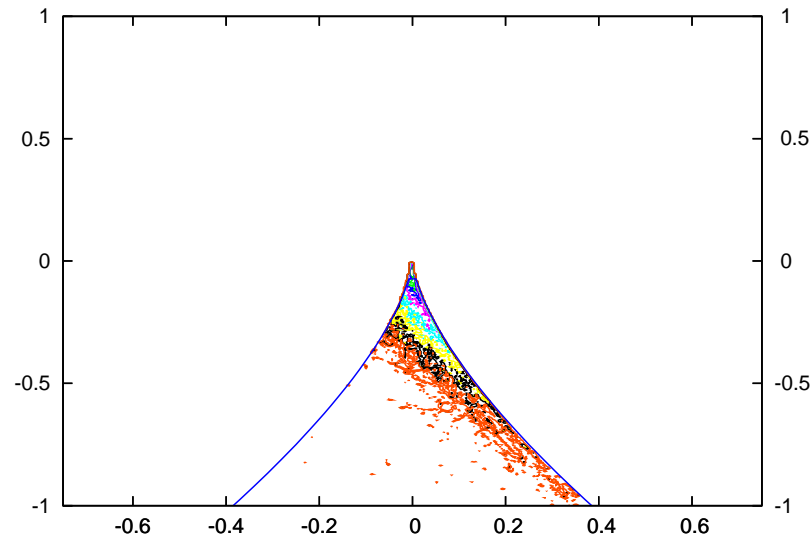
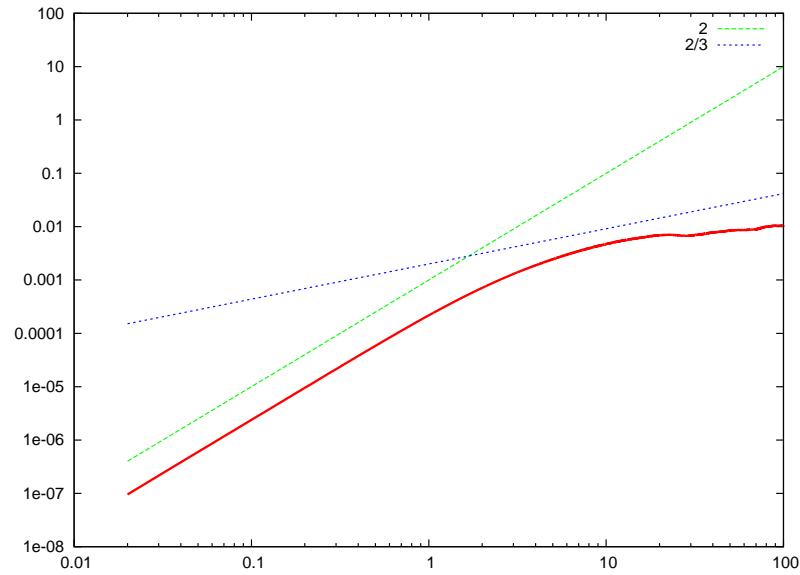
# $\langle \delta u^2(\tau) \rangle$ and $Q_s - R_s$ at $x/x_* = 1.261$



# $\langle \delta u^2(\tau) \rangle$ and $Q_s - R_s$ at $x/x_* = 1.313$

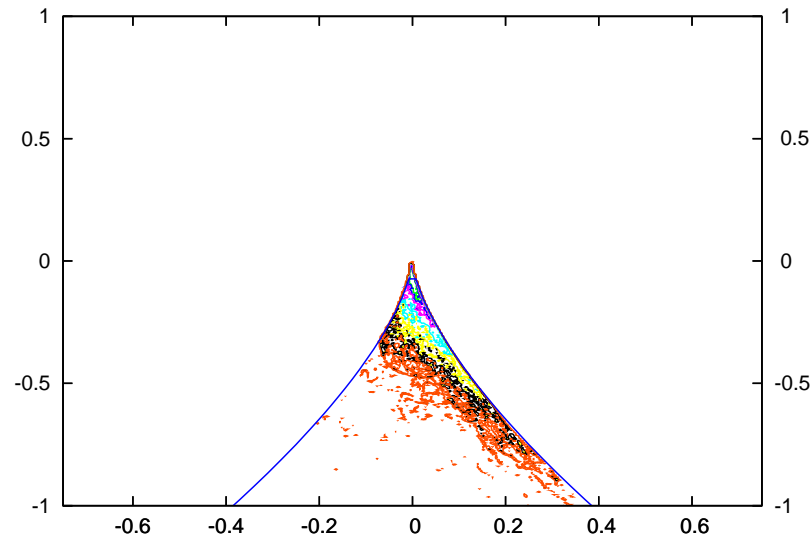
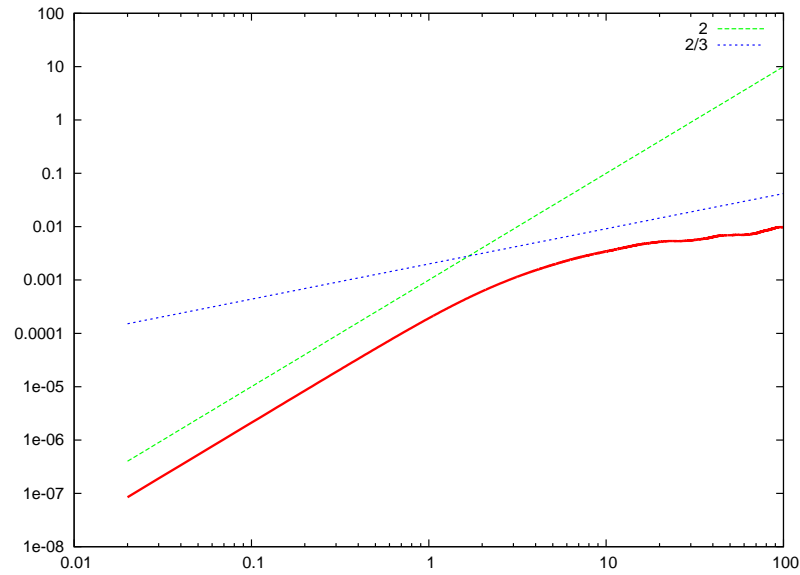


# $\langle \delta u^2(\tau) \rangle$ and $Q_s - R_s$ at $x/x_* = 1.366$

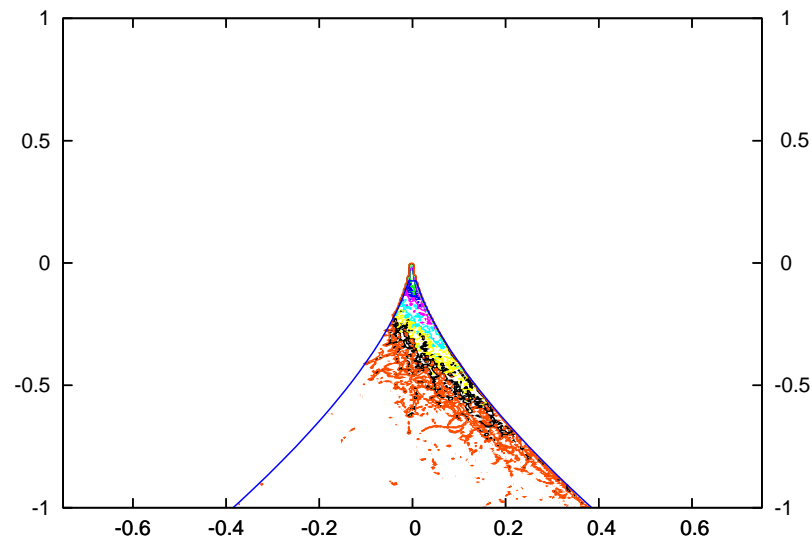
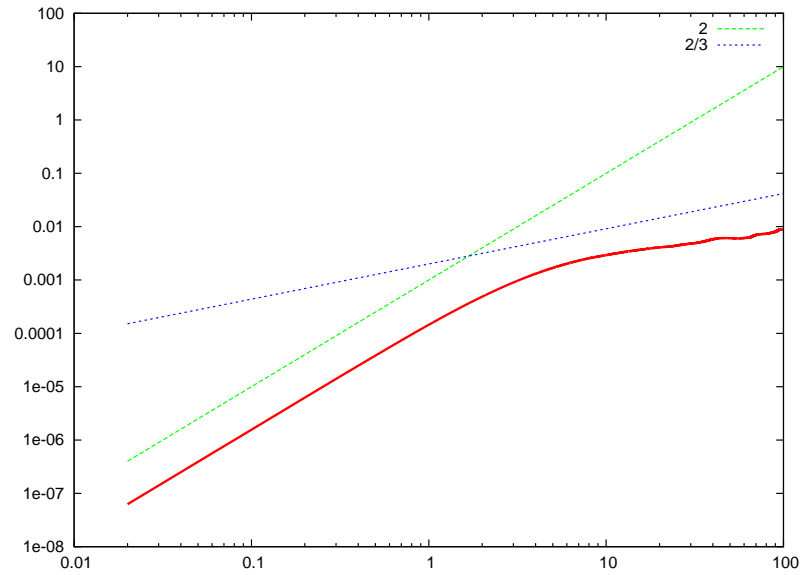




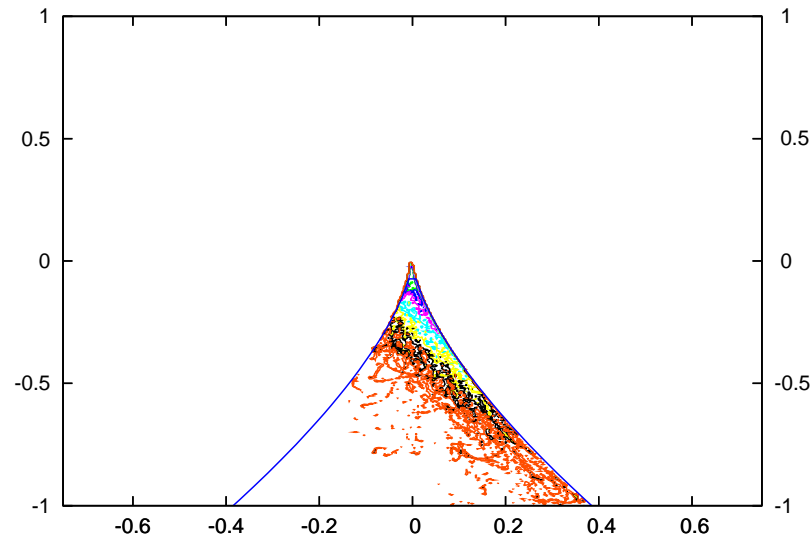
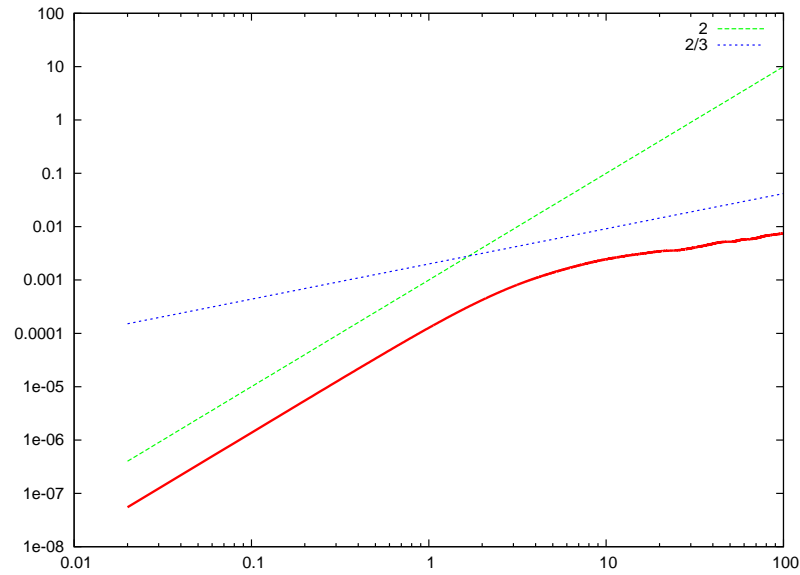
# $\langle \delta u^2(\tau) \rangle$ and $Q_s - R_s$ at $x/x_* = 1.418$



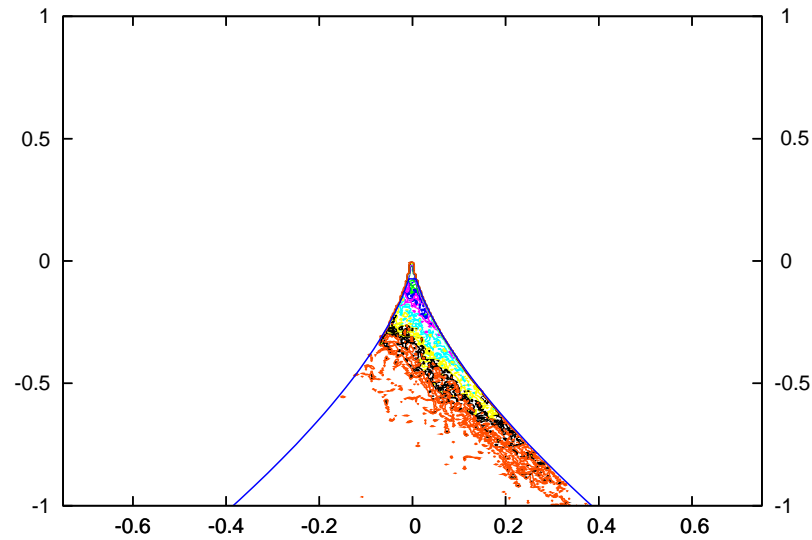
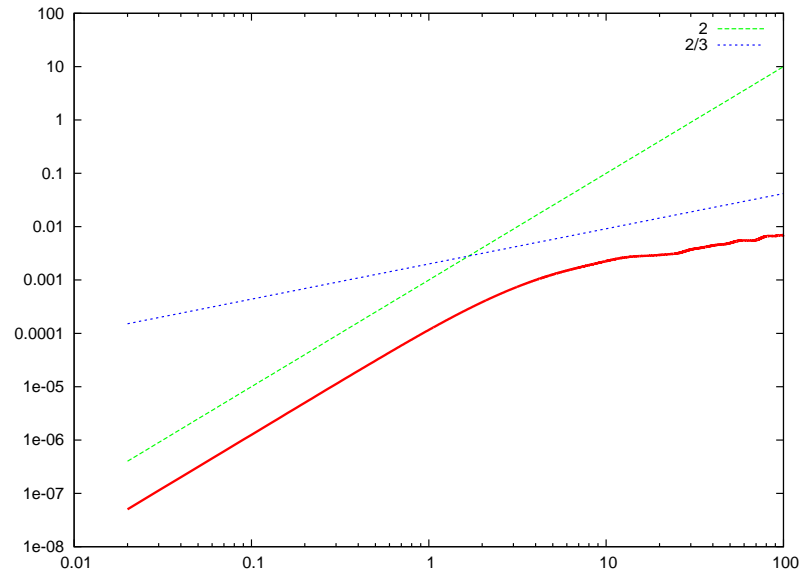
# $\langle \delta u^2(\tau) \rangle$ and $Q_s - R_s$ at $x/x_* = 1.471$



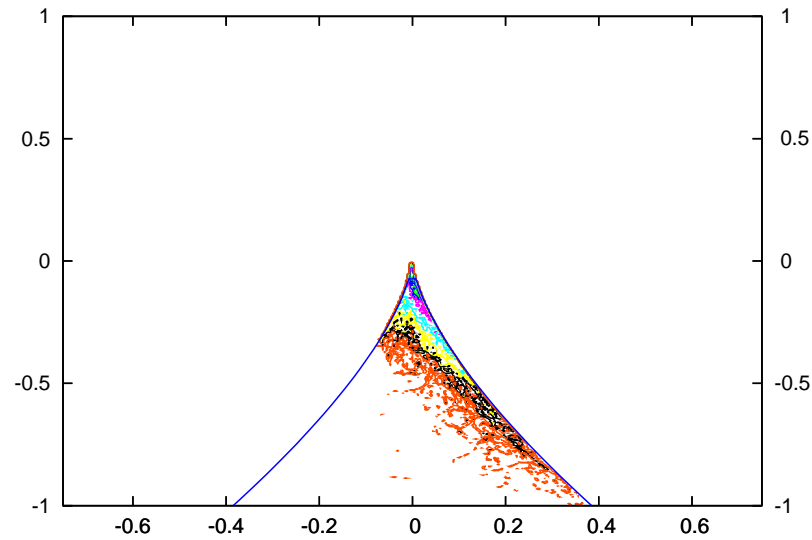
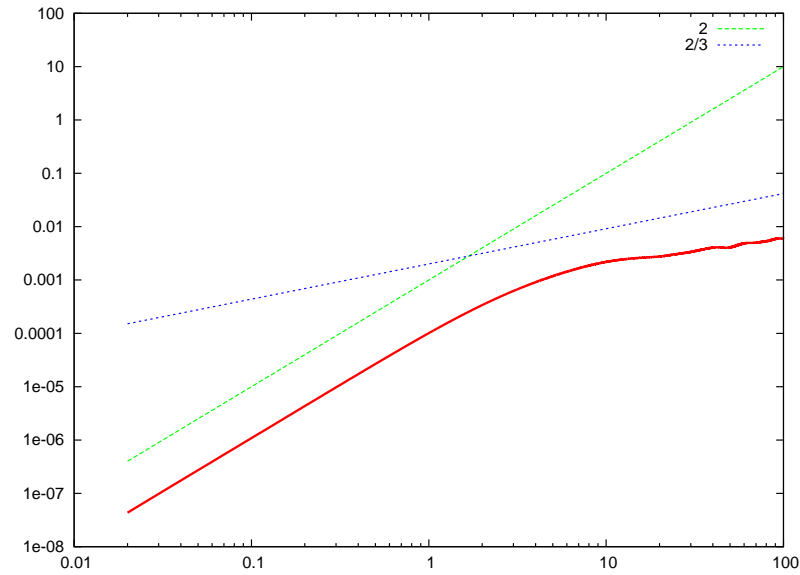
# $\langle \delta u^2(\tau) \rangle$ and $Q_s - R_s$ at $x/x_* = 1.523$



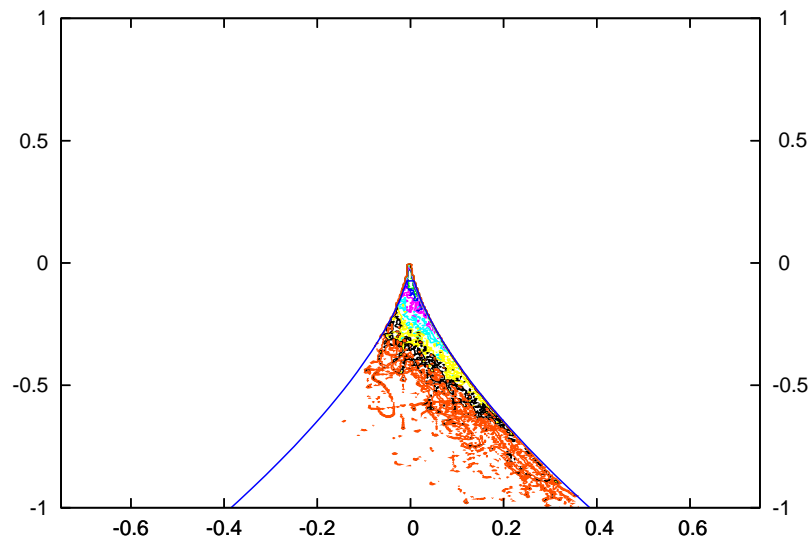
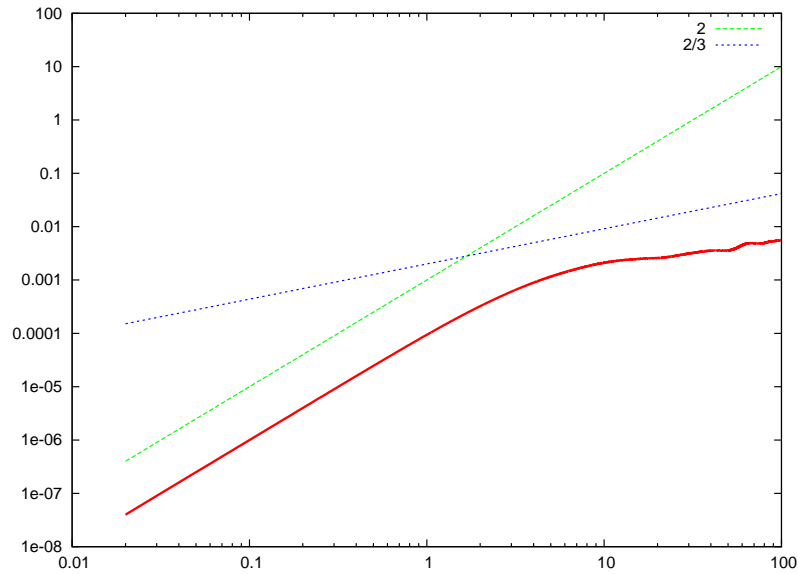
# $\langle \delta u^2(\tau) \rangle$ and $Q_s - R_s$ at $x/x_* = 1.576$



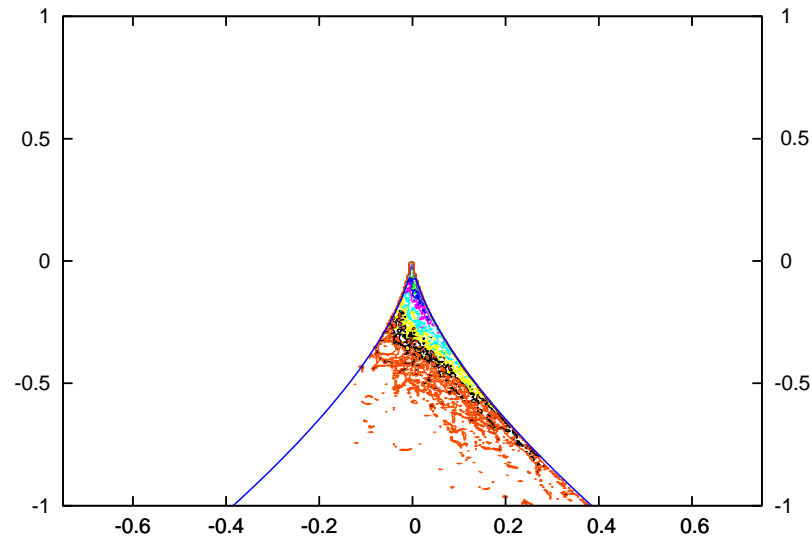
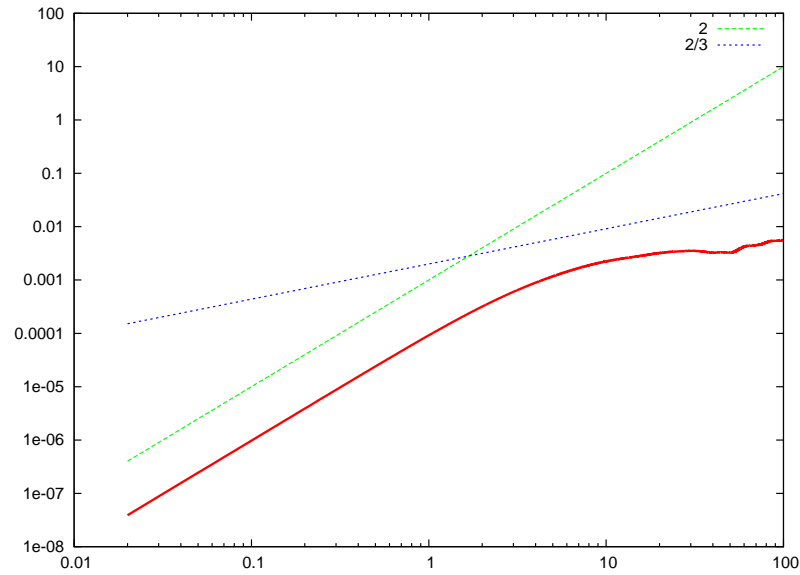
# $\langle \delta u^2(\tau) \rangle$ and $Q_s - R_s$ at $x/x_* = 1.628$



# $\langle \delta u^2(\tau) \rangle$ and $Q_s - R_s$ at $x/x_* = 1.681$

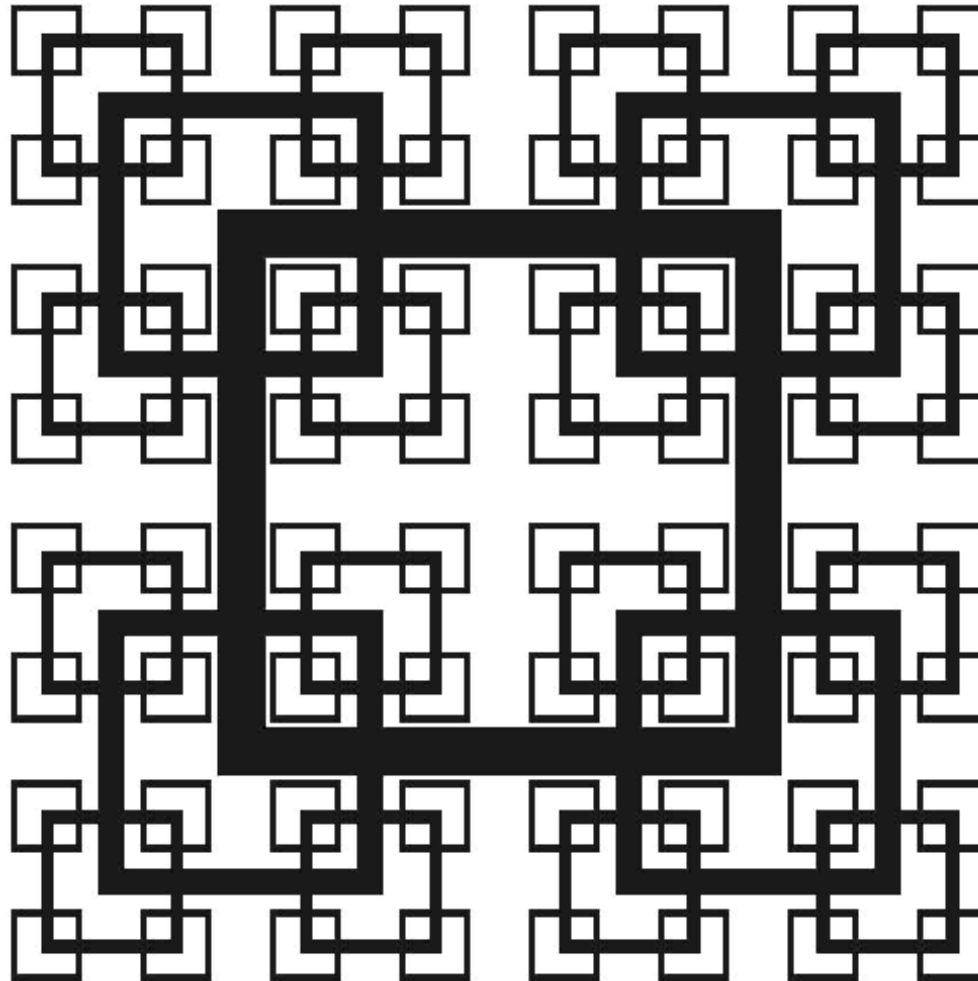


# $\langle \delta u^2(\tau) \rangle$ and $Q_s - R_s$ at $x/x_* = 1.733$



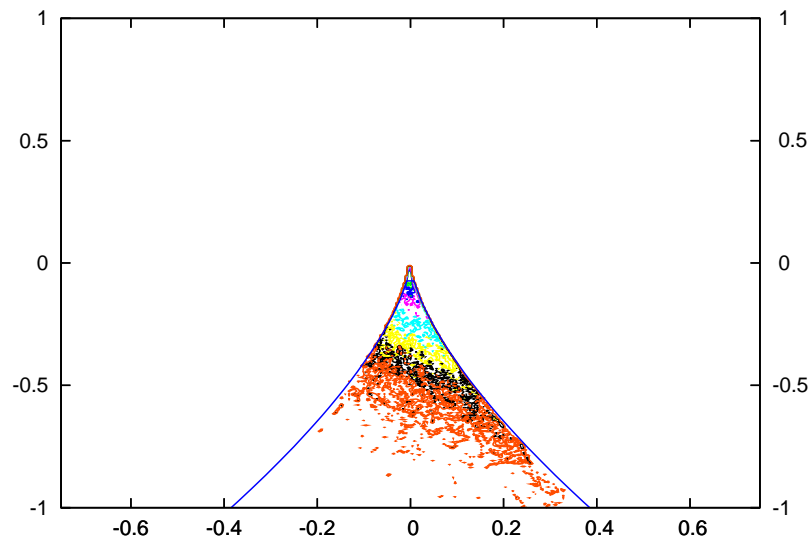
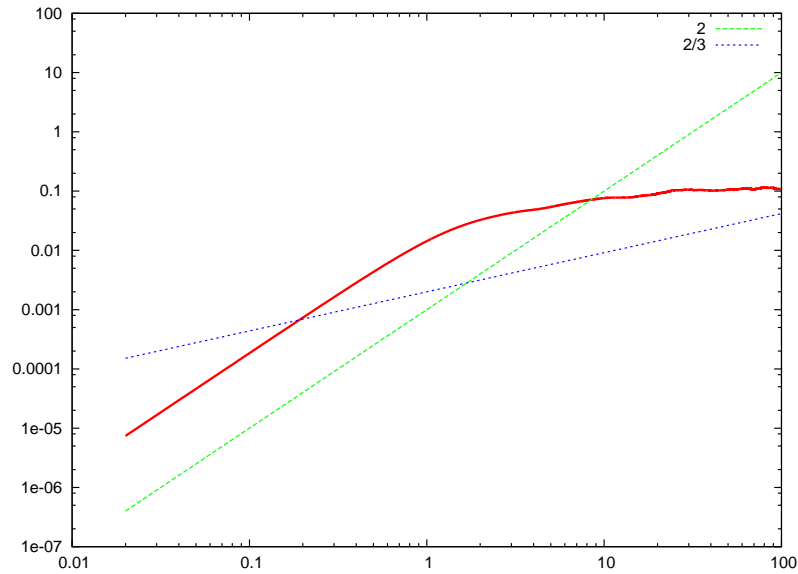
# Next inside wake of big bars

Previous plots were taken along the centreline.  
Next plots are taken along the line normal to the grid and  
crossing a biggest bar at the middle.

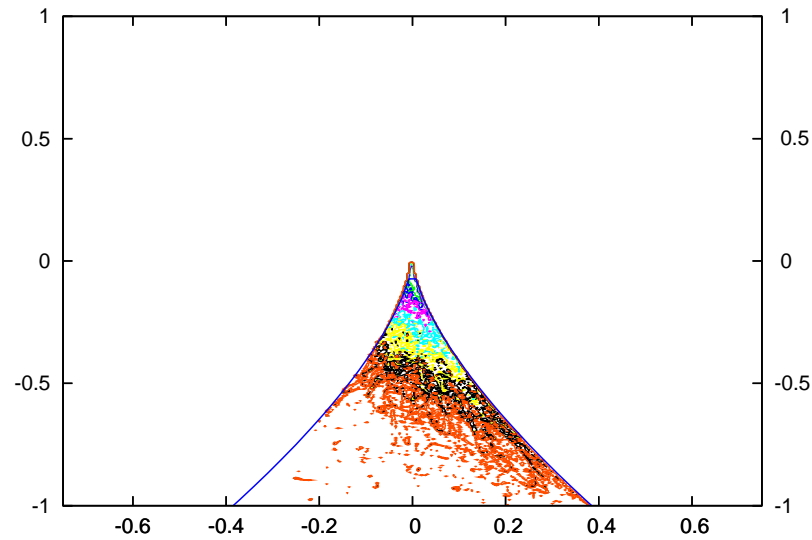
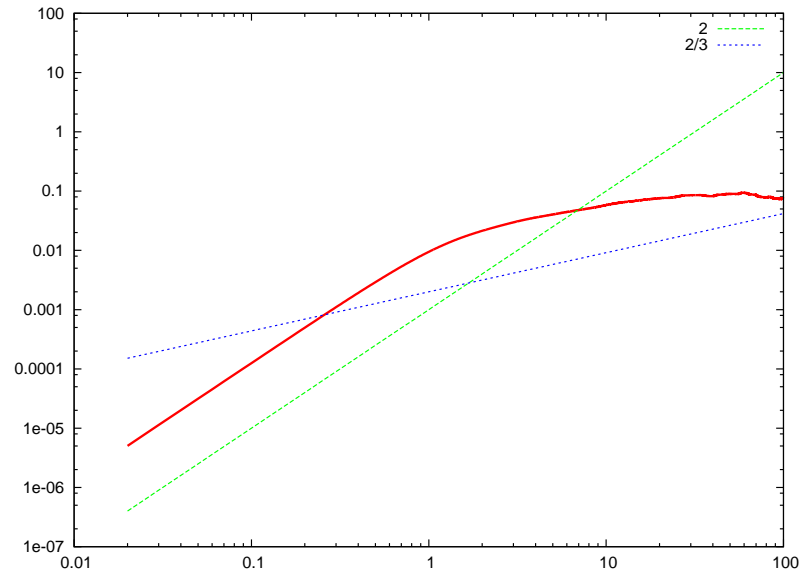




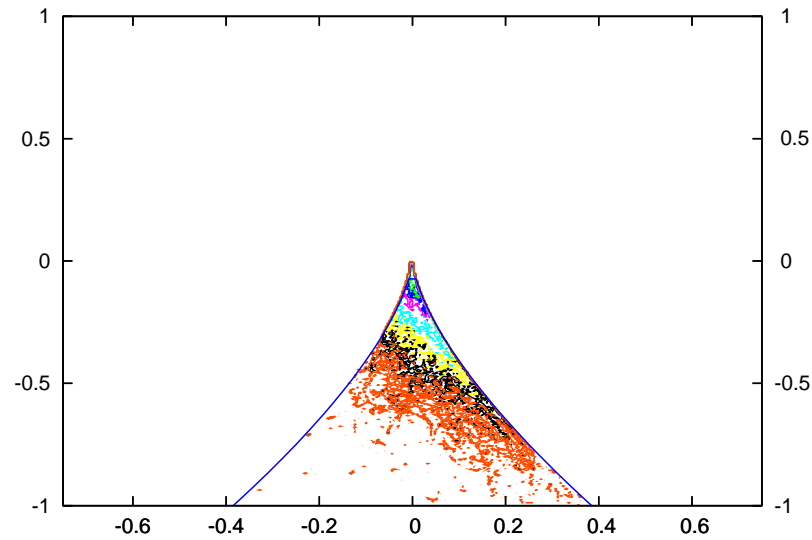
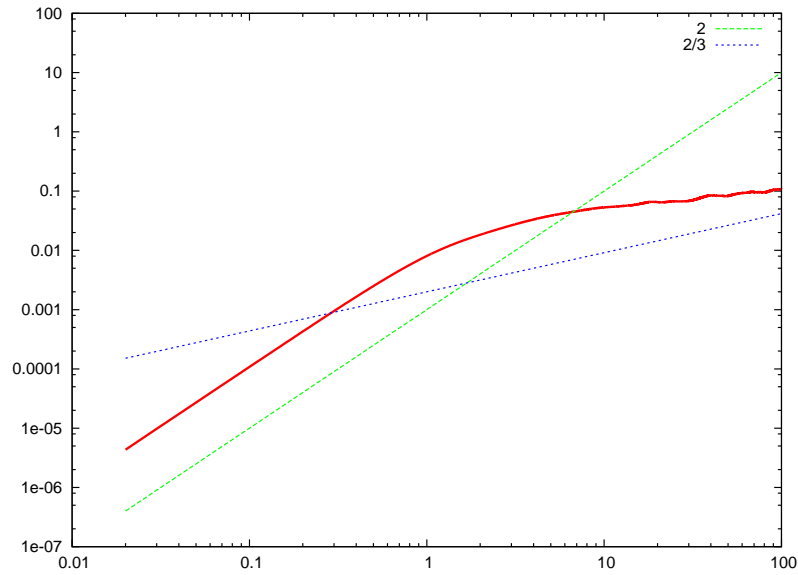
# $\langle \delta u^2(\tau) \rangle$ and $Q_s - R_s$ at $x/x_* = 0.052$



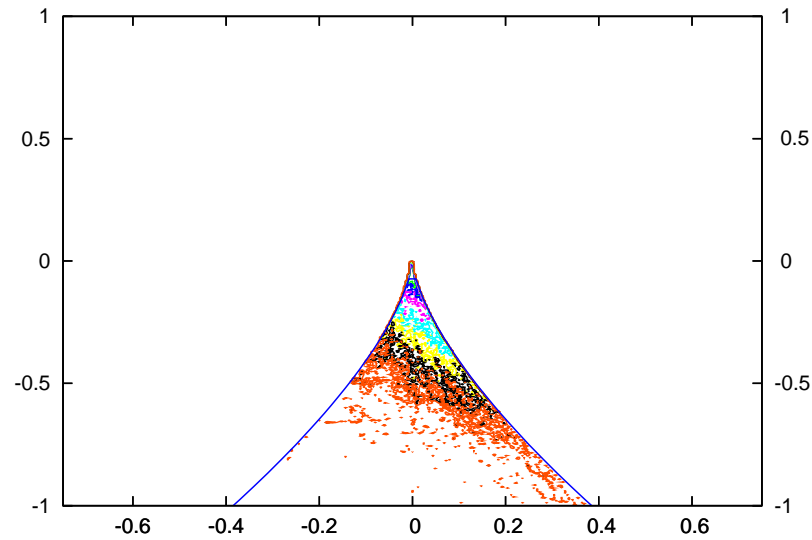
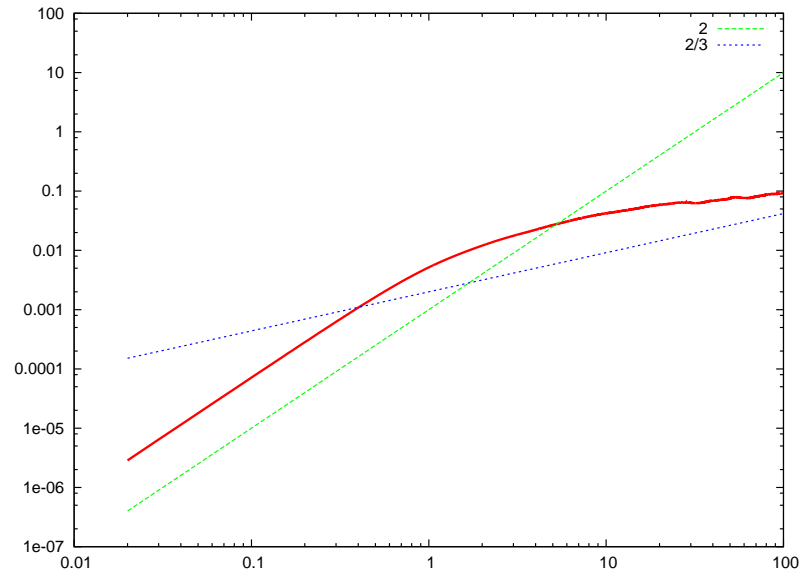
# $\langle \delta u^2(\tau) \rangle$ and $Q_s - R_s$ at $x/x_* = 0.105$



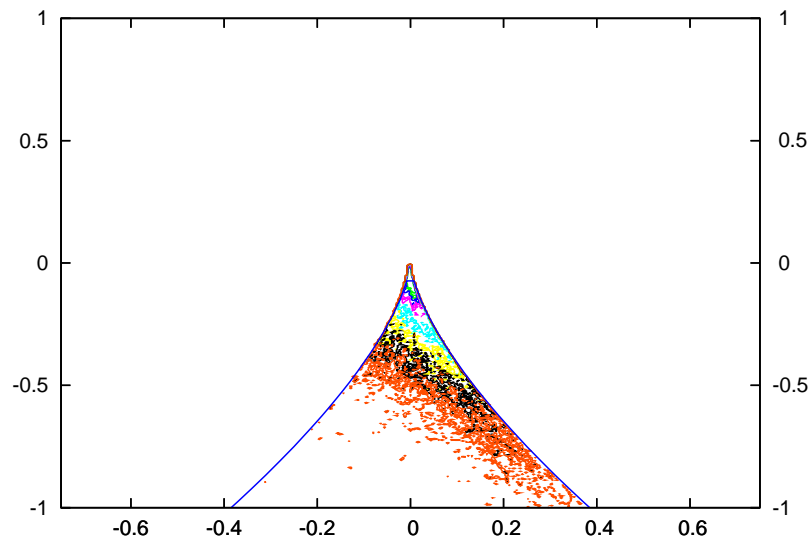
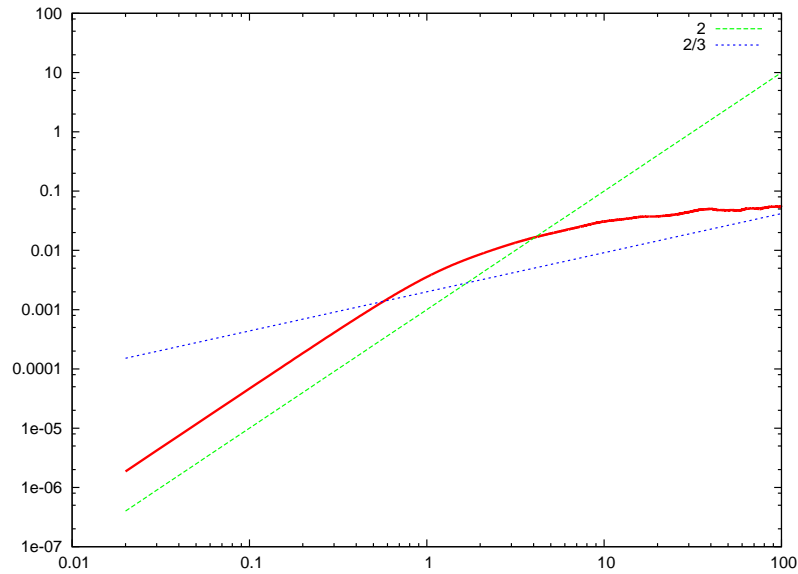
# $\langle \delta u^2(\tau) \rangle$ and $Q_s - R_s$ at $x/x_* = 0.157$



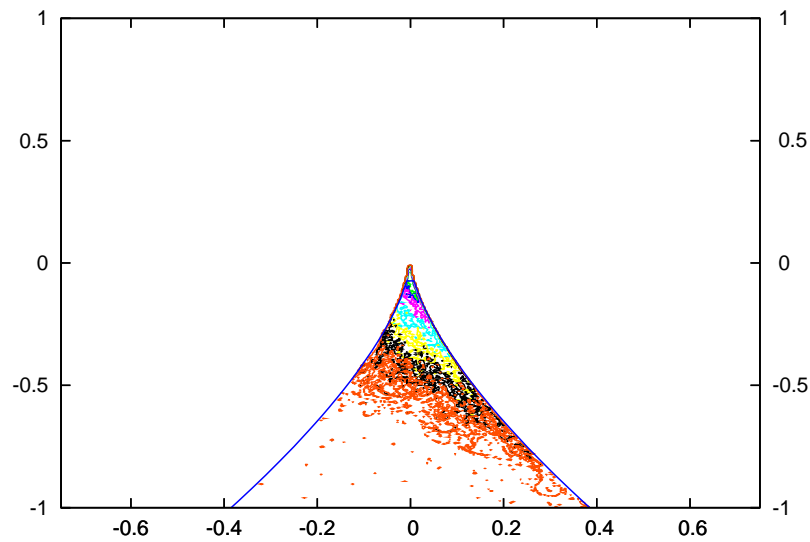
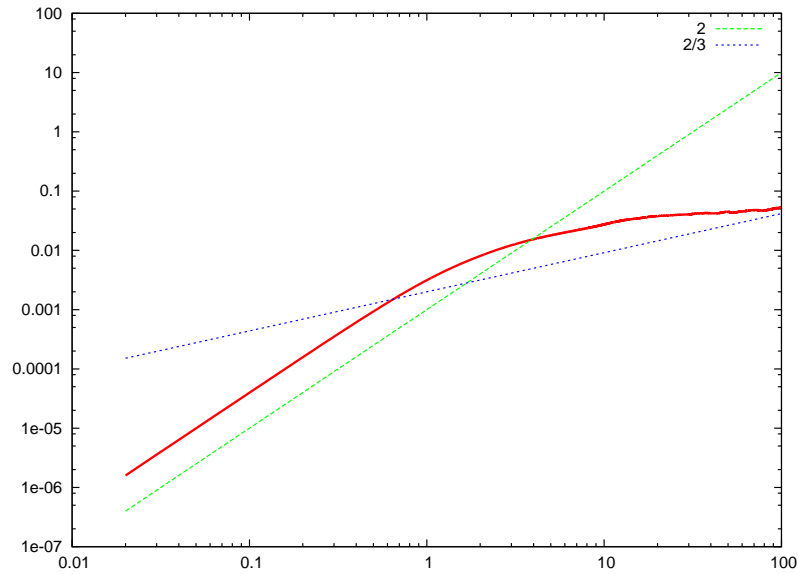
# $\langle \delta u^2(\tau) \rangle$ and $Q_s - R_s$ at $x/x_* = 0.210$



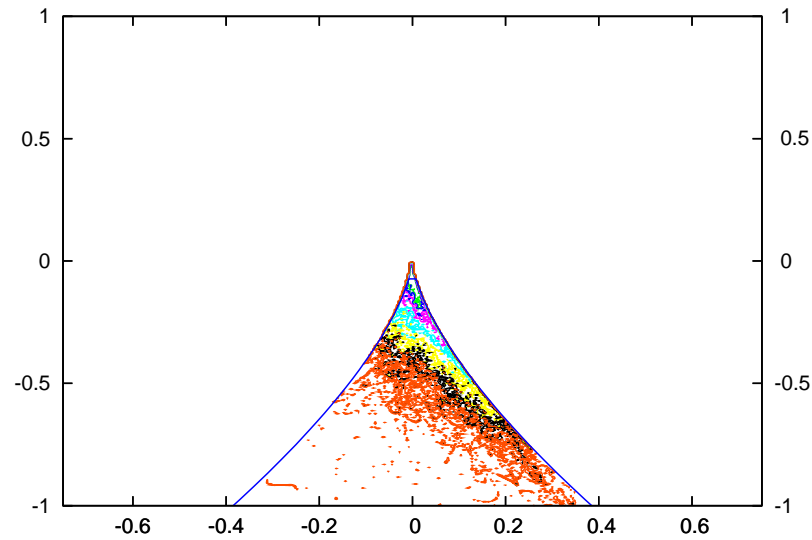
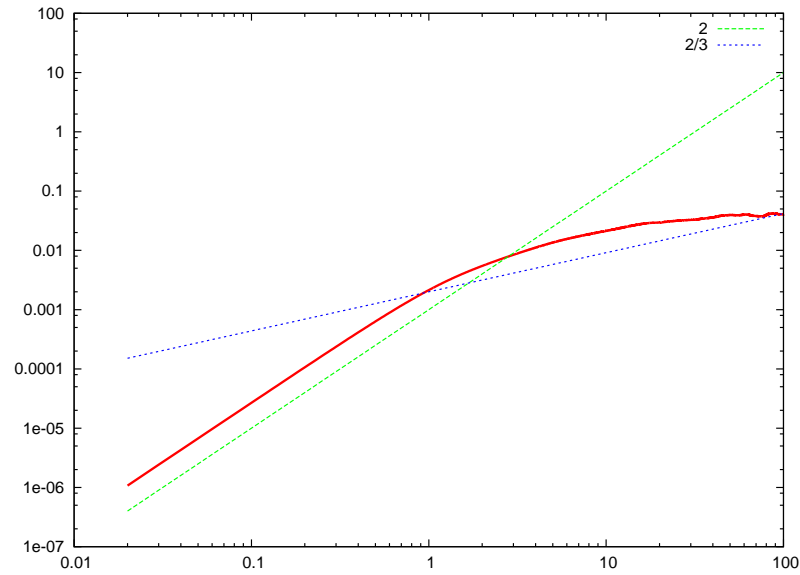
# $\langle \delta u^2(\tau) \rangle$ and $Q_s - R_s$ at $x/x_* = 0.262$



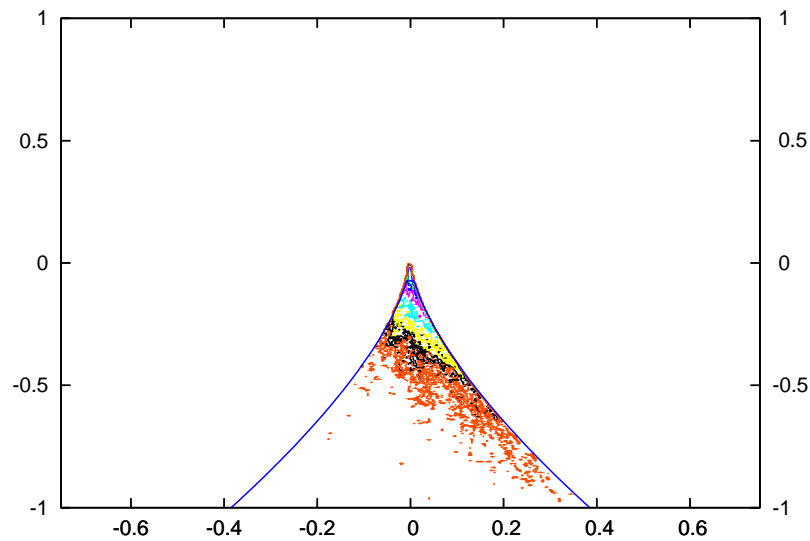
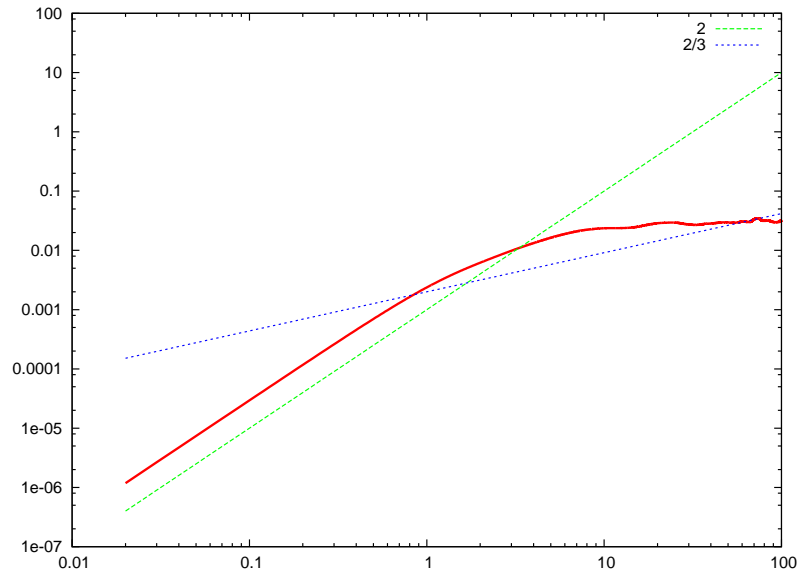
# $\langle \delta u^2(\tau) \rangle$ and $Q_s - R_s$ at $x/x_* = 0.315$



# $\langle \delta u^2(\tau) \rangle$ and $Q_s - R_s$ at $x/x_* = 0.367$

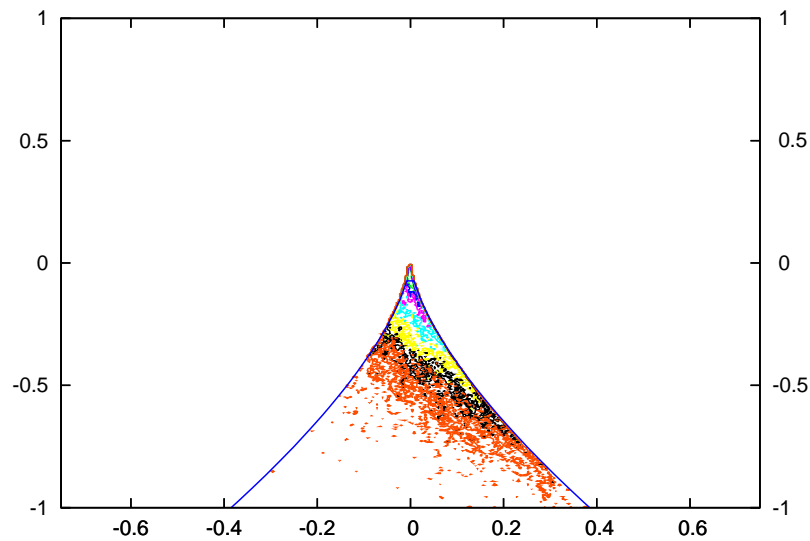
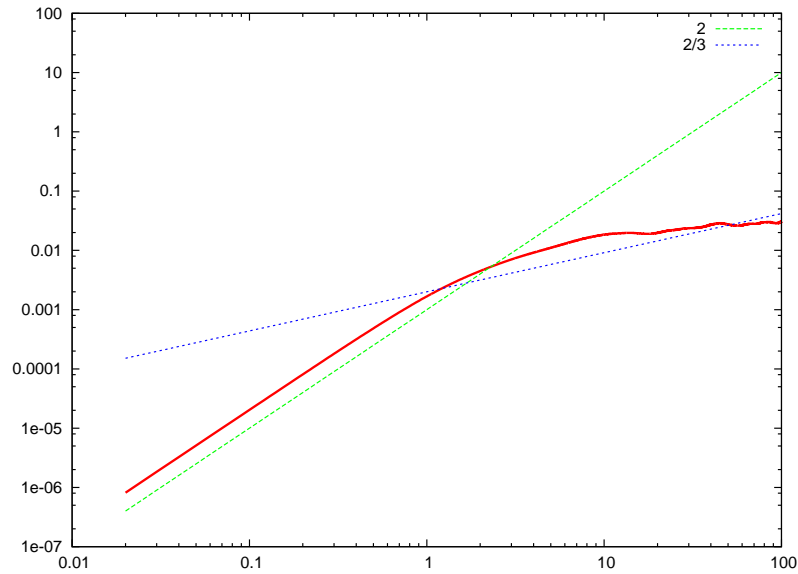


# $\langle \delta u^2(\tau) \rangle$ and $Q_s - R_s$ at $x/x_* = 0.420$

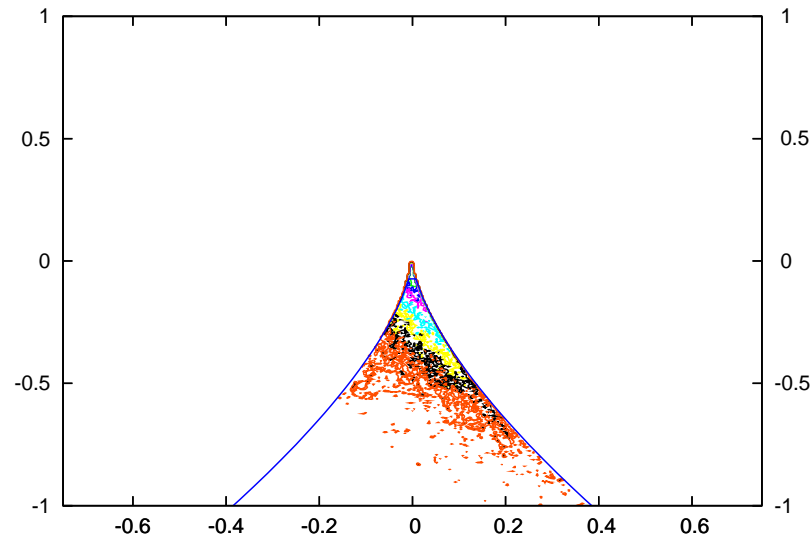
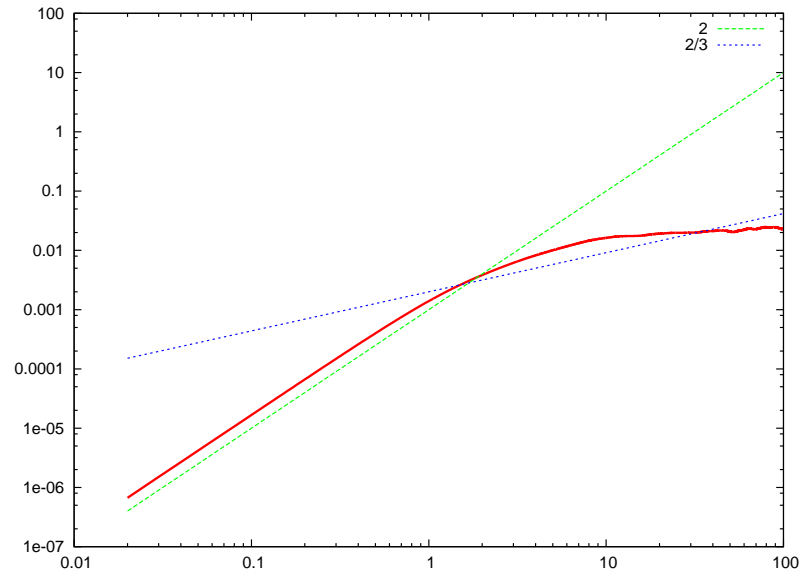




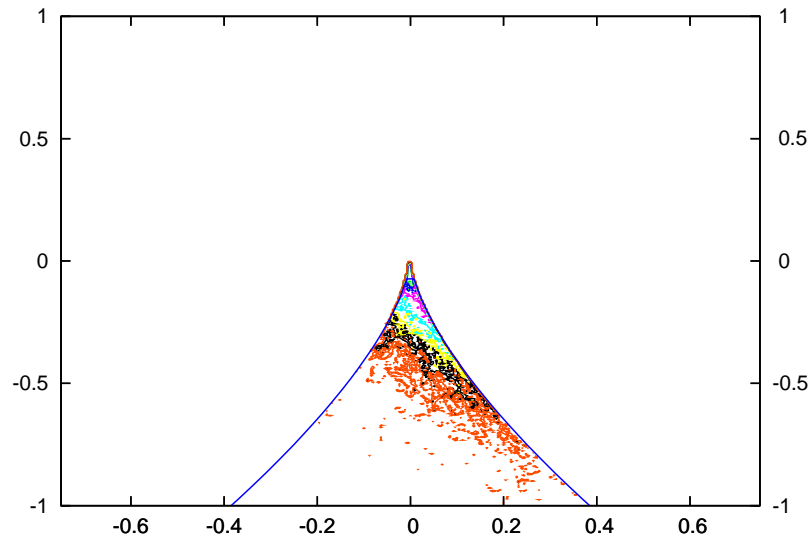
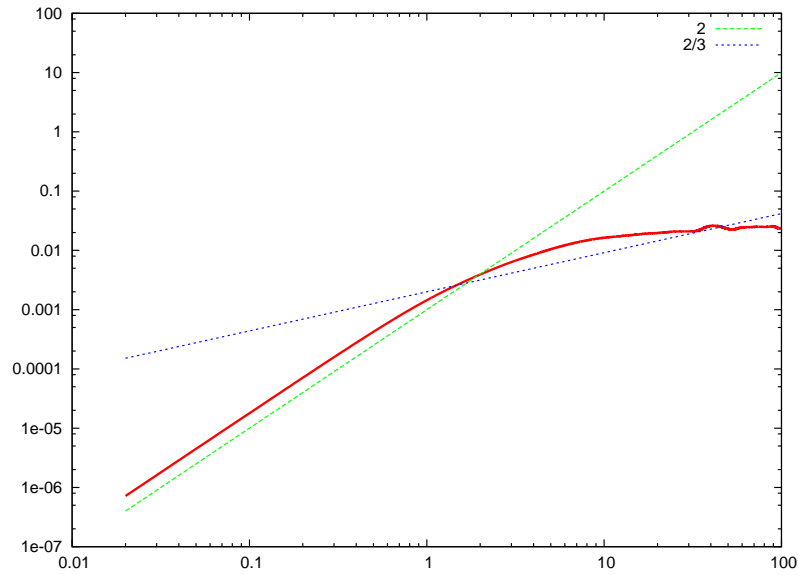
# $\langle \delta u^2(\tau) \rangle$ and $Q_s - R_s$ at $x/x_* = 0.472$



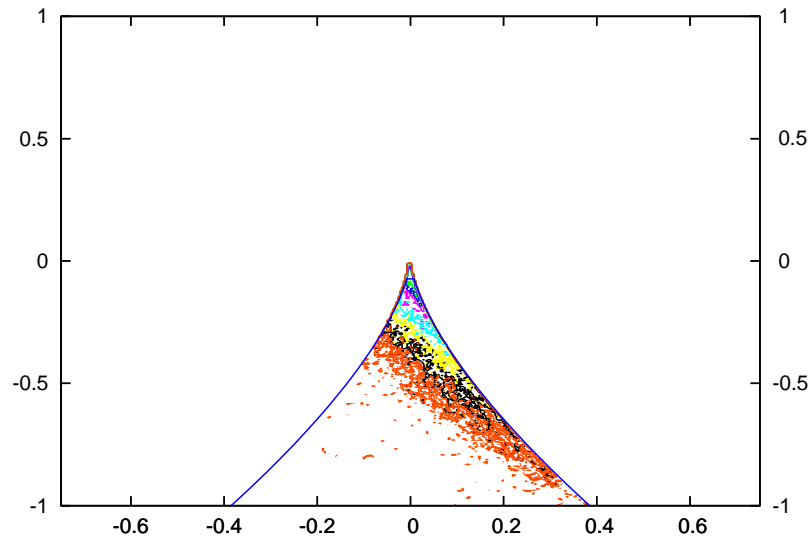
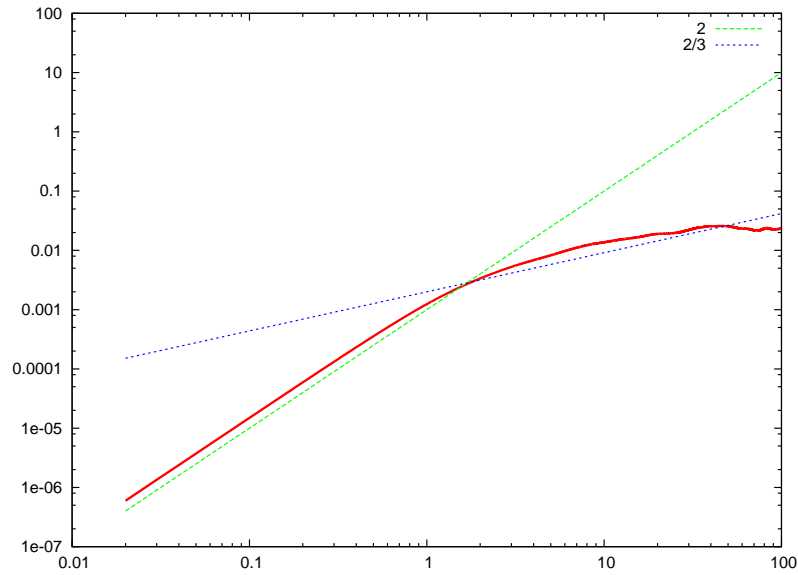
# $\langle \delta u^2(\tau) \rangle$ and $Q_s - R_s$ at $x/x_* = 0.525$



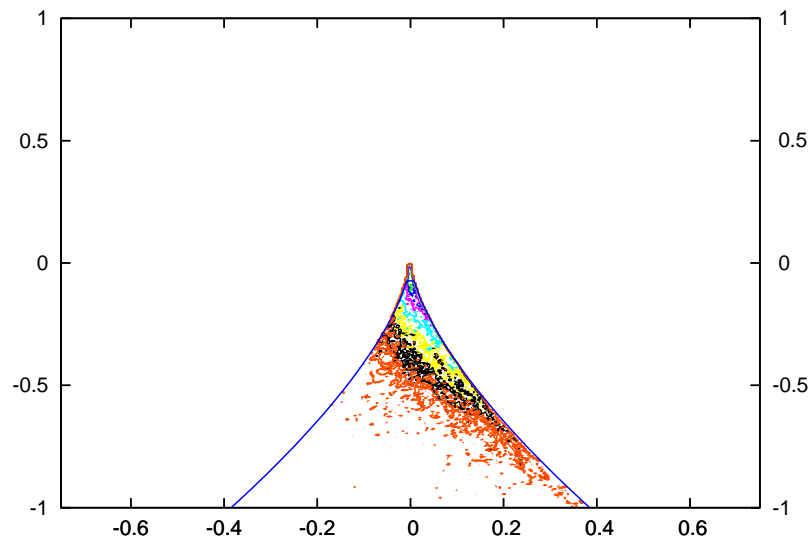
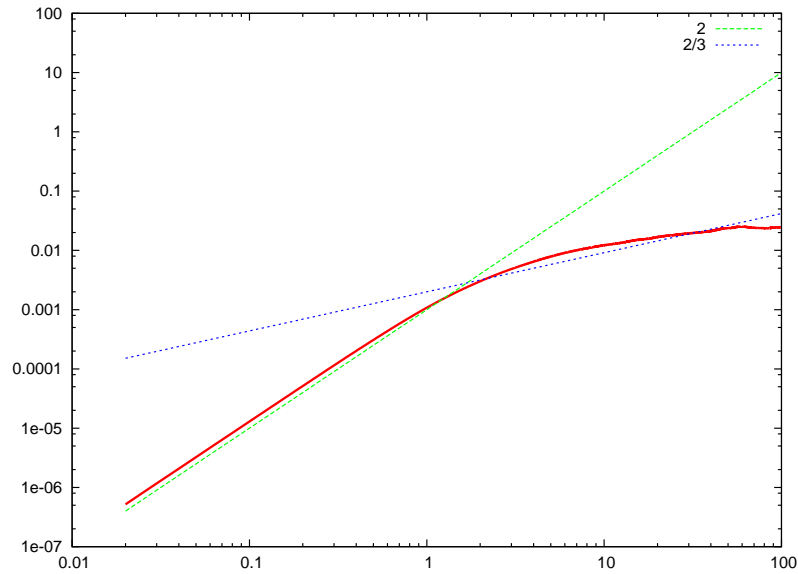
# $\langle \delta u^2(\tau) \rangle$ and $Q_s - R_s$ at $x/x_* = 0.577$



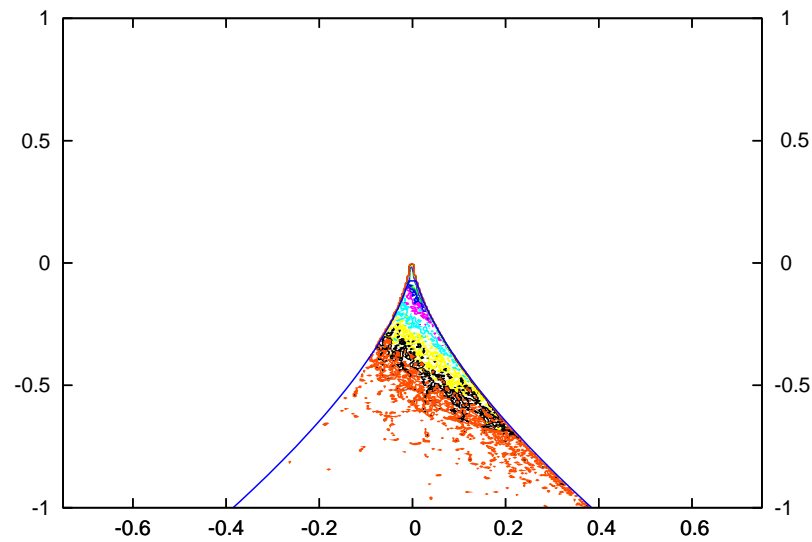
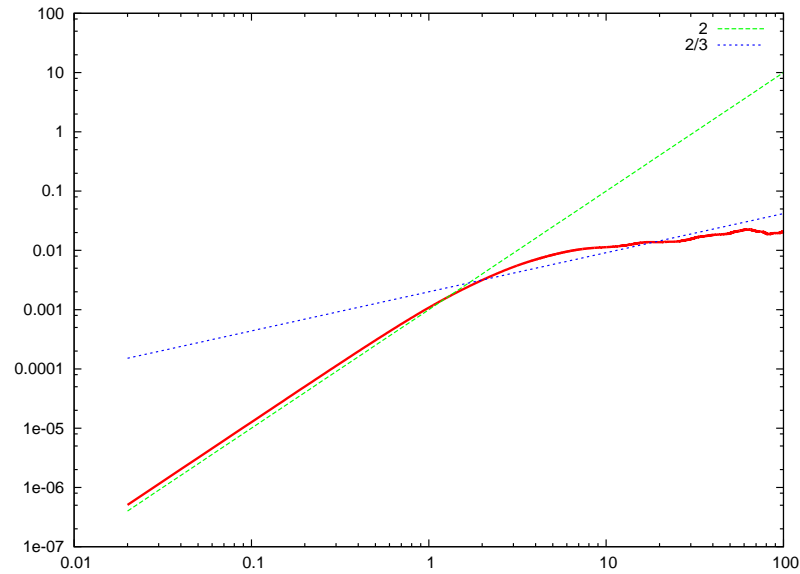
# $\langle \delta u^2(\tau) \rangle$ and $Q_s - R_s$ at $x/x_* = 0.630$



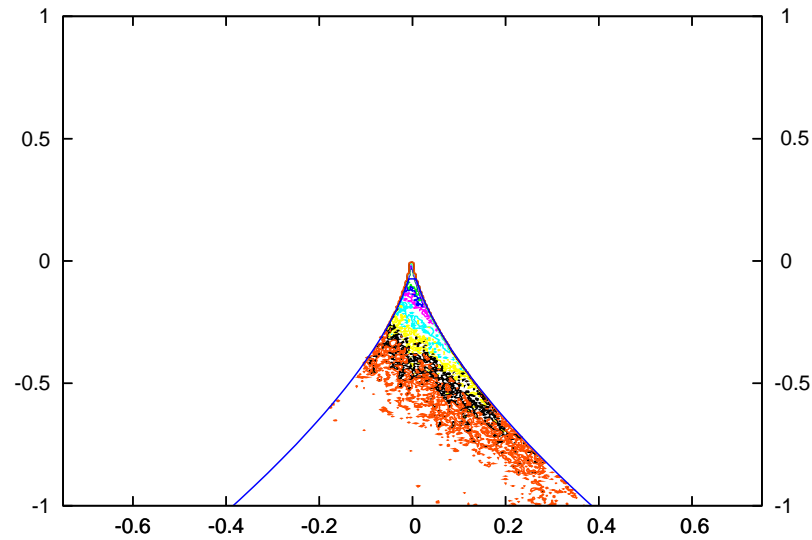
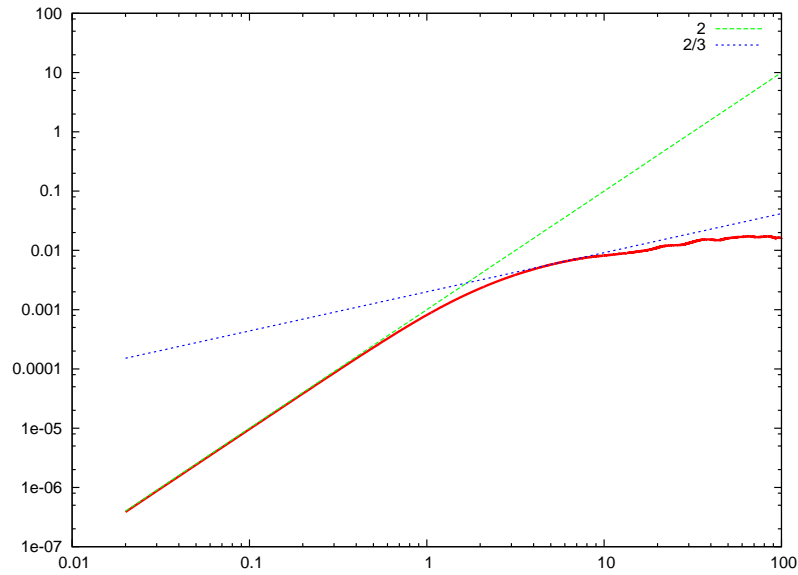
# $\langle \delta u^2(\tau) \rangle$ and $Q_s - R_s$ at $x/x_* = 0.683$



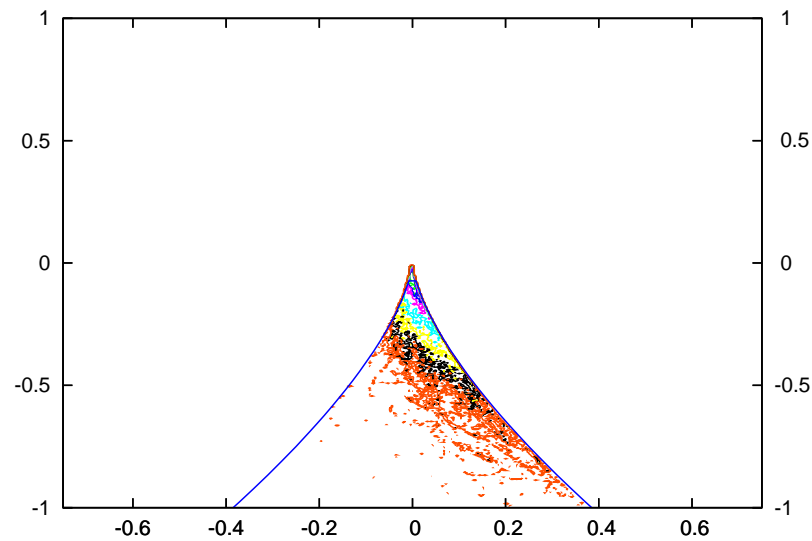
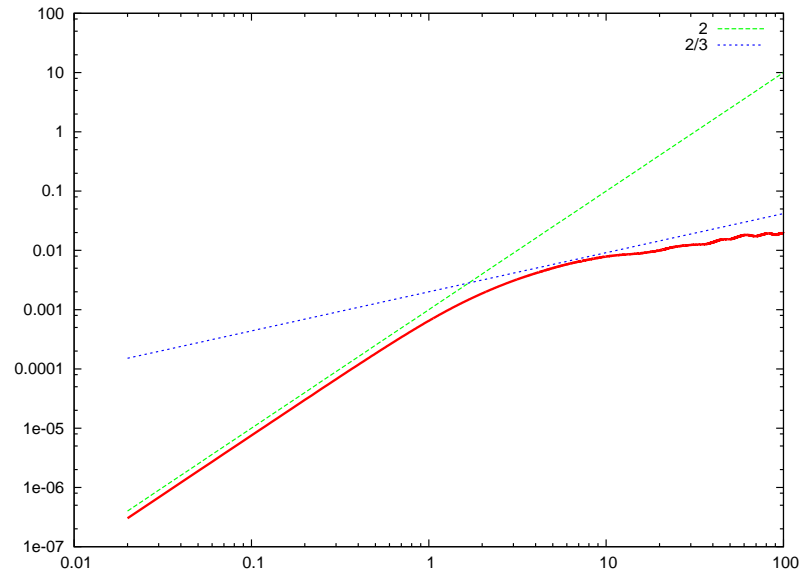
# $\langle \delta u^2(\tau) \rangle$ and $Q_s - R_s$ at $x/x_* = 0.735$



# $\langle \delta u^2(\tau) \rangle$ and $Q_s - R_s$ at $x/x_* = 0.788$

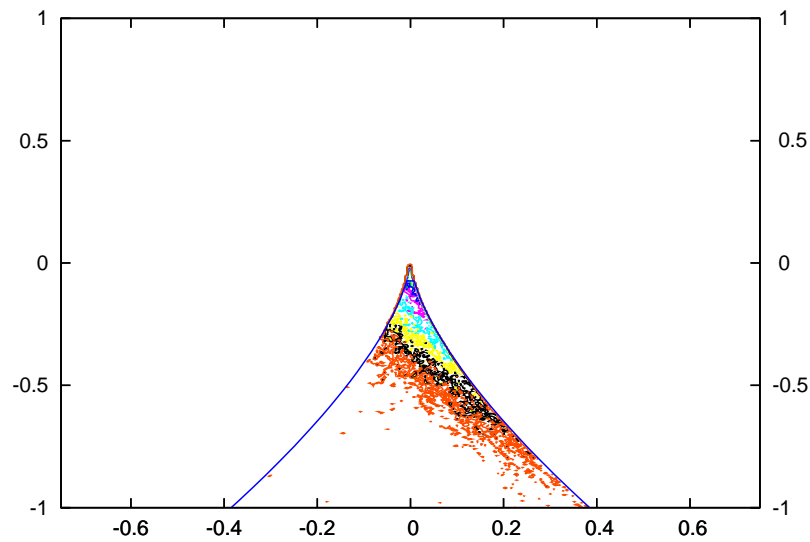
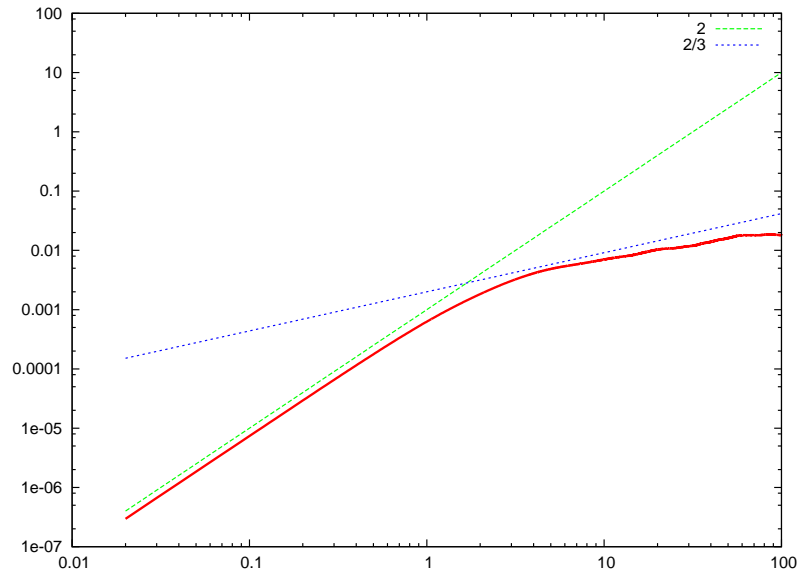


# $\langle \delta u^2(\tau) \rangle$ and $Q_s - R_s$ at $x/x_* = 0.840$

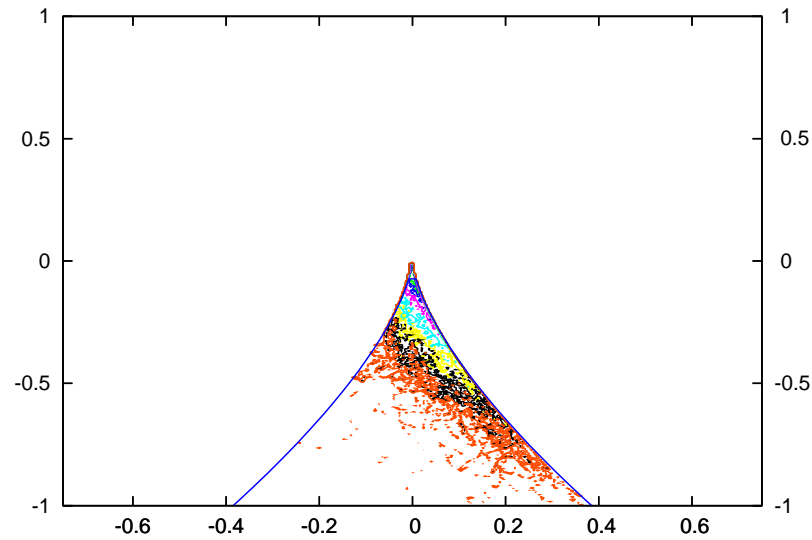
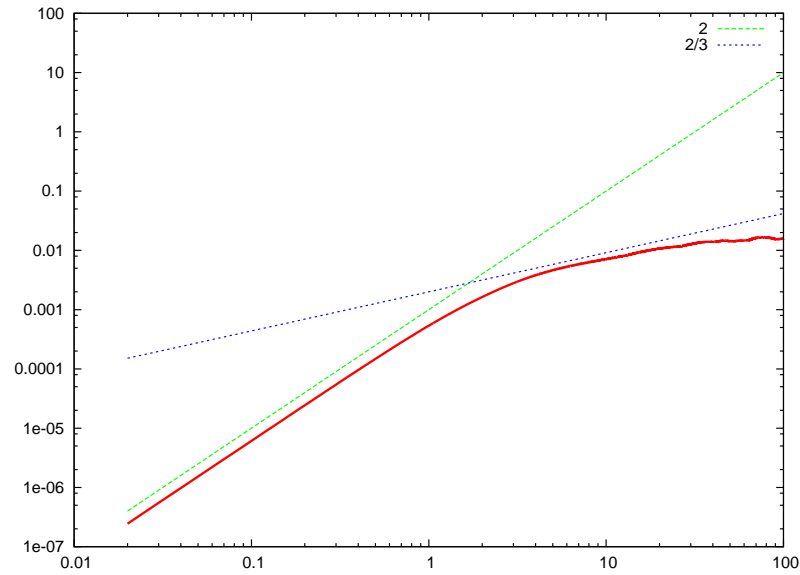




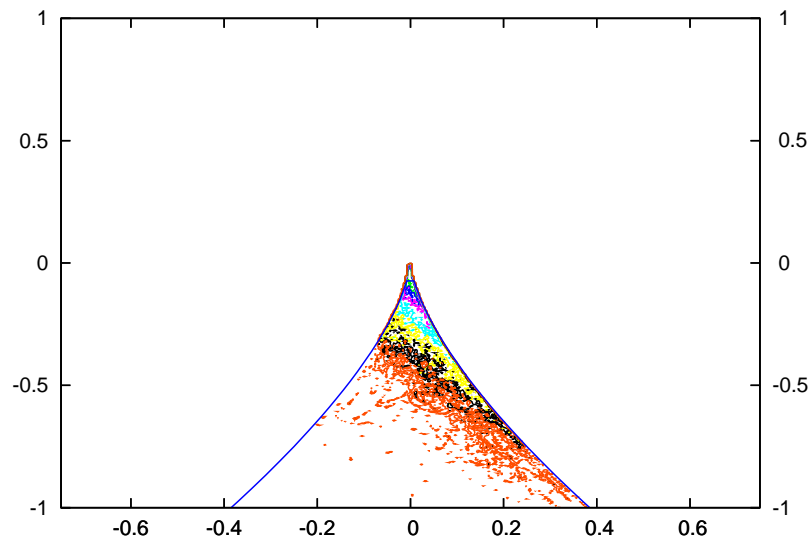
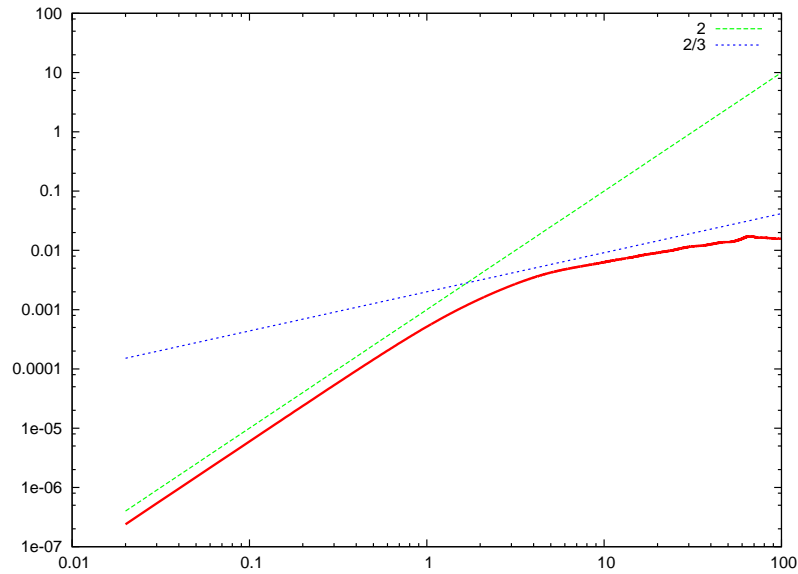
# $\langle \delta u^2(\tau) \rangle$ and $Q_s - R_s$ at $x/x_* = 0.893$



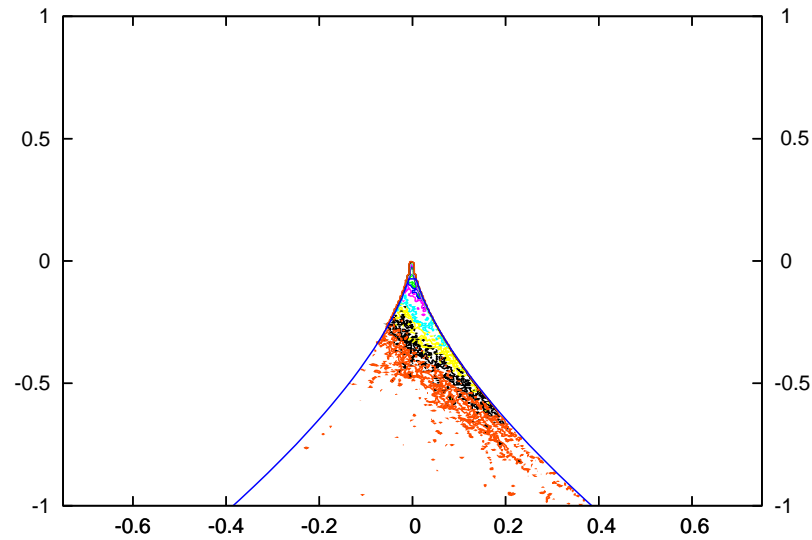
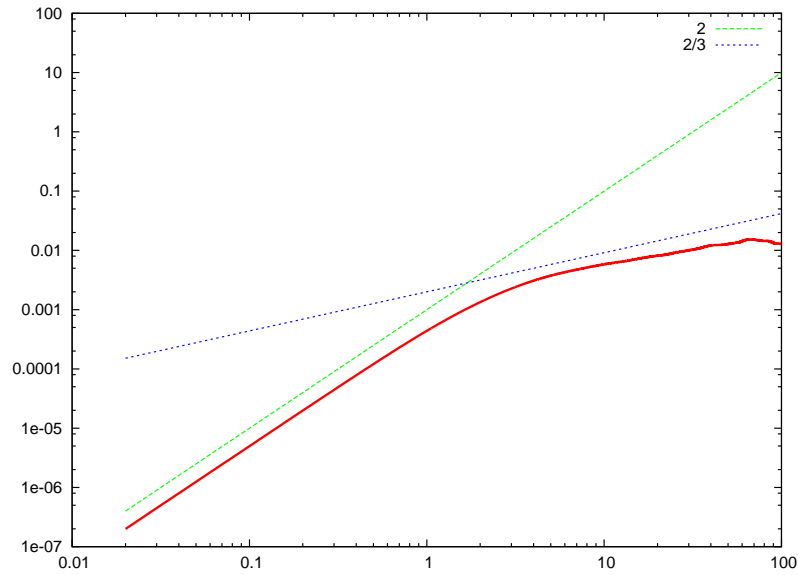
# $\langle \delta u^2(\tau) \rangle$ and $Q_s - R_s$ at $x/x_* = 0.945$



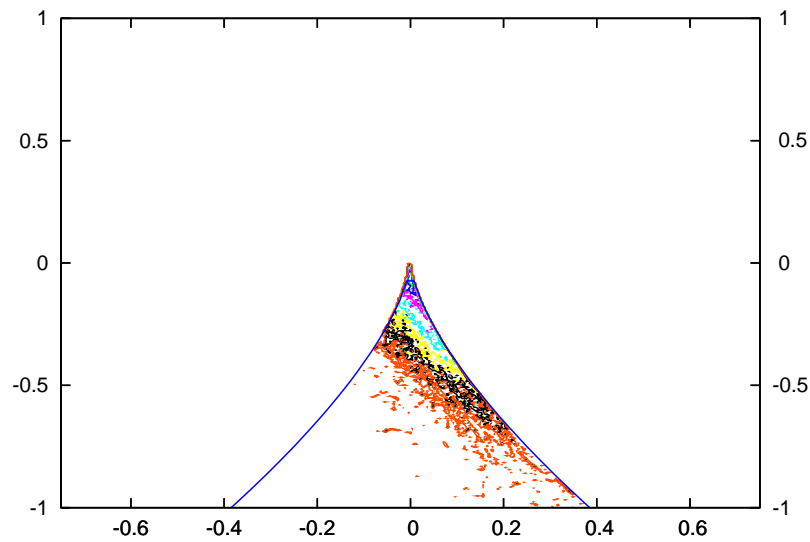
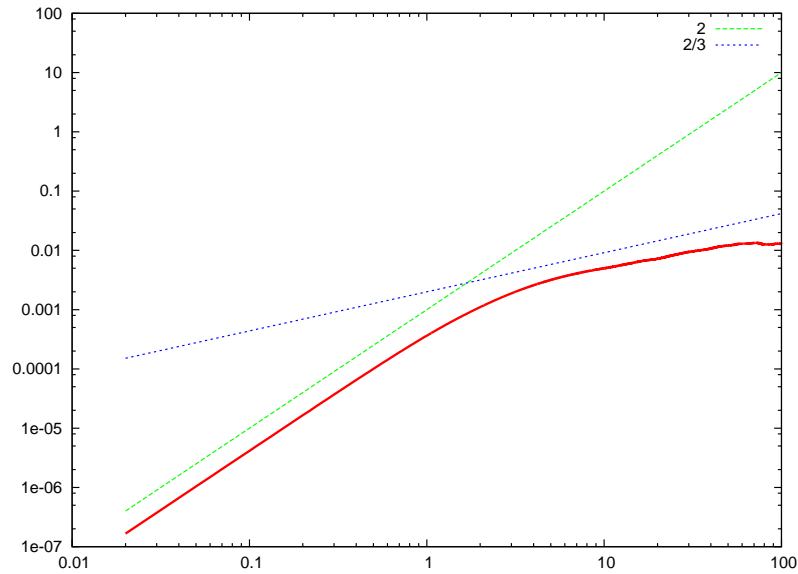
# $\langle \delta u^2(\tau) \rangle$ and $Q_s - R_s$ at $x/x_* = 0.998$



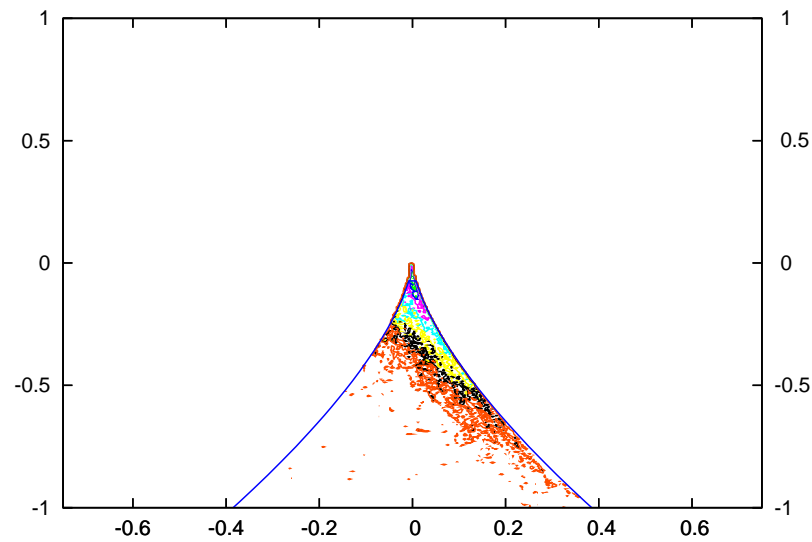
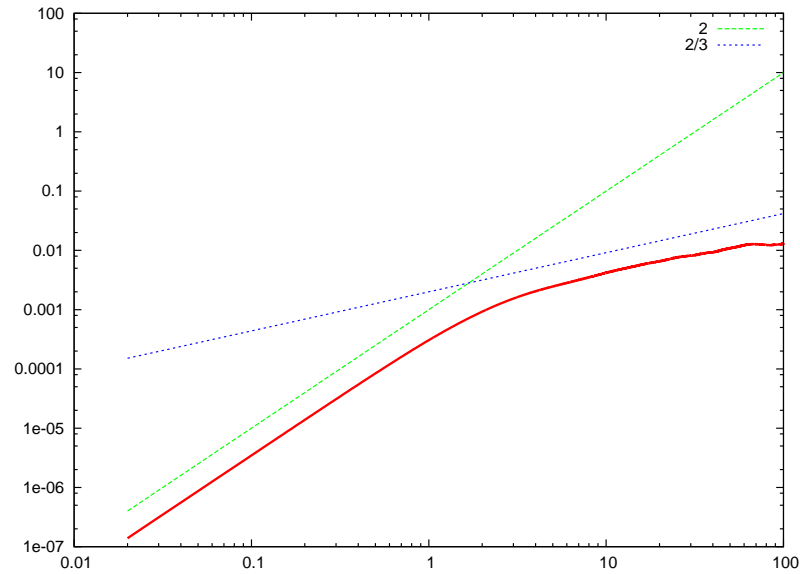
# $\langle \delta u^2(\tau) \rangle$ and $Q_s - R_s$ at $x/x_* = 1.050$



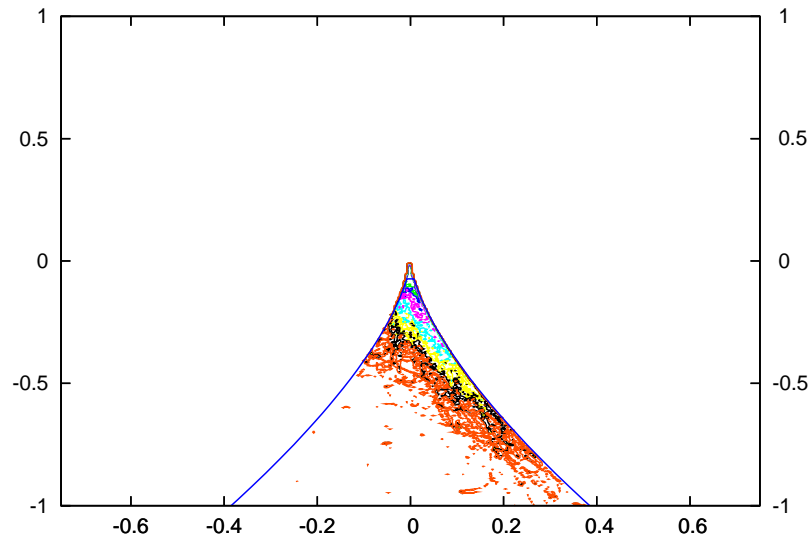
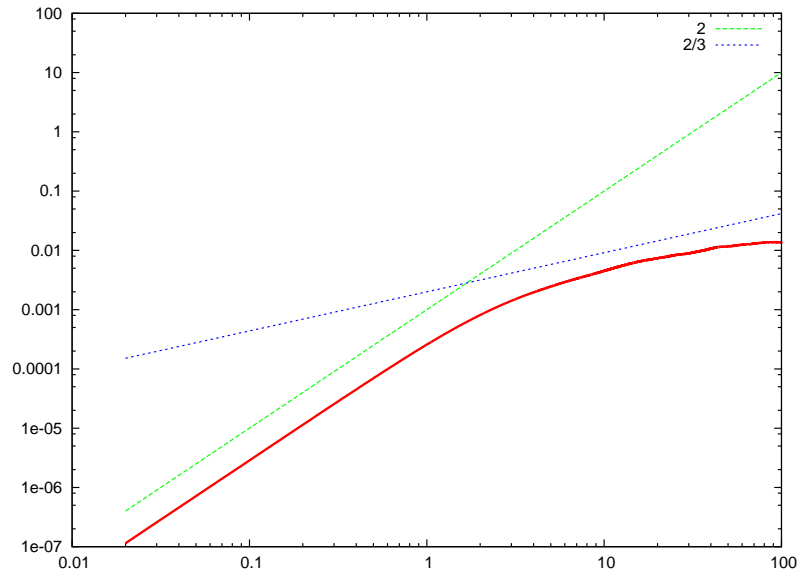
# $\langle \delta u^2(\tau) \rangle$ and $Q_s - R_s$ at $x/x_* = 1.103$



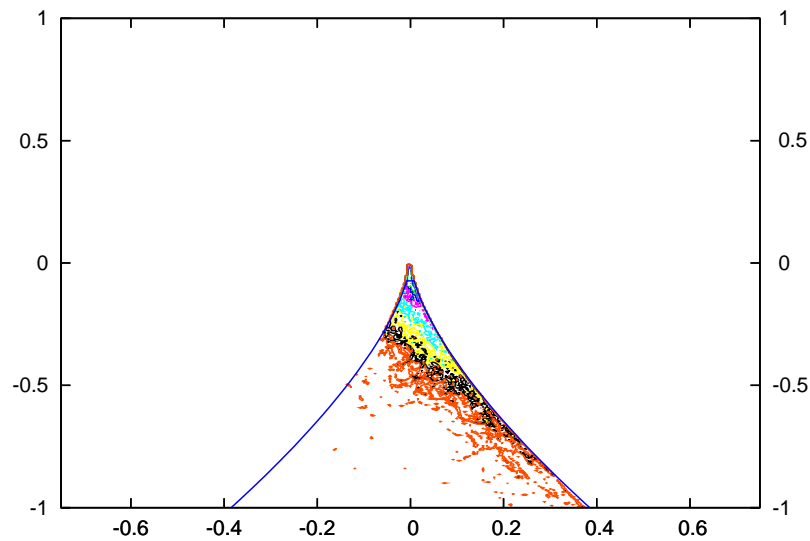
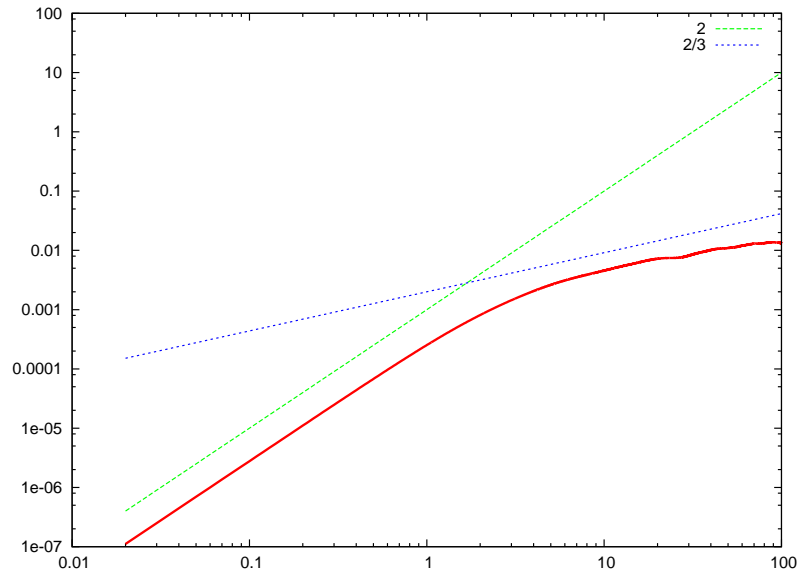
# $\langle \delta u^2(\tau) \rangle$ and $Q_s - R_s$ at $x/x_* = 1.155$



# $\langle \delta u^2(\tau) \rangle$ and $Q_s - R_s$ at $x/x_* = 1.208$

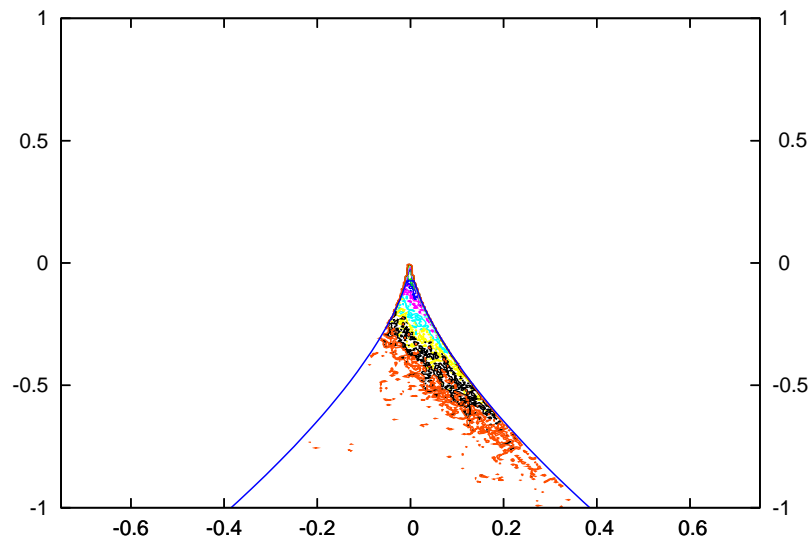
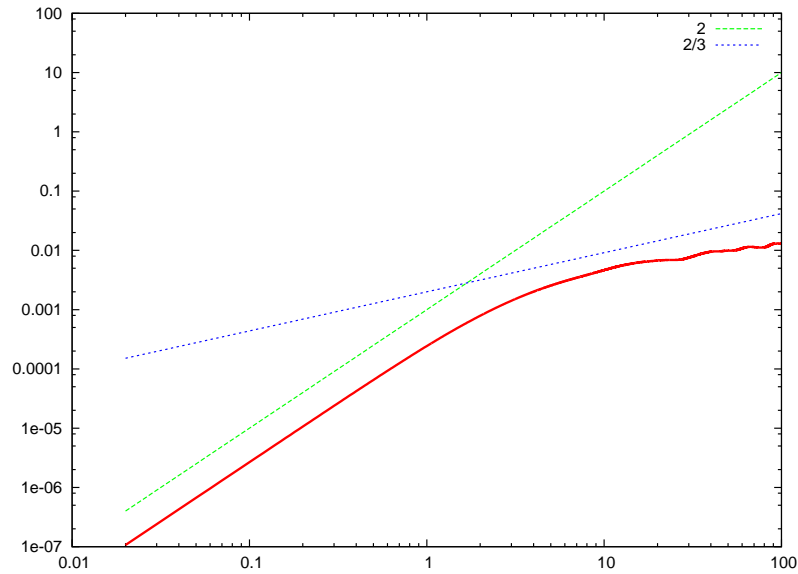


# $\langle \delta u^2(\tau) \rangle$ and $Q_s - R_s$ at $x/x_* = 1.261$

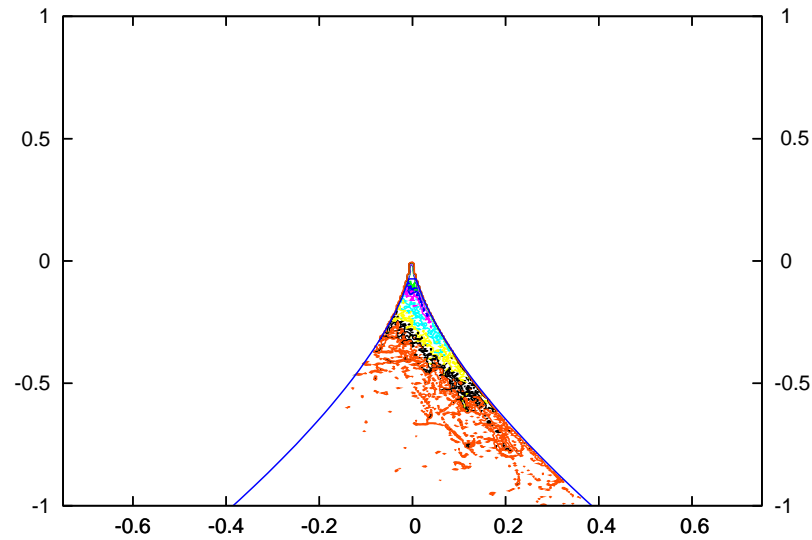
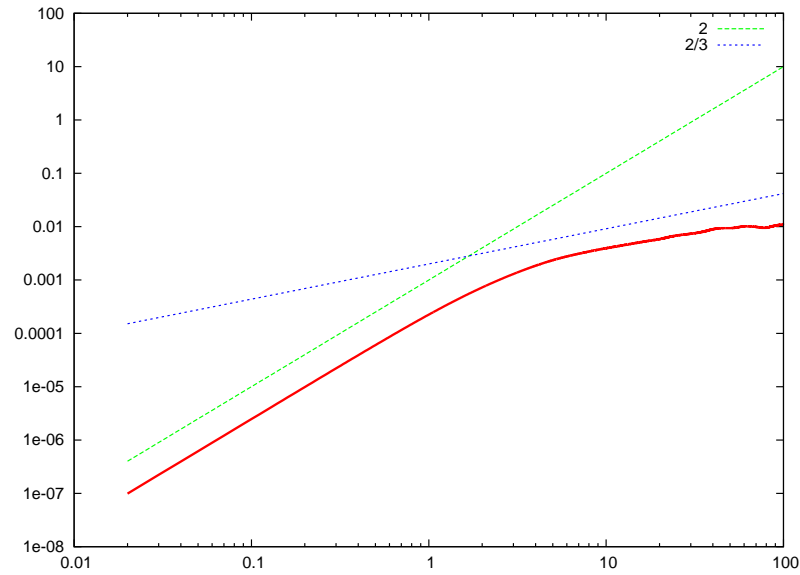




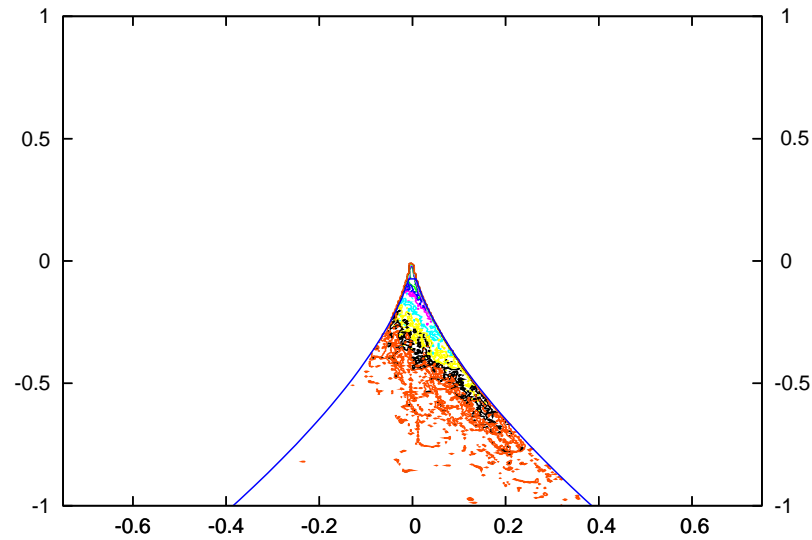
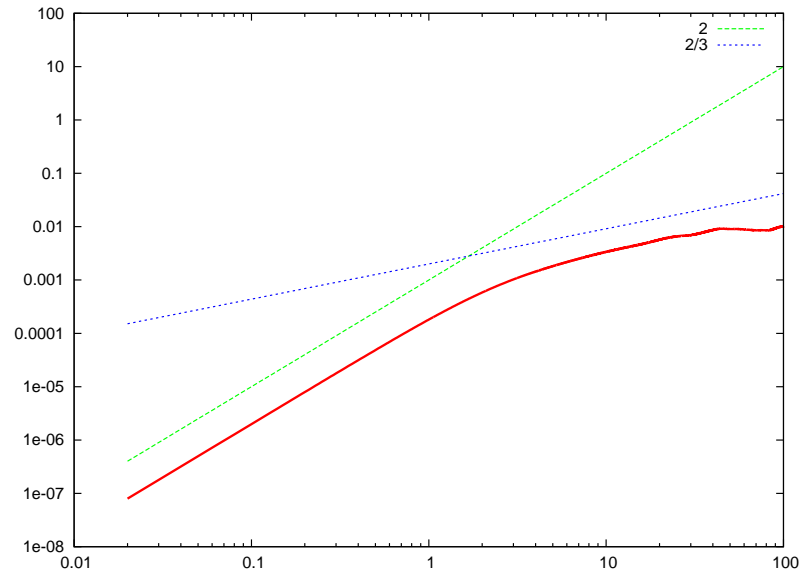
# $\langle \delta u^2(\tau) \rangle$ and $Q_s - R_s$ at $x/x_* = 1.313$



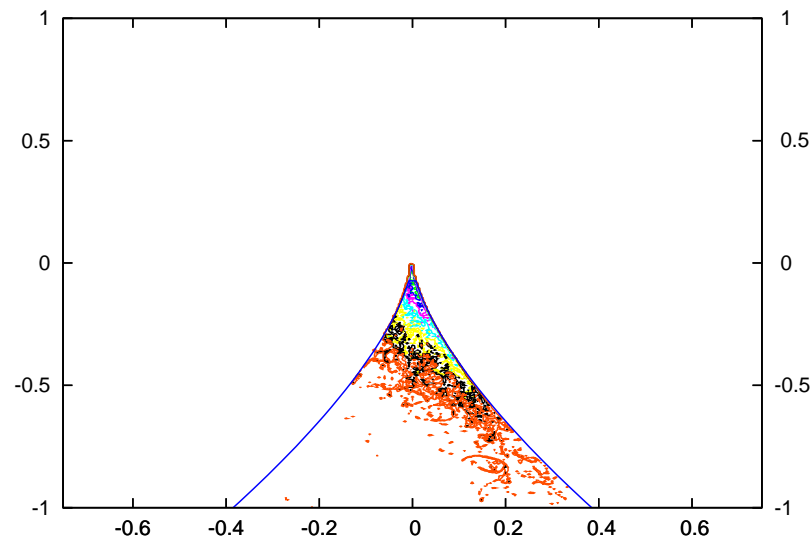
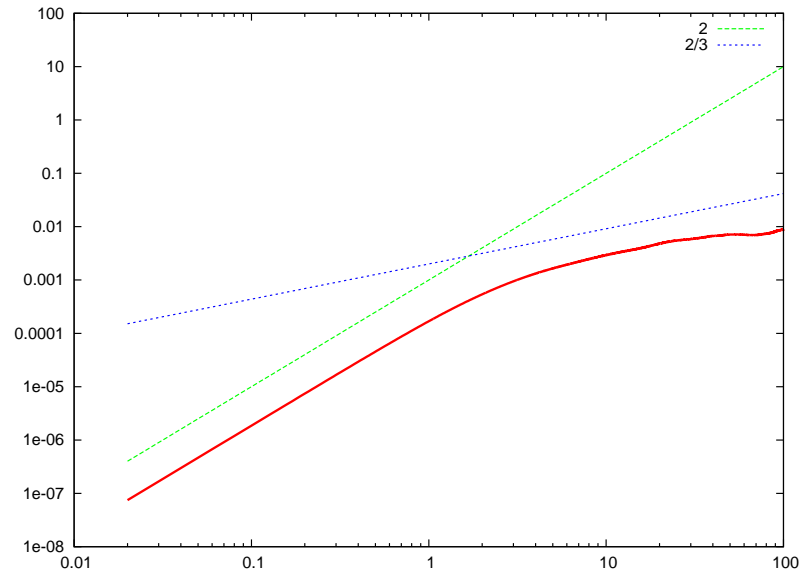
# $\langle \delta u^2(\tau) \rangle$ and $Q_s - R_s$ at $x/x_* = 1.366$



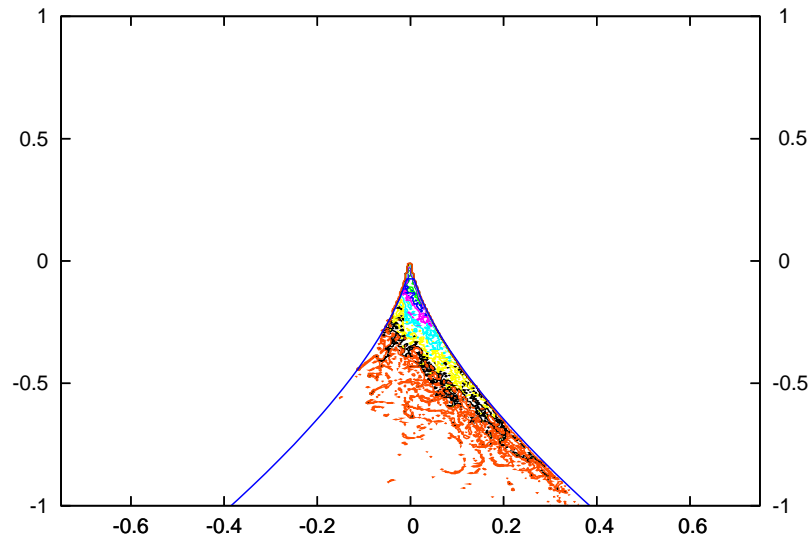
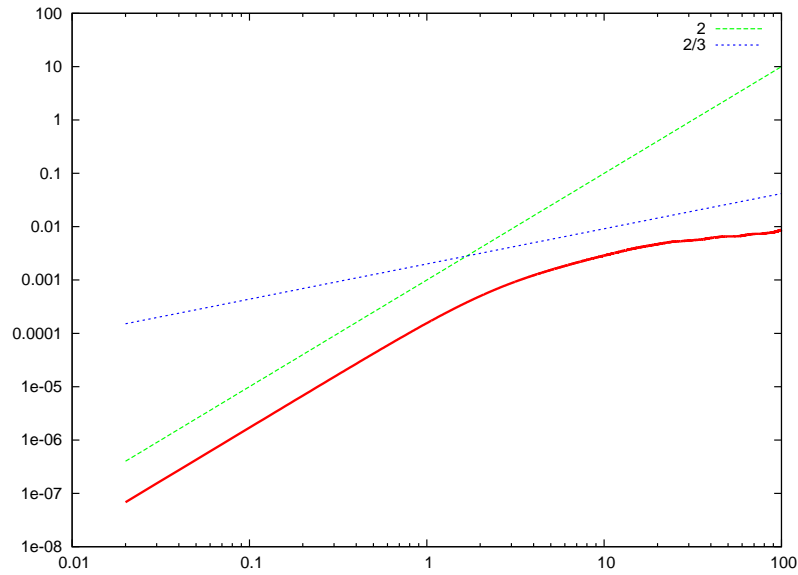
# $\langle \delta u^2(\tau) \rangle$ and $Q_s - R_s$ at $x/x_* = 1.418$



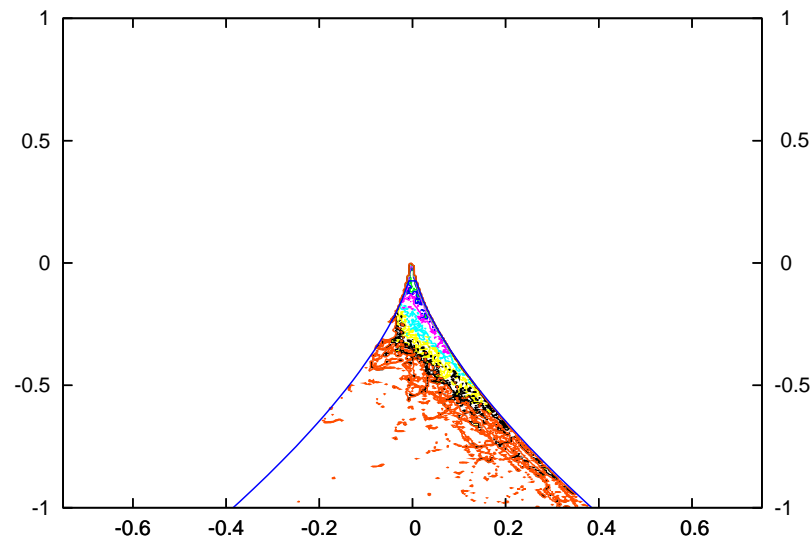
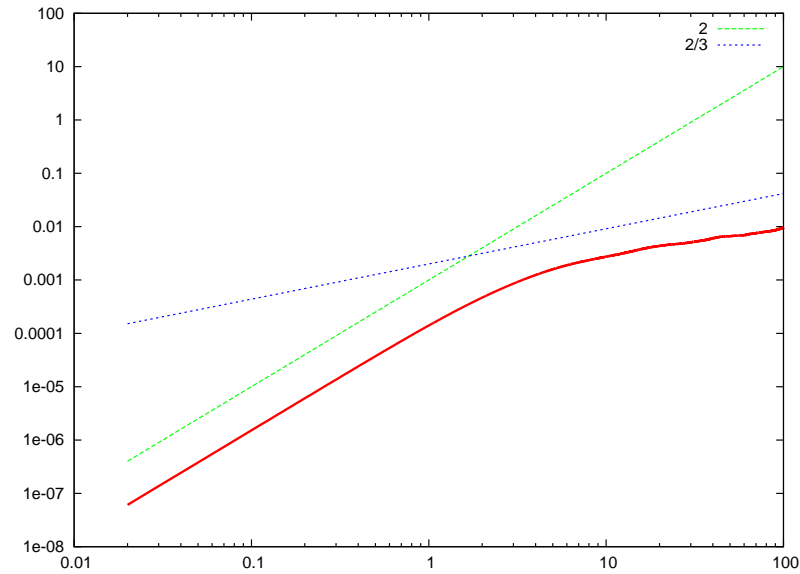
# $\langle \delta u^2(\tau) \rangle$ and $Q_s - R_s$ at $x/x_* = 1.471$



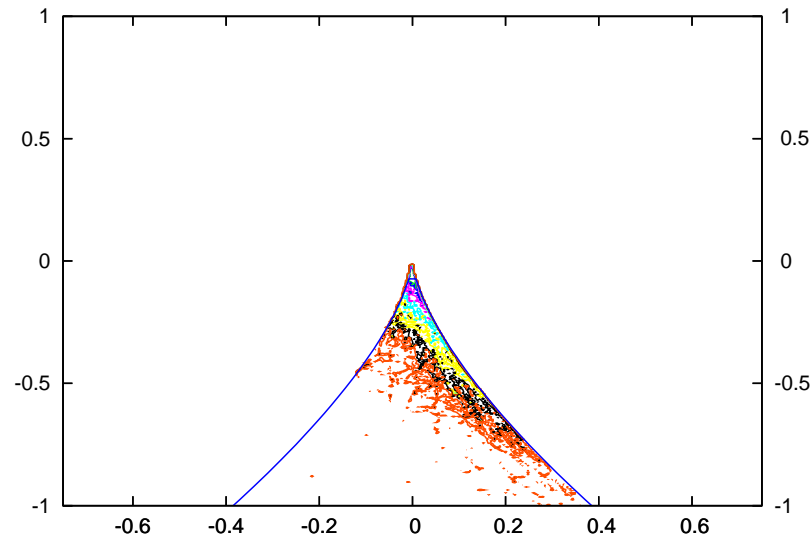
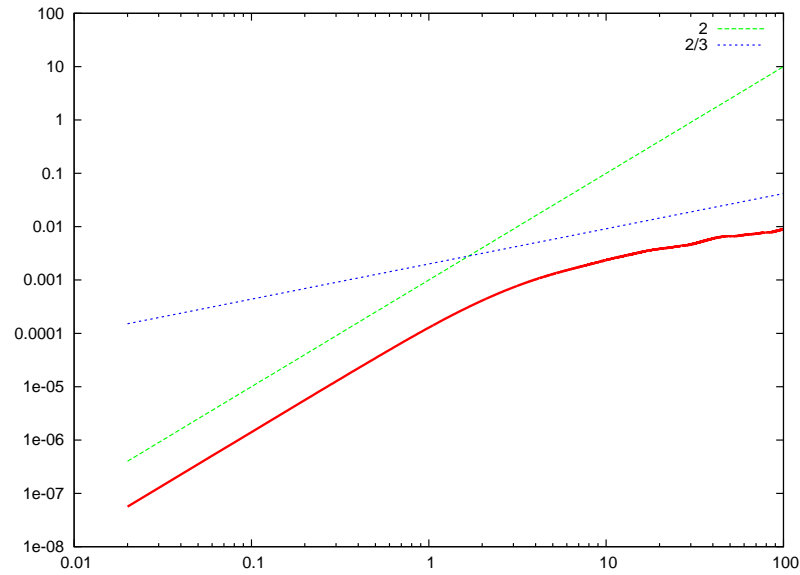
# $\langle \delta u^2(\tau) \rangle$ and $Q_s - R_s$ at $x/x_* = 1.523$



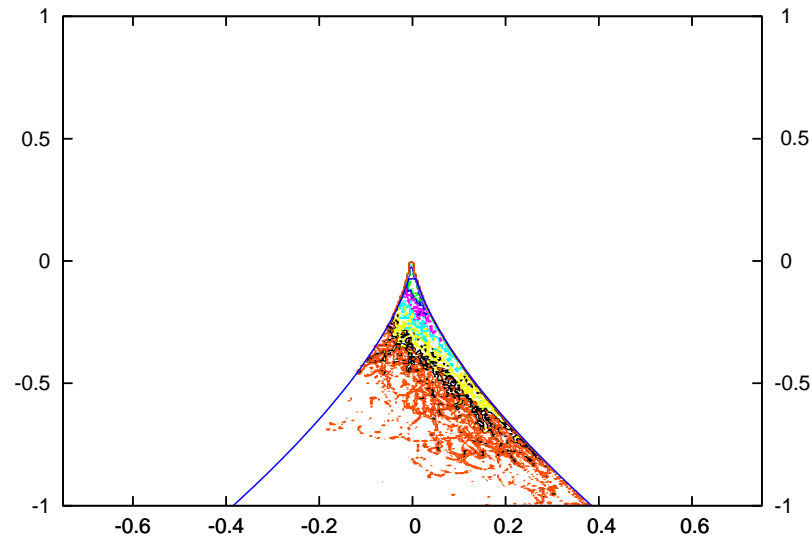
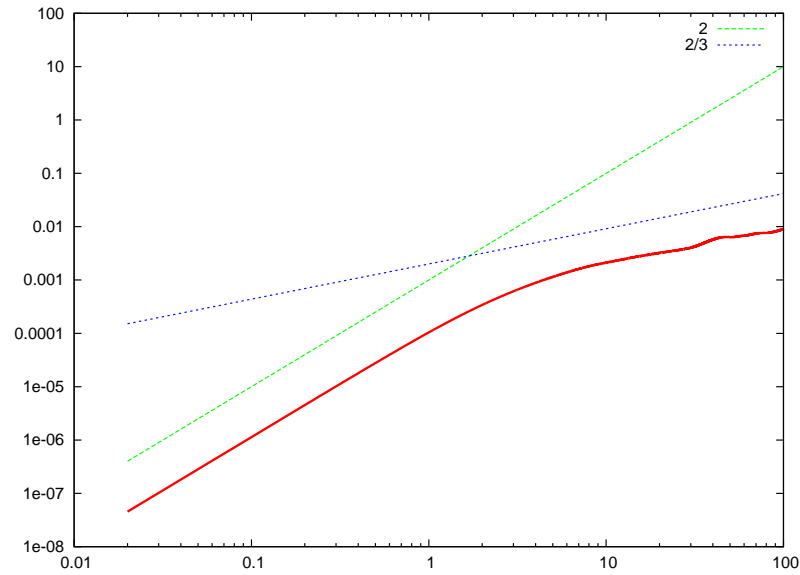
# $\langle \delta u^2(\tau) \rangle$ and $Q_s - R_s$ at $x/x_* = 1.576$



# $\langle \delta u^2(\tau) \rangle$ and $Q_s - R_s$ at $x/x_* = 1.628$

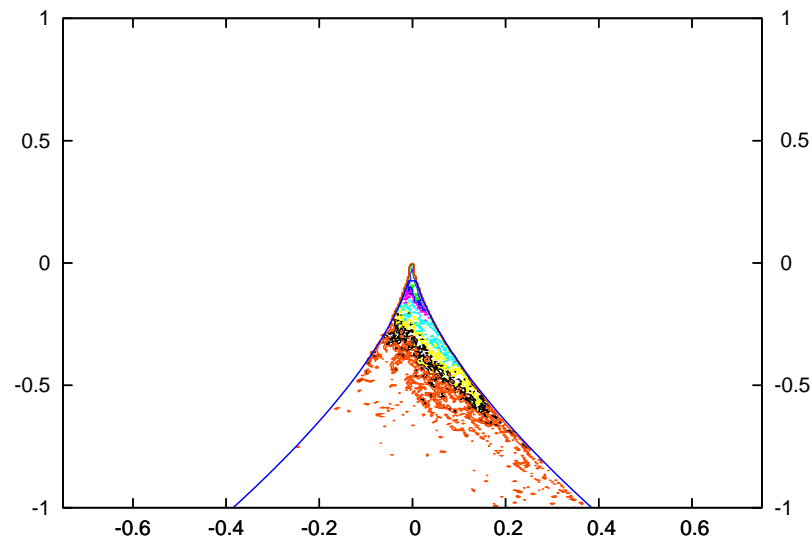
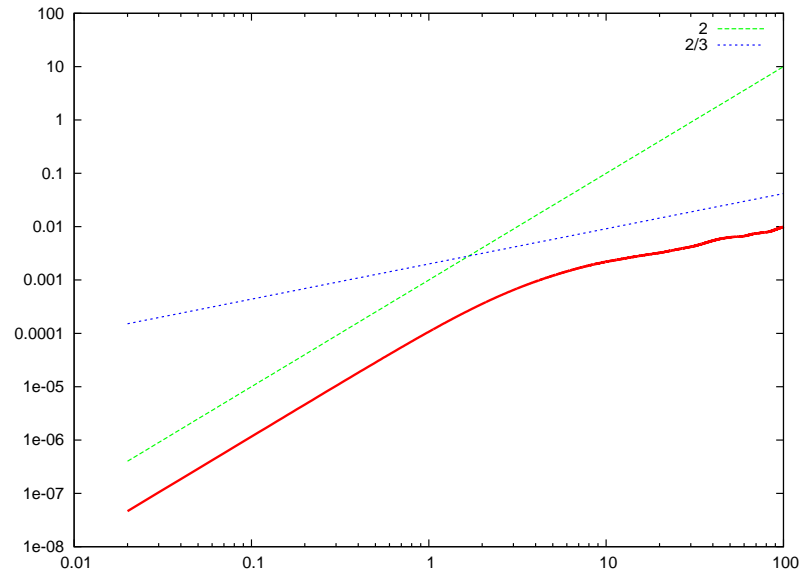


# $\langle \delta u^2(\tau) \rangle$ and $Q_s - R_s$ at $x/x_* = 1.681$





# $\langle \delta u^2(\tau) \rangle$ and $Q_s - R_s$ at $x/x_* = 1.733$



# Conclusion of Q-R study

$\langle \delta u^2(\tau) \rangle \sim \tau^{2/3}$  appears in the lee of the less blocked part of the grid and well before the appearance of the usual Q-R tear drop shape, in fact in the very near-grid region where the turbulent fluctuating velocity is highly non-gaussian and intermittent (sudden chirps between much quieter activity).

# Conclusions

1. **Space-Scale Unfolding mechanism** in turbulence generated by fractal square grids. Reduced pressure-drop, increased scalar transfer/turbulent diffusion. Two new length-scales: Effective mesh size  $M_{eff}$  and wake-interaction length-scale  $x_*$ .
2. **Potential applications**: energy-efficient mixers and heat exchangers, lean premixed combustion, silent airbrakes, wind tunnel simulations of thick turbulent boundary layers.
3. In non-equilibrium region  $\frac{1}{2}x_* \leq x \leq x_e$  (where  $x_e = 2x_*$  for RG),  $\epsilon \sim \frac{U_\infty u'^2}{L} \frac{L_b}{L}$ . There seems to be a universal dissipation law for non-equilibrium near -5/3 turbulence!

see <http://www3.imperial.ac.uk/tmfc>